

Complement-Mediated Microglial Priming: *An In Vitro* Study

Richard Wheat

A thesis submitted to Cardiff University in candidature for the degree of
Doctor of Philosophy

Division of Infection and Immunity
Systems Immunology Research Institute
School of Medicine
Cardiff University

September 2016

Declaration

This work has not previously been accepted in substance for any degree and is not concurrently submitted in candidature for any other degree.

Signed **Date**

This thesis is being submitted in partial fulfilment of the requirements for the degree of PhD.

Signed **Date**

This thesis is the result of my own independent work/investigation, except where otherwise stated. Other sources are acknowledged by explicit references. This thesis is the product of work conducted entirely since the official commencement date of the approved research program.

Signed **Date**

I hereby give consent for my thesis, if accepted, to be available for photocopying and for inter-library loan, and for the title and summary to be made available to outside organisations.

Signed **Date**

Richard Andrew Wheat

Table of Contents

Declaration	i
Table of Contents.....	ii
List of Abbreviations	v
List of Figures.....	x
List of Tables	xiv
Abstract	1
1 Introduction	3
1.1 The Complement System	3
1.1.1 Components	3
1.1.2 Activation	6
1.1.3 Regulation	14
1.1.4 Functions/Roles	18
1.1.5 Human Vs Mouse C.....	23
1.2 Microglia	29
1.2.1 Microglial Activation	32
1.2.2 Microglial Functions.....	33
1.2.3 Tools for Microglial Research	34
1.2.4 Microglia, C, Development & Dysfunction	34
1.2.5 Microglial Priming.....	37
1.3 Aims & Hypotheses.....	40
2 Materials & Methods	42
2.1 Cell Culture.....	42
2.1.1 BV2 Microglial Cell Line	42
2.1.2 Primary Microglia.....	43
2.2 Cell Treatments/Exposures	45
2.2.1 LPS.....	45
2.2.2 Fluid-phase iC3b	45
2.2.3 Zymosan	50
2.2.4 Immobilised C3 Activation Fragments	52
2.2.5 Serum/Complement Deposition & Killing Assay.....	54
2.3 Assays.....	54
2.3.1 Flow Cytometry.....	54
2.3.2 ICC	57
2.3.3 TC Supernatant Analysis.....	58

2.3.4	Rt-qPCR.....	59
2.4	Serum Preparation for use as a C Source.....	65
2.4.1	Mouse	65
2.4.2	Human.....	66
2.5	Statistics	66
3	Isolation of Primary Adult Murine Microglia	67
3.1	Introduction	67
3.1.1	Microglial Culture Systems.....	67
3.1.2	Microglial Phenotyping, Stimulation and Response Detection	70
3.1.3	Chapter Aims	70
3.2	Results.....	71
3.2.1	Establishment of Ongoing Pure Cultures of Primary Adult Murine Microglia.....	71
3.2.2	Mixed Vs Pure Microglial Cultures: Surface CD11b LPS Response	97
3.3	Discussion.....	98
3.3.1	Primary Adult Murine Microglia: Culture, Phenotyping and Activation	98
3.3.2	Primary Microglia vs BV2 Cells	99
3.3.3	Microglial Cultures: Pure Vs Mixed.....	100
4	iC3b Engagement of Microglial CR3: Phenotypic Consequences.....	102
4.1	Introduction	102
4.1.1	CR3 Discovery and Structure	102
4.1.2	The Many Ligands of CR3	108
4.1.3	Cell Signaling of Ligated β 2/CD11:CD18 Integrins	109
4.1.4	CR3 Functions	112
4.1.5	Chapter Aims	114
4.2	Results.....	116
4.2.1	Fluid-Phase iC3b.....	116
4.2.2	Zymosan	129
4.2.3	C3-Activation Fragments Immobilised on Tissue Culture Plastic.....	136
4.3	Discussion.....	150
4.3.1	Fluid-phase iC3b	150
4.3.2	Zymosan	151
4.3.3	C3-Activation Fragments Immobilised on Tissue Culture Plastic.....	154
4.3.4	General.....	155
5	The <i>In Vitro</i> Crry KO Microglial Phenotype.....	157
5.1	Introduction	157

5.1.1	Biological Role of Crry	157
5.1.2	Crry and the CNS.....	158
5.1.3	Chapter Aims	159
5.2	Results.....	160
5.2.1	Specific Detection of Surface Crry Expression	160
5.2.2	<i>In Vitro</i> Phenotype of Crry KO Microglia	162
5.2.3	Sensitivity to C Activation: C3-Activation Fragment Deposition and MAC-Mediated Lysis	163
5.2.4	Phenotypic Effects of C Activation on Crry KO Microglia <i>in Vitro</i>	171
5.3	Discussion.....	173
5.3.1	The <i>in Vitro</i> Crry KO Microglial Phenotype and the Mechanism of C-dependent Priming	173
5.3.2	Crry as the Key Regulator of Microglial Sensitivity to Autologous C Activation	177
6	Discussion	179
6.1	Study Outline.....	179
6.2	Summary of Main Findings	179
6.2.1	The Influence of C on <i>In Vitro</i> Microglial Phenotypes.....	179
6.2.2	Microglial Culture Systems.....	182
6.3	Future Directions	184
6.3.1	Purified iC3b	184
6.3.2	The Priming Effect of Immobilised Mouse iC3b Derived from Serum Borne C3	185
6.3.3	Crry KO Microglia	186
6.3.4	The Assessment of IL-1 β as a Priming Marker.....	186
6.3.5	Exploiting CR3 Non-Inflammatory Responses	187
6.4	Concluding Remarks	187
	References.....	189
	Appendix	209

List of Abbreviations

7-AAD	7-Aminoactinomycin D	cDNA	Complementary DNA
Ab	Antibody	CNS	Central Nervous System
Ag	Antigen	CO₂	Carbon Dioxide
aHUS	Atypical Haemolytic Uremic Syndrome	CR	Complement Receptor
AIHA	Autoimmune Haemolytic Anaemia	CRD	Carbohydrate Recognition Domain
AP	Alternative Pathway	CR1g	Complement Receptor of the Immunoglobulin Superfamily
APC	Antigen Presenting Cell	CRP	C-Reactive Protein
APS	Ammonium Persulphate	CSF	Cerebrospinal Fluid
ASPA	Animals (Scientific Procedures) Act	Crry	CR1-Related Gene/Protein Y
BBB	Blood Brain Barrier	Ct	Cycle Threshold
BLAST	Basic Local Alignment Search Tool	CVF	Cobra Venom Factor
BSA	Bovine Serum Albumin	DAF	Decay Accelerating Factor
C	Complement/the Complement System	DAMP	Danger Associated Molecular Pattern
C1Inh	C1 Inhibitor	DAP12	DNAX-activating protein of molecular mass 12 kDa
C4BP	C4 Binding Protein	DAPI	Diamidino-2-Phenylindole
C5aR	C5a Receptor	dH₂O	De-ionised/Distilled Water
CCP	Complement Control Protein	DMEM	Dulbecco's Modified Eagle's Medium
CD	Cluster of Differentiation	DMSO	Dimethyl-Sulphoxide
Cdc42	Cell division control protein 42 homolog	DNA	Deoxyribonucleic Acid

EAE	Excitatory Autoimmune Encephalomyelitis	GPI	Glycosylphosphatidylinositol
EAMG	Excitatory Autoimmune Myasthenia Gravis	H₂SO₄	Sulphuric Acid
ECM	Extracellular Matrix	HAE	Hereditary Angioedema
EDTA	Ethylenediaminetetraacetic Acid	HBSS	Hank's Balanced Salt Solution
EGFP	Enhanced Green Fluorescent Protein	HCK	Haematopoietic Cell Kinase
EGTA	Ethylene Glycol Tetraacetic Acid	HI	Heat Inactivated
ELISA	Enzyme-linked Immunosorbent Assay	HKG	Housekeeping Gene
ERK	Extracellular-signal Regulated Kinase	HRP	Horse Radish Peroxidase
FACS	Flow/Fluorescence Assisted Cell Sorting	ICC	Immunocytochemistry
FBS	Foetal Bovine Serum	Ig	Immunoglobulin
Fc	Fragment crystallisable/Constant	IHC	Immunohistochemistry
FcR	Fc Receptor	IL	Interleukin
fH	Factor H	ITAM	Immunoreceptor Tyrosine- based Activation Motif
fl	Factor I	KO	Knockout
FITC	Fluorescein Isothiocyanate	LAD	Leukocyte Adhesion Deficiency
GEF	guanine nucleotide exchange factor	LFA	Lymphocyte Function- Associated Antigen
GFAP	Glial Fibrillary Acidic Protein	LPS	Lipopolysaccharide
		mAb	Monoclonal Antibody
		MAC	Membrane Attack Complex
		MACPF	Membrane Attack Complex/Perforin

MACS	Magnetic Cell Separation System	OmCI	<i>Ornithodoros moubata</i> Complement Inhibitor
MAPK	Mitogen-Activated Protein Kinase	OPD	o-Phenylenediamine Dihydrochloride
MASP	MBL Associated Serine Protease	PAGE	Polyacrylamide Gel Electrophoresis
MBL	Mannose Binding lectin	PAMP	Pathogen Associated Molecular Pattern
MCP	Membrane Cofactor Protein	PBS	Phosphate Buffered Saline
M-CSF	Macrophage Colony Stimulating Factor	PC	Personal Computer
MFI	Mean Fluorescence Intensity	PCR	Polymerase Chain Reaction
MHC	Major Histocompatibility Complex	PD	Parkinson's Disease
MOG	Myelin Oligodendrocyte Glycoprotein	PFA	Paraformaldehyde
mRNA	Messenger RNA	PI	Propidium Iodide
MS	Multiple Sclerosis	PKC	Protein Kinase C
MyD88	Myeloid Differentiation Factor 88	PNH	Paroxysmal Nocturnal Haemoglobinuria
N₂	Nitrogen	PRR	Pattern Recognition Receptor
NCBI	National Center for Biotechnology Information	qPCR	Quantitative PCR
NHS	Normal Human Serum	RBC	Red Blood Cell
NIH	National Institute of Health	RCA	Regulators of Complement Activation
NK	Natural Killer	Rac	Ras-related C3 botulinum toxin substrate
NO	Nitric Oxide	rm	Recombinant Mouse
		rMOG	Recombinant MOG

RNA	Ribonucleic Acid	TBI	Traumatic Brain Injury
ROS	Reactive Oxygen Species	TC	Tissue Culture
RT	Room Temperature	TCR	T Cell Receptor
Rt	Reverse Transcription	TED	Thioester Domain
SAP	Serum Amyloid Protein	TCC	Terminal Complement Complex
SDS	Sodium Dodecyl Sulphate	TLR	Toll-Like Receptor
Serpin	Serine Protease Inhibitor	TM-GPCR	Transmembrane G-Protein Coupled Receptor
SCR	Short Consensus Repeat	TMS	Transmembrane Segment
SFK	Src Family Kinase	TNF	Tumour Necrosis Factor
SH2	Src Homology 2	TRIF	TIR-domain-containing adapter-inducing interferon- β
Slp	Sex-linked Protein	UV	Ultra-Violet
SP	Surfactant Protein	WT	Wildtype
Ss	Serological System	ZAP70	Zeta chain-associated protein of 70 kDa
Syk	Spleen Tyrosine Kinase		
TAPA	Target of the Anti-proliferative Antibody		

List of Figures

Fig. 1.1	The C system	Page 7
Fig. 1.2	Regulation of the C activation pathways	Page 15
Fig. 1.3	Origins and organisation of the mouse and human CR1/CR2/Crry gene family	Page 27
Fig. 1.4	Evolution of microglia during phagocytic activity	Page 31
Fig. 1.5	Resting microglia in the mouse cerebral cortex	Page 32
Fig. 1.6	Model of C-dependent microglial priming	Page 39
Fig. 3.1	Successful purification of primary cells from adult mouse CNS tissue (i)	Page 72
Fig. 3.2	Successful purification of primary cells from adult mouse CNS tissue (ii)	Page 73
Fig. 3.3	Continued survival and expansion of purified primary cells	Page 74
Fig. 3.4	Distinct morphologies and proliferation rates of primary and BV2 cells	Page 75
Fig. 3.5	Flow cytometric analysis of surface CD11b expression by primary and BV2 cells	Page 76
Fig. 3.6	Flow cytometric analysis of surface CD45 expression by primary and BV2 cells	Page 76
Fig. 3.7	Flow cytometric analysis of surface CD200R expression by primary and BV2 cells	Page 77
Fig. 3.8	Flow cytometric analysis of surface F4/80 expression by primary and BV2 cells	Page 77
Fig. 3.9	Flow cytometric analysis of surface Crry expression by primary and BV2 cells	Page 77
Fig. 3.10	Flow cytometric analysis of surface C5aR expression by primary and BV2 cells	Page 78
Fig. 3.11	Flow cytometric analysis of surface CD59 expression by primary and BV2 cells	Page 78
Fig. 3.12	Rt-PCR analysis of microglial transcript expression by primary and BV2 cells	Page 80
Fig. 3.13	Increased zymosan phagocytosis by primary microglia Vs BV2 cells – flow cytometry	Page 81

Fig. 3.14	Opsonisation- and dose- dependent increases in zymosan phagocytosis by BV2 cells – fluorescence microscopy	Page 82
Fig. 3.15	Nitric oxide production by primary and BV2 cells in response to LPS – dose and time responses	Page 84
Fig. 3.16	Dose-dependent cytokine production by primary and BV2 cells in response to LPS – TNF- α and IL-6 responses	Page 87
Fig. 3.17	Flow cytometric analysis of change in primary and BV2 cell surface markers in response to LPS – dose and time responses	Page 90
Fig. 3.18	Analysis of primary cell surface CD11b expression by immunocytochemistry – response to LPS over time	Page 92
Fig. 3.19	Confirmation of RNA integrity	Page 93
Fig. 3.20	Confirmation of PCR specificity	Page 93
Fig. 3.21	Induction of transcripts following microglial LPS treatment	Page 94
Fig. 3.22	Morphological change of primary microglia in response to LPS (i)	Page 95
Fig. 3.23	Morphological change of primary microglia in response to LPS (ii)	Page 96
Fig. 3.24	Flow cytometric analysis of change in microglial surface CD11b in response to increasing LPS concentration - pure Vs mixed CNS culture	Page 97
Fig. 4.1	The 24 integrin heterodimers in humans	Page 106
Fig. 4.2	Structure of the Leukocyte/ β 2 (CD11/CD18) Integrins	Page 107
Fig. 4.3	Signal transduction pathways of the β 2 integrins	Page 111
Fig. 4.4	Confirmation of iC3b Chain Structure	Page 116
Fig. 4.5	Specific immuno-detection of immobilised human iC3b: confirmation of identity and ligand binding capacity	Page 117
Fig. 4.6	Specific fluorescence/immuno-detection of fluid-phase iC3b-Fluorescein by immobilised rat anti-human iC3b mAb: confirmation of fluorescent-labelling and ligand binding capacity from fluid-phase	Page 119
Fig. 4.7	Assessment of iC3b-Fluorescein binding to BV2 cell CR3	Page 120
Fig. 4.8	Comparison of human and mouse C3 bioinformatic data	Page 121
Fig. 4.9	Charting C3-activation fragment deposition during NHS-opsonisation of zymosan particles	Page 125

Fig. 4.10	Assessment of CR3-mediated mouse microglial phagocytosis of NHS-opsonised and non-opsonised zymosan particles	Page 126
Fig. 4.11	Effects of fluid-phase iC3b on basal and LPS-activated microglial phenotype – surface markers and NO production	Page 128
Fig. 4.12	Charting C3-activation fragment deposition during mouse serum-opsonisation of zymosan particles	Page 130
Fig. 4.13	Assessment of the specific contributions of CR3 and C3 to opsonic and non-opsonic microglial zymosan phagocytosis	Page 131
Fig. 4.14	Impact of opsonic and non-opsonic zymosan exposure on microglial cytokine mRNA production—the role of zymosan borne iC3b	Page 133
Fig. 4.15	The effect of zymosan borne iC3b on microglial activation status — secreted effectors and surface markers	Page 135
Fig. 4.16	Specific binding of anti-rMOG mAbs to immobilised Ag	Page 137
Fig. 4.17	Specific detection of C3 activation fragments deposited on TC plastic: the effects of sensitisation via the classical pathway	Page 138
Fig. 4.18	C3-activation fragment deposition on TC plastic sensitised by Z4 mAb: effect on microglial phenotype — secreted effectors	Page 140
Fig. 4.19	C3-activation fragment deposition on TC plastic sensitised by Z4 mAb: effect on microglial phenotype — surface markers	Page 142
Fig. 4.20	C3-activation fragment deposition on non-sensitised TC plastic: effect on microglial phenotype — secreted effectors and surface markers	Page 144
Fig. 4.21	C3-activation fragment deposition on non-sensitised TC plastic: effect on primary microglial cell phenotype — morphology	Page 146
Fig. 4.22	C3-activation fragment deposition on non-sensitised TC plastic: effect on primary microglial cell phenotype — secreted effectors	Page 147
Fig. 4.23	C3-activation fragment deposition on non-sensitised TC plastic: effect on primary microglial cell phenotype — surface markers	Page 149
Fig. 5.1	Flow cytometric analysis of surface CD59 and Crry expression by WT, Crry KO and CD59 KO RBCs	Page 161
Fig. 5.2	Flow cytometric analysis of surface F4/80 Ag and Crry expression by WT and Crry KO primary microglia	Page 162
Fig. 5.3	Assessment of the <i>in vitro</i> Crry KO microglial phenotype	Page 163

Fig. 5.4	Activated C3 deposition and MAC formation on BV2 cells: development of assay of murine microglial C activation	Page 165
Fig. 5.5	C3-activation fragment deposition and MAC formation on Crry KO Vs WT primary microglial cells: human serum	Page 169
Fig. 5.6	C3-activation fragment deposition and viability of Crry KO Vs WT primary microglial cells in response to mouse serum incubation	Page 170
Fig. 5.7	Assessment of the <i>in vitro</i> Crry KO microglial phenotype in response to C3-activation fragment deposition resulting from sensitivity to autologous C activation	Page 172

List of Tables

Table 1.1	Component proteins of the C pathways	Page 3
Table 1.2	Regulatory proteins of the C pathways	Page 4
Table 1.3	Receptors for products of C activation	Page 4
Table 1.4	Physiological functions of the C System	Page 18
Table 2.1	Formulae of cell culture media	Page 41
Table 2.2	Formulae of gels and complex solutions utilised for SDS-PAGE and sample visualisation	Page 46
Table 2.3	Antibodies used in flow cytometry	Page 55
Table 2.4	Antibodies used in ICC	Page 57
Table 2.5	Formulation and thermocycling conditions for Rt reactions	Page 61
Table 2.6	qPCR thermal-cycling and fluorescence detection conditions	Page 62
Table 2.7	Primers used in qPCR	Page 63
Table 3.1	Flow cytometric analysis of microglial marker expression by primary and BV2 cells	Page 78
Table 3.2	Microglial cytokine levels in response to different LPS concentrations (i)	Page 85
Table 3.3	Microglial cytokine increases in response to different LPS concentrations (ii)	Page 85
Table 3.4	Microglial surface CD11b and C5aR expression in response to LPS – time course	Page 88
Table 3.5	Microglial surface CD11b and C5aR expression in response to LPS - dose response	Page 88
Table 3.6	BV2 transcriptional responses to LPS exposure	Page 94
Table 4.1	β 2/CD11:CD18 Integrins, their expression and ligands	Page 108

Abstract

The concept of microglial priming has developed through *in vivo* studies and is operationally defined as an exaggerated microglial production of soluble mediators (NO and cytokines e.g. IL-1 β , TNF- α , IL-6) following a pro-inflammatory activation event (e.g. LPS-treatment). In practice microglial priming predisposes the brain to degeneration through the promotion of inflammatory mechanisms. *In vivo* studies of Crry (a major murine cell-surface C3-regulator) KO mice previously identified a novel role for C in the induction of the primed microglial phenotype, implicating iC3b ligation of microglial CR3. The purpose of this study was to further investigate C-dependent microglial priming and its mechanism(s) through study of microglia in isolation *in vitro*.

Experiments using purified fluid-phase human iC3b failed to demonstrate any phenotypic effects of ligand exposure. Given the results of previous investigations concerning CR3 ligands, combined with the results of binding studies and sequence comparisons, it appears likely that, while still able to engage the cell-borne CR3, fluid-phase iC3b is incapable of exerting significant effects on the microglial phenotype.

Studies using Zymosan and C-fixing mAb-sensitised TC plastic as a means to generate ligands to investigate the consequences of microglial CR3 engagement by iC3b were confounded by the stimulatory effects of the C-activating agents (i.e. zymosan or mAb) which prevented attempts to dissect the effects of the isolated interaction. Nonetheless, specific effects were attributable to the C3-derived CR3 ligands generated, which dramatically and significantly reduced the pro-inflammatory responses evoked by the C-activating agents.

Investigations using C3-activation fragments immobilised on native (i.e. non-sensitised) TC plastic demonstrated phenotypic effects of microglial iC3b-CR3 ligation consistent with the previously reported mechanism of C-dependent microglial priming.

Experiments using cultured Crry KO microglia demonstrated increased sensitivity to autologous C activation. Phenotyping experiments, however, failed to show any consequence of Crry expression status, even when the intrinsic sensitivity of Crry KO cells to C3 activation and deposition was effected, thus mimicking the *in vivo* scenario (including the potential for iC3b ligation of CR3).

Data gathered from the several systems designed to ligate CR3 of microglial cells with C3-derived ligands highlight the broad range of potential cellular responses mediated by CR3 and emphasise the importance of context for the consequence of this interaction. In so doing, these data also

further evidence that under certain circumstances, iC3b-CR3 binding can induce a primed microglial phenotype.

1 Introduction

1.1 The Complement System

1.1.1 Components

The C system consists of a complex network of more than thirty interacting partners, comprising effector proteins found in the fluid-phase when inactivated, an array of cell membrane bound receptors, some of which possess important regulatory activity, along with a number of dedicated regulators present both on membranes and in the fluid phase (2, 5, 10-14). The system can be subdivided into discrete parts, with three defined activation pathways (antibody, alternative and lectin) converging on the key central component, C3, activation of which leads into the terminal pathway, concluding with the generation of a protein complex with the ability to form a pore in a target membrane (Table 1.1 – 1.3). To accomplish their defined role in the C system, many components possess catalytic activity; specifically the activators possess serine protease activity while the regulators catalyse Factor I activity and/or the decay of the convertases (10, 15-17). C is found in all body fluids, but the composition is best characterised in blood, with levels of individual components ranging widely. Unsurprisingly, the central and multifunctional component, C3 is most abundant with levels of $\sim 1.2\text{mg mL}^{-1}$ in human serum, constituting $\sim 1\%$ (by mass) of total protein. All told, C components make up $\sim 15\%$ of the total serum globulin fraction (2, 5, 15, 16). The C components are mainly produced by hepatocytes but other cell types such as monocytes and macrophages, epithelial cells, fibroblasts and dendritic cells also make important contributions (18, 19). The expression of the various receptors and regulators is cell type and context specific. Examples of well established cell-C receptor/regulator combinations include CR3 expression by phagocytes and CD59 expression by RBCs (14, 20). Through their various characteristic binding and functional (e.g. catalytic) domains the different groups of C components interact with triggering stimuli and each other, along with components of other biological systems, in multifaceted and complex ways to effect the system's functions (discussed in later sections).

Pathway/ Component	Structure	Function	Plasma Level
Classical pathway			
C1q	460 kDa collectin, six subunits each of three 25 kDa chains	Binds immobilized IgG/IgM to initiate the CP	150 mg/L
C1r	85 kDa single chain	In C1 complex, activates C1s	50 mg/L
C1s	85 kDa single chain	In C1 complex, cleaves C4/C2	50 mg/L
C4	S-S bonded heterotrimer, α , 97 kDa, β , 75 kDa, γ , 33 kDa	C4b fragment target-bound via thioester is the receptor for C2	500 mg/L
C2	100 kDa single chain	C2a fragment bound to C4b cleaves/activates C3	25 mg/L
Alternative pathway			
Factor B	110 kDa single chain, C2 homologue	Bb fragment bound to C3b cleaves and activates C3	200 mg/L
Factor D	25 kDa single chain protease	Cleaves factor B to activate	5 mg/L
Properdin	Oligomers of 53 kDa chain	Stabilizes the C3bBb complex	20 mg/L
Lectin pathway			
MBL	200–600 kDa collectin, two to six subunits each comprising three 32 kDa chains	Binds mannan sugars on pathogens to initiate the LP	0–5 mg/L (broad normal range)
Ficolin-1 (M-ficolin)	440 kDa lectin, 12 subunits each 36 kDa	Binds carbohydrate epitopes on pathogens to initiate the LP	0.05 mg/L
Ficolin-2 (L-ficolin)	420 kDa lectin, 12 subunits each 35 kDa	Binds carbohydrate epitopes on pathogens to initiate the LP	5 mg/L
Ficolin-3 (H-ficolin)	590 kDa lectin, 18 subunits each 3 kDa	Binds carbohydrate epitopes on pathogens to initiate the LP	5 mg/L
MASP-1	90 kDa single chain	Uncertain; in mouse, activates pro-fD to active fD	5 mg/L
MASP-2	74 kDa single chain	In complex with MBL or ficolin, cleaves C4/C2	0.4 mg/L
MASP-3	94 kDa single chain	Uncertain, perhaps as MASP-2	4 mg/L
MAp19 (s-MAP)	19 kDa single chain	Suggested MASP-2 inhibitor	0.2 mg/L
MAp44 (MAP-1)	44 kDa single chain	Suggested MASP-2 inhibitor	1.4 mg/L
Common			
C3	S-S bonded heterodimer, α , 110 kDa, β , 75 kDa	Central component in all pathways, C3b major opsonin	1200 mg/L
C5	S-S bonded heterodimer, α , 115 kDa, β , 75 kDa	Binds C6 to initiate TP, C5a major effector molecule	75 mg/L
Factor I	S-S linked heterodimer, heavy (50 kDa) and light (38 kDa) chains	Serine protease cleaves C3b/C4b in presence of cofactor	30 mg/L
Terminal pathway			
C6	110 kDa single chain	Binds C5b, C5b6 receives C7	50 mg/L
C7	100 kDa single chain	Binds C5b6, C5b-7 attaches to target cell	90 mg/L
C8	α (64 kDa) and γ (22 kDa) chains S-S linked, β chain (65 kDa) noncovalently associated	Binds C5b-7, C5b-8 receives C9	60 mg/L
C9	70 kDa single chain	Binds C5b-8 to form MAC	60 mg/L

CP, classical pathway; fD, factor D; Ig, immunoglobulin; LP, lectin pathway; MAC, membrane attack complex; MASP, mannan-binding lectin-associated serine protease; MBL, mannan-binding lectin; TP, terminal pathway.

Table 1.1: Component proteins of the C pathways [from Morgan, BP; Chapter 36: Complement (2)]

Regulator	Structure	Function	Plasma Level/ Cell Expression
Fluid phase			
C1 inhibitor	Single chain, 100 kDa, heavily glycosylated	Serine protease inhibitor binds and inactivates C1r, C1s, MASP-2, others	150 mg/L
Factor H	Single chain, 150 kDa, 20 SCRs	AP convertase decay accelerator and fl cofactor	300 mg/L
Factor H-like 1	Single chain, 42 kDa, seven SCRs	As for fH	10 mg/L
C4b binding protein	550 kDa oligomer comprising seven α chains (eight SCRs) and one β chain (three SCRs)*	CP convertase decay accelerator and fl cofactor	200 mg/L
Carboxypeptidase N	280 kDa dimer of heterodimers of 83 kDa and 55 kDa	Inactivates C3a/C5a by removing C-terminal Arg	30 mg/L
S protein/vitronectin	84 kDa single chain	Binds C5b67 in fluid phase to inhibit MAC formation	250 mg/L
Clusterin	70 kDa heterodimer of 35 kDa chains	Binds C5b67 in fluid phase to inhibit MAC formation	150 mg/L
Membrane-bound			
CR1/CD35	220 kDa single chain, 30 SCRs, [†] TM	CP/AP convertase decay accelerator and fl cofactor	RBC, WBC, renal, others
DAF/CD55	70 kDa single chain, four SCRs, GPI	CP/AP convertase decay accelerator	Broadly distributed
MCP/CD46	60 kDa, single chain, four SCRs, TM	CP/AP fl cofactor	Broad, absent from RBCs
CD59	20 kDa globular protein, four S-S bonds, heavy glycosylation, GPI	Binds C5b-8 on membrane to inhibit MAC formation	Broad, all blood cells, etc.

AP, alternative pathway; Arg, arginine; CP, classical pathway; DAF, decay accelerating factor; fH, factor H; fl, factor I; GPI, glycosyl phosphoinositol; LHR, long homologous repeat; MAC, membrane attack complex; MASP-2, mannan-binding lectin-associated serine protease-2; RBC, red blood cell; SCR, short consensus repeat; TM, transmembrane; WBC, white blood cell.

*Common isoform; other oligomers of C4bp, $\alpha7\beta0$, and $\alpha6\beta1$, are also found in plasma.

[†]Common isoform; forms comprising 37 SCRs (gain of LHR) and, rarely, 23 SCRs (loss of LHR) occur.

The fH-related proteins 1 to 5 are omitted for simplicity and because their functions are unconfirmed.

Table 1.2: Regulatory proteins of the C pathways [from Morgan, BP; Chapter 36: Complement (2)]

Receptor	Structure	Ligand; Function	Cell Expression
C3/C4/C5 fragment receptors			
CR1 (CD35)	TM, single chain, 30 SCRs	C3b/C4b; binds immune complexes; B-cell activation	RBC, WBC, FDC, renal, others
CR2 (CD21)	TM, single chain, 15 or 16 SCRs	iC3b/C3dg/C3d; sensitizes B cells for response to antigen	B cells, some T cells, FDC
CR3 (CD11b/CD18)	Integrin heterodimer, α 160 kDa, β 95 kDa, TM proteins	iC3b; phagocytic receptor, leukocyte migration	Myeloid cells, NK cells
CR4 (CD11c/CD18)	Integrin heterodimer, α 150 kDa, β 95 kDa, TM proteins	iC3b; phagocytic receptor, leukocyte migration	Myeloid cells, T cells, NK cells
CRlg	45 kDa single chain Ig super-family member	C3b/iC3b; phagocytic receptor	Tissue macrophages
C3a receptor (C3aR)	54 kDa heptaspan G protein-coupled receptor	C3a; activates cell responses	WBC, brain and renal cells, etc.
C5a receptor (CD88)	45 kDa heptaspan G protein-coupled receptor	C5a > C5adesArg; activates cell responses	Broadly expressed
C5L2	37 kDa heptaspan; G protein coupling uncertain	C5a/C5adesArg/C3a/C3adesArg; activates cell responses?	Broadly expressed
Receptors for C1q			
CR1 (CD35)	See above	C1q; uncertain	See above
C1qRp (CD93)	125 kDa single chain TM	C1q/MBL/SP-A; phagocytic receptor	Myeloid cells, endothelium
gC1qR	Tetramer 33 kDa subunits	C1q; phagocytic receptor	WBC, platelets
$\alpha2\beta1$ integrin	Integrin, heterodimer	C1q, collagens, laminins, decorin, etc.; cell activation	Broadly expressed

CR1, complement receptor 1; CR2, complement receptor 2; CR3, complement receptor 3; CR4, complement receptor 4; CRlg, complement receptor of the immunoglobulin superfamily; FDC, follicular dendritic cell; Ig, immunoglobulin; MBL, mannan-binding lectin; NK, natural killer; RBC, red blood cell; SCR, short consensus repeat; TM, transmembrane; WBC, white blood cell.

Table 1.3: Receptors for products of C activation [from Morgan, BP; Chapter 36: Complement (2)]

1.1.2 Activation

Activation of the multi-component C cascade is multifaceted and complex. This has arisen due to the diverse array of stimuli which can trigger activation and the many regulators which may modulate the process. During the activation process the recognition components of the distinct activation pathways engage their cognate molecular entities within the locality, triggering a cascade of protein-protein interactions occurring through enzymatic cleavage (along with enzymatic activity acquisition), conformational change, covalent association and complex formation events. The active fragments and complexes generated in this process interact with sequential system targets, receptors and regulators, to exert the effects of C (5, 10-12, 21).

C comprises three activation pathways (Fig. 1.1). Although the activation pathways of C converge, they each have distinct recognition and initiating components, the biochemical interactions of which have been studied intensively and are considered fairly well defined (17). The classical pathway was by far the earliest recognised (22, 23), followed by the alternative pathway (24-27) and finally the lectin pathway (28). Since the classical pathway is largely dependent on antibody for activation, it cannot be considered a true innate immune effector response. Indeed, the emergence of the classical pathway appears to have been closely if not directly linked to the evolution of adaptive immunity (29-33). The alternative and lectin pathways, however, are triggered independently of any adaptive immune entity and are therefore true innate immune mechanisms.

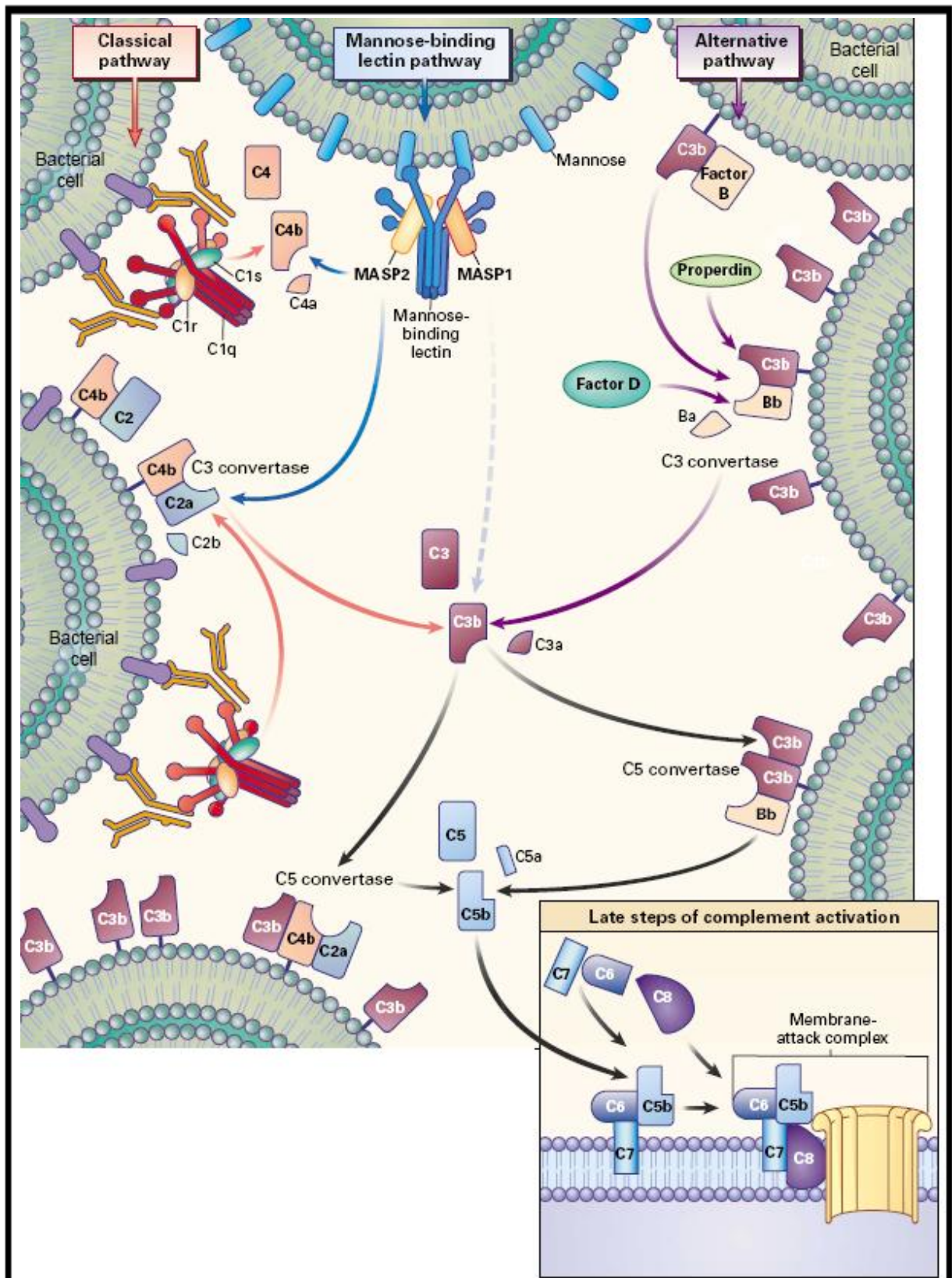


Fig. 1.1: The C system. Figure illustrating the 3 complement activation pathways and their interactions, including convergence and amplification at the level of C3 and formation of the lytic complement multi-protein complex, the Membrane Attack Complex (MAC) [from (5)].

1.1.2.1 Classical Pathway

As has been known since the work of Bordet in 1894, the chief trigger of the classical pathway is antibody-antigen complex (22, 23). C1, the first component of the classical pathway, is a large multi-protein complex of C1q (460kD) and a heterotetrameric complex of C1r₂S₂ (360kD) which is formed in the sequence C1s-C1r-C1r-C1s. C1q itself is formed from three highly homologous polypeptide chains derived from three closely linked genes (34). Six copies of each C1q subunit are present and one of each combine in alignment to form a total of six trimeric strands, each with characteristic C-terminal globular head (~135aa) and N-terminal collagen-like (~80aa) regions. The A and B chains within each trimer associate through disulphide bonds formed by half-cysteine residues at their N-termini, and the C chain in each trimer associates in the same way with the C chain in an adjacent strand, forming a structural unit ABC-CBA. These then associate *via* strong non-covalent interactions through their central fibril-like portions to form the hexameric C1q molecule with its characteristic “bunch of tulips” structure (Fig.1.1). C1r and C1s associate in a Ca²⁺ dependent manner to form a pro-enzyme complex (C1r₂C1s₂) which binds between the collagenous central region of the assembled C1q, which acts as a scaffold. C1 fulfils the role of immune complex recognition through the six globular heads of C1q and that of first enzymatic cleavage events through C1r₂C1s₂ (13, 35-37).

C1 is able to complex with antigen-bound IgG and IgM *via* its globular heads and upon doing so is thought to undergo a conformational change in the C1q collagen domain leading to the activation of the pro-enzyme complex. The C1r subunits first cleave each other and then their neighbouring C1s molecules, which are then able to extend away from the C1q scaffolding to act on C4 and C2. C4 is cleaved to C4a which is released and the larger C4b molecule which, similarly to newly cleaved/nascent C3b, possesses a metastable binding site containing a thioester. In the same manner as C3b, C4b binds to locally available hydroxyl and amino groups and can thus become covalently attached to proximal/nearby surfaces. Following its binding to C4b in a metal cation dependant manner, C2 can be cleaved by active C1s subunits in adjacent C1 complexes releasing the C2b fragment and forming the classical pathway C3 convertase, C4bC2a (2, 15, 38).

Complexed antibody is the archetypical classical C pathway activator, but it is well known that different isotypes (i.e. IgA, IgD, IgE, etc.) and sub-classes (i.e. IgG₁, IgG₂, etc.) have different classical C-activating potential. For example, IgA and IgE are considered non-activating, whereas certain IgG subclasses and IgM are classical pathway activators; in humans IgG₁ and IgG₃ are potent activators whereas IgG₄ is not. Additionally, the density of complexed antibody is also of major significance, with greater density leading to more efficient activation. C1 initiates the classical cascade through binding to Fc portions of complexed antibodies *via* the six globular heads of C1q and it is believed that multivalent C1q Fc binding leads to more efficient activation

of the C1r₂C1s₂ pro-enzyme (14, 39-41). Recent studies show that mutations in Fc domains which lead to formation of hexameric IgG complexes drastically enhance the efficiency of classical C activation (42-44). Indeed, it is known that per mole, IgM is a far more efficient activator because of its multiple Fc portions which act as a pre-assembled array for the multiple globular heads of C1q to simultaneously engage (14).

Further to C1, C4 and C2, another component unique to the classical pathway is the Serpin family member, C1Inh, which displaces the C1r₂C1s₂ enzyme complex from the activated C1 complex, exposing binding sites for C1q receptors in the N-terminal collagenous domains of immune complex-bound C1q. Since C1q is still able to engage its ligands *via* its globular heads, this process leads to acquisition of opsonic functionality (13, 15, 45). In addition to this non-C activating (opsonic) function of C1q, another non-classical activity of C1 is C activation through binding to non-antibody ligands, such as CRP, SAP and certain microbial ligands (2, 12, 14, 46).

1.1.2.2 Alternative Pathway

The AP was originally identified by Pillemer through the observation that C3 and the terminal components activated on yeast cell walls without consumption of the classical pathway components, in a process that involved the newly identified properdin (named from the Latin *perdere*, to destroy) (24-27).

The sequence of events in the AP activation cascade is as follows: C3 exists in a dynamic state, the majority existing as the native C3 form but a small fraction existing as C3 which has been hydrolysed at the intramolecular thioester, known as C3(H₂O) (47-49) (sometimes called Pangburn's molecule). Although uncleaved, this C3(H₂O) has all the functional activity of C3b, being subject to factor I mediated degradation and capable of binding to CR1 (50). Importantly, C3(H₂O) is able to bind factor B in a metal cation dependant manner and then be cleaved by factor D to release Ba and produce a C3(H₂O)Bb complex which, although unstable, is able to briefly act as a C3 convertase (47-50). Indeed, the instability of this C3(H₂O)Bb convertase confounded characterisation attempts, until it was found that coordination of the C3-factor B components by nickel rather than magnesium (the physiological element) ions produced a far more stable convertase (47-49, 51). Metastable C3b produced by the convertases can, with some preference based on physicochemistry, become covalently attached to surfaces *via* its thioester, or is hydrolysed in the fluid phase (52). If this C3b is generated in a locality in which there is insufficient negative regulation (through the combined actions of C3 binding proteins and factor I) then the active C3b is able to persist for long enough to complex with factor B which is then subject to cleavage by factor D, forming the amplification C3 convertase of the AP (C3bBb). This enzyme is unstable, but its half-life can be extended significantly through stabilisation by

properdin. A key feature of this amplification convertase is that it can be formed from C3b produced by any of the activating pathways i.e. by the C4bC2a convertases of the classical and lectin pathways (not just C3[H₂O]Bb), and therefore, represents the actual convergence point between the three recognised activation pathways. The concept of the AP being triggered as a consequence of conversion of C3 to C3(H₂O) and the subsequent sequence of events described above, as proposed by Lachmann, Pangburn and Müller-Eberhard, is known as the “tick-over” theory (13, 49, 53-55).

Thus, unlike the other activation pathways, the AP has no true recognition element since (in the absence of other activation pathways) its initiation is reliant on a spontaneous, non-specific process i.e. hydrolysis of the intramolecular thioester. In this regard it could be said that AP functions, not through activation in response to a certain molecular trigger, rather its default mode is low grade activation which is allowed to proceed and amplify in the absence of sufficient regulation. Therefore, the classical and lectin pathways could be considered true recognition pathways, whereas the AP could be considered a pure activation pathway. However, the vast majority of the activation products produced by the AP are generated *via* the amplification loop, which is reliant on C3b formation (13). Since C3b is known to have variable affinity for different molecular entities, which results in different levels of C3b deposition on various target surfaces (and subsequently different rates of AP amplification) (56), it could be argued that C3b acts as the recognition molecule of the AP. Indeed, the AP does possess some capacity for recognition of self vs. non-self, since it is well known that foreign microbial molecules and particles such as zymosan can activate the AP (27). This capacity to activate on “foreign” surfaces is underlined in model haemolytic assays by the documented activation of the AP of one species on the erythrocytes of another (13).

Several groups of AP activators exist: particulate polysaccharides (e.g. inulin, β -glucan/zymosan); some cell types (e.g. rabbit erythrocytes, pneumococcal cells); immune complex precipitates (13, 16, 20, 27, 57, 58). Despite little obvious resemblance in chemical and fine structural detail, the particulate nature of these activators is notable. Indeed, soluble inulin (polysaccharide) is completely devoid of activating capacity (16, 20). If factor B is the alternative pathway equivalent of C2, then C3 is the parallel of C4 and factor D is the partial equivalent of C1. Properdin is required for efficient AP activation by stabilising the AP convertases (56, 59), but has no homologue in the other pathways, being the only known positive regulator of C activation. Factor D is by far the smallest of the C activation components (25kD) and can thus be excluded from serum by gel filtration, while all the other C components are retained, providing a means to eliminate AP activity (13, 16, 60, 61). Additionally, since formation of the C1q₂S₂ and C3bB complexes is physiologically dependant on Ca²⁺ and Mg²⁺ ions, respectively, it is possible to

selectively inactivate the classical pathway by specific Ca^{2+} chelation with EGTA or to inhibit all activation pathways with EDTA (13, 16).

1.1.2.3 Lectin Pathway

Lectins are carbohydrate specific binding proteins and are ubiquitous, being found in plants, animals and microbes. The term derives from the Latin, “*legere*”, meaning to read or select. Lectins are found both intra- and extra- cellularly and perform diverse roles in animals, including protein folding (e.g. calnexin) and mediating intercellular and cell-matrix interactions (e.g. selectins) (62). Through MBL and ficolins, this also extends to activation of C. MBL is an example of a collectin, a collagenous lectin with a C-type (Ca dependant) CRD, other examples of which include the surfactant proteins SP-A and SP-D which play an important role in pulmonary innate immunity. Ficolins (fibrinogen-like collagen-like lectins) possess a collagenous domain and a fibrinogen like domain, which displays homology to the C-terminal portions of the fibrinogen β and γ chains, in place of a CRD. Their classification as lectins is controversial since the fibrinogen (ligand binding domain) is specific for acetyl groups on non-carbohydrates as well as carbohydrates, and concerning the latter, the binding isn’t primarily dependent on the sugar ring . However, many of their natural ligands have carbohydrate moieties and they have similar higher order structures and functional properties to lectins (63). In humans there is a single MBL protein arising from a single gene, whereas in mice there are two forms, MBL-A and MBL-C. In humans there are three ficolins, H, L and M, whereas mice have two forms, A and B. MBL and ficolins H and L are produced in the liver and secreted into the circulation, whereas ficolins L and M are housed in secretory granules of neutrophils and macrophages in the lung. MBL polypeptides have a structure consisting of an N-terminal cysteine rich sequence, a collagen-like domain, an α -helical coiled coil domain and a C-terminal CRD, which is reminiscent of that of C1q, with the CRD replacing the globular (head) domain. Ficolin polypeptides also possess a similar structure with the fibrinogen-like domain replacing the CRD. Similarly to C1q, the MBL and ficolin polypeptides assemble into trimeric subunits *via* disulphide bonds formed in the N-terminal domain, along with hydrophobic interactions. Again, similarly to C1q, these subunits then assemble into higher order/multimeric structures, which possess functional activity, through their collagen-like stalks/fibrils, forming characteristic “bouquet” like structures reminiscent of the C1q “bunch of tulips” structure. However, unlike C1q which forms hexameric structures, the lectins are known to form structures containing variable numbers of subunits which are thought to possess different functional activities. MBL and the ficolins circulate in complex with serine proteases known as MASP1-MASP3, originally identified through their binding to MBL (64), along with non-protease molecules derived from the MASP genes, known as sMAP/MAP19 and MAP-1. Upon lectin binding conformational changes lead to activation of the MASPs which are then able to cleave C4 and C2

in the same manner as the activated C1 complex, thus initiating C activation in a cascade which converges with the classical pathway with the formation of the C4bC2a C3 convertase (14, 17, 62, 65-67). The precise specificities and functions of the MASPs and related proteins are still being characterised (17, 62).

MBL deficiency is relatively common and is associated with a defect in C3-dependent opsonic phagocytosis of yeast and several mutations have been identified in exon 1 and the promotor of the MBL gene which account for this (11, 68-70). Polymorphisms in the gene coding for ficolin L (FCN2) are associated with variable serum levels and ligand binding (62). The variable distribution of ficolins and the formation of lectin-protein complexes with enzymatic partners of different activities/specificities, along with non-enzymatic partners, illustrate the importance of regulated activation in the lectin pathway and is suggestive of distinct biological roles.

1.1.2.4 C3

Each of the three distinct C activation pathways converge on the enzymatic cleavage of C3 (187kD) at the N-terminal α chain to form the small (9kD, 77 amino acid) C3a anaphylatoxin fragment and C3b. As a consequence of this cleavage step the major C3b portion of the native C3 molecule undergoes significant conformational change with important functional consequences. Binding sites for other C components, including activators, receptors and regulators are formed, and importantly, an intramolecular metastable surface binding/activation site, which includes a thioester bond, becomes exposed. If C3b is formed in the vicinity of suitable molecular entities on an activating surface (e.g. sugar hydroxyl or amine [polarised] groups on microbial cell walls) it can become covalently attached to them *via* nucleophilic attack on the carbonyl group of the thioester, also resulting in the formation of a free sulfhydryl. If metastable C3b does not attach to a surface the thioester is subject to fluid phase hydrolysis, stabilising the reactive intermediate. Binding studies indicate the metastable active/binding site of C3 encompasses more than just the thioester moiety. Kinetic studies demonstrate that within minutes of C activation, millions of C3b molecules can be deposited on an activating cell membrane (11, 13-15, 46).

1.1.2.5 Terminal Pathway

With the formation of the C3 convertase by any activation pathway comes the production of C3b. In addition to the labile thioester-containing active site which permits it to perform its opsonic role, C3b has binding sites which permit it to combine with the C3 convertases (C4bC2a and C3bBb) shifting the specificity of the enzymes to C5, thus forming the C5 convertases (C4bC2aC3b and C3bBbC3b) and initiating the terminal pathway by C5b production through C5 cleavage (52).

The reaction cascade of the terminal pathway can be summarised as the molecular fusion of the terminal components (C5b-C9), with the ability to insert into cell membranes, through alterations

in reactant physicochemistry acquired *via* conformational changes, produced during sequential interactions. If the pathway is activated on a membrane, the assembling C5b-9 complex can penetrate and is capable of spanning the membrane, forming a lytic pore (diameter: up to ~100 Å). The terminal is unique amongst the C pathways since after the cleavage of C5 no further enzymatic cleavage events take place, all further activation occurring through binding to newly exposed sites and subsequent conformational change exposing further potential sites for the next protein to bind to (11, 13-15, 46).

The C5 convertases cleave C5 into the small, potent anaphylatoxin fragment, C5a, and the larger C5b. Upon formation of C5b, similarly to the homologous C3b and C4b, significant conformational changes occur within the molecule, pre-dominantly in the α chain, with the β chain forming a stable ring-like structure. Unlike C3, C4 and other members of the α 2M family, C5 lacks the prototypical thioester within its TED and thus C5b isn't able to covalently bind to target surfaces in the same way, thereby stabilising its active conformation. Indeed, despite similarities in adjacent domains, the final position of the TED in C5b is distinctly different to that in C3b. However, the structural changes in C5 do produce a labile-binding site (half-life: 2 mins) for the next component (C6), which if not engaged, decays irreversibly to a form incapable of C6 binding. The active conformation of the nascent C5b is captured by C6 binding. C6 interfaces predominantly in its C-terminal region, which undergoes major rearrangement, in contrast with the N-terminal region containing the "core" domain region common to C6-C9, which is highly similar to that of free C6. Indeed, the two putative transmembrane segments located in the MACPF domain of this core region remain loosely folded on the central β sheet (also in the MACPF domain) suggestive of a pre-membrane insertion state, which is consistent with the soluble nature of C5b6. Unlike the other terminal components, C7 also shares the C-terminal domains of C6 which, similarly to C6, mediate binding of C7 to C5b, which aligns the MACPF domains of C6 and C7. Formation of the C5b-7 complex also leads to rearrangement of the TMS regions which represents a hydrophilic-amphiphilic transition causing separation from the parent C5 convertase and permitting the binding of the C5b-7 complex to available surface phospholipids in target membranes. Conformational change as a result of C5b-7 formation also generates a C8 binding site. The C8 β is known to bind to C5b and subsequent alignment of the C8 β and C8 α MACPF domains with those of C7 and C6 relocates C8 γ , which is thought to then stabilise the complex. Bound C8 anchors the complex into target membranes *via* its α chain and is now able to recruit C9, the association of which results in lytic activity. It is thought that C8 γ may block C9 recruitment before its relocation as a result of C5b-8 formation, thus preventing C9 polymerisation before C activation. Up to ~15 C9 molecules may be incorporated into the complex, in which case it takes on a circular/ring structure which appears identical to poly(C9)

under electron microscopy, a complex produced when C9 is incubated with metal ions or subject to mild proteolysis (11, 13-15, 46, 71).

C6 – C9 are related proteins which all share structural domains (72). It is unclear whether the acquisition of new domains by the most basic component (C9), deletion of existing domains from the most complex component (C6), or a combination of addition and deletion of domains to an intermediate component is responsible for their generation (46).

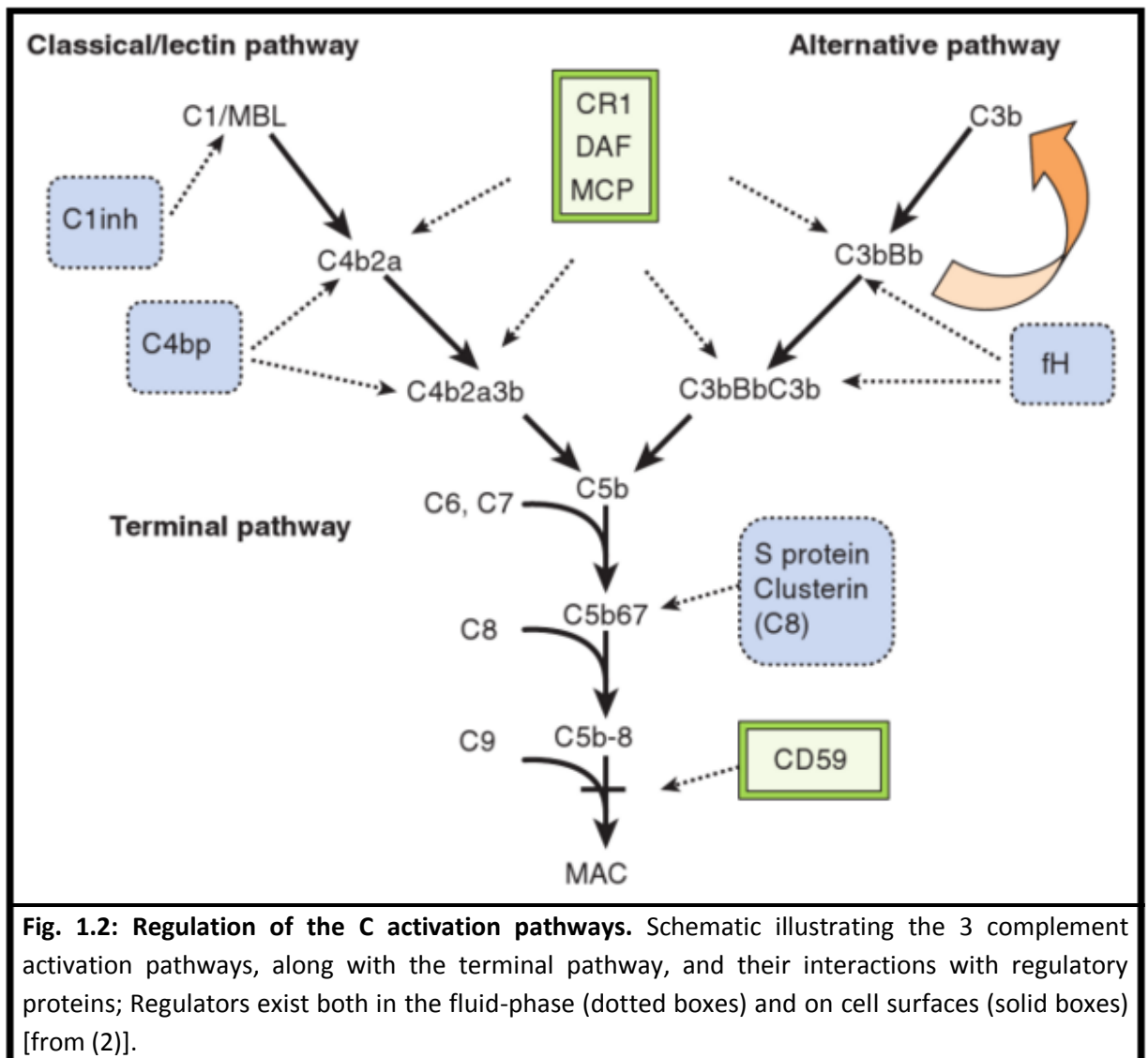
The existence of the terminal lytic pathway of C has been appreciated since the late 19th century and much of the early research on C and immunology as a whole made use of assays which depend on its function (16, 20, 22). Indeed, a great deal of study has been conducted on the biology of the terminal pathway components. Nonetheless, the fact that the pathological consequences of terminal component deficiency are limited to predisposition to Neisserial infections suggests that the MAC has limited biological function (73). However, the presence of specific regulators to prevent its aberrant activity (11) and the dramatic results of their absence, particularly in the case of PNH, illustrate its potency as a destructive agent (73).

1.1.3 Regulation

C activation can be considered the default mode of the system as C is constantly activated through the tick-over and amplification mechanism of the alternative pathway. Indeed, an isotonic 37°C solution of C components will spontaneously activate *via* the alternative pathway until activity decays (13, 56, 59). Given the powerful inflammatory effects of the anaphylatoxins, the directly damaging effects of the MAC, and the adhesive, opsonic and signalling capacity of the C3/C4 activation fragments, along with roles in other non-immune processes, tight, finely controlled C regulation is of paramount importance to avoid pathological consequences to self tissues. Furthermore, due to the default nature of activation, a lack of regulation can rapidly lead to the exhaustion of C, as exemplified by the effects of C3f (74), rendering the individual susceptible to infection and immune complex disease (73).

Regulation is intrinsic to C activation in that the convertases and the metastable binding sites of the activated TED containing components (i.e. C3b and C4b) have relatively short half-lives, decaying quite rapidly. This is important in preventing prolonged and off-target activation (75). Nonetheless, the presence of C regulatory proteins is essential to prevent the default activation of C damaging self and thus, roughly one third of C components possess regulatory activity. C regulators are present in the fluid phase and on cell surface. Through mechanisms such as alternative splicing and gene duplication, some have both membrane bound and soluble forms (e.g. mouse DAF, CR1). Regulators can be dedicated solely to C inhibition (e.g. C4BP, fI) or also possess adhesion/receptor activity (e.g. CR1, CR2) for C fragments. The regulatory action of the

RCA family members is characterised by the ability to catalyse the factor-I mediated decay of C3b and C4b, thus preventing the formation of more convertases, and/or the ability to accelerate the dissociation and prevent the formation of the convertases through binding to C3b/C4b and inhibiting their interaction with convertase components. Through the actions of the RCA family members and a number of other regulator components (e.g. fI, C1Inh, properdin, CD59), C activation is controlled at virtually all steps in the cascade, providing robust and fine control of the reaction (2, 11) (Fig. 1.2).



1.1.3.1 Fluid-Phase Regulation

Soluble regulators control activation in the fluid phase and include C4BP, factors I and H, properdin and C1Inh. Mouse DAF, which in humans is found solely as a GPI-anchored form, also exists as a secreted molecule (76). Through binding and stabilising the alternative pathway

convertases, the oligomeric protein properdin has unique status as the only known positive regulator of C activation (77).

C4BP is a large (570kD) glycoprotein with a plasma concentration of $\sim 200\mu\text{g mL}^{-1}$, formed of multiple copies of α subunit and a single β subunit derived from the C4bp α and β genes (respectively) within the RCA cluster (11, 15). C4BP primarily binds C4b and acts as a cofactor for its cleavage by factor I to C4c and C4d, which are believed to be inactive. Through its binding to C4b, C4BP also prevents formation of the C4bC2a convertase and accelerates decay of established convertases (15). C4BP is thought to be the main inhibitor of the classical and lectin pathways. C4BP forms a high affinity complex with vitamin-k dependent protein S (also known as S-protein or vitronectin; see below) in the plasma (78).

Factor I (88kD) is a key serine protease regulator of C which processes C3b and C4b to products which can no longer form the convertases (iC3b and iC4b, respectively) (79). Thus factor I has regulatory activity in all three activation pathways. Factor I cleaves the α' chains of C3b and C4b to form products with smaller and larger α' chain fragments held together by intra-chain disulphide bonds. Factor I then further cleaves these products (iC3b and iC4b) between the intra α chain disulphide bonds to produce the fragments, C3c and C4c, together with the smaller fragments, C3d and C4d (which contain the TEDs). If the C3b/C4b precursors were bound to a surface prior to the factor I activity, the second cleavage step leaves the smaller C3d/C4d TED-containing products bound to the surface. In the case of C3 degradation products, factor I mediated degradation results in the acquisition of new specificity as C receptor ligands (80). Factor I cleavage is dependent on the catalytic activity of a cofactor which is provided by one of several other C regulators such as MCP/CD46, C4BP, factor H, CR1, CR2 and Crry. However, only the membrane bound C regulators CR1 and Crry (in rodents) are known to catalyse the second cleavage event and are therefore essential in the formation of C3d, the ligand for CR2 (11), which has important functions in adaptive immunity (as discussed below).

C1Inh, a serpin family member, inhibits the serine proteases of the classical pathway by displacing them from the active C1 complex (15). This process has been proposed to expose binding sites in the ligated C1q which enable it to function as an opsonin. Through displacement of the serine proteases which act on C4 and C2, C1Inh prevents formation of the C4bC2a convertase and thereby shuts down the classical pathway.

Other, perhaps lesser known soluble regulators include clusterin, otherwise known as apolipoprotein J, and S-protein, otherwise known as vitronectin, which have been described as 'membrane mimics'. This lipid membrane-like structure is thought to underlie the role of these proteins in binding to off-target assembling terminal components which fail to insert into cell

membranes. Since it is upon the insertion of C7 into the nascent C5b6 complex that the assembling TCC becomes lipophilic, it is at this stage where binding by the soluble regulators is initiated resulting in the formation of non-lytic soluble C5b-9. Structural studies illustrate that the regulated soluble C5b-9 complex has a butterfly-like structural element formed from clusterin and S-protein which is proposed to inhibit membrane binding by blocking TCC hydrophobic residues and prevent C9 oligomerisation by capping the terminal C8/C9, thus inhibiting MAC activity (71). It has been demonstrated that removal of clusterin and S-protein by proteolysis or detergents restores membrane binding ability (81, 82).

Some of the soluble C regulators are known to have other functions. For example, S-protein is known to have a vitamin-K dependent anti-coagulation role and C1Inh also inhibits serine proteases of the kininogen system. This is in fact the main cause of clinical consequences in the case of C1Inh deficiency where elevated bradykinin production leads to HAE attacks (83).

1.1.3.2 Regulation on Surfaces/Membranes

Host cells are protected from inadvertent C attack by the presence of a number of regulatory proteins expressed on the cell surface. These have evolved as integral transmembrane and/or GPI anchored proteins. These regulators control C in similar ways to the fluid phase equivalents, albeit with some differences in the fine details. Importantly, many of the membrane localised C regulators, due to their intrinsic ability to bind C-activation fragments, have roles in immune adherence. Furthermore, many of the membrane bound C regulators have some role in cell signalling. For example, in addition to possessing decay and cofactor activity, CR1, which is widely expressed on myeloid cells, is able to mediate phagocytosis of the particle on which its C ligand is bound. CR1 expressed on human erythrocytes mediates the transport of C opsonised immune complexes to phagocytes for elimination while also catalysing the cleavage of C3b to iC3b (84). In mice Crry, plays a similar role in immune adherence of immune complexes to RBCs (85-87). CR2, expressed on B cells, follicular dendritic cells and some T cells, has weak co-factor activity but also plays a key role in control of adaptive immune responses (87). Examples of membrane bound C regulators include DAF, CR1, CR2, Crry (in rodents), MCP and CD59, with all but the latter being formed of variable numbers of SCR domains (11, 84). In humans, the terminal pathway regulator CD59 appears to be particularly important in preventing C mediated damage to self by binding C8 in the C5b-8 complex and blocking C9 incorporation, thereby preventing MAC formation. In PNH a defect in GPI anchoring leads to deficiency of CD59, among other proteins, on RBCs and it is CD59 deficiency in particular which is believed to be responsible for the C mediated intravascular haemolysis and thrombosis, and subsequent pathological sequelae, which characterise the disease (73). The critical role of CD59 in protection is underlined by the efficacy of the only current effective treatment for the disease: eculizumab is a C5 blocking mAb which effectively

inhibits the generation of the MAC through the terminal pathway (88-90). Additionally, disorders involving primary CD59 deficiency are known to feature neurological impairment (along with intravascular haemolysis and thrombosis), highlighting the importance of terminal pathway regulation on multiple cell types (91).

1.1.4 Functions/Roles

Reflecting the intricacy of the system, C has multifaceted and complex functions (Table 1.4). This is perhaps also unsurprising given the evolutionary ancient nature of C. The C system is classically considered a key humoral effector of innate immunity, which functions to protect against infection (5). Indeed, analogous functions for the C homologues in members of ancient/distant phylogenetic groups such as the sea-urchin (a nervous system-lacking deuterostome invertebrate) (33) illustrate that innate protection against infection was an/the original function of C in evolution. However, it has long been known that C has important roles in other immune-related processes (92-94) and in more recent times it has become clear that C also has key roles in many non-immune and/or destructive activities (95, 96). The importance of C in normal physiology is illustrated in patients with deficiencies of the activation components who, depending on the exact component, are predisposed to bacterial infections and immune complex diseases. Furthermore, the dramatic pathophysiological consequences of aberrant C activation in states such as regulator deficiency and antibody-mediated autoimmunity illustrate the potency of the system's activities (73, 91, 97, 98).

ACTIVITY	COMPLEMENT PROTEIN RESPONSIBLE FOR ACTIVITY
<p>Host defence against infection and waste disposal (immune-complexes; apoptotic & necrotic cells)</p> <p>Opsonization Chemotaxis and activation of leukocytes Lysis of bacteria and cells</p>	<p>Covalently bound fragments of C3 and C4 Anaphylatoxins (C5a, C3a, and C4a); anaphylatoxin receptors on leukocytes Membrane-attack complex (C5b–C9)</p>
<p>Interface between innate and adaptive immunity</p> <p>Augmentation of antibody responses Enhancement of immunologic memory</p>	<p>C3b and C4b bound to immune complexes and to antigen; C3 receptors on B cells and antigen-presenting cells C3b and C4b bound to immune complexes and to antigen; C3 receptors on follicular dendritic cells</p>

Table 1.4: Physiological functions of the C system [adapted from (5)]

1.1.4.1 Opsonisation of Targets

C activation on a surface leads to the deposition of C3-activation fragments (C3b, iC3b, C3dg) on that surface *via* the thioester-containing metastable site generated upon C3 cleavage by a convertase, and millions of C3-derived molecules can be deposited on a cell-sized target with efficient activation (13, 15, 16). Bound C3 fragments “tag” the material to which they are anchored as being a phagocytic target for cells bearing the appropriate receptors, and they are therefore known as opsonins (16, 99), derived from ancient Greek, meaning “to prepare for ingestion”. The cognate receptors for the C3-activation fragments, C3b, iC3b and C3dg are CR1, CR3 and CR4, and CR2, respectively (16, 100). Additionally, these receptors also possess some affinity for C4b (87), which is deposited onto activating surfaces *via* the classical and lectin pathways (100). With the exception of CR2 which is expressed mainly by B and T cells, these receptors are widely expressed by leukocytes and some other cell types (e.g. human CR1 by erythrocytes). Additionally, CR1g is expressed by tissue macrophages and binds both C3b and iC3b (16, 100). These receptors are integral transmembrane molecules possessing cytoplasmic domains which can associate with various intracellular mediators (e.g. kinases and phosphatases) and structural components (e.g. the cytoskeleton), and are thus able to function in cell signalling.

Although the fine details of the signalling mechanisms are poorly defined, the various C receptors mediate phagocytosis of C opsonised material through this process (101, 102). Furthermore, in similar fashion to some antibodies, it is thought that C1q and MBL may act as opsonins directly without the requirement for downstream C activation and C3/C4-fragment deposition (103-105). However, the receptors which mediate such activity remain controversial, with many of the original C1q receptors (e.g. cC1qR, gC1qR) now linked chiefly with other functions (36, 106).

In vivo: the fact that MBL deficiency causes a deficiency in yeast opsonic phagocytosis and predisposes to microbial infections illustrates the importance of this pathway in the clearance of foreign material (11, 63, 70). C activation and opsonic-fragment deposition occurs on foreign (microbial) material as a key part of infection control, but also on endogenous materials such as immune complexes and apoptotic cells as a major homeostatic mechanism. Indeed, the rapid clearance of immune complexes from the circulation, essential in preventing their pathological accumulation, precipitation and deposition in numerous tissues, is accomplished through C opsonisation (17, 107). Opsonised immune complexes bind to erythrocyte CR1 and are subsequently transported to the liver and spleen, where they are transferred to phagocytes which also express C receptors and Fc receptors. Deficiency of classical pathway components or C3 both predispose to derangement of immune complex-handling along with susceptibility to microbial infections, illustrating the importance of C1q in the recognition of complexed antigen and the central role of C3 in C opsonic processes (5, 17, 73, 107-109).

1.1.4.2 Induction of Inflammation via Anaphylatoxin Production

Along with the opsonic sub-components and the lytic TCC, C activation results in the production of the small (10kD; ~75 aa) hydrophilic α helical anaphylatoxin fragments, which have a potency hierarchy of C5a>C3a>C4a (16, 110). A minimum of ~30% sequence identity exists between anaphylatoxins within or between species (human, mouse, rat, pig, cow), but there is more similarity between the same peptide in different species than the different peptides in the same species. Thirteen conserved amino acids exist, six of which are cysteines and form intrachain disulphide bonds, thereby stabilising the structure (16). The C-terminal pentapeptide sequence (LGLAR) of C3a has been conserved in each species examined to date and it has long been known that a synthetic peptide of this sequence is sufficient to illicit C3a activity (13). The anaphylatoxins bind to 7 TM-GPCRs present on numerous cell types to produce dramatic but distinct tissue effects. Anaphylatoxin signalling results in smooth muscle cell contraction and release of histamine from basophils and mast cells to mediate the characteristic activity of increasing vascular permeability. C5a is also a potent chemotactic factor which acts to draw neutrophils and other leukocytes to site of acute inflammation (13, 100). Limited, compartmentalised anaphylatoxin production results in a localised inflammatory response, which contributes to the

resolution of the initial trigger. However when robust, acute and disseminated C activation occurs, excessive systemic anaphylatoxin activity results in a shock-like reaction, first observed experimentally by the French physiologist Francois Magendie in 1837 (20, 111). Anaphylatoxin activity is lost upon cleavage of the C-terminal arginine by carboxypeptidase enzymes (N, B), resulting in the production of des-arginated forms (e.g. C3a *des-arg*). Originally believed to be biologically inactive, it is now known the des-arginated products can mediate new effects through signalling mechanism believed to involve the same receptors used by the intact anaphylatoxins (13, 100).

1.1.4.3 Direct Lysis of Targets via MAC Formation

The ability to lyse cellular targets was the very first action of C to be recognised (22) and it has subsequently been established that this is the consequence of the sequential assembly of the C5b-9 components, although the precise molecular mechanism which leads to cell death remains unclear. Early theories on the mechanism of MAC mediated cytotoxicity included the suggestion that it was an enzyme, based largely on the enzymatic nature of the preceding reaction steps, and that it was a detergent (16). However, it has subsequently been demonstrated that the MAC forms membrane pores of varying size (112, 113) which are similar to the immune (perforin)-pores of cytotoxic T-cells and bacterial CDCs (114). It has been known since the 1970s that a MAC containing a single C9 is sufficient to lyse erythrocytes, whereas at-least three copies of C9 are required for bactericidal activity, illustrating, in-addition to the requirement of C9 for lytic action, MAC's heterogenous composition and relative potency (2, 16, 115, 116). Freeze-fracture electron microscopy has convincingly demonstrated that C9 is the only MAC component which penetrates beyond the outer leaflet of the lipid bilayer. Prior to C9 insertion, the putative amphiphilic α helices of C6-C8 remain parallel with the target membrane surface, but upon the insertion of multiple copies of C9, those of the earlier components also insert into the target membrane to form the β barrel pore. Cell death is primarily believed to be a consequence of disruption of the selective permeability of the membrane, leading to dissipation of cytosolic solutes and cellular energy, and in some cases colloid osmotic lysis (117-119). In nucleated eukaryotic cells (which actively resist MAC-mediated disruption), calcium influx can cause secondary organelle (mitochondrial) dysfunction leading to the induction of cell death pathways (2).

Despite strong evidence for lytic activity as a consequence of pore formation, it is important to note the physicochemical effects of the actual presence of the MAC components in the membrane, which are intrinsically disruptive to the lipid bilayer. Indeed, it has been shown that, independently of any changes in solutes, the presence of MAC components in membranes has the capacity to alter the lipid arrangements and is thereby potentially damaging in isolation. It is

conceivable that this disruption constitutes the main effect on cellular targets during early stages of MAC assembly (46).

MAC formation plays an undisputed *in vivo* role in infection control through the direct destruction of pathogens. However, the fact that terminal component deficiency only predisposes to Neisserial infections (as mentioned earlier) suggests that this is of limited biological importance (73, 120). In actuality it is likely that MAC mediated lysis is somewhat redundant, with cellular destructive pathways (e.g. phagocytes, NK- and cytotoxic T- cells) compensating. Although no definitive classification can be applied regarding the sensitivity of bacteria to MAC-mediated cytotoxicity, it is known that some bacteria are protected from MAC by larger LPS constituents and more extensive carbohydrate encapsulation. These characteristics are associated with “smooth” (as opposed to “rough”) phenotypes and convey hydrophobic properties on the membrane, thus rendering it less amenable to the proper formation of the MAC pore with its hydrophobic residue-lined channel (120, 121). Nonetheless, the potent lytic activity of the MAC on sensitive cells is clearly illustrated in disorders of aberrant C activation, such as PNH, AIHA and aHUS, where MAC formation in autologous erythrocyte membranes leads to destruction of red-cells and associated pathological sequelae (73, 122).

1.1.4.4 Modulation/Regulation of Adaptive Immune Responses

Although evolutionary very old in its own right, having emerged at the time of the jawed vertebrates some 500 million years ago (123, 124), C precedes the advent of adaptive immunity by at least 1000 million years (29-33). It is therefore unsurprising that C and adaptive immunity co-evolved, as amply demonstrated by the intimate relationship between antibody and C in the classical pathway, which is key for defence against pathogens and in immune complex clearance. However, other links between C and adaptive immunity are less well understood. Nonetheless, it has long been known that C has a key role in modulating the B cell antibody response through CR2 present on B cells, providing a survival and proliferation signal and reducing the threshold for B cell activation. It has since been established that many other facets of B cell function, including memory processes, are influenced by C3dg-CR2 signalling (46, 92). An appreciation that the C3dg-CR2 interaction is important in antibody responses to specific antigens came originally from the work of Pepys, who in 1974 showed that mice had impaired antibody responses to sheep RBCs when depleted of C3 using C3d (93). This concept was then confirmed in humans and other species with defined genetic deficiencies of early C components (73, 92, 94). Some of the strongest evidence of the role of CR2 in regulating antibody responses comes from the demonstration that only one ten-thousandth of the quantity of antigen is required to induce a detectable antibody response when the antigen is coupled to C3dg (125). Additionally, Cr2 *-/-* mice have an impaired antibody response to sheep RBC antigen which is restored by transgenic

expression of human CR2 (126). CR2 is known to associate in a tri-molecular complex with CD19 and TAPA-1/CD81, molecules which mediate cell signalling (127). More recently, the expression of CR1 on B cells and CR1 and CR2 on human T cells illustrates a wider role for C in adaptive immunity (92). Additional reports for MCP/CD46 having an important role in T cell processes such as response to TCR ligation and regulatory T cell activity further support this idea (128, 129). It is believed that the qualitative and quantitative nature of the C receptor engagement in lymphocytes influences their specific, cognate responses, along with non-specific/antigen-independent responses, thereby playing an important regulatory role in adaptive immunity. Derangement of C membrane protein activity in B and T cells has been implicated in the establishment and maintenance of autoimmunity. In addition to the long-established classical pathway, these observations place C at the interface of innate and adaptive immunity.

1.1.4.5 Non-Immune & Emerging Roles

Beyond the important roles in classical innate and adaptive immune processes described above there are additional established and emerging roles for C in other diverse processes ranging from cancer (130), metabolism (21, 131), development (95) and reproduction (132-134), expanding further the degree of physiological and pathophysiological complexity of the system. Indeed, the presence of response elements for signalling molecules intuitively unrelated to immunity in the regulatory sequences of key C genes are suggestive of roles beyond conventional immune processes (73, 135).

1.1.5 Human Vs Mouse C

With the “modern” C system having been established by the time of the divergence of the actinopterygii class from the vertebrate lineage some 500 million years ago, as co-members of the most recently emerged mammalia class of the vertebrata subphylum of the phylum chordata (within the kingdom Animalia), humans and mice have broadly similar C systems, with all of the component groups in place (29-33). However, important C-specific differences exist, along with differences in many other aspects of human and murine immunity, innate and adaptive, cellular and humoral, which are not inconsequential (136); it is therefore essential that the key differences in C are understood when using systems involving mouse C during investigations geared towards human disease.

1.1.5.1 Homology

There are varying degrees of homology between the components of the mouse and human C systems, along with examples of species specific components. There is a higher degree of genetic homology between the early activation components along with the central C3 molecule (87), possibly reflecting the evolutionary pressure to conserve these core cascade components,

although some key functional differences do exist (discussed below). Greater genetic and structural variation is observed in the C regulators, but the utilisation of similar regulatory mechanisms possibly reflects the recombination-prone repetitive nature of the genetic sequences, most notably in the case of the RCA gene members, and the apparent limited structural requirements for effective function in this role, with binding capacity for just 1 or 2 factors (C activation fragment & membrane/fl) being the basic pre-requisite (87). Polymorphisms exist in certain C regulatory proteins, notably CR1, which are associated with lupus-like disease and certain microbial infections and it has been suggested that microbial and genetic stress could have driven rapid evolution in C regulator genes (137, 138). Obvious differences in the pathogenic environments between species could have also driven the divergence of these key genes in humans and mice.

1.1.5.2 Activity

One of the main differences between mouse and human C is that mouse C has dramatically reduced lytic activity (139). Indeed, mouse serum has reduced lytic activity relative to other common laboratory species in assays using antibody sensitised cells and early reports suggested that this was due to an absence of classical pathway components. However, it was subsequently shown that this is not the case - all of the classical pathway components are present in mouse serum (139). The lytic activity of mouse serum is also affected by gender and later studies showed that levels of mouse C4 (originally termed Ss antigen and then Slp) are dependent on MHC alleles and gender (73, 140, 141), however these variations could not fully account for the low haemolytic activity of mouse serum. It was finally shown that C5 requires a particular amino acid sequence of the human C4 β chain in order to bind to the C4b subunit of the classical pathway C5 convertase (C4bC2aC3b) (142, 143). In the mouse C4 harbours mutations in this key segment rendering it unable to bind C5 (144), thus all terminal pathway activity in the mouse is attributable to the alternative pathway C5 convertase ([C3b]₂Bb). Implicit in these findings is the fact that no C5a anaphylatoxin is generated directly by the classical pathway in mice, which has implications for the mechanisms of inflammation and immune cell activation. The reduced lytic activity of female mouse serum is believed to be due mainly to reduced terminal pathway components, along with C4 to a lesser extent, and a function of endocrine (sex) steroid hormone signalling (73). Naturally, these issues pertaining to the relative activity of mouse C must be appreciated when designing experimental assays dependent on it, and when implementing and interpreting mouse disease models in which C plays a role.

1.1.5.3 Regulators and Receptors

Most of the regulators of the mouse and human C systems are members of the RCA gene family, the central inactivating protease enzyme, factor I, being a notable exception. These characteristic

genes are composed of variable numbers of short repetitive nucleotide sequences which code for functional units known as SCR, CCP or Sushi domains (known henceforth as SCRs) – roughly 60 amino acid domains with triple-loop structures maintained by disulphide bonds. In humans the RCA genes are clustered on the long arm of chromosome 1q32 and six of the genes are located in a ~700kb segment (5'- C4BP α , C4BP β , DAF, CR1, CR2, MCP-3'), with factor H located some 5Mb 5' (11). In the mouse the RCA gene cluster has undergone a deletion and translocation event altering the organisation of this gene family. Comparisons between these components in mice and man have led to the conclusion that despite significant structural variations, major functional homologies exist (87).

1.1.5.3.1 Crry and Mouse and Human CR1 and CR2

A key species difference between the molecular organisation of the RCA family is the production of both the murine CR1 and CR2 through alternative splicing of a transcript from a single gene, designated mCr2 (145, 146), and the presence of an additional smaller (65kD) mouse C3-binding protein, originally anticipated to be DAF or MCP (87, 147). This protein, known initially as p65 (147), was found to be a genetic homologue of human CR1 (148, 149) and is now therefore known as Crry.

1.1.5.3.1.1 *The Discovery of Crry*

Following the characterisation of the human system and the identification of receptors and regulatory proteins, their mouse homologues were sought – after all, the existence of equivalent receptors for fixed-C3 was inferred long before, given the known binding characteristic of C3-coated bodies to mouse leukocytes and platelets (86, 150). Combined use of chromatographic, immunological and genetic screening methods identified important differences and similarities in the molecular organisation and functions of the mouse homologues of the human C3/C4 binding and regulatory proteins (85, 87, 145, 147-149, 151-154). Initially, studies using mouse C3-binding proteins isolated from solubilised phagocyte membranes showed that antibodies against human CR1 cross-reacted with a 65KDa mouse glycoprotein (P65), distinct from mouse CR1 based on size, wide-distribution and inability to mediate adhesion of cells to C3b coated targets (147). Indeed, due to its similar size, this relatively small protein was suspected to be the mouse homologue of DAF or MCP (as mentioned above) (87, 147). Later, two genetic homologues of the human Cr1 were found: 1) a discrete gene; 2) a 6-SCR encoding portion of the mouse Cr1/Cr2 which contributes the first 6 SCRs of the mouse CR1 alternative splice-variant (in addition to the 15 SCR Cr2 encoded portion) (145, 153). Use of human CR1-derived probes initially identified two genes in the mouse, arbitrarily named 'X' and 'Y' (chromosomes 8 and 1, respectively), which while very similar to each other, appeared to encode a different product to human CR1 (149, 154). It was

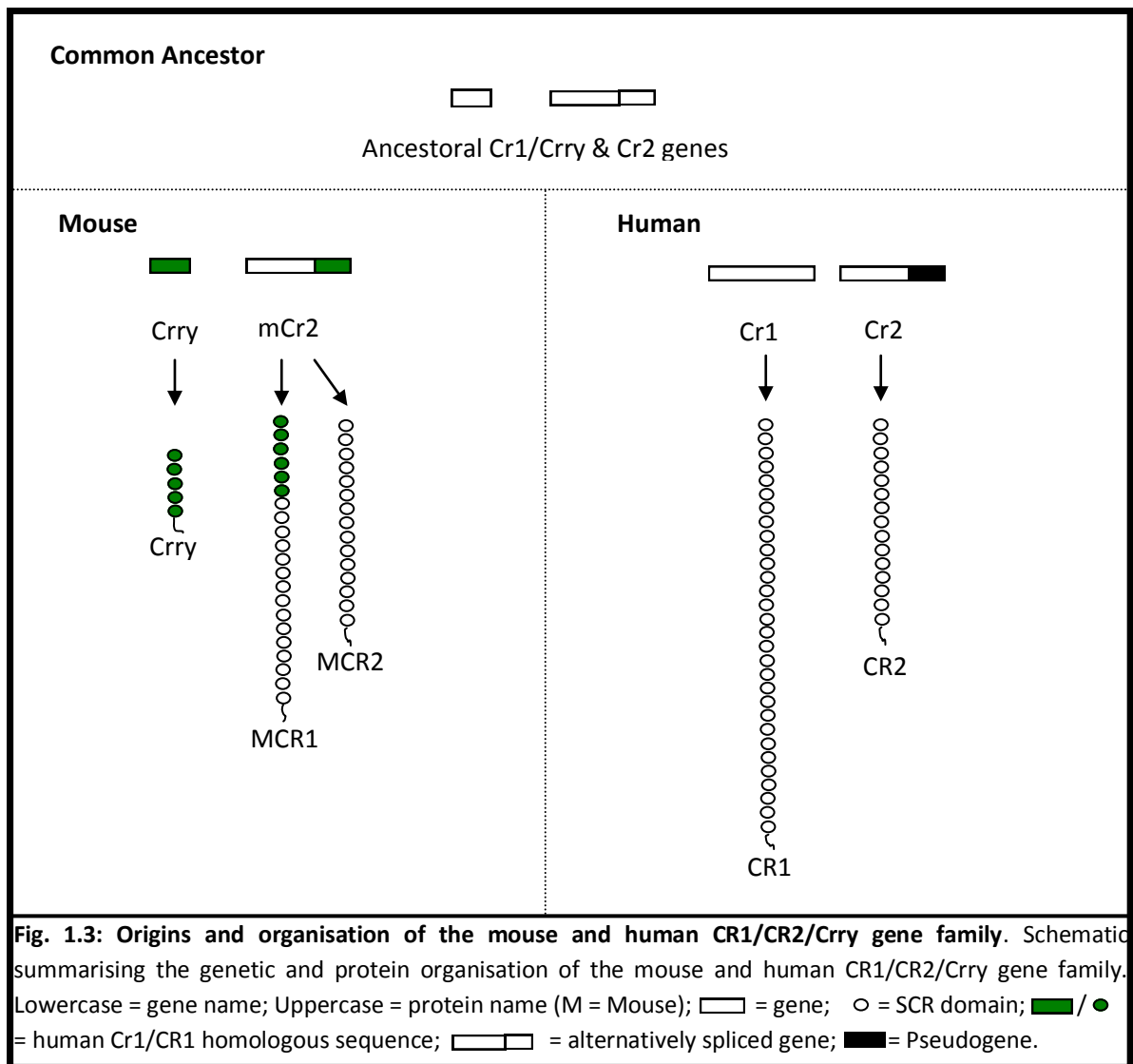
noted that the sequences of the mRNA species derived from the X/Y genes, like CRs 1 and 2, fH and C4bp, corresponded to products composed of the 60 amino acid SCR/CCP domains, but were shorter than for human CR1 and also were far more widely expressed, indicating a different product (148, 149, 154). Through genomic sequence and RNA protection analysis it became apparent that the CR-X gene represents a processed pseudogene derived from the CR-Y gene: the CR-Y gene was subsequently termed complement receptor 1-related gene Y/Crry, while the CR-X gene was termed Crry-ps (154). Molecular cloning and recombinant expression of the Crry gene enabled the subsequent identification of P65 as its protein product (155).

1.1.5.3.1.2 Function

Given its homology to human CR1 and identity as a C3-binding protein, the function of Crry as a C regulator at the C3-level, employing the mechanism of decay-acceleration and/or cofactor activity, was suspected (87). The recognition of Crry's function as an inhibitor of the classical (156), and later the alternative (157) activation, but not the terminal, pathways, further indicated a C-inhibitory function for Crry at or prior-to the level of C3 in the process of C activation. Further studies subsequently confirmed that Crry, indeed possesses both decay-acceleration and fl-cofactor activity (155). Given the limited expression of mouse CR1 across the body and the testis-restricted expression of MCP (158), Crry represents the only known ubiquitous mouse membrane C regulator with fl-cofactor activity (84).

1.1.5.3.1.3 Evolution

Further investigation has subsequently revealed that the human Cr1 gene is actually derived from the precursor of the mouse Crry, but appears to have undergone expansions and at least one recent duplication. Indeed, the human Cr1 gene has undergone very recent exon shuffling events leading to the emergence of common allotypes (87). Additionally, the presence of a pseudogene-like element and stop codons indicates that the human Cr2 gene has lost its ability to form two alternatively spliced transcripts (159) (Fig. 1.3).



To summarise the functional differences with the mouse genetic homologues of human CR1 and CR2: Crry doesn't possess receptor or immune adherence functions, but does possess potent regulatory activity; mouse CR1 and CR2 have overlapping receptor activities along with immune adherence and some regulator activity; human CR1 and CR2 have discrete receptor activities and only CR1 plays a role in immune adherence, but both have some regulatory activity. The biological functions of these components are in-part achieved through their differential distribution, with broad expression of human CR1 including on erythrocytes providing a means for transport of C3b-bearing immune complexes to C3 receptors on phagocytic cells in tissues (160-162). The system for immune complex clearance in mice is markedly different: with no C3 binding protein with immune adherence activity present on erythrocytes [which are protected from autologous lysis by Crry instead of CR1 (163, 164)], the immune adherence-active mouse CR1 protein present on platelets fulfils the requirement to bind and transport opsonised immune complexes (87).

1.1.5.3.1.4 *Requirements for Immune-Adherence Activity*

Human CR1 has a structure of many (~30) SCRs which means it has the capacity to engage ligands at a relatively large distance from the surface of the cell membrane (>1000 Angstroms). It has been suggested that this capacity is important in processes involving cellular engagement of C3 opsonised particles in the fluid phase, particularly immune complex trafficking and maturation of adaptive responses (13). The lack of immune adherence and receptor activity of the relatively small but widespread, five SCR containing Crry, coupled with the role of the larger CRs in these processes in the mouse (156) suggests that this could be the case. Furthermore, the fact that CR1 is the dominant mouse C3 binding protein with receptor and immune adherence activity, which only differs from mouse CR2 by the presence of the six additional human CR1 homologous SCRs at the N-terminal, coupled with the known physiological roles of human CR1, indicates that there may be some CR1 specific structural features required for efficient handling of C3-bearing immune complexes.

1.1.5.3.2 *Other Regulators*

1.1.5.3.2.1 *DAF*

The mouse homologs of DAF, CD59 and MCP were identified after the homologues of the human CR1 and CR2. The human DAF gene encodes a widely expressed GPI anchored form. It also appears to encode a putative secreted transcript but no fluid phase DAF protein has ever been identified. Evidence hinting of the existence of a murine counterpart of human DAF was reported in 1989 (165). Later (in 1995), two DAF genes were definitively identified in the mouse which differ in their C terminal attachment sites: one encodes a GPI anchored form (*Daf-GPI*) and another encodes a protein with a transmembrane domain (*Daf-TM*) (166). The genes lie adjacent to one another in a “head to tail” orientation, *Daf-GPI* 5' to *Daf-TM*. Similar to the human GPI anchored DAF, *Daf-GPI* is widely expressed. However, the expression of the transmembrane form, *Daf-TM*, is limited with preferential expression in certain tissue, notably testis and spleen. Further investigation showed that the mouse DAF genes are subject to alternative splicing producing novel transcripts, including versions with novel GPI anchoring sequences from *Daf-TM* and versions with sequences suggestive of a secreted protein from *Daf-GPI* (76).

1.1.5.3.2.2 *CD59*

Human CD59, a regulator outside of the RCA family (167), was identified in the late 1980's by several groups and was found to be encoded by a single gene (91). Homologues were later identified in other species including mouse in 1997 (168). It was shown that this gene coded for a structural and functional homologue of human CD59 and was widely expressed. It was subsequently shown that a second CD59 gene termed mCd59b (the originally identified gene being termed mCD59a) existed and that the protein product was also a structural and functional

homologue of human CD59 (134). It was also shown that the mCD59b gene is subject to limited expression, predominantly in the testis/by germ line cells. The fact that mCd59a expression is relatively low in this compartment suggests discrete biological roles of the two gene products, despite similar C inhibitory function *in vitro*.

1.1.5.3.2.3 MCP

Human MCP is broadly expressed, although notably not on erythrocytes, with the transcript undergoing alternative splicing to generate distinct forms of the protein with different molecular masses. The mouse homologue of MCP was identified in 1998 (133, 158). Unlike human MCP, but similarly to the rat and as previously shown in the guinea pig, mouse MCP mRNA was found to be preferentially expressed in the testis, indicating, in addition to complement regulatory capacity, a possible specialised role in fertilisation and/or other reproductive processes for MCP in these species. Furthermore, the selective expression of distinct forms of DAF and CD59 in the reproductive organs in the mouse (as described above), suggests an important, wider role for C and/or the regulators in these processes. The fact that deletion of *Crry* results in embryonic lethality (169) which can be reversed with C3 deficiency (170) or inhibition of maternal C strengthens (171) this argument.

Other inter-species differences in the C system have been identified, including the binding properties of C3 to O-linked carbohydrates and the nature of the C4A, C4B/Slp, C4 gene equivalents (172). However, further discussion is beyond the scope of this section.

1.2 Microglia

Microglia are the resident innate immune cells within the CNS parenchyma and as the name suggests, are the smallest of the four principle CNS cell types (neurones, astrocytes, oligodendrocytes and microglia). Their original identification is usually attributed to a notable early Spanish neuroscientist, Pio del Rio-Hortega, through use of a novel silver stain technique (3, 173). A characteristic feature of the CNS is the longevity of its cell types, and microglia are no exception, with evidence to suggest that at least some will persist the entire lifetime of the host (174, 175). The exact origin of the microglia and the question of whether they are renewed entirely from within the CNS or by infiltrating bone marrow-derived myelomonocytic cells from the circulation has been contentious (176). It is now generally accepted that the amoeboid microglia which populate the neonatal brain are derived from myeloid precursors which migrate from the yolk sac/mesoderm to the developing CNS early during embryonic development and occupy all CNS regions, using the vasculature and white matter tracts for guidance (175). They are found almost evenly dispersed throughout the mature CNS, with somewhat higher density in the white matter, and show little variation (173). It appears likely that some microglia, particularly

those generated during responses to CNS insults, are derived from peripheral monocytes (176). In the normal mature CNS microglia adopt a ramified (from the Latin, “ramosa” meaning “branching” or “forked”) morphology and are said to be in a “resting” state, whereas in the perturbed CNS, microglia migrate towards the damage site, proliferate and take on an amoeboid morphology in what is said to be an “activated” state: a notable microglial feature included in del Rio-Hortega’s original nine postulates (3, 173) (Fig. 1.4). Studies utilising fluorophore-expressing microglia and/or *in vivo* live cell imaging have demonstrated that microglia occupy defined spatial territories with limited overlap (thus confirming another of del Rio Hortega’s original postulates) and, even in the normal brain, actively scan their local microenvironment through the dynamic movement of their extensive processes which are equipped with numerous receptor types (4, 177-181) (Fig. 1.5).

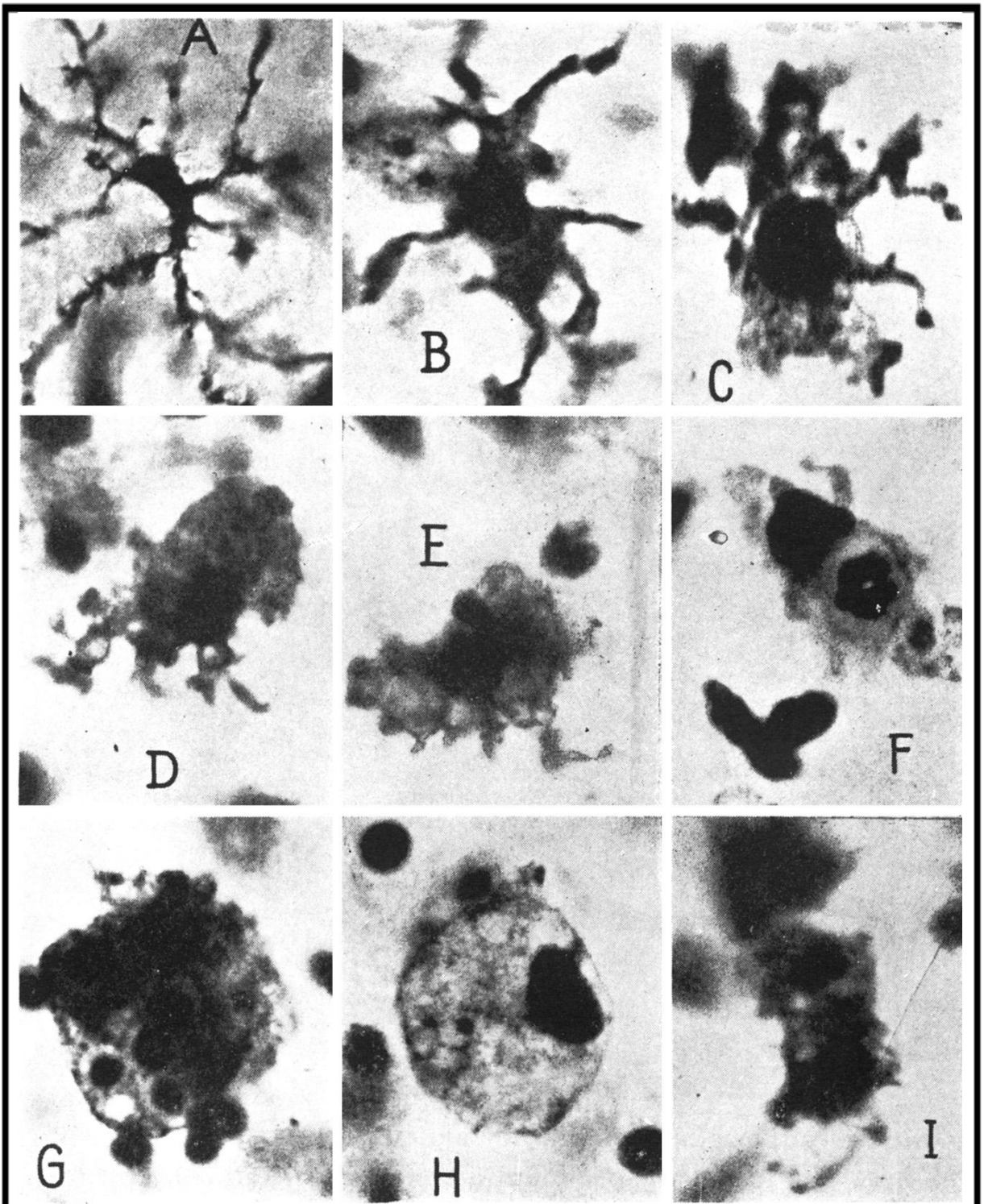


Fig. 1.4: Evolution of microglia during phagocytic activity. *A*, cell with thick, rough prolongations; *B*, cells with short prolongations and enlarged cell body; *C*, hypertrophic cell with pseudopodia; *D* and *E*, amoeboid and pseudopodic forms; *F*, cell with phagocytosed leukocyte; *G*, cell with numerous phagocytosed erythrocytes; *H*, fat-granule cell; *I*, cell in mitotic division. [Photomicrographs from del Rio-Hortega, P; *Microglia* (3)].

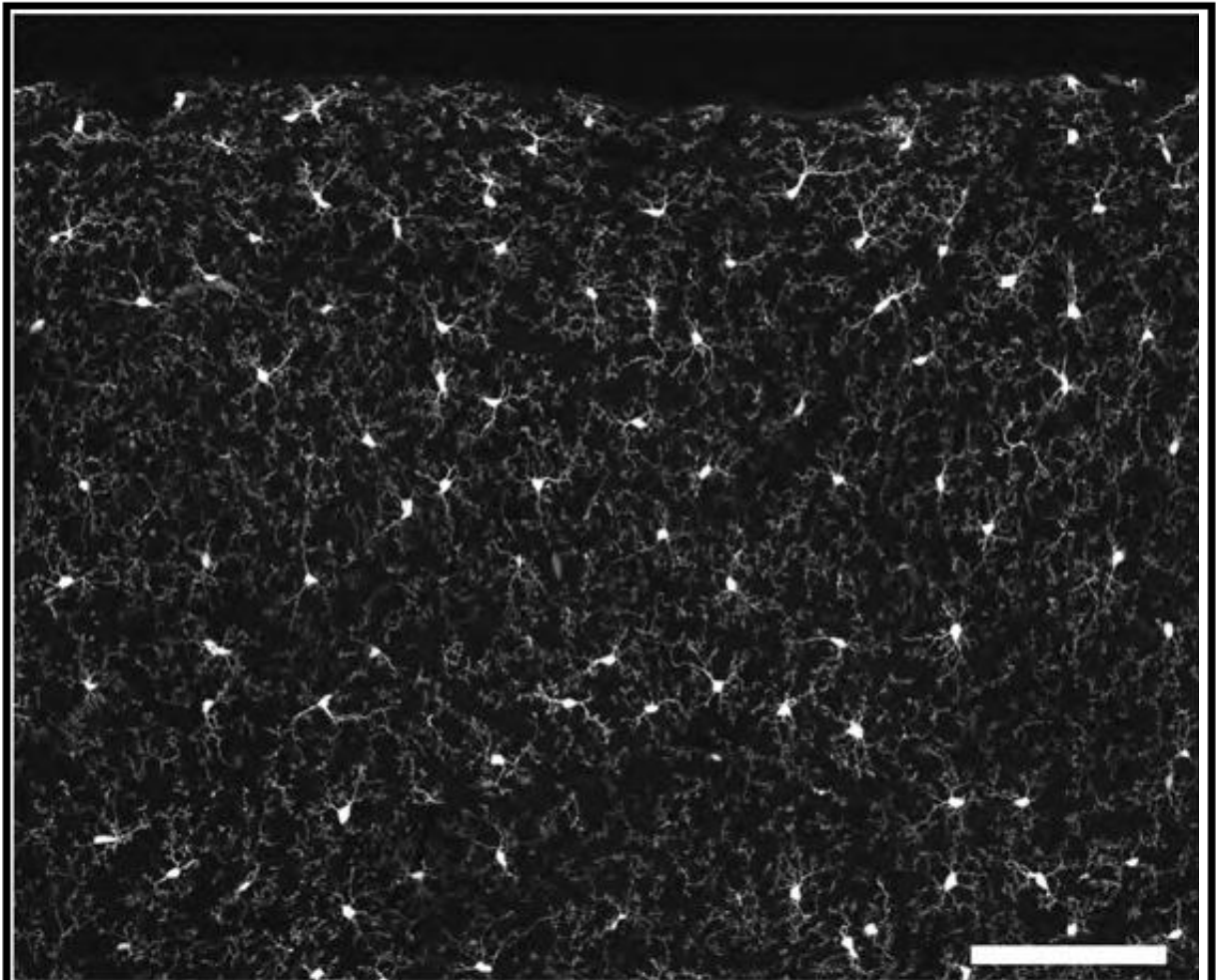


Fig. 1.5: Resting microglia in the mouse cerebral cortex. Microglia are labelled by EGFP expressed from the CX3CR1 promoter. Note the highly ramified appearance of individual microglial cells, as well as the 'tiled' or non-overlapping processes of microglia in the cortex; Scale bar = 100 μ m [from (4)]

1.2.1 Microglial Activation

The resting microglial state observed in the normal brain is induced by their two-directional interaction with neurones, macroglia and other immune cells, in-addition to the ECM, which is mediated by a plethora of soluble (e.g. cytokines) and membrane bound (e.g. CD200) factors, coupled with cellular receptors. Additionally, the resting phenotype is maintained by virtue of the BBB's exclusion of components from the circulatory system (173). The changes in the microglial sensory input which occur upon damage to or infection of the CNS, along with perturbations in neuronal activity, initiate and inform the qualitative and quantitative responses which result in the change to the activated/amoeboid phenotype. The variable magnitude and diversity of CNS damage and derangement seen in different pathologies gives rise to a wide range of potential alterations in the microenvironment which regulates the microglial phenotype. This gives rise to a spectrum of microglial activation/effector phenotypes which vary in their gene expression profiles

and functional activities, and reflect the requirements for the resolution of the distinct activating trigger(s) (182, 183). Microglial functional responses include phagocytosis and release of toxic effector (e.g. ROS, proteases) and immune active molecules, the latter including cytokines and chemokines (etc.) which promote expansion (or resolution) of inflammation. In addition to the potential for collateral damage caused directly by the release of toxic effectors and aberrant phagocytosis, by signalling to other immune active cells, microglial functional responses can initiate, guide and perpetuate expansion of inflammation, which if excessive, can be potentially self-destructive. Thus, along with the possibility of failure to adequately resolve inflammatory triggers when not sufficiently intense, perturbed microglial activation responses can be dangerous when excessively intense or misdirected, and this is believed to play a role in diverse neurological diseases (173).

1.2.2 Microglial Functions

The reactive nature and phenotypic diversity of microglia means they participate in numerous processes in the mature CNS and (as described above) these have potential to become pathophysiological if functional activity is misdirected or not properly gauged. This includes defence against infection, although microglia are known to be targets of some intracellular pathogens such-as HIV-1, which mainly targets microglia for productive infection in the CNS and enters the cell in a CD4 dependent manner, leading to HIV-associated dementia through release of neurotoxic immune modulators resulting in neuronal degeneration and death (184, 185). Other roles of microglia include containment and repair of CNS injury, both traumatic and non-traumatic (e.g. ischaemic), and antigen presentation. During elevated responses as part of infection control or following injury, microglia initiate and coordinate the involvement of peripheral immune cells through cytokine and chemokine release. By upregulating their antigen presentation capacity and permitting the sampling of the CNS by other APCs, along with causing lymphocyte influx, microglia thereby activate adaptive immune responses which are key for the resolution of complex immune challenges (e.g. established/active infections). However, deranged/aberrant adaptive immune responses in the CNS, which is normally relatively insulated from adaptive immunity, is particularly hazardous and is thought to contribute to the establishment of autoimmunity (173). The above functions all pertain to the roles of microglia in the context of immunity. Through their sentinel and phagocytic nature, microglia also mediate the homeostatic clearance of debris and aged and/or damaged proteins. Additionally, *via* their capacity to detect the activity of and communicate with neurones and macroglial cell types, microglia also have emerging roles in modulating neural activity and plasticity (186, 187).

1.2.3 Tools for Microglial Research

The early studies of microglia relied on histology and special staining procedures, the first of which was developed by del Rio-Hortega in the early twentieth century (173). Although of great historical importance and utility, revealing the identity and fundamental biology of microglia, such methods are laborious and inconsistent (188). Advances which led to the development of IHC, a technique for the detection in tissue of specific antigens related to cell type and activation status, and *in situ* hybridisation, for detection of specific RNAs in tissues, provided powerful tools for microglial research. A further notable development was the introduction of the facial nerve lesion model in the late 1960s which permitted investigation of activated microglia without BBB disruption (189). In 1986 a key step forward was made by Giulian and Baker who established protocols for the *in vitro* culture of microglia from the postnatal rodent brain in sufficient volumes for investigation of cell features and functional responses (190). Culture protocols involve generating a single cell suspension of CNS tissues through enzymatic and/or physical methods, and many (including the originals) are based on the differential adhesive properties of neural/CNS cells. Refinements to these techniques have included isolation steps based on distinct CNS cell densities (i.e. density gradient centrifugation) and antigen expression (i.e. MACS sorting) (191). Several cell lines (e.g. BV2, N9) have been developed and used extensively since they provide a ready source of large cell numbers, a shortfall of primary cell culture protocols which typically take a matter of days to weeks to yield relatively small numbers of cells (192). Unsurprisingly, as a result of the extraction process and recognition of the culture environment as foreign/alien, extracted cells typically have an activated phenotype, readily illustrated by an amoeboid morphology (190) and also apparent in an ion channel distribution akin to that observed in activated cells in acute brain slices (173, 193), illustrating the importance of careful interpretation of *in vitro* data. Acute and cultured brain slices have also been employed in microglial research in more recent times, particularly concerning electrophysiological properties and responses to various agents in different contexts/scenarios (193-196). The development of mice with genetically-based cell type specific markers, such as EGFP expressed under the control of the fractalkane receptor (CX3CR1) (197) or Iba-1 (198) promoter, combined with the use of advanced imaging techniques has recently permitted microglial study in the undisturbed living brain (179-181). Despite this, more *in vivo* methodologies are needed for the investigation of microglial activities and interactions in the intact CNS.

1.2.4 Microglia, C, Development & Dysfunction

1.2.4.1 Microglia & C in the CNS: a Dichotomy of Function

As the resident immune cells within the parenchyma, microglia are traditionally known for their involvement in the mechanisms of numerous CNS pathologies ranging in nature from infection,

traumatic, ischaemic and excitotoxic injury, inflammation (e.g. MS), degeneration (e.g. Alzheimer's), neoplasia and even behavioural disorders (e.g. Schizophrenia, Rett syndrome) (173, 178, 199). Indeed, some form of microglial activation and effector function appears ubiquitous in scenarios of CNS perturbation. However, in addition to participation in pathological events, it has become increasingly recognised in more recent times that microglia are involved in non-pathological CNS events in the normal mature tissue and also in development, with roles in surveillance, homeostasis, neuroprotection, repair and wiring of the neural circuitry (177, 178, 200). This reveals a dichotomy of microglial function with potential for harmful and beneficial effects, leading to a realisation that therapeutic modulation of microglial activation will require suppression of negative effects while simultaneously preserving or enhancing beneficial effects. Furthermore, a similar situation has emerged regarding the role of C in the CNS. Previously, C activation in the CNS had been viewed in terms of its known function as an immune effector system, owing largely to the lack of other ascribed functions and the immunohistochemical detection of C activation products in and around CNS lesion (e.g. amyloid plaques, demyelinated lesions). It should also be noted that the methodology of detecting deposited C activation products in pathological/damaged tissue precludes the function of other non-immobilised products and functions in non-pathological scenarios (e.g. development, normality/health) and thus biases towards the view of C as a CNS damage mediator. However, in recent times it has become established that all the CNS cells combined produce all the C components and C is found, albeit at relatively low levels, in normal CSF (18, 96, 201-207). Since the BBB excludes blood borne C under physiological circumstances (18, 207), the discovery of C in the normal CNS led to reassessment of the traditional view of C's role in CNS pathology, previously thought to reside solely in protection against neisserial meningitis (which is more common in individuals deficient in terminal C components) (96). It has subsequently been established that C activation plays physiological roles in development and additionally, some products have beneficial effects in terms of neuronal and cognitive integrity in some settings, with roles in neuroprotection and regeneration. This has been described as "a renaissance" of C research in neuroscience (207) and has led to the recognition of C activation in the CNS as, similarly to that of microglial function, another "dual-edged sword", the beneficial effects of which must be promoted and the negative obviated if modulation will ever be a valid therapeutic target. Moreover, through an array of/being equipped with C receptors and as a source of C components, microglia play central roles in initiating and effecting C-mediated functions in the CNS (173), both beneficial and detrimental. Thus understanding the roles of and the links between microglia and C in the CNS during development, health and disease will be of great value for both basic and applied/clinical neuroscience.

1.2.4.2 C as a Therapeutic Target for CNS Disease/Pathology

Despite these data illustrating the neurogenic, refinement, protective and proliferative effects of C on neurones and glial cells (96), there are ample data defining an inflammatory and damaging role for C in various pathological CNS settings, including demyelinating and degenerative disorders, infection, and acute neurodegeneration resulting from injury (i.e. ischaemia, haemorrhage, trauma, toxicity) (208). Through direct tissue damage *via* MAC formation, opsonisation of cells and matrix components, and the recruitment of cells and immune molecules to sites of pathology, C is a potent mediator of neuroinflammation and neurodegeneration. Nonetheless, mechanisms of neuroprotection and regeneration are active in similarly diverse pathological processes. C is active in the low level turnover of certain neural populations in the normal brain and can mediate protective mechanisms, in addition to widespread regenerative processes at the cellular and synaptic level. Additionally, the lytic, opsonic and inflammatory actions of C activation can have beneficial effects, clearing infections, senescent, dying and damaged host cells and debris, and generally creating a favourable environment for healing (96, 207). However, if the inflammatory trigger is qualitatively and quantitatively sufficient, and the underlying genetic and temporal-spatial status of the system is conducive, it seems the balance between C's homeostatic and protective effects can be outstripped by the tendency of this protean system for robust activation and pro-inflammatory effects, resulting in secondary damage and exacerbation of pathology (207). Given this current knowledge regarding the role of C in CNS health and disease, targeted therapeutic modulation of C in the CNS, although clearly challenging, appears potentially attractive, offering the exciting possibility to inhibit and reverse degeneration. However, owing to C's inherently dangerous nature, such targeted modulation would require highly tuned control and careful monitoring.

1.2.4.3 Links between C and Microglia

Microglia interact with other neural and immune cells, in-addition to the ECM and other entities from outside the CNS (both foreign and endogenous), through a plethora of soluble (e.g. cytokines) and membrane bound (e.g. CD200) factors coupled with cellular receptors in-order to affect their functions. Included amongst this multitude are a number of soluble and membrane bound C components and products, along with C receptors (173). As discussed above, microglia and C participate in diverse processes within the CNS ranging from developmental to dysfunctional; in some cases, this is accomplished through cooperation. Perhaps the most notable physiological interaction between C and microglia established to date is that involved in the mechanism of synaptic pruning in the early postnatal brain, where C1q is deposited on weak synapses leading to C activation and opsonisation with C3 activation fragments and subsequent phagocytosis by microglia *via* CR3 (95, 177). Other notable defined interactions between C and

microglia include the C5a-mediated neuroprotective mechanisms of microglial glutamate transporter-1 up-regulation (which increases the clearance of extracellular glutamate) (209) and C3a-mediated increased microglial nerve growth factor expression (210). In-terms of pathological C-microglia interactions: Rapid, high-grade C activation which can occur in acute disease settings (e.g. ischaemic/haemorrhagic stroke, trauma), where sudden BBB brake-down permits access of C from the circulation to the CNS parenchyma (211, 212), can lead to excessive C-mediated microglial phagocytosis of tissue components and release of proinflammatory (e.g. cytokines) and damaging molecules (e.g. reactive oxygen and nitrogen species, proteases) which outweighs the beneficial effects of C-microglial activation, becoming pathological; A similar situation applies in chronic disease settings, but it is the slow, low-grade C activation, which results from the failure to adequately resolve the activation trigger (e.g. Alzheimer's disease, MS), which can result in ongoing C-mediated microglial phagocytosis of tissue components and release of proinflammatory and damaging molecules which, again, outweighs the beneficial effects of C-microglial activation in terms of clearing the environment of aberrant contents, restoring homeostasis and supporting neuroprotection and neurogenesis. It is almost certain that other links between C and microglia which are (of course) relevant for health and disease in the CNS will be established. For example, given that microglia are known to secrete factors which regulate the proliferation, migration and differentiation of neural progenitor cells (213), and C3a-C3aR signalling has been shown to impact on these same parameters in neural progenitors (96, 207), it is tempting to speculate that the C3a may prove to be among those (if not the sole) microglial molecules which are responsible for this activity. A further link between C and microglia was recently established in the pathological realm and is particularly relevant for CNS diseases involving microglial activation, especially those in-which triggering events (e.g. infections, injuries) can precipitate disease symptoms and progression (e.g. Alzheimer's, MS, aging): this link derives from studies of the microglial phenotype in Crry KO mice, a system of chronic C activation, and relates to the phenomenon of microglial priming (1), which is discussed below.

1.2.5 Microglial Priming

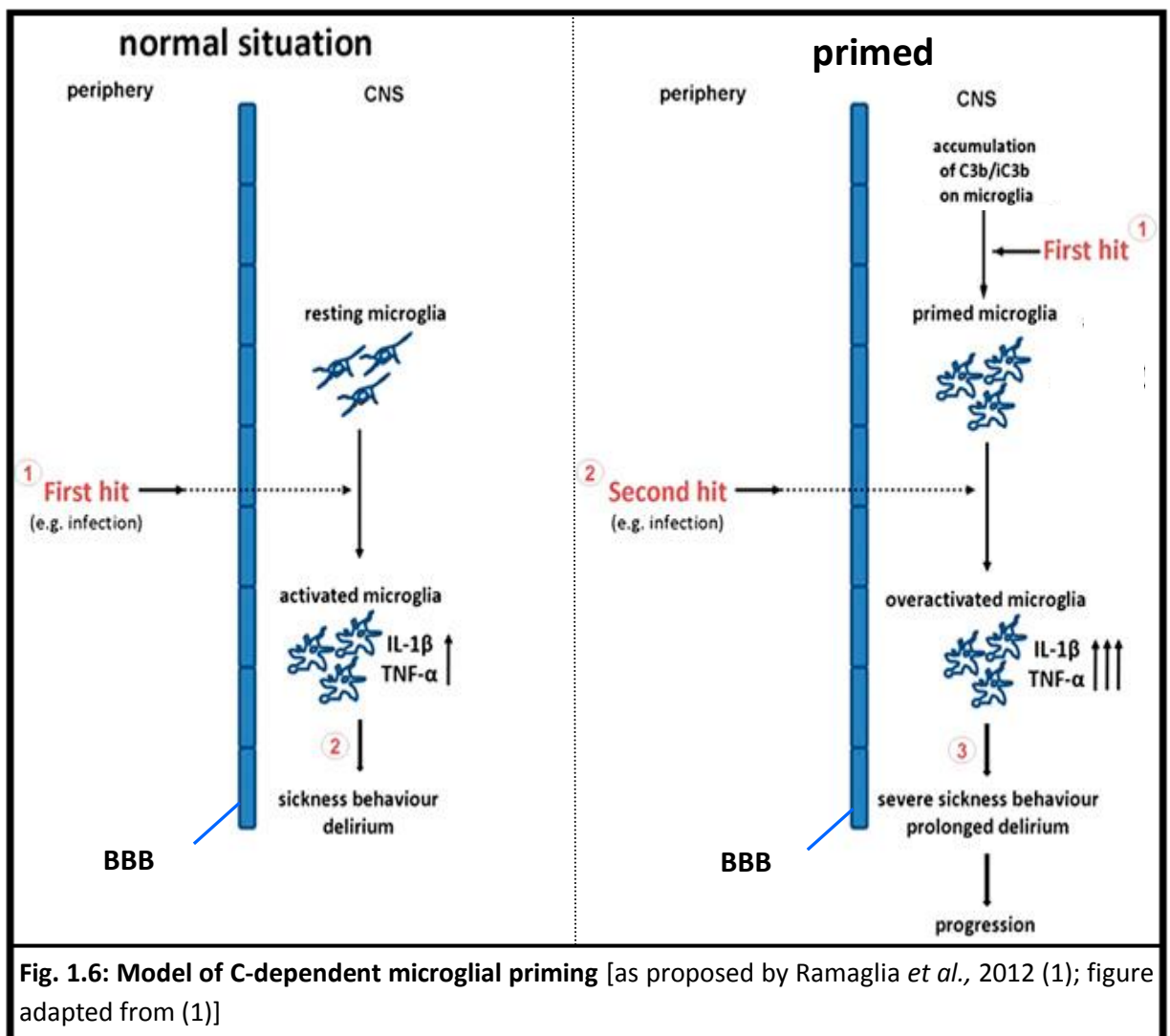
Microglial priming is the concept that previous exposures can sensitise microglia to subsequent challenges such that their inflammatory response becomes exaggerated or they respond to what is normally a sub-threshold challenge. Owing to the longevity which makes microglia susceptible to inflammatory exposures over time, coupled with the sensitivity of the CNS to disruptions and its poor capacity for regeneration, the increased neuroinflammation associated with priming of microglia is particularly problematic/dangerous. Some evidence from infectious models illustrates that priming, like typical modes of microglial response, is potentially an adaptive response which has beneficial effects (214). However, as evidenced by animal models of neurodegeneration,

normal human aging, along with patients suffering from head injuries and dementia, the exaggerated neuroinflammation associated with microglial priming can have deleterious impacts on CNS health and disease, leading to cognitive decline, exaggerated sickness-behaviour and depression, along with physical degeneration of the neural network (1, 214-220). Currently, since there is no clear-cut molecular distinguisher to identify primed microglia; the concept of microglial priming remains operationally defined, although available evidence illustrates that underlying differences in morphology, gene expression and cell number are important. Microglial priming was first described in the last decade in mice with pre-clinical ME7 prion disease, a model of neurodegeneration featuring chronic microglial activation without inflammatory effector release, where it was shown that systemic inflammation induced by intraperitoneal LPS administration led to exaggeration of sickness behaviour (temperature and activity responses), microglial production of IL-1 β and neuronal apoptosis (217). The term 'primed', to describe hyper-reactive microglia, was coined by the same group a few years later, in further studies using the ME7 model of prion disease (221). Priming has since been recognised in diverse scenarios including deficiency of specific neuroimmune inhibitory molecules which are ligands for microglial receptors i.e. CD200 and CX3CR1 (215), acute and chronic psychosocial stress (where catecholamine, glucocorticoid and IL-1 β signalling has been implicated) (219), aging (216, 218), traumatic CNS injury, chronic systemic inflammation and neurodegeneration (214). Similar to the molecular signature of priming, the molecular mechanism(s) which induces priming remains unclear, yet this is essential if microglial priming, an important driver of neuroinflammation, is to be successfully targeted therapeutically.

1.2.5.1 Complement & Microglial Priming

A recent study into the *in vivo* consequences of Crry deficiency revealed a novel microglial phenotype in naïve Crry KO animals involving global hypercellularity and morphological changes (thickening of processes, enlargement of soma). Critically, inducing robust microglial activation by modelling systemic infection with peripheral LPS administration led to a dramatically enhanced pro-inflammatory response thus fulfilling the criteria of priming. Additionally, Crry KOs also experienced accelerated and exacerbated EAE, further illustrating the relevance of microglial priming for CNS degeneration. The microglial phenotype in naïve Crry/C3 and Crry/fB double KOs didn't differ to that observed in WT mice, illustrating the dependence of the Crry KO phenotype on C activation, specifically *via* the alternative pathway. Furthermore, systemic/peripheral administration of sCR1 reversed the microglial phenotype observed in naïve animals during the pre-clinical/symptomatic stages of EAE, but failed to do so in the absence of BBB disruption, indicating that the Crry KO primed microglial phenotype is dependent on intrathecal C activation/C activation within the CNS. Similarly to Crry/C3 and Crry/fB double KOs, a normal

microglial phenotype was observed in factor H KO mice, another system of uncontrolled C activation: in the mouse, factor H is the non-essential cofactor for the factor I-mediated cleavage of C3b to iC3b and C3f, whereas Crry is the essential cofactor for processing of iC3b to C3dg and C3c; factor H KOs therefore have elevated C3b in their system whereas Crry KOs have elevated iC3b. The fact that the primed microglial phenotype was only observed in Crry KOs with an otherwise intact C system (and not factor H KOs) therefore indicates that it is dependent on the generation of the iC3b cleaved product of activated C3. Further suggestive of the key role for iC3b in the priming mechanism, deposited cleaved products of C3, which (as described) in the Crry KO mouse are primarily the iC3b fragment, were shown to co-localise with CD11b, a key microglial marker and part of the cognate receptor for iC3b (CR3), in the Crry KO CNS (1). Based on these data, a model of C3-dependent microglial priming was developed in-which local deposition of iC3b leads to ligation of microglial CR3, thereby inducing a primed phenotype and resulting in hyper-responsiveness to subsequent pro-inflammatory triggers (Fig. 1.6).



1.3 Aims & Hypotheses

Microglia participate in diverse processes throughout the course of their host's lifetime, ranging from (physiological) pre- and post- natal development, homeostasis, neuroplasticity, neuroprotection, neurotrophism to (pathological) neuroinflammation and neurodegeneration (222). However, having long been known as innate immune cells which rapidly respond to all manner of CNS insults and due to the relatively recent appreciation of their activity in undisturbed tissue, microglia have traditionally been appreciated as cells involved in pathology which have the potential to mediate damage (213). Within the pathological realm of microglial function, the concept of microglial priming has been established within the last decade and is widely applicable to scenarios of CNS injury where it provides a mechanistic explanation of clinical, experimental and anecdotal observations (223). The report of Ramaglia *et al.* which identified and defined a C dependent mechanism of microglial priming and demonstrated its relevance for inflammatory and degenerative CNS disease was a seminal publication which for the first time identified a molecular mechanism of priming, a mechanism which could be applicable to a variety of clinical and experimental settings (1). However, (perhaps unsurprisingly) a number of questions still remain/these findings raise further questions regarding the nature of C-mediated microglial priming, specifically relating to the ability of C to prime genetically un-manipulated cells and the maintenance of the primed state of Crry KO cells in the absence of chronic C activation.

Dementia has a serious impact on quality of life and represents a major cause of age-related mortality, with Alzheimer's disease (the most common form of dementia) estimated to reach >100 million cases by 2050 (224). As a mechanism which promotes neuroinflammation, a recognised component in the pathogenesis of dementia (225, 226), coupled with early and chronic microglial activation during neurodegeneration (173, 214, 227) and the known exaggerated detrimental effects of inflammatory triggers on Alzheimer's/dementia patients (217, 228, 229), microglial priming is of clear relevance for the establishment and progression of dementia. Given the influence of peripheral inflammation (which can be modified by lifestyle and pharmacologically) on microglial priming and activation (1, 214, 216-218, 220, 230), priming may therefore represent a valuable new therapeutic target for strategies to prevent and/or treat dementia and thereby promote healthy aging.

Set against a background of unanswered questions pertaining to C and microglial priming, as a phenomenon which impacts on these cells' contribution to health and disease, this thesis provides an account of investigations into specific mechanisms of C-induced microglial priming based on the findings of and model proposed by Ramaglia *et al.* (1).

The issues and questions raised by the study of Ramaglia *et al.*, which was an exclusively *in vivo* investigation, call for *in vitro* investigations where the properties and responses of normal and genetically manipulated microglial cells can be studied in isolation from other cell types and uncontrolled C exposure.

The hypotheses to be tested are that:

- 1. ligation of microglial CR3 by iC3b on naïve cells will result in a primed phenotype**
- 2. in the absence of chronic C activation (*in vitro*) the primed microglial phenotype observed in Crry KO cells *in vivo* will be lost, but will be restored (through the mechanism of the 1st hypothesis) by exposure to C activation which results from their intrinsic sensitivity**

The key aims of this study are to develop (and characterise) *in vitro*:

- a system for the extended culture of pure populations of primary adult (murine) microglia in a resting state with retained responsiveness to activation stimuli and C factors
- a microglial activation regime and readouts which permit the assessment of activation/phenotypic status
- strategies (and appropriate controls) to ligate/cross-link/engage microglial CR3 with iC3b
- a method to exploit the intrinsic sensitivity of Crry KO microglia to C activation

2 Materials & Methods

2.1 Cell Culture

All cell cultures were maintained at 37°C in a humidified atmosphere with 5% CO₂. All plastic-ware and solutions/reagents were sterile TC grade. Plastic-ware was from Greiner or Nunc; all media and reagents were from Life Technologies (Gibco & Invitrogen), apart from (rm)M-CSF (R&D Systems) and DMSO (Fisher Scientific). Unless specified, all solutions were pre-heated to 37°C before use.

Solution	Formulation
Plain Medium	1 x DMEM, 4.5g L ⁻¹ D-glucose, 2mM L-glutamine
Serum free medium	Plain medium + 50U mL ⁻¹ penicillin G, 50µg mL ⁻¹ streptomycin sulphate, 1mM sodium pyruvate
BV2 Growth medium	Serum free medium + 10% (v/v) heat inactivated FBS
1° Culture medium	Serum free medium + 15% (v/v) heat inactivated FBS
1° Growth medium	1° Culture Medium + 10ngml ⁻¹ rmM-CSF
Freezing medium	60% (v/v) serum free medium, 30% (v/v) FBS and 10% (v/v) DMSO

Table 2.1: Formulae of cell culture media

2.1.1 BV2 Microglial Cell Line

2.1.1.1 Maintenance

The BV2 murine microglial cell line was kindly provided by Dr. David Copland, School of Clinical Sciences, University of Bristol. The BV2 line was selected for its isogenicity to the C57Bl/6 mouse strain which was used for primary cell culture (231). BV2 cells were maintained in BV2 growth medium (Table 2.1) in 25cm² TC flasks. In-order to minimise genetic drift of cells between experiments, cells were maintained in culture for no more than ~2.5 months/20 passages before being discarded and another culture initiated from original frozen stocks.

2.1.1.2 Sub-Culture

Cells were cultured until they were ~75% confluent, at which point they were passaged. The culture medium was discarded and the monolayer rinsed in 5ml sterile PBS, then incubated with 5mL 0.05% trypsin, 0.53mM EDTA (Gibco). When the monolayer was fully detached as evident from microscopy, 8mL BV2 growth medium was added and the total 13mL volume transferred to a 15mL centrifuge tube, which was then centrifuged at 300xg for 4 minutes at RT. The supernatant was discarded and the cell pellet resuspended in 1mL BV2 growth medium. Cell numbers were determined using a haemocytometer and 2.5 x 10⁵ cells in 10ml BV2 growth medium were added to each 25cm² TC flask; the growth rate of BV2 cells necessitated biweekly passaging.

2.1.1.3 Reanimation from Liquid N₂ Storage

BV2 cell aliquots were removed from the liquid N₂ dewar and transported on dry ice to the TC room. Aliquots were rapidly thawed in a 37°C water bath, then cells were washed by transfer to BV2 growth medium (20mL) and pelleted by centrifugation at 300xg for 4 minutes at RT. Cells were then resuspended in BV2 growth medium, counted and seeded at 5 x 10⁴ ml⁻¹ in 25cm² TC flasks.

2.1.1.4 Preparation of Frozen Stocks

BV2 cells were grown to ~85% confluence in a 175cm² TC flask. The spent medium was discarded and the monolayer washed with sterile PBS followed by trypsin-EDTA solution until fully detached (as above [2.1.1.2]). The cell suspension was diluted in BV2 growth medium and centrifuged at 300xg for 4 minutes at RT. The cell pellet was then resuspended in the appropriate volume of freezing medium (Table 2.1) to yield a cell density of ~10⁶ ml⁻¹ and 1ml aliquots were transferred to cryo-vials. Vials were then placed in an isopropanol-containing freezer box which was stored overnight in a -80°C freezer to effect slow cooling (~1°C min⁻¹). Vials were then transferred to vapour phase liquid N₂ for long term storage.

2.1.2 Primary Microglia

2.1.2.1 Initial Culture

2.1.2.1.1 Tissue Acquisition

Primary adult murine microglia were cultured according to the protocol of Yip *et al.* '09 with minor modifications (232). All animal procedures were performed in accordance with UK Home Office legislation under the ASPA act 1986. Mice (genotypes as indicated) of ages 8-12 weeks, housed in a conventional/non-barrier environment were used for all experiments. Animals were sacrificed by exposure to a rising concentration of CO₂ and quickly exsanguinated by cardiac puncture. The thorax was promptly opened and the inferior vena cava severed. The animal was then perfused *via* the left ventricle with 40ml of ice cold autoclaved, 0.22µM filtered PBS in 20ml syringes with 25 gauge needles (sterile; BD) at a flow rate of ~6ml min⁻¹ to remove all blood cells from CNS blood vessels. The skull was exposed and a sagittal incision made along the crest. A cut was then made around the skull cap and the brain exposed and rinsed with ~5ml of ice cold plain medium (Table 2.1). The whole brain was removed from the top of the brain stem before removal of any extraneous membranous tissue and transfer to 20ml of plain medium on ice for transport. The dissected tissue was then transferred to a class 2 TC hood for the remainder of the procedure.

2.1.2.1.2 Tissue Processing

The brain tissue was finely minced in a small volume (2-3mL) of plain medium using a sterile 23 gauge scalpel and transferred to a 15ml tube. Sterile papain solution (Sigma-Aldrich; 4 ml of 2mg ml⁻¹ in plain medium, 0.22μM filtered) was added and incubated at 37°C for 30 minutes with agitation. The tissue was then allowed to settle for 5 minutes and the papain solution removed and replaced with 2mL of 1° culture medium at 37°C (Table 2.1). The tissue was then triturated by passage through a 1mL pipette-tip, allowed to settle for 2 minutes and the supernatant collected. The remaining tissue pellet was resuspended in another 2ml 1° culture medium at 37°C and the process repeated twice such that a total volume of 6ml supernatant/suspension was recovered. This suspension was then centrifuged at 300xg for 5 minutes at RT and the supernatant discarded. The pelleted material was then resuspended in 1ml 1° growth medium (Table 2.1) at 37°C and passed through a sterile 70μM nylon-mesh cell-strainer (Fisher Scientific). The cell strainer was then rinsed with another 1mL of warm 1° growth medium and the total recovered volume gently mixed. The suspension was then seeded into multi-well TC plates at 50μL per cm² and then 4 x the suspension volume of 1° growth medium added to the well and mixed gently by rocking/swirling. Cells were allowed to adhere for a minimum of 2hr [max. 24hr, *as per Yip et al.*, (232)] and then, following gentle agitation to resuspend non-adherent debris and cells/material, the medium was removed from each well and was replaced with 1° culture medium. Following further gentle agitation, this was then finally replaced with 0.5mL 1° growth medium per cm² TC surface. Media was replaced biweekly.

2.1.2.2 MACS Purification

Where indicated, cells were further purified by MACS® technology based on CD11b immunoreactivity according to the manufacturer's (Miltenyi Biotec) instructions. Near confluent cultures were rinsed with sterile PBS and incubated with 10mM warm, sterile EDTA (Fisher Scientific) in PBS for 5 minutes. The cell-suspension in EDTA/PBS was diluted by addition of 1.5x the volume of 1° growth medium and the remaining adherent cells were lifted by gentle pipetting. Cell suspensions were then pooled and centrifuged at 300xg for 4 minutes at RT. Cells were then washed by resuspension in ~5mL of ice-cold MACS buffer (PBS, 2mM EDTA, 10% FBS [0.22μM filtered]) and then pelleted again by centrifugation at 300xg for 4 minutes at 4°C. The supernatant was discarded, the cell pellet resuspended in 90μL ice-cold MACS buffer and 10μL CD11b (microglia) MicroBeads, human and mouse (Miltenyi Biotec), added and mixed thoroughly by gentle pipetting. The mixture was then incubated for 15 minutes at 4°C with occasional agitation and then washed twice in ice-cold MACS buffer by centrifugation (4°C). The microbead labelled cell pellet was then resuspended in 0.5ml of ice-cold MACS buffer and transferred into a pre-

equilibrated (0.5mL MACS buffer) MACS column (MS; Miltenyi Biotec) within the magnetic field of a mini-/octo-MACS magnet (Miltenyi Biotec). The column was then washed thrice within the magnetic field with 0.5mL ice-cold MACS buffer and the run-through (unlabelled cells/material) collected. The column was then removed from the magnetic field and placed onto a 15ml centrifuge tube, at which point another 0.5ml ice-cold MACS buffer was added and the labelled cells flushed out by rapid depression of the column plunger. The collected cell fractions were washed with warm 1° growth medium, pelleted by centrifugation at RT, resuspended in warm 1° growth medium at $5 \times 10^4 \text{ ml}^{-1}$ and seeded onto multiwell TC plates before being incubated. Medium was replaced biweekly.

2.1.2.3 Expression of Microglial Markers

To confirm the identity of the isolated primary cells as microglia, the expression of a range of microglial markers was assessed by flow cytometry (CD11b, CD45, CD200R, C5aR, F4/80 antigen and Crry; *as per* Section 2.3.1) and Rt-qPCR (Iba-1, Crry; *as per* Section 2.3.4), in-addition to comparative assessment of gross morphology by phase-contrast microscopy.

2.2 Cell Treatments/Exposures

2.2.1 LPS

Lyophilised LPS (from *E. coli* 0111:B4; Sigma-Aldrich) was reconstituted at 1 mg ml^{-1} in plain medium then diluted 1:5 in plain medium to a $200 \mu\text{g ml}^{-1}$ stock solution. To achieve final concentrations of $\geq 1 \mu\text{g ml}^{-1}$, stock solution was diluted by direct addition to the TC medium. Where concentrations $< 1 \mu\text{g ml}^{-1}$ were required, stock solution was diluted 1:10 in plain medium for each 10-fold/ \log_{10} reduction in concentration from $1 \mu\text{g ml}^{-1}$ prior to addition to TC medium.

2.2.2 Fluid-phase iC3b

Human iC3b (fluid-phase) was purchased from Complement Technology, Inc.: catalogue number A115; $250 \mu\text{l per vial}$; 1 mg ml^{-1} solution in PBS (10 mM sodium phosphate, 145 mM NaCl, pH 7.2).

2.2.2.1 Characterisation

2.2.2.1.1 SDS-PAGE

SDS-PAGE was performed using the Mini PROTEAN II system (Bio-Rad). SDS-buffered acrylamide gel mixtures were prepared as indicated in Tables 2.2 A & B. The 10% APS (Sigma-Aldrich) solution (which catalyses acrylamide polymerisation and thus setting of the gel) was added immediately prior to pouring of the gel mixtures into the assembled gel-casting moulds. The volume of the resolving gel mixture (sufficient to fill roughly three-quarters of the cast) was poured first; this was then submerged to a level of 3-5mM inside the casting mould with butanol to seal the resolving gel-mixture from the atmosphere in-order to assist setting/polymerisation. After 30

minutes to 1 hour (upon setting of the resolving gel) the layer of butanol was removed and the complete (i.e. + 10% APS) stacking gel mixture was poured into the mould. A Teflon comb (which forms multiple wells in the gel and seals the mixture to assist polymerisation) was inserted into the top of the mould (now full) being careful not to introduce air into the mixture. Once set (after ~1hr) the cast containing the gel was clamped into the running tank and SDS running buffer (Table 2.2B) was filled to the appropriate levels to cover the anode and cathode. The gel was left to equilibrate in the SDS running buffer for at-least 5 minutes prior to the loading of protein. iC3b samples for electrophoresis were prepared by diluting $3\mu\text{L}/3\mu\text{g}$ (1mg mL^{-1}) of the iC3b preparation in $9\mu\text{L}$ loading buffer (Table 2.2B), mixing thoroughly and heating to 90°C for 5-10 minutes; $10\mu\text{L}$ (containing $2.5\mu\text{g}$ iC3b) of this protein/loading-buffer mixture was then transferred to the relevant well of the equilibrated gel alongside $5\mu\text{L}$ of pre-stained broad-range protein standards (New England Biolabs). The electrophoresis apparatus was fully assembled then connected to a Model 500/200 power supply (Bio-Rad) and a potential difference ($\sim 100\text{V}$, 70mA) applied until the dye front reached 0.5 cm from the far-edge of the gel ($\sim 1\text{hr}$).

Following electrophoresis, polyacrylamide gels were stained with Coomassie blue stain (Table 2.2B) for the detection and visualisation of separated proteins. Gels were rinsed in dH_2O to remove surface running buffer and bathed in coomassie stain for 3 hours on a rocker. Coomassie blue stain was removed, the gel rinsed (in dH_2O), then bathed in de-stain buffer (Table 2.2B) and incubated for an hour on a rocker. The destain solution was removed and replaced with fresh destain; this process was repeated until protein bands appeared blue with a sharp-contrast against a clear background. Coomassie stained gels were then scanned.

A

Component	Stacking Gel (3.5%)	Resolving Gel (10%)
SDS stacking gel buffer	1.2mL	N/A
SDS resolving gel buffer	N/A	3.75mL
Acrylamide/Bis (37.5:1)	440µL	3.75mL
dH ₂ O	3.25mL	7.25mL
TEMED	5µL	15µL
10% APS (in dH ₂ O)	50µL	150µL

B

Solution	Formulation
SDS stacking gel buffer	0.5 M Tris, 0.4% (w/v) SDS, pH6.8
SDS resolving gel buffer	1.5 M Tris, 0.4% (w/v) SDS, pH8.8
Loading buffer (reducing)	0.1 M Tris, 10% (v/v) glycerol, 2% (w/v) SDS, 0.01% (w/v) bromophenol blue, 0.71M 2-Mercaptoethanol , pH 6.8
SDS running buffer	25 mM Tris, 191 mM glycine, 1% (w/v) SDS
Coomassie blue staining buffer	0.2% (w/v) coomassie blue R250 in 45% (v/v) methanol, 8% (v/v) glacial acetic acid in dH ₂ O
De-staining buffer	40% (v/v) methanol, 10% (v/v) glacial acetic acid in dH ₂ O

Table 2.2: Formulae of gels (A) and complex solutions (B) utilised for SDS-PAGE and sample visualisation

2.2.2.1.2 Immuno-Reactivity

2.2.2.1.2.1 Plate Coating

Each of the wells in rows 1-3 of a 96 well ELISA plate (Nunc MaxiSorp™; Sigma-Aldrich) were incubated with 100µL of 2.5, 5 and 10 µg mL⁻¹ (respectively) iC3b in PBS, while those in row 4 were incubated with 100µL of 10µg mL⁻¹ purified human C1Inh (Cinryze®; Viropharma) in PBS, for 1hr at 37°C.

2.2.2.1.2.2 Blocking, Probing and Detection

After 3 washes with 0.05% tween in PBS, the protein coated plate was blocked by incubation for 1hr at 37°C with 1% BSA (Fisher Scientific) in PBS. Following decantation of the blocking buffer: all of the protein-coated wells in column 4 of the 96-well plate were incubated with 2µg mL⁻¹ of rat IgG1 isotype control mAb (clone R3-34, BD); all of the protein-coated wells in column 5 and 6 were incubated with 2.5 and 5 µg mL⁻¹ (respectively) mouse anti-human C1Inh mAb (in-house); all of the protein-coated wells in columns 7-12 were incubated with doubling dilutions of rat anti-

human iC3b mAb (clone 9 [rat IgG1]; in-house) ranging from 8-0.25 $\mu\text{g mL}^{-1}$; all remaining/antibody-untreated wells were incubated with 100 μL 1% BSA in PBS. After 1hr at 37°C, each of the incubated wells was washed 3-times with 0.05% tween in PBS. Each of the protein coated wells in column 1 were incubated with 100 μL 1% BSA in PBS, while those in columns 2, 5 and 6 were incubated with HRP-conjugated donkey anti-mouse polyclonal Ab (1:2000; Jackson Immuno Research), while those in 3, 4 and 7-12 were incubated with HRP-conjugated donkey anti-rat polyclonal Ab (1:2000; Jackson Immuno Research). All antibody incubations were in 100 μL 1% BSA in PBS. After 1hr at 37°C, each of the incubated wells were again washed 3-times prior to the addition of 100 μL HRP substrate solution (SIGMAFAST OPD [Sigma-Aldrich; prepared *as per* manufacturer's instructions]) *per* well, and incubation for ~10 minutes at RT in the dark (without sealing of the plate). The peroxidase reaction was then terminated by the addition of 100 μL 10% H_2SO_4 (in dH_2O) *per* well and gentle mixing/swirling. Absorbance was then measured at 492nm using a FLUOstar OPTIMA plate reader (BMG Labtech).

2.2.2.2 Fluorescent iC3b

2.2.2.2.1 Fluorescein Conjugation

Human iC3b was fluorescein conjugated *via* N-hydroxysuccinimide-linkage using the Fluorescein Antibody Labelling Kit (Thermo Scientific) according to the manufacturer's instructions. Briefly, 2 vials of iC3b were mixed together to yield 0.5ml at 1mg ml^{-1} , which was then added to a fluorescein – N-Hydroxysuccinimide reaction vessel and incubated in the dark at RT for 1hr to fluorescein-label the protein. The remaining free dye was then removed from the sample by mixing with- and centrifugation (1000xg, ~40 seconds) through- the supplied purification resin, which had been pre-packed and separated from storage solution by centrifugation (1000xg, ~40 seconds) into the dye removal column. Residual, non-covalently associated/bound dye was removed from the sample by extensive dialysis against PBS at 4°C.

2.2.2.2.2 Confirmation of Labelling & Retained Capacity for Antibody Binding

To confirm the successful fluorescein labelling of the iC3b protein and demonstrate the preservation of its ability to bind specific antibody, a concentration gradient of the reaction product was incubated against a concentration gradient of human iC3b specific rat monoclonal antibody (clone 9; in-house) which had been immobilised on an ELISA microtitre plate, and specific fluorescence detected. FITC conjugated donkey anti-rat polyclonal Ab (as a detection reagent; Jackson Immuno Research) and rat IgG1 isotype control mAb (as an immobilised target; clone R3-34, BD) served as positive and negative control, respectively.

2.2.2.2.1 Plate Coating

200 μ L of 10 μ g ml⁻¹ Clone 9 anti-iC3b in PBS was added to each well in column 6 of a 96 well microtitre plate (Greiner); 100 μ L PBS was added to each well in columns 1-5. A serial doubling-dilution series was then made across the plate from columns 6-2 by consecutive transfer and mixing of 100 μ L of the well from the previous columns contents; 100 μ L was then removed from each well in column 2. This resulted in a concentration gradient across the plate in 100 μ L volume with concentrations of 0, 0.625, 1.25, 2.5, 5 & 10, μ g ml⁻¹ in each well of columns 1-6, respectively. Each well of columns 7-9 was filled with 100 μ L of Clone 9 in PBS, at concentrations of 0.625, 1.25 & 2.5, μ g ml⁻¹ respectively. Each well of columns 10-12 was filled with 100 μ L of a rat IgG1 isotype control mAb (clone R3-34, BD) in PBS, at concentrations of 0.1, 1 & 10, μ g ml⁻¹ respectively. The plate was then sealed with a plastic film and incubated at 37°C for 1hr.

2.2.2.2.2 Blocking, Probing and Detection

After 3 washes with 0.05% tween in PBS, the Ab coated plate was blocked by incubation for 1hr at 37°C with 1% BSA in PBS. In a new 96-well microtitre plate; 220 μ L of a 5% solution of the reaction product in 1% BSA (PBS) was added to wells 1-6 & 10-12 of row A, while 220 μ L of a 5% solution of FITC-labelled anti-rat Ab in 1% BSA was added to wells 7-9. 110 μ L of 1% BSA was added to all the remaining wells. A serial doubling-dilution series was then made down the plate from rows A-G by consecutive transfer and mixing of 110 μ L of the well from the previous rows contents. This resulted in a gradient of fluorescently labelled proteins down the plate with concentrations of 5, 2.5, 1.25, 0.63, 0.31, 0.16, 0.08 & 0 % in each well of rows A-H, respectively, with iC3b-fluorescein in columns 1-6 & 10-12, and FITC-labelled anti-rat Ab in columns 7-9. Following decantation of the blocking medium, 100 μ L of the contents of each well was transferred directly to the corresponding well of the Ab coated plate and incubated in the dark at RT for 1hr. The plate was then washed thrice in PBS 0.05% tween and the fluorescence measured in each well at excitation 485nm and emission 520nm using a FLUOstar OPTIMA plate reader.

2.2.2.2.3 Cell Binding Assays

Cells were harvested *as per* Section 2.3.1.1 with the exception of the use of CR3-binding buffer (Hanks' balanced salt solution [Sigma-Aldrich] supplemented with 1% BSA [0.22 μ M filtered]) in place of FACS buffer. 10⁶ BV2 cells were re-suspended in appropriate volumes of CR3-binding buffer such that addition of the appropriate volume of the iC3b-fluorescein preparation into the respective cell sample resulted in 100 μ L final-volumes with concentrations of iC3b-fluorescein ranging from 0-10%. Where indicated, harvested cells were first treated with 1 μ g of CR3-blocking mAb [clone 5C6 (8); Bio-Rad] for 30 minutes (4°C) prior to incubation with iC3b-fluorescein. Samples were incubated with iC3b-fluorescein for 1hr (4°C) then washed twice by the addition of

0.5mL ice-cold CR3-binding buffer followed by centrifugation at 300xg, 3 minutes at 4°C and re-suspension in 0.5mL ice-cold CR3-binding buffer. Cell samples were then centrifuged again at 300xg, 3 minutes (4°C) and re-suspended in 200µL CR3-binding buffer then immediately assessed for green-fluorescence signal by flow cytometric analysis (*as per* Section 2.3.1).

2.2.2.3 Cell Treatment/Exposure

2.5x10⁵ MACS sorted primary microglia cultured in 24-well plates were left untreated or incubated with 1µg/mL iC3b overnight before treatment with or without 100µg/mL LPS for 48 hours. Unlabelled iC3b 200µg ml⁻¹ stock solution in plain medium was diluted by direct addition to the TC medium.

2.2.3 Zymosan

Alexa Fluor-488 labelled zymosan (Thermo Fisher Scientific) was reconstituted at 20mg ml⁻¹ in 2mM sodium azide in PBS. Unlabelled zymosan was reconstituted at 1mg ml⁻¹ in sterile PBS. Suspended zymosan was washed prior to use by addition of ≥10x volume of PBS followed by centrifugation at 1500xg for 15-20 minutes and discarding of the supernatant.

2.2.3.1 Zymosan Opsonisation

2.2.3.1.1 Serum Incubation

Where indicated, zymosan was opsonised with NHS, or WT or C3 KO mouse serum by incubation (1mg zymosan *per* mL serum) for 1 hr at 37°C. Following incubation particles were washed twice by the addition of ≥5-10x volume PBS 1% BSA at 4°C followed by vortexing, centrifugation at 1500xg for 15-20 minutes at 4°C and discarding of the supernatant. The physical appearance and uniformity of the resuspended particles was assessed by bright-field and fluorescence microscopy using a Nikon eclipse 80i fluorescence microscope system equipped with a Nikon DXM 1200F Digital Camera and ACT-1 Version 2 software. Post-acquisition image analysis and processing was performed using ImageJ software (NIH).

2.2.3.1.2 Confirmation of Activated C3-fragment Deposition

Zymosan is a well-known C activating agent (27, 233). C3-activation fragment deposition on the surface of zymosan particles (unlabelled) as part of the opsonising process was assessed by flow cytometry:

Zymosan was incubated with neat NHS or WT mouse serum for different lengths of time ranging from 0 minutes to 1hr to provide a time-course of particle opsonisation. In-addition to NHS- and WT mouse serum- opsonised and non-opsonised zymosan, samples incubated with isotype control Abs, along with particles incubated with serum containing EDTA (10mM; to inhibit C

activation) and C3 KO serum served as negative controls to confirm the specificity of staining/validity of signal.

Particles were washed twice by the addition of 0.5mL PBS 1% BSA at 4°C followed by vortexing, centrifugation at 1500xg for 15-20 minutes at 4°C and discarding of the supernatant. Samples were then incubated (as appropriate) with anti-human iC3b/C3dg/C3g mAb (clone 9; Table 2.3) or anti-mouse C3b/iC3b/C3c mAb (clone 2/11; Table 2.3) for ~30 minutes at 4°C, washed twice, then incubated with Alexa Fluor-488 conjugated anti-rat Ab (Table 2.3) in 0.25mL PBS 1% BSA for ~ 30 minutes at 4°C, washed twice, then analysed by flow cytometry in a volume of 200µL PBS 1% BSA (*as per* section 2.3.1).

2.2.3.2 Phagocytosis Assays

Phagocytosis assays were performed using alexa-fluor 488 labelled zymosan, with uptake measured by flow cytometry or fluorescence microscopy where indicated.

2.2.3.2.1 Primary Vs. BV2 Cells

Non-opsonised or serum-opsonised zymosan particles were resuspended in growth medium at $10^5 \mu\text{L}^{-1}$. $10 \mu\text{L}/10^6$ serum-opsonised or non-opsonised zymosan particles were added directly to 5×10^4 BV2 or MACS purified primary cells cultured in 0.5mL growth medium in 24-well plates and incubated for ~1hr (37°C, 5% CO₂, humidified atmosphere). Untreated cells or cells treated with non-opsonised or serum-opsonised zymosan were then harvested and stained for surface CD11b and viability and analysed by flow cytometry *as per* Section 2.3.1.

2.2.3.2.2 High : Low Dose

Non-opsonised or serum-opsonised zymosan particles were resuspended in BV2 growth medium at $10^4 \mu\text{L}^{-1}$. 5×10^4 or 1.5×10^5 opsonised or non-opsonised particles were added directly to 5×10^4 BV2 cells cultured in 0.5mL growth medium in 24-well plates and incubated for ~1hr (37°C, 5% CO₂, humidified atmosphere). Cells were cultured on glass coverslips and zymosan uptake was assessed by fluorescence microscopy after DAPI staining of nuclei *as per* Section 2.3.2.

2.2.3.2.3 The Role of CR3

Non-opsonised or NHS-, WT or C3 KO mouse serum- opsonised zymosan particles (where appropriate) were resuspended in BV2 growth medium at $10^5 \mu\text{L}^{-1}$. 2.5×10^5 non-opsonised or NHS-, WT or C3 KO mouse serum- opsonised particles were added directly to 5×10^4 BV2 cells cultured in 0.5mL growth medium in 24-well plates and incubated for ~1hr (37°C, 5% CO₂, humidified atmosphere). Where indicated, CR3 was blocked prior to zymosan treatment by addition of 2µg anti-CR3 mAb [which blocks both the iC3b (8) and β-glucan (234) binding sites] (clone 5C6; Bio-

Rad) to the culture medium, gentle mixing and incubation for ~15 minutes (37°C, 5% CO₂, humidified atmosphere). Untreated cells or cells treated with non-opsonised or NHS-, WT or C3 KO mouse serum-opsonised zymosan, with or without exposure to CR3-blocking Ab, were then harvested and stained for surface CD11b and viability, then analysed by flow cytometry *as per* Section 2.3.1.

2.2.3.3 Microglial Activation Assays

BV2 cells were seeded at 5×10^4 in 0.5mL BV2 growth medium per well in a 24-well plate and cultured overnight. Where indicated 2.5×10^6 unlabelled non-opsonised zymosan particles, or particles opsonised with WT or C3 KO mouse serum, were added directly to the well and mixed by gentle swirling. Following incubation for ~4hrs (37°C, 5% CO₂, humidified atmosphere), cells were exposed to LPS at $1 \mu\text{g mL}^{-1}$ where indicated *as per* Section 2.2.1 and cultured for 48hrs. As indicated, supernatants were assayed for nitrite/nitric oxide, TNF- α and IL-6 *as per* Section 2.3.3, and cells were assayed for surface CD11b, C5aR, CD200R and viability by flow cytometry *as per* Section 2.3.1 and changes in expression of mRNAs encoding TNF- α , IL-1 β and IL-6 by Rt-qPCR *as per* Section 2.3.4.

2.2.4 Immobilised C3 Activation Fragments

2.2.4.1 System Development

2.2.4.1.1 Assay to Determine Specificity of (Immobilised) rMOG : anti-rMOG Binding

2.2.4.1.1.1 Protein Immobilisation

Each of the wells in columns 1-5 of a 96 well ELISA plate were incubated with rMOG ($2.5 \mu\text{g mL}^{-1}$; in-house) while those in columns 7-11 were incubated with purified human C1Inh ($10 \mu\text{g mL}^{-1}$) and those in columns 6 and 12 with PBS alone. All incubations were in 100 μL PBS.

2.2.4.1.1.2 Blocking, Probing and Detection

After 3 washes with 0.05% tween in PBS, the plate was blocked by incubation for 1hr at 37°C with 1% BSA in PBS. Following decantation of the blocking buffer: the wells in rows 8-2 in columns 1-4 and 7-10 were incubated (1hr, 37°C) with a concentration gradient (prepared by serial-doubling dilution) of mAb (in 100 μL 1% BSA/PBS) ranging from 40-0.63 $\mu\text{g mL}^{-1}$ (respectively), with Y10, Z4, Z12 (all in-house) and anti-C1Inh in columns 1-4 and 7-10 (respectively). All remaining wells were incubated with 1% BSA in PBS alone. The plate was then washed 3-times with 0.05% tween in PBS before incubation (1hr, 37°C) of each well with HRP-conjugated donkey anti-mouse polyclonal Ab (1:2000 in 100 μL 1% BSA in PBS). The plate was then washed again 3-times with 0.05% tween in PBS prior to the addition of 100 μL HRP substrate solution (SIGMAFAST OPD [prepared *as per* manufacturer's instructions]) *per* well, and incubation for ~10 minutes at RT in the dark (without

sealing of the plate). The peroxidase reaction was then terminated by the addition of 100 μ L 10% H₂SO₄ (in dH₂O) *per* well and gentle mixing/swirling. Absorbance was then measured at 492nm using a FLUOstar OPTIMA plate reader.

2.2.4.1.2 Complement Activation

2.2.4.1.2.1 Coating of TC Plate with C3-Activation Fragments

Plastic TC plates were pre-coated in rMOG or Z4 anti-rMOG mouse monoclonal Ab by incubation with rMOG at 2.5 μ g mL⁻¹ or Z4 at 10 μ g mL⁻¹ in sterile PBS, 100 μ L *per* 0.5cm² TC surface, for 1hr at 37°C, or incubated with PBS alone. Wells were then washed thrice with sterile PBS (250 μ L *per* 0.5cm² TC surface) and non-specific binding sites were blocked by incubation with 1% BSA in PBS, 200 μ L *per* 0.5cm² TC surface, for 1hr at 37°C. Blocking solution was then removed, replaced where indicated with doubling dilutions (50-0.78%) of WT or C3 KO mouse serum in HBSS or HBSS alone (100 μ L *per* 0.5cm² TC surface), and the plate incubated for 1hr, 37°C. Where indicated, WT serum was pre-treated with 10mM EDTA. In some experiments, rMOG coated wells were incubated with anti-rMOG mAbs, Z4 and Y10 (100 μ L *per* 0.5cm² TC surface at 10 μ g mL⁻¹ in 1% BSA in PBS, 1hr, 37°C), and washed 3 more times (as above), prior to serum incubation. Following the final (serum) incubation step, wells were again washed thrice more as above, before a final wash with BV2 growth/1° culture medium (250 μ L *per* 0.5cm² TC surface; as required). All solutions except for BV2 growth medium were 0.22 μ M filtered prior to use and the procedure was performed entirely within a class II TC hood.

2.2.4.1.2.2 Confirmation of Active C3 Deposition

Confirmation of fixed C3-activation fragment (i.e. C3b/iC3b/C3dg) immobilisation on the TC surface was achieved *via* ELISA. Following coating of TC plate with C3-activation fragments, as above, wells were incubated with rat-anti mouse active C3 mAb (clone 2/11; Hycult Biotech) or rat IgG1 isotype-control mAb (clone R3-34, BD) at 0.2 μ g mL⁻¹ in 1% BSA in PBS, 100 μ L *per* 0.5cm² TC surface, for 1hr at 37°C. Wells were then washed thrice with PBS (250 μ L *per* 0.5cm² TC surface) before the addition of 1:4000 dilution of HRP-conjugated anti-rat polyclonal Ab (Jackson Immuno Research) in 1% BSA in PBS, 100 μ L *per* 0.5cm² TC surface, for 1hr at 37°C. Wells were then washed thrice with PBS and incubated with HRP substrate solution (SIGMAFAST OPD [prepared *as per* manufacturer's instructions]), 100 μ L *per* 0.5cm² TC surface, and incubated for ~10 minutes at RT in the dark (without replacement of the lid). The peroxidase reaction was then terminated by the addition of 100 μ L *per* 0.5cm² TC surface 10% H₂SO₄ (in dH₂O) and gentle mixing/swirling. In the case of 96 well plates, absorbance was then measured at 492nm using a FLUOstar OPTIMA plate reader. In the case of plates of other sizes, the reaction endpoint was captured/imaged using a digital camera. 1% BSA (PBS) solution was 0.22 μ M filtered prior to use.

2.2.4.2 Cell Treatment/Exposure

Following coating of the relevant/specified surfaces of a TC plate as described above (Section 2.2.4.1.2), BV2 or primary microglial cells were seeded at 2.5×10^4 in 0.25mL BV2/1° growth medium *per* cm^2 TC surface and cultured overnight. Cells were then exposed to LPS at 100ng mL^{-1} (*as per* Section 2.2.1) or an equal volume (2.5 μ L) of vehicle (plain medium) and cultured for 48hr-72hrs as indicated. Supernatants were then collected and assayed for nitrite/nitric oxide, TNF- α and IL-6 (*as per* Section 2.3.3), and cells harvested and assayed for surface CD11b, C5aR, CD200R and viability by flow cytometry (*as per* Section 2.3.1).

2.2.5 Serum/Complement Deposition & Killing Assay

Where indicated, BV2 cells or MACS purified primary Crry^{+/+} & Crry^{-/-} microglia, seeded at 5×10^4 or 2.5×10^5 *per* well in 24-well plates were used for experiments. Media volumes were adjusted, where necessary (i.e. for primary cells) to 0.5mL. To achieve the desired serum concentrations, the appropriate volume of medium was removed and replaced with NHS or HI NHS, or WT or C3 KO mouse serum, which had been allowed to equilibrate at RT prior to use. Where indicated, NHS was pre-treated with OmCl (in-house) at $10 \mu\text{g mL}^{-1}$ at RT for 15 minutes to block the terminal C pathway by inhibiting C5 activation (and thus MAC-formation). After gentle mixing by swirling, cells were incubated with serum for 1hr (37°C, 5% CO₂, humidified atmosphere) then harvested and assessed for active C3 fragment deposition, MAC formation and viability by flow cytometry *as per* Section 2.3.1.

2.3 Assays

2.3.1 Flow Cytometry

2.3.1.1 Cell Harvest

To minimise degradation of target cell surface epitopes, cells were harvested from the TC surface without the use of protease (e.g. trypsin) solutions, and following harvest, cells were kept cold at all times prior to analysis to preserve their architecture and viability, and to minimise antibody/ligand shedding or engulfment. Medium was removed and cells rinsed in warm, sterile PBS, then incubated with warm, sterile PBS EDTA (5mM for BV2s, 10mM for primary cells) to detach the cells from the culture surface. After most cells had released, 1.5x volume of warm medium was added (BV2 growth or 1° culture medium, as appropriate) and residual adherent cells lifted by gentle pipetting. Cell suspensions were then collected into sterile centrifuge tubes (Corning B.V. Life Sciences) and placed on ice. Samples were spun at 300xg for 3 minutes at 4°C to pellet the cells, which were then washed by resuspension in 1-2mL ice-cold FACS buffer (1% BSA, 2mM EDTA in PBS [0.22 μ M filtered]) and centrifugation at 300xg for 3 minutes at 4°C. Cell

samples were then resuspended in an appropriate volume (as determined by cell density and the number of separate samples required for staining) of ice-cold FACS buffer and aliquoted into 100µL samples in separate FACS tubes (Fisher Scientific or BD) on ice for staining.

2.3.1.2 *Sample Labelling*

Samples were stained by the addition of antibodies of the type and at the concentration(s) indicated in Table 2.3 for ~30 minutes on ice with occasional agitation/shaking. Samples were then washed twice by the addition of 0.5mL ice-cold FACS buffer followed by centrifugation at 300xg, 3 minutes at 4°C and resuspension in 0.5mL ice-cold FACS buffer. Where a non-conjugated primary antibody had been employed, an additional staining step was performed at this point using species IgG-specific, fluorophore-conjugated secondary antibodies of the type and at the concentration(s) indicated in Table 2.3, followed by an additional washing step. In-order to assess viability for nucleated cellular samples, following centrifugation during the final wash step, the supernatant was discarded by inversion and cells resuspended in the small (~50µL) residual volume in the tube; Cells were then stained with an intercalating membrane-impermeant fluorescent dye (either PI or 7-AAD, [as determined by fluorophores used during antibody labelling] at 2.5µg/mL). Sample volumes were then increased by the addition of 100-300µL ice-cold FACS buffer and then analysed by flow cytometry. Where fluorophore-conjugated antibodies alone were used in an assay, or where assay design required the use of a test antibody type raised in mouse with a cellular sample of murine origin, to minimise the issue of non-specific binding an additional Fc blocking step was performed; prior to the addition of primary/test antibodies, cells were incubated with monoclonal rat anti-mouse Fc receptor blocking antibody (Table 2.3) for 5-10 minutes. Where rat Fc blocking mAb was employed in indirect staining assays, secondary antibody which had been cross adsorbed against rat serum proteins was used.

2.3.1.3 *Fluorescence Analysis*

In all cases, samples were analysed on a BD FACSCanto II flow cytometry instrument using BD FACSDiva version 8 software for acquisition. Post-acquisition analysis was performed using FlowJo version 10.0.7 software (Treestar, Inc./FlowJo, LLC).

Target*	Clone	Conjugate	Host	Isotype	Supplier	Working Concentration
CD11b	M1/70	PE	Rat	IgG2b	eBioscience	0.5-1 μ g mL ⁻¹
CD11b	M1/70	PE-Cy7	Rat	IgG2b	BioLegend	1 μ g mL ⁻¹
CD11b	5C6	N/A	Rat	IgG2b	Bio-Rad	5-10 μ g mL ⁻¹
CD45	30-F11	PerCp-Cy5.5	Rat	IgG2b	eBioscience	2 μ g mL ⁻¹
β III-Tubulin	TUJ1	APC	Mouse	IgG2a	R&D Systems	1:50
CD200R	OX-110	PE	Rat	IgG2a	BioLegend	2 μ g mL ⁻¹
F4/80	Cl:A3-1	N/A	Rat	IgG2b	Bio-Rad	10 μ g mL ⁻¹
Cry	1F2	N/A	Rat	IgG2a	Becton Dickinson	5 μ g mL ⁻¹
C5aR	20/70	APC	Rat	IgG2b	BioLegend	2 μ g mL ⁻¹
CD59	MEL-2	N/A	Rat	IgG2a	N/A (In-house)	5 μ g mL ⁻¹
C3b/iC3b/C3c	2/11	N/A	Rat	IgG1	Hycult Biotech	1 μ g mL ⁻¹
Human iC3b/C3dg/C3g	mAb 9; YB2/90-5-20	N/A	Rat	IgG1	N/A (In-house)	9 μ g mL ⁻¹
Human TCC/MAC	aE11	N/A	Mouse	IgG2a	Hycult Biotech	1 μ g mL ⁻¹
N/A (Isotype Control)	eB149/10H5	PE	Rat	IgG2b	eBioscience	0.5-1 μ g mL ⁻¹ (to match test)
N/A (Isotype Control)	RTK4530	PE-Cy7	Rat	IgG2b	BioLegend	1 μ g mL ⁻¹ (to match test)
N/A (Isotype Control)	RTK4530	N/A	Rat	IgG2b	BioLegend	5-10 μ g mL ⁻¹ (to match test)
N/A (Isotype Control)	eB149/10H5	PerCp-Cy5.5	Rat	IgG2b	eBioscience	2 μ g mL ⁻¹ (to match test)
N/A (Isotype Control)	20102	APC	Mouse	IgG2a	R&D Systems	1:50 (to match test)
N/A (Isotype Control)	RTK2758	PE	Rat	IgG2a	BioLegend	2 μ g mL ⁻¹ (to match test)
N/A (Isotype Control)	RTK2758	N/A	Rat	IgG2a	BioLegend	5 μ g mL ⁻¹ (to match test)
N/A (Isotype Control)	RTK4530	APC	Rat	IgG2b	BioLegend	2 μ g mL ⁻¹ (to match test)
N/A (Isotype Control)	R3-34	N/A	Rat	IgG1	Becton Dickinson	1-9 μ g mL ⁻¹ (to match test)
Rat IgG	Polyclonal (Secondary)	AF-488	Goat	IgG (Polyclonal)	Life Technologies	~5 μ g mL ⁻¹
Rat IgG	Polyclonal (Secondary)	PE	Donkey	IgG (Polyclonal)	Jackson Laboratories	1:200

Mouse IgG (X-absorbed against rat)	Polyclonal (Secondary)	FITC	Donkey	IgG F(ab) ₂ (Polyclonal)	Jackson Laboratories	1:200
CD16/32 (Fc Block)	2.4G2	N/A	Rat	IgG2b	Becton Dickinson	2.5-5µg mL ⁻¹

Table 2.3: Antibodies used in flow cytometry; * all test primary antibodies reactive against mouse antigens unless otherwise stated; Test, isotype control, secondary and miscellaneous.

2.3.2 ICC

13mM glass coverslips (Fisher Scientific) where autoclaved, then immersed in 70% ethanol and rinsed thrice in plain medium in a class 2 TC hood, before being placed into the wells of a 24-well plate. Cells were seeded onto the glass surface in 0.5mL medium at 10⁵ cells ml⁻¹; cells were cultured and stimulated as indicated.

2.3.2.1 Staining

Medium was removed from the wells and cells rinsed with warm, sterile PBS, which was then replaced with cold 4% PFA in PBS. Cells were incubated in the fixative for 15 minutes at 4°C then rinsed thrice in PBS at RT. In the case of staining for internal GFAP protein, cells were then permeabilised by incubation in 100% ethanol at 4°C then washed thrice in PBS at RT. Cells were then incubated in blocking solution (0.22µM filtered 10% goat serum [Gibco], 1% BSA in PBS) for 1 hour at RT, rinsed thrice with PBS at RT, then stained with primary antibodies of the type and at the concentration(s) indicated in Table 2.4 by inversion of the coverslip onto ~100uL blocking solution containing the relevant antibodies in a new 24 well plate and incubation for 1 hour at RT. Coverslips were then returned to their original 'face-up' position (with cells on the upper surface) in a 24 well plate and washed thrice with PBS at RT. Fluorophore labelled secondary antibody in 0.3mL blocking solution, of the type and at the concentration(s) indicated in Table 2.4, was then added to the relevant wells and incubated for 1hr at RT in the dark. Staining solution was then removed and coverslips rinsed thrice with PBS at room temperature. Coverslips were then mounted onto standard 1" x 3" glass microscope slides using Vectashield mounting medium for fluorescence containing DAPI (Vector Laboratories).

Target	Clone	Conjugate	Host	Isotype	Supplier	Working Concentration
CD11b	5C6	N/A	Rat	IgG2b	Bio-Rad	20µg mL ⁻¹
GFAP	GA5	AF488	Mouse	IgG1	eBioscience	10µg mL ⁻¹
N/A (Isotype Control)	RTK4530	N/A	Rat	IgG2b	BioLegend	20µg mL ⁻¹ (to match test)
N/A (Isotype Control)	P3.6.2.8.1	AF488	Mouse	IgG1	eBioscience	10µg mL ⁻¹ (to match test)
Rat IgG	Polyclonal (Secondary)	AF555	Goat	IgG (Polyclonal)	Life Technologies	10µg mL ⁻¹

Table 2.4: Antibodies used in ICC; Test, isotype control and secondary

2.3.2.2 Imaging and Analysis

Imaging was performed using a Nikon eclipse 80i fluorescence microscope system equipped with a Nikon DXM 1200F Digital Camera and ACT-1 Version 2 software. Post-acquisition image analysis and processing was performed using ImageJ software (NIH).

2.3.3 TC Supernatant Analysis

2.3.3.1 Sample Preparation

Supernatant from individual samples was collected into separate sterile centrifuge tubes. Dead and dying cells, along with debris, were removed by centrifugation at 350xg for 5 minutes (RT). Ninety percent of the sample volume was then transferred to a sterile bijoux tube (Fisher Scientific), with care taken not to disturb any pelleted material from the bottom of the centrifuge tube. Samples were assayed immediately.

2.3.3.2 Assays

2.3.3.2.1 Griess Assay

Nitrite was assayed as an indirect measure of NO production using the Griess Reagent System (Promega) according to the manufacturer's instructions. Briefly: A high standard of 100µM sodium nitrite was prepared by 1:1000 dilution of the 0.1M stock solution in growth medium (BV2 of 1° where relevant). High standard (100µl) was added to triplicate wells in row A of a 96-well microtitre plate and a doubling-dilution series was made down the plate from rows A-G to create a nitrite gradient with concentrations of 100, 50, 25, 12.5, 6.25, 3.13, 1.56 and 0 µM in each well of rows A-H, respectively, with 50µL volume in each well. Sample (50µL) was dispensed into test wells; 50µL of the sulphanilamide solution was then added to standards and samples, mixed gently and incubated in the dark at RT for 5-10mins. This was followed by 50µL of the N-1-naphthylethylenediamine dihydrochloride solution, which was also mixed gently and incubated in the dark at RT for 5-10 minutes before the absorbance was measured at 544nm using a FLUOstar

OPTIMA plate reader. Sulphanilamide and N-1-naphthylethylenediamine dihydrochloride solutions were equilibrated at RT before use.

2.3.3.2.2 ELISAs: IL-6 & TNF- α

IL-6 and TNF- α ELISAs (R&D Systems) were performed according to the manufacturer's instructions. Capture antibodies were reconstituted in 0.5mL sterile, 0.22 μ M filtered PBS. Detection antibodies and standards were reconstituted in 0.22 μ M filtered 1% BSA in sterile PBS, 1mL & 0.5mL respectively. ELISA plates were coated overnight at RT with 50 μ L of capture antibody diluted 1:120 in plain PBS *per well*. Wells were then washed thrice with 250 μ L 0.1% tween in PBS and subsequently blocked by incubation with 125 μ L *per well*, 1% BSA in PBS (0.22 μ M filtered) for at least 1hr at RT. Blocking solution was then thoroughly decanted before addition of 50 μ L *per well* standards or samples. A high standard was prepared, 2 μ g mL⁻¹ for TNF- α , 1 μ g mL⁻¹ for IL-6, by dilution of the stock solution in TC medium (BV2 or 1^o where applicable) to a final volume of 1mL, and 6 doubling dilutions performed with 0.5mL standard into 0.5mL TC medium. Along with the inclusion of a TC medium only sample, this generated an 8-point standard curve for each analyte (2000-0 & 1000-0 pg mL⁻¹, TNF- α & IL-6 respectively). Samples and standards were incubated at RT for 2hr before being decanted and wells washed thrice in 250 μ L PBS 0.1% tween. Biotinylated-detection antibody diluted 1:60 in 1% BSA in PBS (50 μ L *per well*; 0.22 μ M filtered) was added and incubated for 2hr at RT. Wells were washed thrice as above then incubated with 50 μ L of HRP-conjugated streptavidin (1:40 in PBS 1% BSA, 0.22 μ M filtered) for 20 mins at RT in the dark. Wells were washed again before addition of 50 μ L *per well* HRP substrate solution (SIGMAFAST OPD [prepared *as per* manufacturer's instructions]) then incubated for various times at RT in the dark. The peroxidase reaction was terminated by the addition of 50 μ L *per well* 10% H₂SO₄ (in dH₂O) and gentle mixing/swirling. The absorbance was then measured at 492nm using a FLUOstar OPTIMA plate reader.

Apart from during the HRP reaction, the plate was sealed with an adhesive film during each incubation step. Samples and standards were assayed in triplicate.

2.3.3.3 Analysis/Quantification

Regression analysis of standards and interpolation of unknowns/test samples was performed using GraphPad Prism (version 5.02; GraphPad Software Inc.).

2.3.4 Rt-qPCR

All steps in the Rt-qPCR process were performed within a class II biosafety cabinet with all surfaces thoroughly cleansed with ethanol. Filter-equipped pipette tips (Starlab) were used throughout and all plastic ware (Starlab) was certified RNase/DNase and pyrogen/endotoxin free.

2.3.4.1 RNA

2.3.4.1.1 Extraction

RNA was extracted from cells in culture using the GenElute™ Mammalian Total RNA Miniprep Kit (Sigma-Aldrich) according to the manufacturer's instruction. Unless otherwise stated all steps were performed at RT. Ten microlitres of 2-mercaptoethanol was added *per* mL of lysis buffer to facilitate RNase inactivation. Prior to lysis, cell samples were harvested and pelleted: TC medium was replaced with an equal volume of sterile 0.22µM filtered PBS, which was then replaced with half the volume of 10mM sterile EDTA in PBS, with the subsequent addition of twice the EDTA volume of culture medium; TC surfaces were then rinsed in the EDTA/medium solution to remove remaining adherent cells before transfer of the solution to sterile centrifuge tubes and centrifugation at 300xg for 3mins at RT. The supernatant was aspirated entirely from the pellet before addition of 250µL lysis buffer and immediate thorough vortex &/or pipetting to disrupt cells. The lysed sample was then added to a blue filtration column in a 2mL collection tube and spun in a microcentrifuge at full speed (13,000rpm) for 1min to remove cellular debris and to shear contaminating DNA. An equal volume (250µL) of 70% ethanol prepared from molecular grade water (Sigma-Aldrich) and absolute ethanol (Sigma-Aldrich) was then added to the sample and thoroughly mixed by vortex &/or pipetting. The sample was then transferred to a nucleic acid binding column inside a 2mL collection tube and RNA bound to the silica membrane by centrifugation at 13,000rpm for 15 seconds. The flow-through was discarded and 0.5mL Wash Solution 1 (guanidine thiocyanate-containing) added to the column which was again spun at 13,000rpm for 15 seconds. The binding column was then transferred to a new 2mL collection tube and 0.5mL Wash Solution 2 (ethanol-containing) added before centrifugation at 13,00rpm for 15 seconds. The flow through was then discarded and another 0.5mL Wash Solution 2 added before centrifugation at 13,000rpm for 2 minutes (longer spin to dry column membrane). The column was then transferred to a final 2mL collection tube before the addition of 50µL of the Elution Solution and centrifugation at 13,000rpm for 1 minute. Eluted RNA was immediately transferred on to ice and the binding column discarded. Where necessary RNA was stored at -80°C and kept on ice at all times during use and when thawing. Assessment of RNA concentration and purity was made by spectrophotometric analysis according to Section 2.3.4.1.3 below.

2.3.4.1.2 DNase Treatment

Extracted RNA was treated/processed with the TURBO DNA-free™ Kit (Ambion) according to the manufacturer's instructions to remove trace DNA contamination, and subsequently remove the DNase enzyme along with divalent cations which can catalyse thermo-dependent RNA degradation. Reactions were conducted in 500µL micro-centrifuge tubes to maximise RNA recovery efficiency post-treatment with the DNase Inactivation Reagent.

Where necessary, RNA samples were diluted to $\leq 200 \text{ ng } \mu\text{l}^{-1}$ (based on spectrophotometric analysis) using cold ultrapure/PCR grade water. TURBO DNase buffer (5 μL of 10x stock) was mixed with 45 μL RNA before addition and mixing of 1 μL TURBO DNase and incubation at 37°C for 20-30mins. Resuspended DNase Inactivation Reagent (5 μL) was then added to the sample and incubated for 5 minutes at RT with frequent agitation to maintain the reagent in suspension &/or dispersion. Samples were then centrifuged at 10,000xg for 1.5mins at 4°C to pellet the DNase Inactivation Reagent; the RNA-harboring supernatant was then transferred to a fresh 0.2mL or 0.5mL collection tube and placed on ice, with great care taken not to reintroduce the DNase Inactivation Reagent by disturbing the pellet. Assessment of DNase treated RNA preparations was made by spectrophotometric and electrophoretic analysis according to Sections 2.3.4.1.3 and 2.3.4.3 (respectively).

2.3.4.1.3 Spectrophotometric Analysis of RNA Preparations

Quantitative and qualitative assessment of RNA preparations was carried-out by spectrophotometric analysis using a NanoDrop spectrophotometer (Thermo Fisher Scientific); 2 μL RNA samples were diluted 1:10 with Tris EDTA buffer (10mM Tris, 1mM EDTA, pH8). The machine was initialised with dH₂O and blanked with TE buffer. Individual samples were then analysed and absorbance values at 230nM, 260nM and 280nM noted. RNA concentration was then calculated using the Beer-Lambert Law according to the equation below. Nucleic acid purity was assessed by measuring non-specific absorbance at 280nM (protein) and 230nM (organics). The A₂₆₀/280 and A₂₆₀/A₂₃₀ ratios were calculated with 2.0 +/- 0.2 being deemed satisfactory.

$$\text{Nucleic acid concentration} = \left(\frac{A_{260}}{\text{Pathlength}} \right) \times \text{standard coefficient} \times \text{dilution factor}$$

Given that RNA has a 1cm pathlength standard coefficient of 40 $\mu\text{g mL}^{-1}$:

$$\text{RNA concentration } (\mu\text{g mL}^{-1}) = (A_{260}/1\text{cm}) \times 40\mu\text{g mL}^{-1} \text{ cm}^{-1} \times 10$$

(Where A₂₆₀ = Absorbance at 260nM)

2.3.4.2 Assessment of mRNA Expression

2.3.4.2.1 Reverse Transcription

First strand cDNA synthesis was performed using the TaqMan Reverse Transcription Reagents (Applied Biosystems). Rt reactions were performed with 1 μg RNA *per* 50 μL volume (the stated capacity for conversion of RNA to cDNA using the recommended master mix formulation [https://tools.thermofisher.com/content/sfs/manuals/MAN0009791_TaqMan_RT_Reagents_Kit_UG.pdf]). Rt components were thawed on ice, mixed by inversion or vortex then briefly

centrifuged at low speed to draw liquid to the tube bottom. Common/non sample-specific master mixes were prepared according to the recommended formulation, with 1x Rt Buffer, 1.75mM MgCl₂, 500μM of each dNTP, 1U μL⁻¹ RNase inhibitor, 2.5U μL⁻¹ MultiScribe Reverse Transcriptase and 2.5μM oligo d(T)₁₆ or random hexamers (Table 2.5A). The master mix was vortexed and centrifuged at low speed prior to enzyme and inhibitor addition, then mixed by inversion and centrifuged at low speed post-addition. The master mix and components were kept on ice during and following preparation. 0.57x the final reaction volume of the common master mix was added to a PCR tube on ice and RNA was added at a rate of 1μg RNA *per* 50μL final reaction volume (volume dependent on RNA sample concentration). The total volume was then made up to the appropriate, pre-determined final reaction volume with cold PCR/molecular grade H₂O (Table 2.5A) before gentle mixing by inversion and low speed centrifugation. Reaction mixtures were placed in a DNA Engine Dyad PCR thermal-cycler (MJ Research) and Rt performed using the recommended parameters as indicated in Table 2.5B. Rt reactions lacking template RNA or reverse transcriptase were included as negative controls.

A

Reactant	Volume Per 50μL Reaction	Final Concentration
10 x Rt buffer	5 μL	1 x
25mM MgCl ₂	3.5μL	1.75mM
10mM dNTP mixture (2.5mM each dATP, dCTP, dGTP, dTTP)	10μL	2mM (0.5mM each dATP, dCTP, dGTP, dTTP)
RNase Inhibitor (20U μL ⁻¹)	2.5μL	1U μL ⁻¹
RTase (Multiscribe; 50U μL ⁻¹)	2.5μL	2.5U μL ⁻¹
Primers: 50μM oligo d(T) ₁₆ or 50μM random hexamers	2.5μL	2.5μM
Template RNA	Volume dependent on RNA sample concentration - 1μg	20ng μL ⁻¹ (1μg 50μL ⁻¹)
Molecular/PCR- grade H ₂ O	To 50μL (dependent on RNA sample concentration)	N/A

B

Step	Temperature (°C)	Duration (mins)
1	25	10
2	37	30
3	95	5
4	4	∞

Table 2.5: Formulation (A) and thermocycling conditions (B) for Rt reactions

2.3.4.2.2 qPCR

Relative gene expression was determined by qPCR. Reactions were carried-out in 20µL volumes containing 10µL 2x SYBR Green JumpStart Taq Ready Mix (Sigma-Aldrich), 0.4µL of each (i.e. forward & reverse) 10µM gene-specific primer (biomers.net GmbH) and 9.2µL relevant cDNA diluted 1 in 5.75 in PCR/molecular grade H₂O (equivalent to cDNA Rt product of 32ng RNA). Gene specific master mixes (i.e. SYBR Green JumpStart Taq ReadyMix & primers) were prepared prior to the preparation of individual reactions. At least 10% surplus volumes of gene-specific master mixes were prepared. 10.8µL gene-specific master mix was added to each of the relevant wells of a 48-well qPCR plate (Bio-Rad) followed by 9.2µL of the relevant diluted cDNA and the wells sealed using qPCR-grade/optical flat 8-cap strips (Bio-Rad). Reactants were mixed by combined plate inversion and shaking before the plate was centrifuged briefly at low-speed and then placed in the stage of a MJ Mini cycler (MJ Research) equipped-with a MiniOpticon Real-Time PCR Detection System (Bio-Rad) controlled by PC using Opticon Monitor 3.1 software (Bio-Rad). Thermal cycling and real-time detection was then performed using the recommended parameters as indicated in Table 2.6. Primer sequences for mouse target genes (Table 2.7) were taken from published research and validated using the Primer BLAST programme (NCBI). Primers sequences were submitted to biomers.net for synthesis. As negative controls and to determine the relative magnitude of any contribution of contaminant/false template from the possible sources, qPCRs were performed in which no template was added (i.e. master mix, primers and water only), or the products from Rt reactions in which either no reverse transcriptase/enzyme or RNA was included were used as templates. To validate the PCRs, products were run on 2% agarose gels *as per* Section 2.3.4.3. qPCR reactions were performed in duplicate or triplicate.

Step	Temperature (°C)	Duration (mins)
1	94	5
2	94	0.25
3	60	1
4	Fluorescence read	N/A
5	Return to 'Step 2' 40x	N/A
6	Melt-Curve from 70-90°C	0.3°C every 0.25m + fluorescence read
7	4	∞

Table 2.6: qPCR thermal-cycling and fluorescence detection conditions

Relative gene expression was calculated using the $\Delta\Delta C_t$ method, with β -Actin used as the housekeeping/reference gene, according to the following equation:

$$\text{Relative mRNA expression (\%)} = 2^{-\Delta\Delta C_t}$$

C_t was defined as the cycle number at which fluorescence crossed a threshold level, chosen as the point at which the PCR expansion was exponential/linear in all samples. The C_t values for β -actin (housekeeping/reference gene) and the target gene were determined and referred to as the C_t [HKG] and C_t [target], respectively; ΔC_t was calculated for each target gene of each sample by subtracting mean C_t [HKG] from mean C_t [target]. $\Delta\Delta C_t$ for each target gene of each test sample was calculated by subtracting the ΔC_t of the relevant gene in test sample from the ΔC_t of the relevant gene in the control/baseline sample. Relative gene expression was not calculated/results were rejected if the difference in replicate $C_t \geq 1$.

Target mRNA/cDNA	Forward/Reverse	Sequence (5'-3')	Length (oligonucleotide bases)
Iba-1	Forward	GTCCTGAAGCGAATGCTGG	20
	Reverse	CATTCTCAAGATGGCAGATC	20
Crry	Forward	CCCATCACAGCTTCCTTCTG	20
	Reverse	CTTCAGCACTCGTCCAGGTT	20
GFAP	Forward	TCCTGGAACAGCAAACAAG	20
	Reverse	CAGCCTCAGGTTGGTTTCAT	20
B-Actin	Forward	ACGGCCAGGTCATCACTATTG	21
	Reverse	AGTTTCATGGATGCCACAGGAT	22
C3	Forward	AAGCATCAACACACCCAACA	20
	Reverse	CTTGAGCTCCATTCTGTGACA	20
iNOS	Forward	TTCCAGAATCCCTGGACAAG	20
	Reverse	GGTCAAACCTCTGGGGTTCA	20
COX-2	Forward	CCACTTCAAGGGAGTCTGGA	20
	Reverse	GAGAAGGCTTCCCAGCTTTT	20
IL-1 β	Forward	GCACACCCACCCTGCA	16
	Reverse	ACCGCTTTTCCATCTTCTTCTT	22
IL-6	Forward	TCCAGAAACCGCTATGAAGTTC	22
	Reverse	CACCAGCATCAGTCCAAGA	20
TNF- α	Forward	CTCCAGGCGGTGCCTATG	18
	Reverse	GGCCATAGAACTGATGAGAGG	22
TGF- β	Forward	CGTGGAATCAACGGGATCA	20
	Reverse	GGCCATGAGGAGCAGGAA	18
CD40	Forward	GCCATCGTGGAGGTAAGTGT	20
	Reverse	CTGCGATGGTGTCTTTGCCT	20
CD80	Forward	GGCAAGGCAGCAATACCTTA	20
	Reverse	CTCTTTGTGCTGCTGATTCCG	20
CD86	Forward	TCTCCACGAAACAGCATCT	20
	Reverse	CTTACGGAAGCACCCATGAT	20

Table 2.7: Primers used in qPCR

2.3.4.3 Agarose Gel Electrophoresis

RNA preparations and PCR products were electrophoresed on 1.2% and 2% (w/v) agarose gels, respectively. Molecular grade agarose powder (Life Technologies) was weighed out and suspended in TAE buffer in a conical flask and dissolved by heating at full power in an 800W microwave and swirling of the flask for 30 second intervals, until no trace of powder was visible. Cold water was run over the surface of the flask to cool the molten agarose before $0.5\mu\text{g mL}^{-1}$ ethidium bromide (Sigma-Aldrich) was added and mixed in by gentle swirling. Agarose was then poured into a gel casting tray fitted with a well-forming comb with teeth of $\sim 30\mu\text{L}$ volume and allowed to set for a minimum of 30 minutes before submersion in an electrophoresis tank filled with TAE buffer. RNA ($1\mu\text{g}$) or $25\mu\text{L}$ DNA samples mixed 1:1 with nucleic acid loading dye (New England Biolabs) were transferred to the relevant agarose gel wells. An appropriate quantity of pre-formulated DNA ladder/molecular weight marker (100bp fragments; New England Biolabs) was added to at least 1 well in each gel. Samples were electrophoresed at $\sim 100\text{V}$ until the dye front had migrated to the opposite end of the gel. Gels/samples were then imaged under UV light using a GelDoc system equipped with a digital camera (Bio-Rad) operated by Labworks or UVP software.

2.4 Serum Preparation for use as a C Source

All plastic ware and needles utilised for serum preparation were sterile and all fluid-transfers were performed in a class II bio-safety cabinet after the initial bleed.

2.4.1 Mouse

Mice of specified genotype (housed in a conventional/non-barrier environment) were sacrificed by exposure to a rising concentration of CO_2 or anaesthetised with isoflurane (5% knockdown [chamber], 3% maintenance [ventilator]; Fisher Scientific) and quickly exsanguinated by cardiac puncture using 1mL syringes and 25 gauge needles. Blood was transferred to 0.6mL or 1.5mL microcentrifuge tubes and placed upright at RT for ~ 5 minutes before being placed on ice for a minimum of 30 minutes. Clotted blood was then fractionated by centrifugation at $\sim 9,500\text{g}$ at 4°C for 45 minutes – 1 hour and the serum transferred to a fresh tube and placed on ice (with care taken not to contact the lower fractions with the pipette tip). Sera were pooled, mixed and $0.22\mu\text{M}$ filtered, then aliquoted into 0.3-0.4mL volumes before storage at -80°C .

Excess stock colony members were used for serum preparation and thus were of varying age and sex. All animal procedures were performed in accordance with UK Home Office legislation under the ASPA act (1986).

2.4.2 Human

Blood was collected from a healthy consenting volunteer (male, 27yrs) by venepuncture and transferred immediately to autoclaved glass tubes (~25mL volume). Whole blood was left to clot at RT for 30 minutes before transfer on to ice for a further 30 minutes. Clotted blood was fractionated by centrifugation at 3000xg for 30 minutes at 4°C and the serum transferred to a fresh tube and placed on ice (with care taken not to contact the lower fractions with the pipette tip during transfer). Serum was 0.22µM filtered and aliquoted into 1mL volumes before storage at -80°C.

2.5 Statistics

All statistical data analysis was performed using GraphPad Prism (Version 5) software. Student's t-test was performed when comparing 2 unpaired groups. One-way ANOVA was utilised when studying more than 2 unpaired groups. When comparing 2 unpaired groups within a data set comprising 3 or more groups, One-Way ANOVA was performed, with post-hoc t-test(s) with Bonferroni correction subsequently performed contingent on a significant ($P < 0.05$) main effect of the subject variable (as determined by the ANOVA result). Two-way ANOVAs were performed when assessing more than 2 groups with 2 independent variables and results of Bonferroni post-tests are indicated. Again, post-hoc testing was performed contingent on a significant ($P < 0.05$) main effect of the subject variable, as determined by the ANOVA result. The statistical results displayed on figures/graphs throughout are the output of post-hoc analyses. Mean and standard deviation/error are stated throughout the results sections as indicated. The relevant statistical analysis is indicated throughout in appropriate figure legends.

3 Isolation of Primary Adult Murine Microglia

3.1 Introduction

The establishment of methods to culture both microglial cell lines and primary isolated microglia *in vitro* together with suitable assays for phenotyping and the detection of responses to various C-derived (and other) stimuli were critical to fulfilling the aims of the thesis and form the basis of this chapter. Additionally, prompted by the evidence generated during *in vivo* studies using transgenic animals (1), the *in vitro* consequences of total deficiency in a specific rodent microglial membrane C regulator (i.e. Crry) is a key subject of this investigation. Thus, the capability to culture microglia isolated from adult murine CNS tissue was a key requirement, since the phenomenon of microglial priming is most relevant in scenarios of aging and degeneration (178, 223, 235, 236). This is of particular importance since microglia in adult animals have morphology distinct from those seen in neonates (amoeboid vs ramified) and are therefore likely to be functionally different (173, 178, 237). This is underlined by the inability of microglia cultured from adult animals, unlike neonatal, to readily survive and proliferate *in vitro* (232, 237-239). The establishment of microglial culture systems as described in this chapter thus permitted the further aims of the thesis to be addressed, namely: 1) to investigate the ability of naïve WT microglia to be primed *in vitro* by exposure to C activation products, specifically CR3 ligands (i.e. iC3b); 2) to investigate the *in vitro* phenotype of Crry KO microglia, cells previously shown to be primed *in vivo*. Furthermore the use of a validated and well characterised (178, 192, 240, 241) microglial cell line (BV2) as comparator provided an alternative and reliable source of microglial cells to explore techniques and assays for modification of microglial phenotype and responses to stimulation.

3.1.1 Microglial Culture Systems

3.1.1.1 Primary

Microglial cultures were first described long ago by Costero in 1930 (178). However, their widespread use as a resource for the study of microglial biology emerged almost half a century later, after the 1986 publication by Giulian and Baker (190) describing a technique for the isolation and expansion of high-purity primary microglia from the neonatal rodent brain in sufficient numbers to perform phenotypic and functional assessments. Giulian and Baker's principle "warm-shake method" is still widely employed today, although numerous derivations and modifications have taken place, with various sources of CNS tissues from different species (mouse or rat in the vast majority of cases), different enzyme cocktails and tissue dissociation and homogenisation techniques, cell adhesion-interference techniques, along with myelin removal techniques and immunomagnetic separation steps (191, 232, 238, 239, 242-244). A notable

feature of Giulian and Baker's culture system (190) and others which employ neonatal tissue (192), is that the isolated microglia display an amoeboid morphology which gradually transitions to ramified. This process can be accelerated using retinoic acid or DMSO and mirrors the transition observed *in vivo* from microglia present in developing embryos and neonates to that seen in the mature CNS.

The vast majority of early protocols for the culture of pure microglial populations were based on the use of perinatal rodent (rat or mouse) CNS tissue and of the few protocols designed to isolate adult microglia, some have been used for immediate *ex vivo* analysis of microglia post-isolation (235, 239, 244). Notably, despite displaying a quiescent phenotype consistent with that observed *in vivo* in the normal mature brain, cultured adult microglia typically do not proliferate or survive for extended periods, exhibit unusual phenotypic features (e.g. non-adherence) or are of low purity (191, 192, 232, 238, 239, 242-244). Culture of pure, adult, phenotypically and responsively normal microglia over extended periods in sufficient numbers for experimental investigation therefore constitutes a significant but essential challenge for further progress in understanding the biology of these cells in the various neuropathologies.

One approach to overcoming this problem has been to use M-CSF (238), a mitogen which stimulates myeloid cell proliferation and differentiation of precursors. In this case Ponomarev *et al.* developed a culture system which supported adult microglial cell proliferation and maintenance in the resting state with retained responsiveness to stimulation. Indeed, the importance of CSF receptor signalling for the maintenance of the microglial compartment has been demonstrated in the brain (245). Thus, although it adds significant cost, the addition of M-CSF to the culture medium offers a potential means to circumvent the difficulties associated with adult microglial culture over extended periods.

3.1.1.2 Cell Lines

Despite their close physiological resemblance to microglia *in situ*, there are major drawbacks associated with the use of primary cell culture approaches, namely: 1) the relatively low cell numbers (both from low initial yield and proliferation rate); 2) extensive preparations times and lengthy protocols; 3) the latent period during initial expansion; 4) high cost in terms of time, reagents and experimental animal usage (192). The issue of low cell numbers is particularly pertinent in the case of human microglial research, where suitable donor tissue is not readily available (for obvious reasons). In order to bypass these drawbacks, clonal microglial cell lines have been developed which are highly homogenous and exhibit rapid proliferation with standard cell culture media formulations and protocols, yet retain key properties of *in vivo* and *in vitro* primary microglia (e.g. morphology, immunophenotype, function, electrophysiology), and thus

represent valuable tools for microglial research (192). Like immortalised lines of other cell types, microglial lines have been generated in several species (including human and rodent). These cell lines were derived from initial primary cultures and were immortalised either spontaneously (e.g. HAPI, EOC, C8-B4) or through manipulation (e.g. HMO6, BV2, N9 [retroviral transformation]) (192). Examples of human microglial cell lines include HMO6, CHME3/5 and SV40, while examples of rodent equivalents include BV2, C8-B4, HAPI, EOC and N9 (192). Despite their value as an experimental tool and widespread use, by definition cell lines are transformed and are thus not subject to the normal regulation of progression through the cell cycle and therefore display proliferative properties dramatically different to those of non-transformed cells. Additionally, other aspects of their biology often becomes altered, such as immunophenotype, adhesion, morphology and functional responses (e.g. phagocytosis, migration), further distancing them from their origins and diminishing their value as a research tool. Nonetheless, microglial cell lines have been highly valuable tools for neuroscience (including neuro-immunological) research and will continue to be so for the foreseeable future.

3.1.1.3 Issues Associated with Microglial Culture in Isolation

Microglial isolation and culture systems have been essential in elucidating the molecular signals and responses, along with “macro-responses” (e.g. phagocytosis, migration, proliferation), which govern the microglial lifecycle. The majority of the published *in vitro* data concerning microglial biology comes from studies which employ purified primary cell culture systems, or homogenous cultures of microglial cell lines. However, despite the value and utility of such approaches, there is an increasing appreciation of the importance of basal microglial interactions with factors on or secreted by other neighbouring cell types (e.g. CD200; TGF- β). (173, 177, 246-249). Cultured microglia may deviate markedly from their natural phenotype because of the absence of other interacting cell types. While it is difficult to envisage a system where a pure culture of microglial cells will ever behave exactly as their *in vivo* counterparts we might hope to see the significant improvements in the degree to which the behaviour of these *in vitro* models approach the *in vivo* scenario. As has been touched upon previously, supplementation of the culture system with various purified and synthetic factors which reflect the natural microglial environment, may allow a more normal microglial phenotype to be established whilst maintaining purity, thus permitting the optimised study of microglia-specific responses. As proof of concept, it has been demonstrated that supplementation of the culture medium with soluble CX3CL1/fractalkine (a ligand for microglial CX3CR1; ubiquitously expressed by neurones) results in N9 microglial cells adopting a more ramified morphology and reduces the up-regulation of proinflammatory gene expression induced by LPS treatment (249). These findings are consistent with a shift towards the quiescent state observed *in vivo* in the mature CNS. Additionally, it has been shown that culturing

primary microglial cells in the presence of M-CSF and TGF- β resulted in a shift in their molecular profile towards a unique signature observed only in acutely isolated/*ex vivo* adult cells (although such an effect was absent in cell lines [BV2 and N9]) (183). These studies provide conceptual validation and highlight the potential of such an approach to the optimisation of microglial culture methodologies. Nonetheless, further research is required in-order to define the individual and combined effects of physiological factors which maintain *in vivo* microglia in their resting state.

3.1.2 Microglial Phenotyping, Stimulation and Response Detection

The earliest method of distinguishing microglial phenotype was through morphology and this remains a useful if limited determinant (173, 188). With their development, the full ranges of cellular and molecular techniques have been applied to the study of microglial phenotypes *in vitro* and *in vivo*. Thus, global approaches to microglial phenotyping have been employed in the form of large-scale transcriptome and protein analyses using microarray technology and quantitative mass spectrometry (tandem mass tagging/TMT) (183, 235, 250). Studies exploring microglial responses to various agents have been carried out *in vitro* and *in vivo*. Such agents include typical activators of innate immune cells such as PAMPs (e.g. LPS, poly[I:C]), DAMPs (e.g. AGEs, β -amyloid), microbes and cytokines. Factors specific to scenarios of CNS perturbation have also been investigated such as those promoting apoptotic neurones or neuronal fragments/blebs, myelin, amyloid- β and mutant Huntingtin. As the archetypical PAMP which is used almost ubiquitously in studies of immune cell activation, LPS is the most common agent utilised in studies concerned with microglial responses.

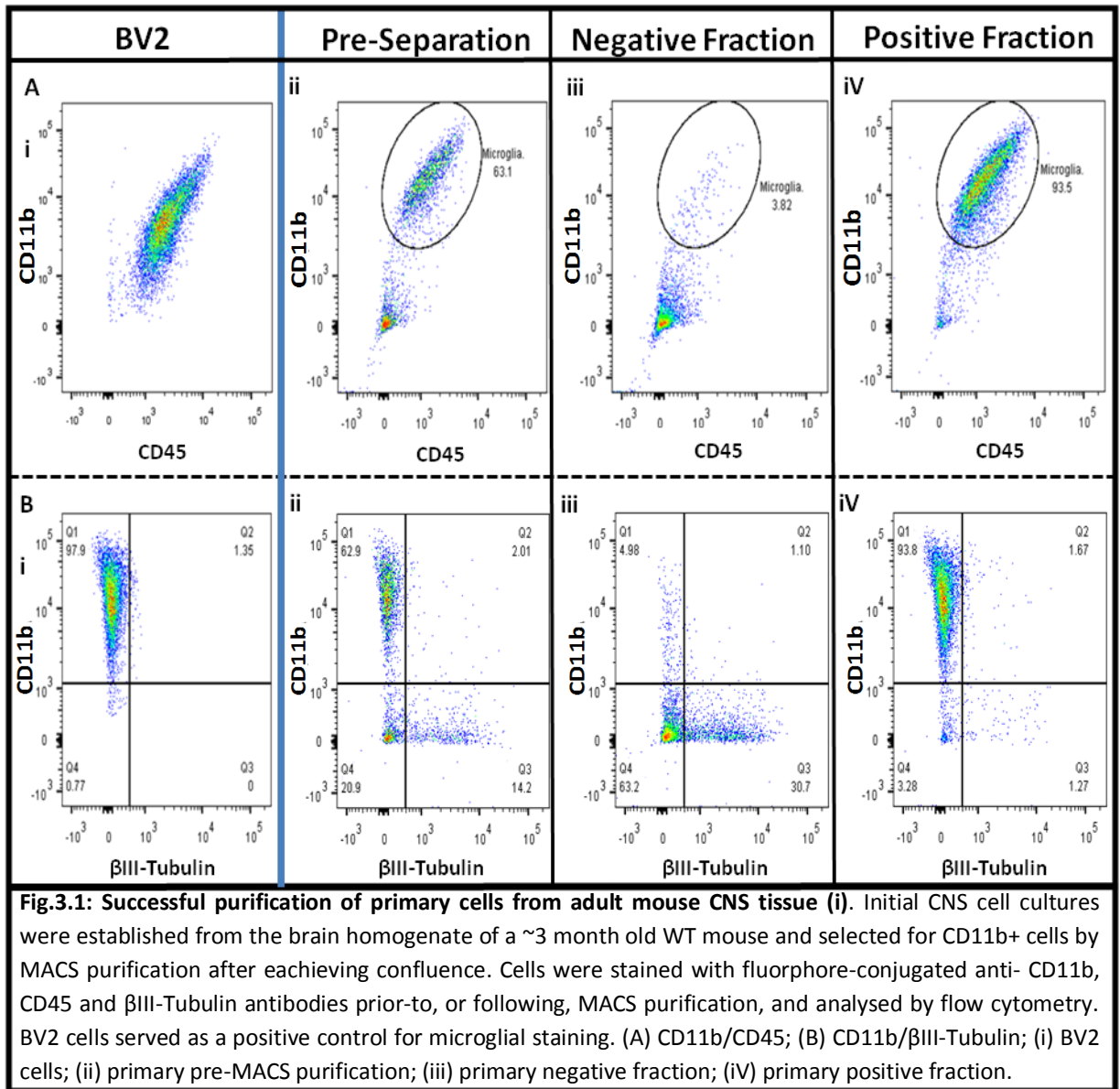
3.1.3 Chapter Aims

The principle aim of the work set out in this chapter was to establish a system for the extended culture of pure populations of primary adult (murine) microglia in a resting state with retained responsiveness to activation stimuli and C factors, along with the development of a regime for their activation and readouts to permit the assessment of their phenotypic status. Additional aims of this chapter were to characterise the identity of isolated primary cells and compare them to a microglial cell line, both to confirm their identity and to assess the differences between primary microglia and cell lines, and compare the properties of microglia maintained in isolation with those maintained in mixed CNS cell cultures.

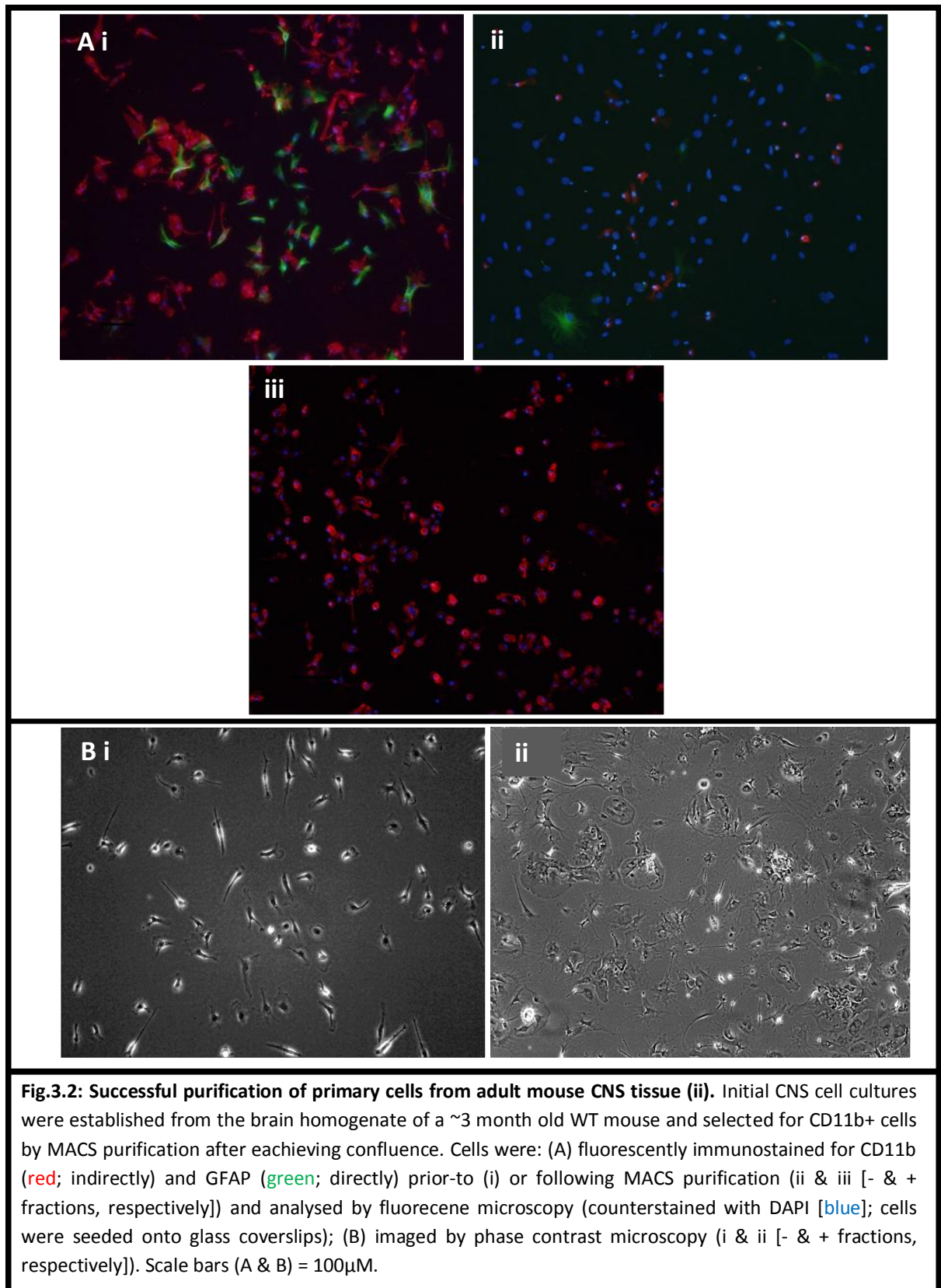
3.2 Results

3.2.1 Establishment of Ongoing Pure Cultures of Primary Adult Murine Microglia

Initial mixed CNS cell cultures were established from the tissues of young adult mice and then purified to homogeneity by MACS sorting (as described in Section 2.1.2). According to the protocol of Ponomarev *et al.* (238), the medium was supplemented throughout the culture process with 10ng mL^{-1} rmM-CSF (R&D Systems) to support the survival of adult murine microglia and their maintenance in a resting/quiescent state, along with their expansion. Initial mixed CNS cell cultures were seeded at a density which afforded individual cells discrete spatial territories; cells proliferated and reached confluence over the course of a week to ten days. As described in Sections 2.3.1 and 2.3.2 (respectively), FACS and fluorescent ICC analysis were utilised to assay the purity of cell cultures using cell type-specific markers. Quantitative FACS analysis demonstrated that 63.1% of cells in initial mixed CNS cell cultures were positive for the microglial surface markers, CD11b and CD45 (Fig.3.1 A ii), while 14.2% stained for the intracellular neuronal marker, β III-tubulin (Fig.3.1 B ii). The remaining 22.7% of cells in initial mixed cultures were unidentified but likely represented other CNS cell types (e.g. astrocytes and oligodendrocytes). Following MACS sorting based on surface CD11b immunoreactivity the vast majority (~95%) of cells in the positive fraction were CD11b and CD45+ (Fig.3.1 A iv), while β III-tubulin+ cells were virtually undetectable (1.3%; Fig.3.1 B iv). Conversely, only a small minority (3.8%) of cells in the negative fraction were CD11b and CD45+ (Fig.3.1 A iii), while the β III-tubulin+ compartment was enriched roughly two-fold (14.2% Vs 30.7%) compared to baseline levels (Fig.3.1 B iii). The staining profile of purified cells closely resembled that observed for the BV2 murine microglial cell line (Fig.3.1 i).



The results of ICC analysis of initial mixed cultures and post-separation fractions closely mirrored those of the FACS analysis (Fig.3.2A), and phase contrast microscopy of positive and negative fractions maintained in culture post-separation illustrated a clear difference in morphology (Fig.3.2B).



Phase contrast microscopy illustrated that purified primary cells generally adopted a ramified morphology, consistent with a resting/quiescent phenotype, and continued to survive in the culture environment. Although growth was very slow, the purified cell cultures, in-which initial seeding density yielded cells with non-overlapping territorial domains (Fig.3.3 Ai), gradually reached confluence over the course of ~3 weeks (Fig.3.3 Aii-iv). FACS analysis of purified primary cells for surface CD11b expression and viability demonstrated that established cultures were highly pure (~99% CD11b+) and the vast majority of cells (~95%) were viable (Fig.3.3 B).

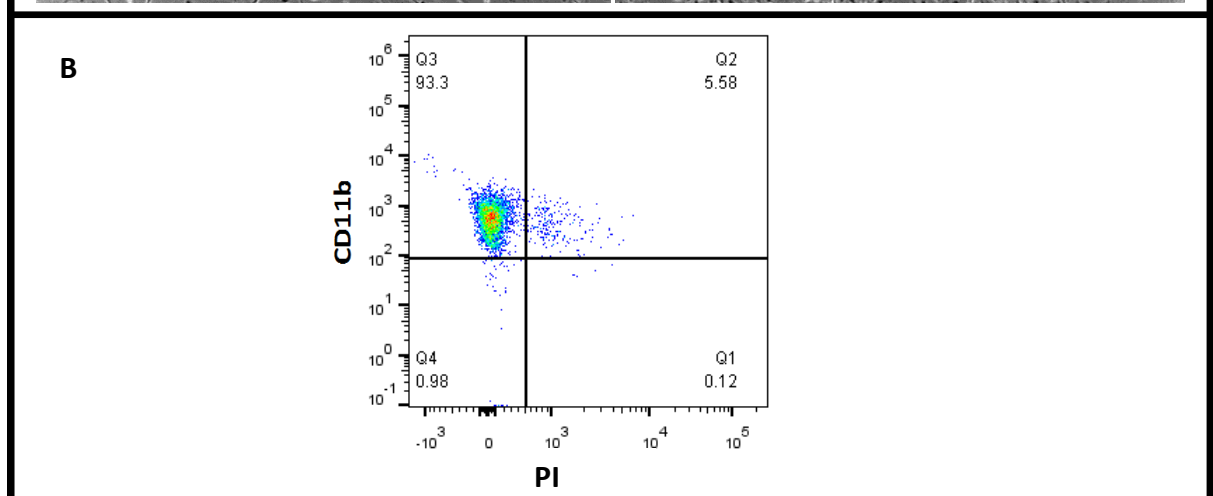
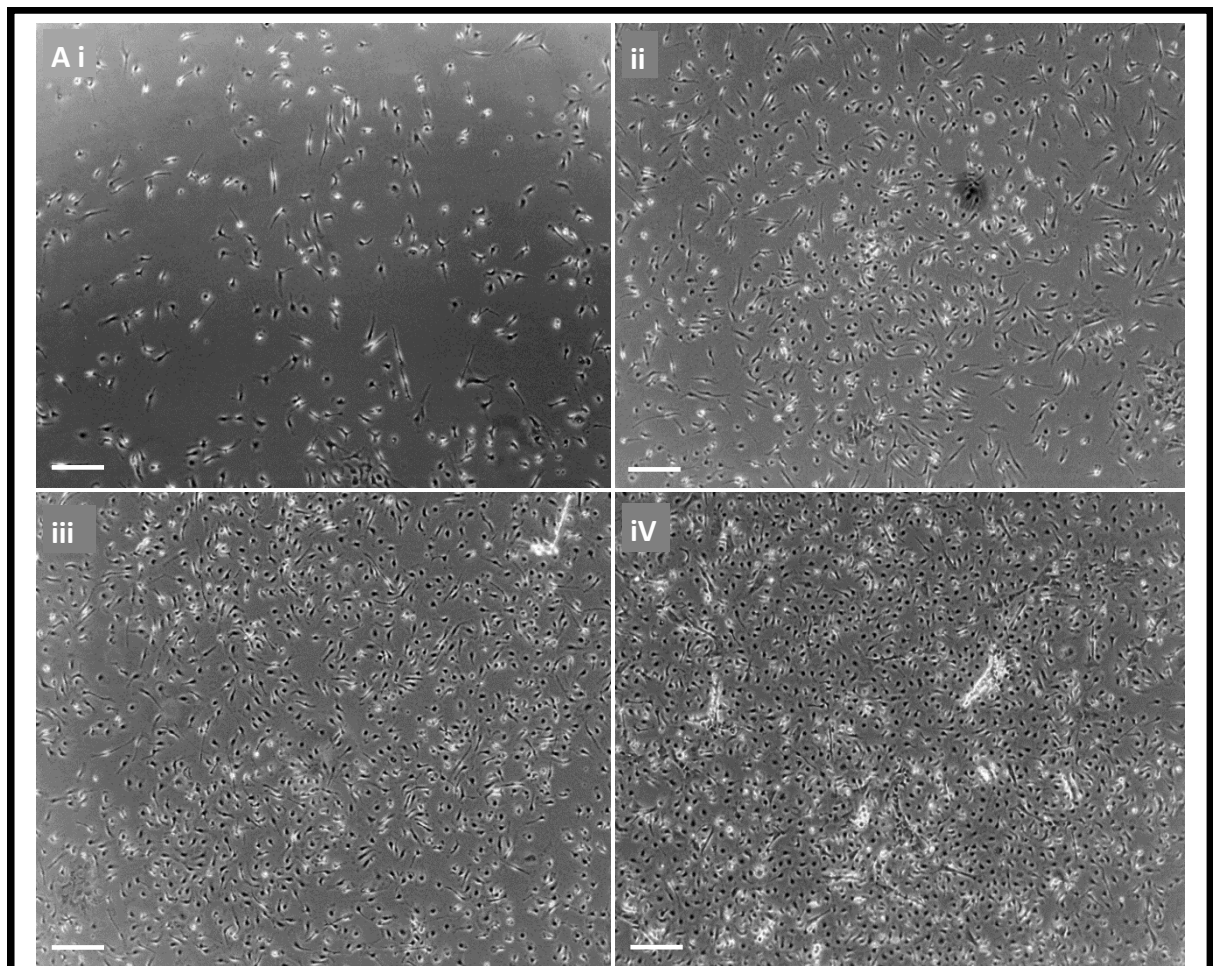


Fig.3.3: Continued survival and expansion of purified primary cells. (A) Primary microglia were cultured for 1, 2, 3 and 4 weeks post-immunomagnetic separation and imaged by phase contrast microscopy (i-iv, respectively). Scale bar (i - iv) = 200 μ M; (B) Primary cells were cultured for 3 weeks post-immunomagnetic separation and stained with anti-CD11b PE-Cy7 (microglial marker; Y-axis) and PI (dead cell marker (X-axis) before analysis by flow cytometry.

3.2.1.1 Assessment of Identity

To confirm their responsiveness to an activator and identity as microglia, and to investigate the differences between primary adult and immortalised microglia as *in vitro* models, purified primary cells and BV2 cells were subjected to phenotyping assays along with LPS exposure.

3.2.1.1.1 Morphology

Morphological examination by phase-contrast microscopy revealed a distinct difference between primary microglia and the cell line: although both cell types were adherent, primary cells generally adopted a ramified/branching morphology with a proportionally smaller cell body (Fig.3.4A) and BV2 cells generally had an amoeboid circular form (Fig.3.4B). This morphological difference is well documented and reflects the activated status of the immortalised cells and their progression through the cell cycle (241, 251, 252), which is particularly rapid when compared to adult primary cells. Only a small minority of BV2 cells adopted a ramified morphology associated with resting cells, while in the case of primary cells, only a minority adopted a rounded morphology, associated with progression through the cell cycle. The time to achieve a similar expansion of cell numbers (~2.5-fold Vs baseline) was much greater for primary compared with BV2 cells (2 weeks Vs 36 hours for primary Vs BV2 cells, respectively; Fig.3.4 Aii & Bii).

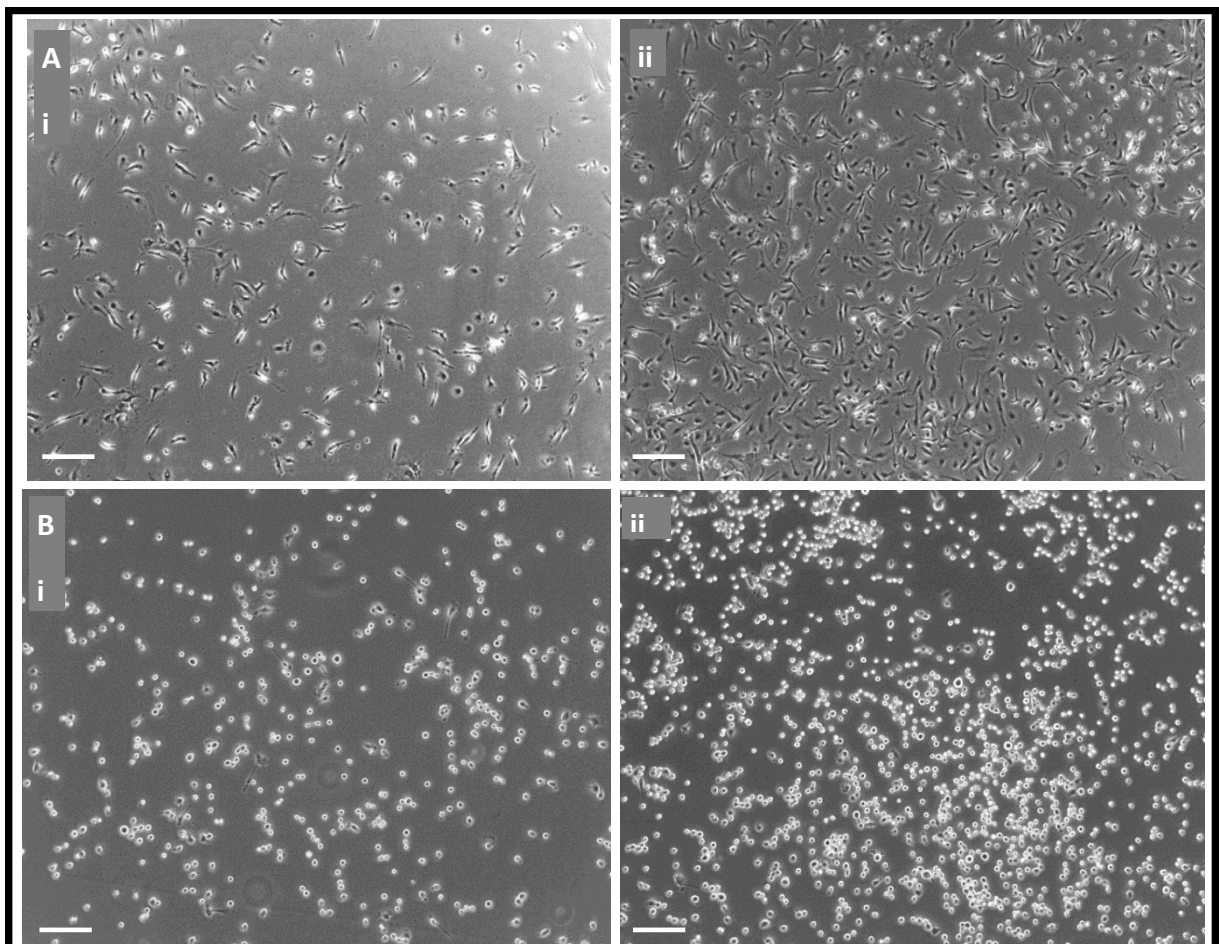


Fig.3.4: Distinct morphologies and proliferation rates of primary and BV2 cells. Representative phase-contrast images of purified primary cells after 1 or 3 weeks in culture post-immunomagnetic separation (A i & ii, respectively), or BV2 cells after 12 or 48 hours in culture post-passage (B i & ii, respectively). Scale bars (A & B) = 200 μ M.

3.2.1.1.2 Immunophenotype

As described above, FACS analysis of primary microglia and BV2 cells showed very similar patterns of staining for both of the microglial markers CD11b and CD45. This analysis was further extended to directly assess the relative expression of a panel of microglial markers on purified primary microglia and BV2 cells. Markers analysed (*as per* Section 2.3.1) were CD11b, CD45, CD200R, F4/80 antigen, Crry, C5aR and CD59a. Specific staining for each marker was detected on both cell types and is summarised in Figures 3.5-3.11 and Table 3.1.

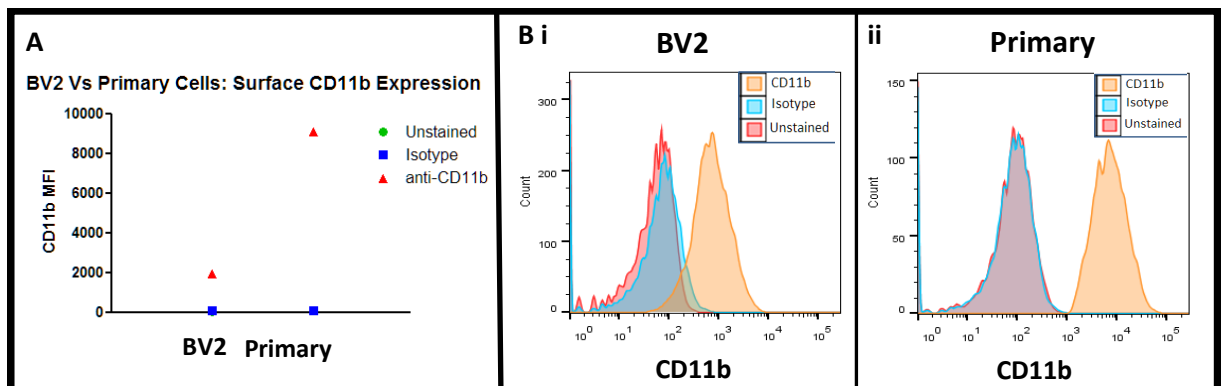


Fig.3.5: Flow cytometric analysis of surface CD11b expression by primary and BV2 cells. MACS + primary and BV2 cells were left unstained or incubated with fluorescently conjugated anti-mouse CD11b (M1/70) Ab or an appropriate isotype control and analysed by flow cytometry. (A) MFIs (+/- SDs; N ≥ 3); (B) Representative histograms of fluorescence quantified in (A) for BV2 (i) and primary cells (ii).

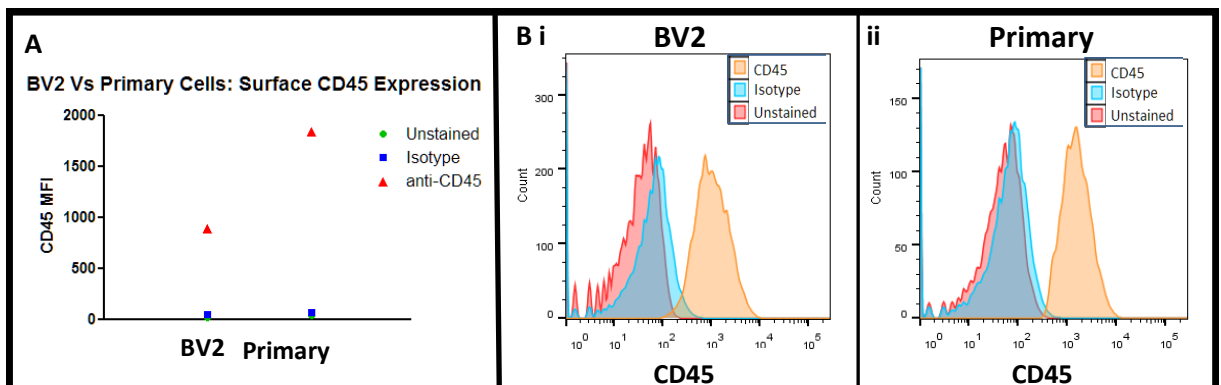


Fig.3.6: Flow cytometric analysis of surface CD45 expression by primary and BV2 cells. MACS + primary and BV2 cells were left unstained or incubated with fluorescently conjugated anti-mouse CD45 (30-F11) Ab or an appropriate isotype control and analysed by flow cytometry. (A) MFIs (+/- SDs; N ≥ 3); (B) Representative histograms of fluorescence quantified in (A) for BV2 (i) and primary cells (ii).

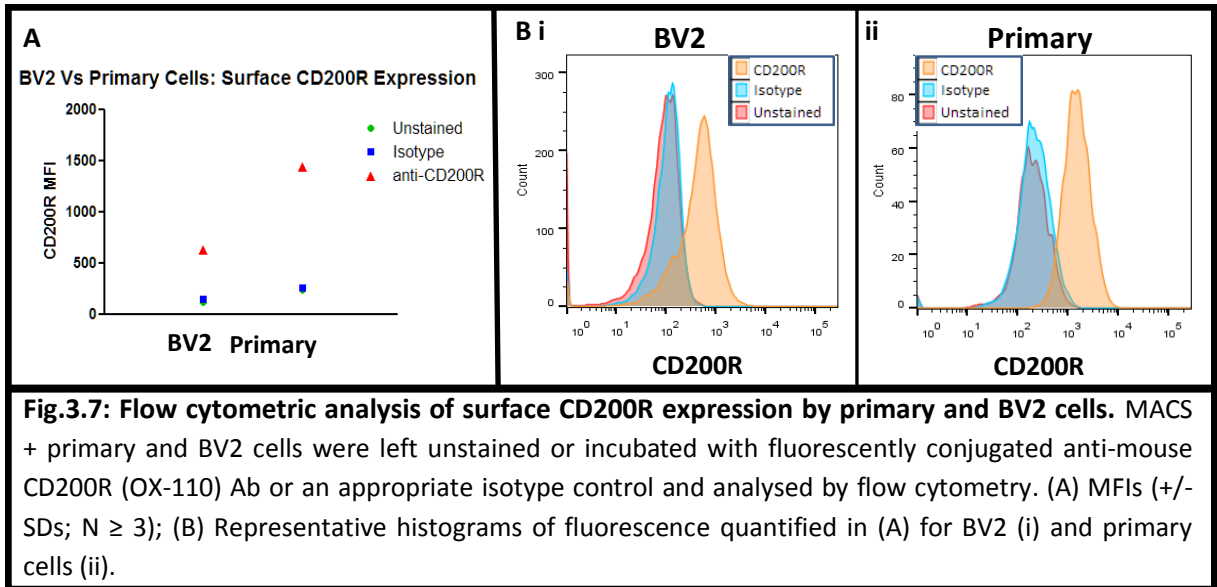


Fig.3.7: Flow cytometric analysis of surface CD200R expression by primary and BV2 cells. MACS + primary and BV2 cells were left unstained or incubated with fluorescently conjugated anti-mouse CD200R (OX-110) Ab or an appropriate isotype control and analysed by flow cytometry. (A) MFIs (+/- SDs; N ≥ 3); (B) Representative histograms of fluorescence quantified in (A) for BV2 (i) and primary cells (ii).

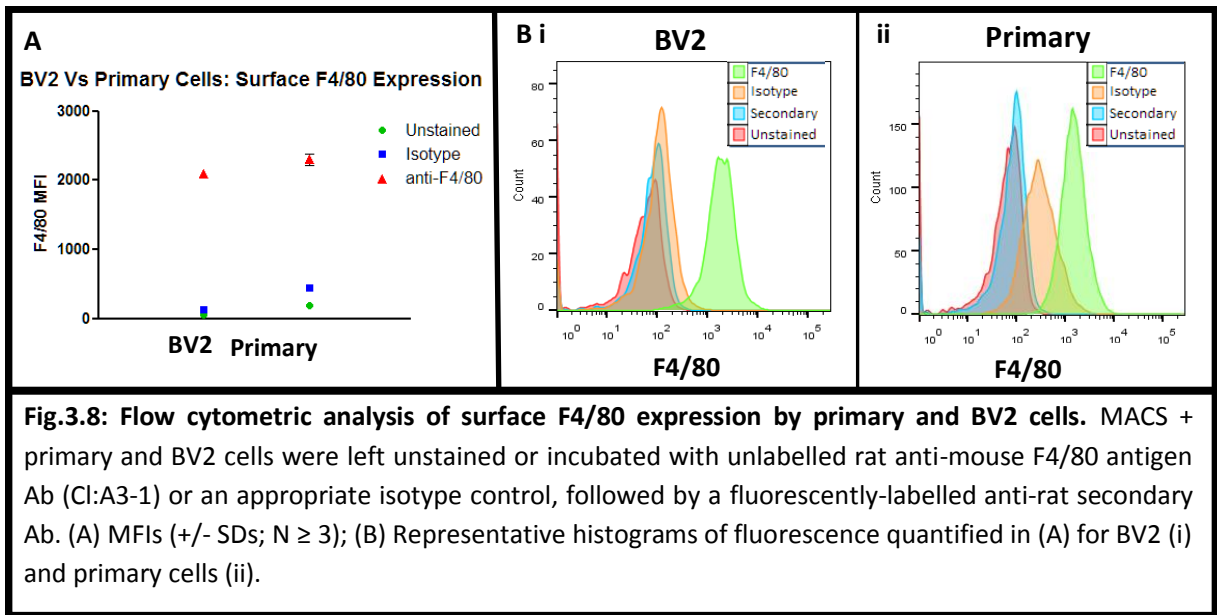


Fig.3.8: Flow cytometric analysis of surface F4/80 expression by primary and BV2 cells. MACS + primary and BV2 cells were left unstained or incubated with unlabelled rat anti-mouse F4/80 antigen Ab (Cl:A3-1) or an appropriate isotype control, followed by a fluorescently-labelled anti-rat secondary Ab. (A) MFIs (+/- SDs; N ≥ 3); (B) Representative histograms of fluorescence quantified in (A) for BV2 (i) and primary cells (ii).

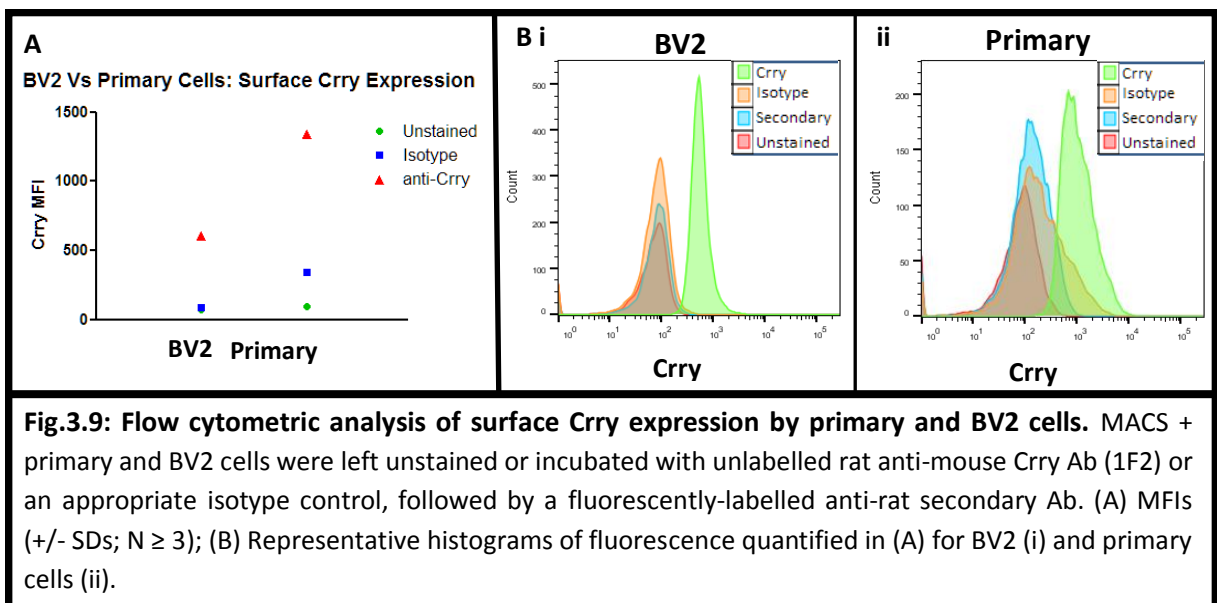
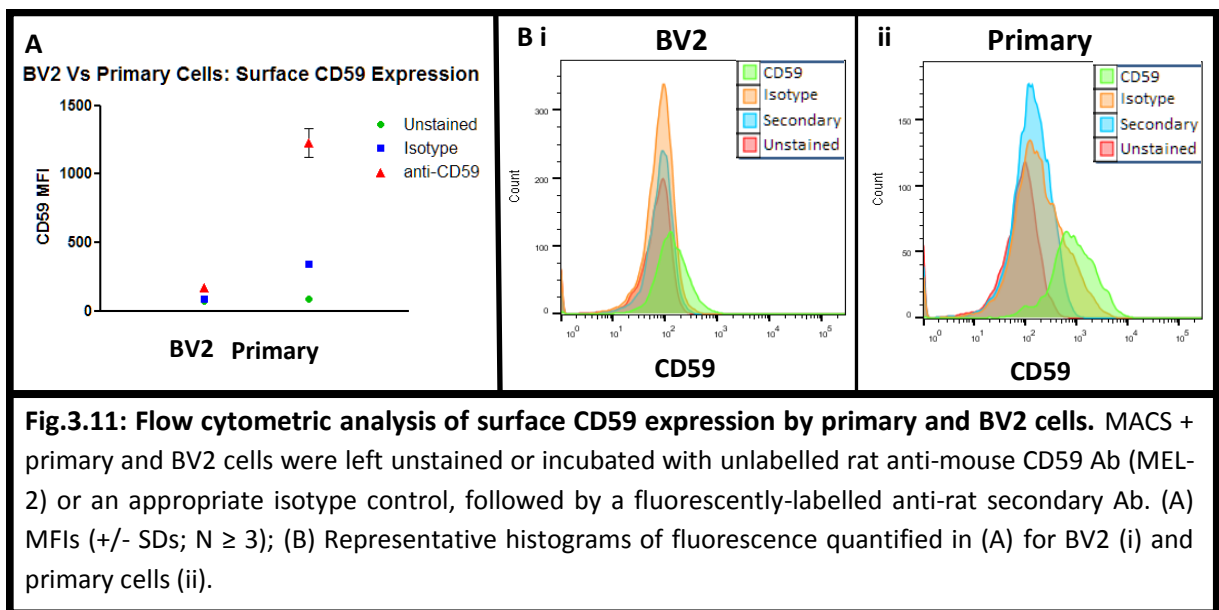
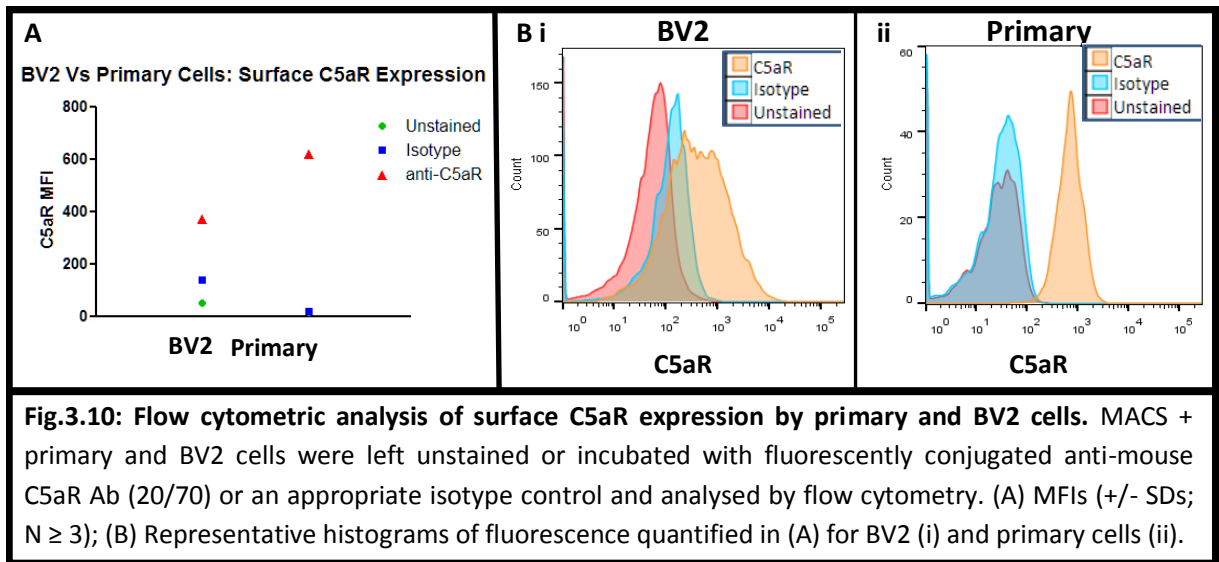


Fig.3.9: Flow cytometric analysis of surface Crry expression by primary and BV2 cells. MACS + primary and BV2 cells were left unstained or incubated with unlabelled rat anti-mouse Crry Ab (1F2) or an appropriate isotype control, followed by a fluorescently-labelled anti-rat secondary Ab. (A) MFIs (+/- SDs; N ≥ 3); (B) Representative histograms of fluorescence quantified in (A) for BV2 (i) and primary cells (ii).



With the exception of F4/80 antigen, primary microglial cells expressed higher levels of all surface markers than BV2 cells. In the case of CD11b/CR3, this could be of particular consequence, since investigation of the specific functional effects of microglial CR3 ligation by iC3b is a key aim of this study; these findings would suggest that primary cells would be better suited to highlighting the consequences of this interaction.

As the key regulator implicated in the C3-dependent mechanism of microglial priming reported by Ramaglia *et al.* (1), the phenotypic consequences of microglial Crry deficiency are a major focus of this study. Thus, the demonstration of Crry expression by FACS analysis on the surface of cultured primary and BV2 microglial cells (Fig.3.9; Table 3.1) is central to the work in this thesis. Higher expression of surface Crry by primary microglia is also significant, since this indicates that primary microglia will more readily illustrate the functional consequence of Crry deficiency and it is with primary cells cultured from CNS tissue from WT and Crry KO mice that the functional consequences of this deficiency in microglia are intended to be investigated.

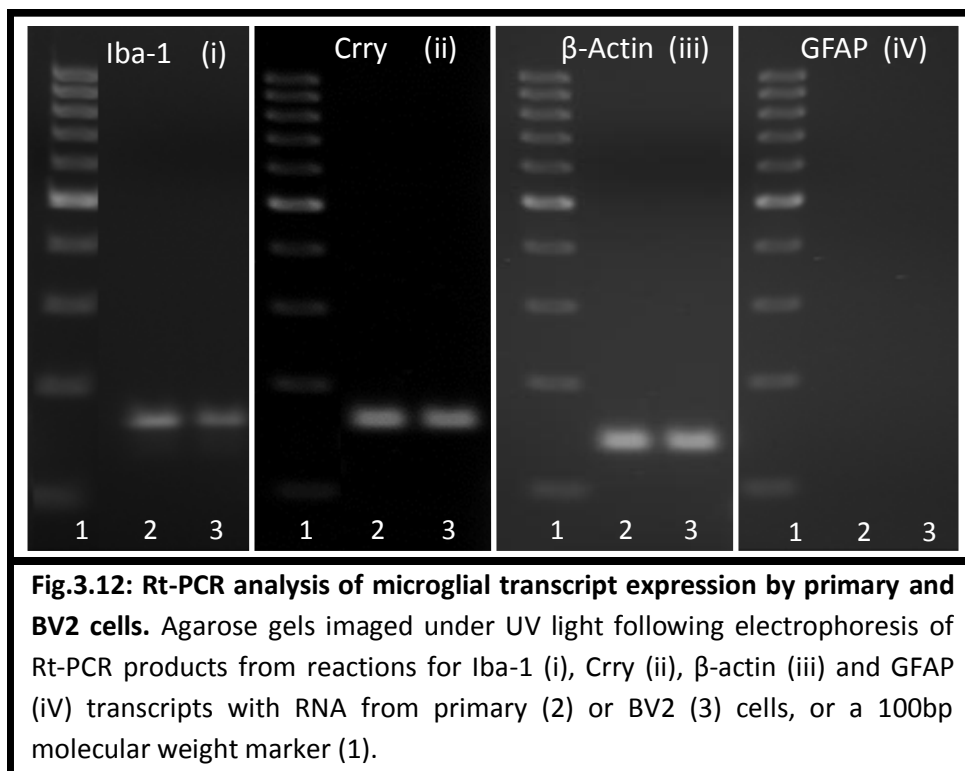
As illustrated in Figures 3.1 and 3.2, CD11b+ cells were negative for markers of other CNS cell types i.e. β -III tubulin (neuronal) and GFAP (astrocytic), whereas cells which were CD11b- were positive for those same markers of other CNS cell types.

Primary Cells					
Marker	Autofluorescence (MFI)	Background (MFI)	Test (MFI)	Signal – Background	Signal: Background
CD11b	81.6 +/- 0.90	88.9 +/- 2.69	9045 +/- 31.75	8956.1	101.7
CD45	41.6 +/- 0.50	69.8 +/- 1.62	1814 +/- 59.80	1744.2	25.9
CD200R	230 +/- 15.63	259 +/- 7.10	1425 +/- 40.38	1166	5.5
F4/80	198 +/- 15.10	439 +/- 17.52	2299 +/- 150.0	1860	5.2
Crry	98.7 +/- 18.16	345 +/- 25.50	1310 +/- 34.78	965	3.8
C5aR	12.8 +/- 0.26	20.5 +/- 0.13	616 +/- 17.01	595.5	30.1
CD59	85.3 +/- 8.65	358.5 +/- 26.01	1142 +/- 186.4	783.5	3.2
BV2 Cells					
Marker	Autofluorescence (MFI)	Background (MFI)	Test (MFI)	Signal – Background	Signal: Background
CD11b	52.5 +/- 0.31	59.8 +/- 4.50	1935 +/- 31.53	1875.2	32.3
CD45	17.2 +/- 1.47	45.4 +/- 0.72	886 +/- 7.50	840.6	19.5
CD200R	121 +/- 5.51	151.7 +/- 5.10	626 +/- 7.77	474.3	4.1
F4/80	61.7 +/- 5.10	127 +/- 4.73	2098 +/- 98.00	1971	16.5
Crry	74.3 +/- 7.51	88.1 +/- 6.51	605 +/- 20.21	516.9	6.8
C5aR	51 +/- 3.00	138 +/- 7.51	371 +/- 17.52	233	2.7
CD59	74.3 +/- 3.57	88.1 +/- 9.07	169 +/- 7.55	80.9	1.9

Table 3.1: Flow cytometric analysis of microglial marker expression by primary and BV2 cells. MFIs (+/- SDs) of primary and BV2 cells due to autofluorescence (Autofluorescence) or staining with a fluorophore-labelled (direct or indirect) antibody against the indicated marker/target (Test), or an appropriate isotype control (Background) (N \geq 3). Signal – Background = Test MFI – Background MFI; Signal : Background = Test MFI/Background MFI.

3.2.1.1.3 Microglial mRNA/Transcript Expression

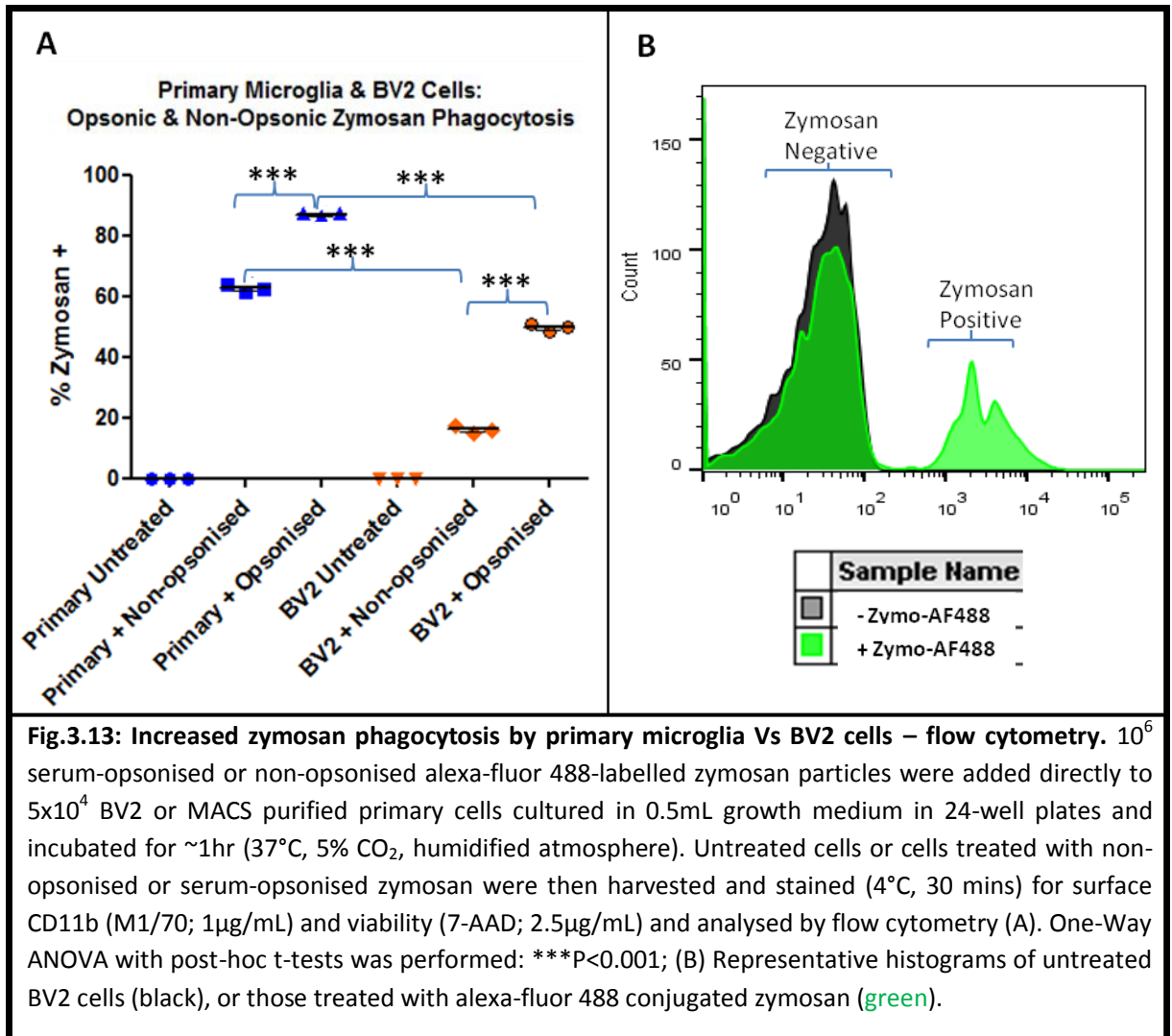
Purified primary microglia and BV2 cells were also assayed by Rt-PCR (*as per* Section 2.3.4) for expression of the transcripts for the microglial markers Iba-1 and Crry, along with β -actin and the astrocytic marker GFAP as positive and negative controls (respectively). Visualisation of PCR products following agarose gel electrophoresis revealed that both cell types were positive for the expression of the microglial marker Iba-1 and Crry transcripts, along with β -actin, but were negative for GFAP (Fig.3.12).



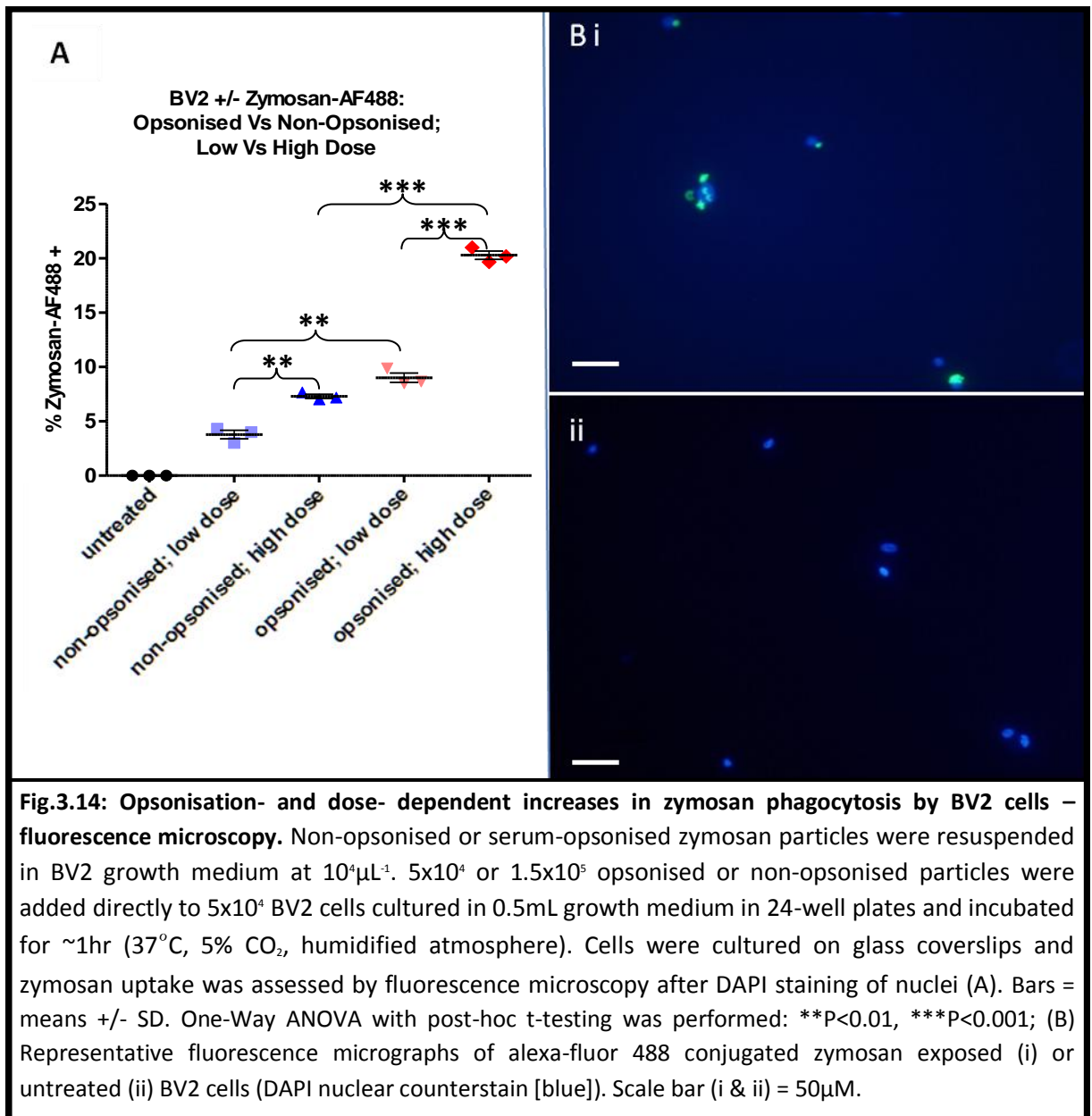
3.2.1.1.4 Zymosan Phagocytosis

As microglia are professional phagocytes (253, 254), purified primary and BV2 cells were also assayed for phagocytosis of both non-opsonised and serum-opsonised zymosan particles. Both cell types were exposed to equal amounts of non-opsonised or opsonised alexa-fluor 488 conjugated zymosan and assayed for the frequency of uptake by FACS analysis (as described in Sections 2.2.3.2.1 and 2.3.1 respectively). As expected, in the case of both cell types, serum opsonisation significantly increased the proportion of cells which were positive for ingested fluorescent zymosan (24.7% primary and 32.5% BV2, $P < 0.001^{***}$ for both). However, the level of ingestion of both non-opsonised and opsonised fluorescent zymosan was significantly higher for

primary compared with BV2 cells (non-opsonised: 61.95% primary vs. 16.65% BV2, $P < 0.001^{***}$; opsonised: 86.6% primary vs. 49.1% BV2, $P < 0.001^{***}$) (Fig.3.13).



Fluorescence microscopy of BV2 cells exposed to different amounts of alexafluor-488 conjugated zymosan particles (*as per* Sections 2.2.3.2.2 and 2.3.2 respectively) also demonstrated significantly increased uptake in an opsonisation- and dose- dependent manner (Fig.3.14).



3.2.1.1.5 LPS Responses

Purified primary and BV2 cells were exposed to LPS over a range of concentrations and times (as described in Section 2.2.1) and assessed for responses.

3.2.1.1.5.1 Secreted Effectors

Both cell types were assayed for the release of secreted effectors by ELISA for mouse IL-6 and TNF- α and Griess assay for nitrite (in accordance with Section 2.3.3).

3.2.1.1.5.1.1 Griess Assay

3.2.1.1.5.1.1.1 Dose Response

As demonstrated in Figure 3.15A, after 48 hours exposure to LPS, both cell types had a similar NO response LPS as determined by Griess assay. NO production increased with LPS concentration across similar ranges (max. nitrite concentration = 5.72 μ M and 4.40 μ M for BV2 and primary cells, respectively; basal nitrite concentration = 0.46 μ M and 1.44 μ M for BV2 and primary cells, respectively). For BV2 cells NO production continued to increase even at the maximum LPS doses whereas the response of primary cells plateaued at LPS concentrations of 1000ng/ml (Fig.3.15 Ai & Aii). The basal NO production of untreated primary cells was greater than that of untreated BV2 cells (1.44 μ M vs 0.46 μ M for primary and BV2 cells respectively). However, the maximal response of primary cells was lower than that of BV2 cell (max nitrite concentration - nitrite concentration untreated cells = 2.97 vs 5.27 μ M for primary and BV2 cells, respectively). Furthermore, while significant increases in nitrite concentrations above basal levels were detectable at LPS doses of 10ng/mL for BV2 cells (BV2 [nitrite] 10ng/mL – [nitrite] untreated = 0.73 μ M; P = 0.048*; Fig.3.15 Aii), detectable increases in nitrite levels produced by primary cells only emerged at 10-fold greater LPS doses (100ng/mL) and significant increases did not appear until doses of 1000ng/ml were used (Fig.3.15 Ai). However, as evidenced below, this may reflect the expansion of the BV2 cell line (which is dramatically more rapid than that of primary cells) during the course of the experiment, which invariably means that by the selected endpoint cell numbers are no longer in balance.

3.2.1.1.5.1.1.2 Time Course

To examine the effect of LPS on NO production over time a longitudinal experiment was carried out on both cells types using a mid-range dose of 1 μ g/mL LPS. Nitrite concentration increased over time in both primary and BV2 cells (Fig.3.15B i & ii, respectively). This is to be expected given that while NO itself is unstable, its product, nitrite (NO₂⁻; the Griess assay analyte), is stable and accumulates in the media. The fact that nitrite concentrations were continuing to increase even at the latest time points, indicates that induction of NO production was still ongoing in both cell types after 48 hours. Nitrite concentration did not increase significantly in untreated or BSA-treated (negative control) primary cells over time (Fig.3.15B i). However, in the case of control BV2 cells there was a modest increase in the level of nitrite in control cells over time (Fig.3.15B ii), (mean nitrite concentration at 72hr – mean nitrite concentration at 0hr = 3.45 and 0.65 μ M for untreated BV2 and primary cells, respectively; Fig.3.15B). Since the BV2 cell line proliferates at a much faster rate than primary cells and the basal nitrite level remains stable in primary cells, it is likely that the production of NO by untreated BV2 cells over time is a result of increasing cell numbers, with increased cellular stress at increased confluence probably playing a role. Indeed,

the fact that the increase in nitrite is far greater for both control and LPS-treated BV2 cells between the final time points (i.e. 48 and 72 hours) than any other equivalent period (nitrite concentration 72-48hr = 12.25 and 3.15 μM , 48-24hr = 1.75 and 0.1 μM , 24-0hr = 2.2 and 0 μM , for LPS and BSA treated BV2, respectively), indicates that their exponential proliferation is probably responsible for the increased production of NO by untreated BV2 cells (Fig.3.15B).

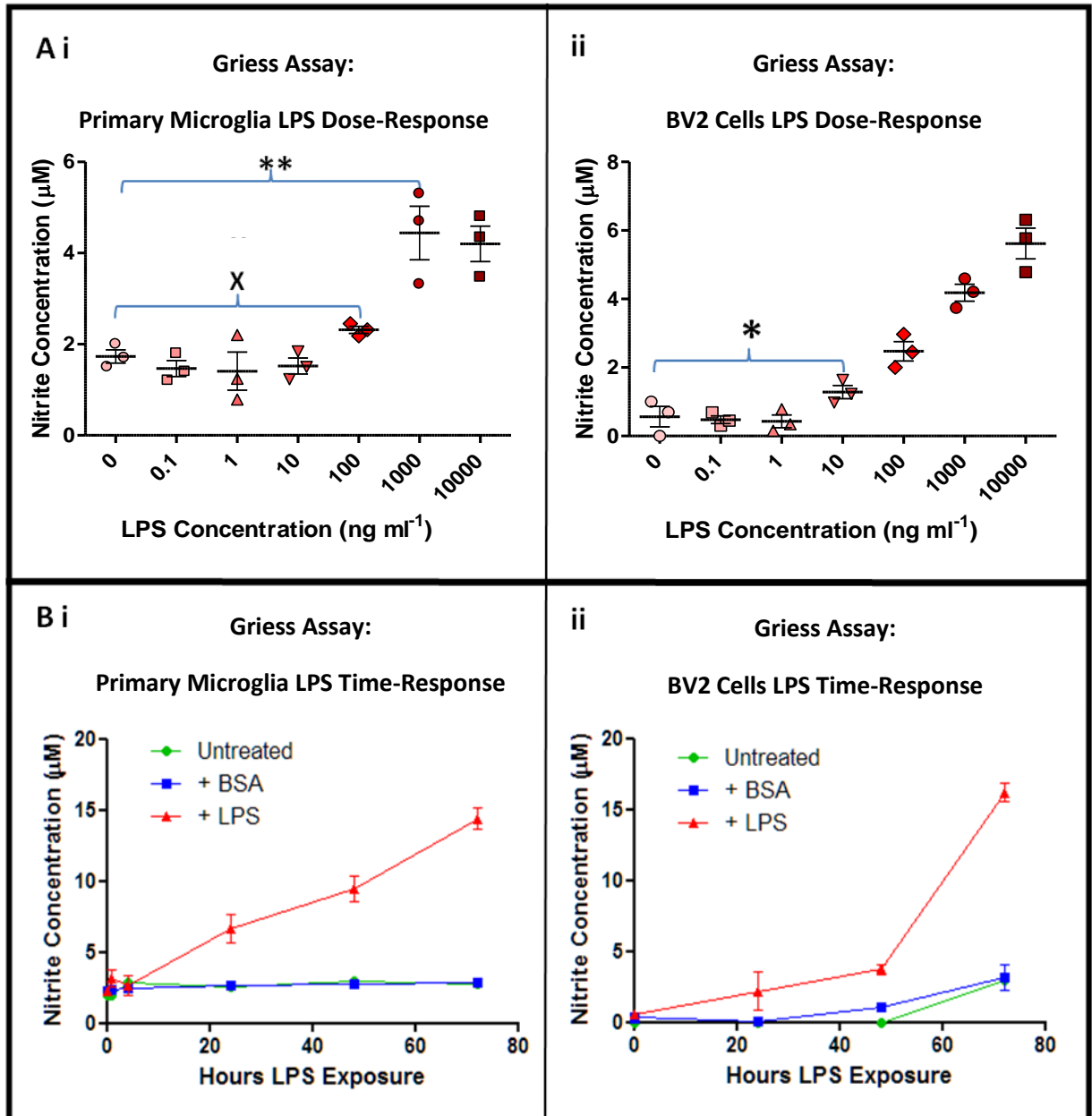


Fig.3.15: Nitric oxide production by primary and BV2 cells in response to LPS – dose and time responses. 2.5×10^5 primary microglia or BV2 cells cultured in 0.5mL growth medium in 24-well plates were treated with LPS concentrations ranging from 0-10,000ng/mL (deepening red) for 48 hours (A [data points represent individual replicates]) or $1\mu\text{g}/\text{mL}$ LPS for time periods ranging from 0-72 hours (B [bars = means +/- SD]) and supernatant nitrite levels determined by Griess assay. One-Way ANOVA with post-hoc t-testing was performed: X $P > 0.05$, * $P < 0.05$, ** $P < 0.01$.

3.2.1.1.5.1.2 TNF- α and IL-6 ELISAs

Primary microglia and BV2 cells were stimulated with LPS for 24h at concentrations ranging from 0-10 μ g/mL. Supernatants were then assayed by ELISA for IL-6 and TNF- α . Cytokine production increased with LPS concentration in both cell types, although the scale of increase and the point at which responses became significant, along with the basal level of production, differed for the two cell types and analytes.

The LPS-induced increases in cytokine production by BV2 cells were relatively modest, being in the order of hundreds of picograms per millilitre (BV max. TNF- α and IL-6 increase = 331.1 and 98.5 pg/mL, respectively). In contrast, the increases in cytokine production by primary microglia in response to LPS were several orders of magnitude greater (Tables 3.2 & 3.3; Fig.3.16).

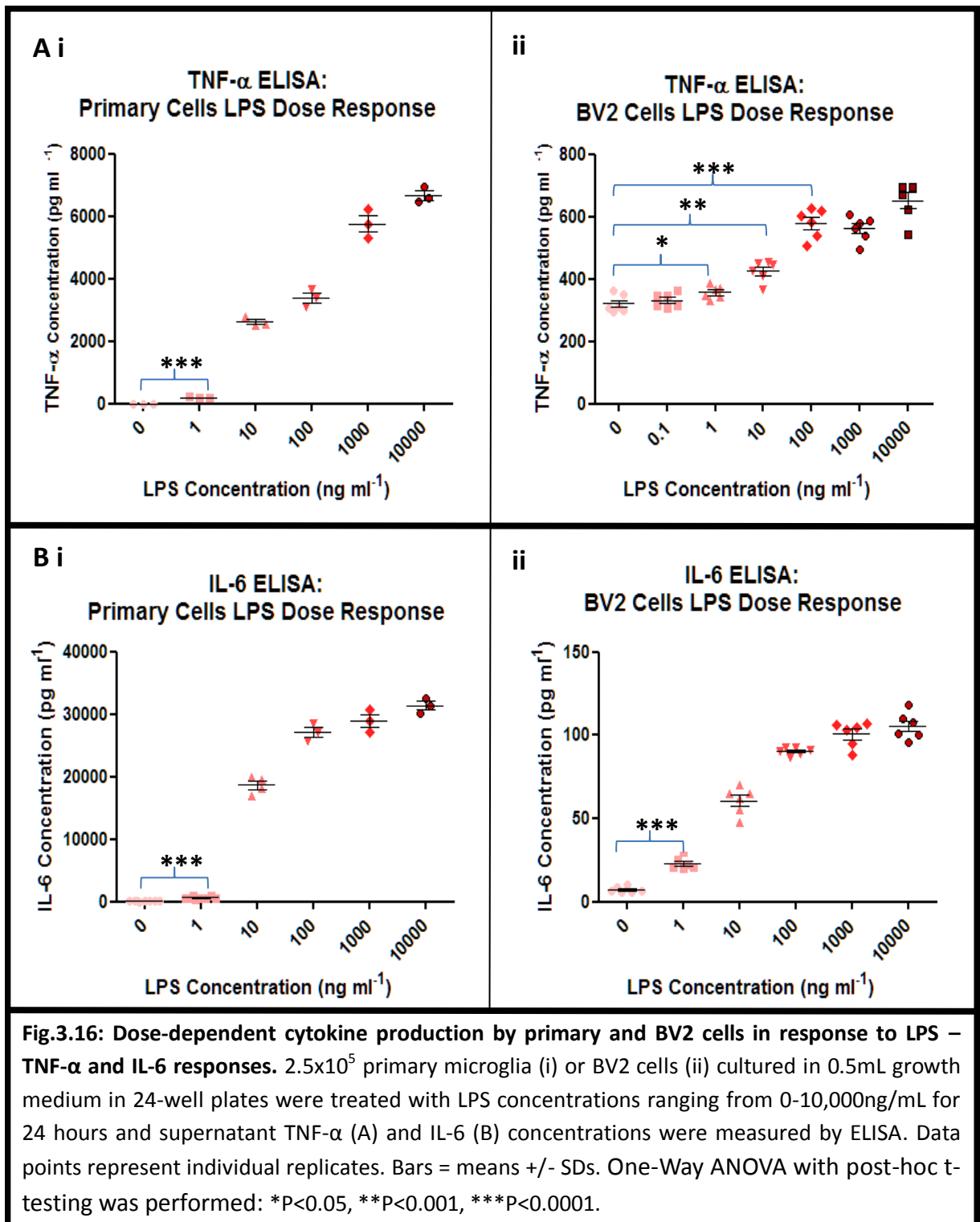
An LPS concentration of 1ng/mL resulted in a small but significant ($P = 0.0001$) cytokine induction from primary cells (198.0pg/mL and 544.9pg/mL for TNF- α and IL-6, respectively) while BV2 cells showed little cytokine production at this dose. LPS doses of 10ng/mL and above resulted in a much greater induction of IL-6 and TNF- α in primary microglia whereas responses in BV2 remained low (Tables 3.2 & 3.3; Fig.3.16).

TNF- α Concentration (pg/mL)						
Cell Type	LPS Concentration (ng/mL)					
	0	1	10	100	1000	10,000
BV2	321.4	357.0	425.0	578.8	561.0	652.5
Primary	0	198.0	2620.8	3385.5	5760.1	6582.0
IL-6 Concentration (pg/mL)						
Cell Type	LPS Concentration (ng/mL)					
	0	1	10	100	1000	10,000
BV2	7.5	23.0	60.2	88.4	100.5	106.0
Primary	89.6	634.5	18669.8	27097.1	28957.7	31342.1

Table 3.2: Microglial cytokine levels in response to different LPS concentrations (i). 2.5×10^5 primary microglia or BV2 cells cultured in 0.5mL growth medium in 24-well plates were treated with LPS concentrations ranging from 0-10,000ng/mL for 24 hours and supernatant TNF- α and IL-6 concentrations were measured by ELISA (N \geq 3).

TNF- α					
Cell Type	TNF- α increase 1ng/mL LPS (A)	TNF- α increase 10ng/mL LPS (B)	TNF- α increase 10 μ g/mL LPS (C)	B/A	C/A
BV2	35.6	103.6	331.1	2.9	9.3
Primary	198.0	2620.8	6582.0	13.2	33.3
IL-6					
Cell Type	IL-6 increase 1ng/mL LPS (A)	IL-6 increase 10ng/mL LPS (B)	IL-6 increase 10 μ g/mL LPS (C)	B/A	C/A
BV2	15.5	52.7	98.5	3.4	6.35
Primary	544.9	18580.2	31252.5	34.1	57.4

Table 3.3: Microglial cytokine increases in response to different LPS concentrations (ii). Increase (pg/mL; from baseline) in mean TNF- α and IL-6 concentrations for primary and BV2 cells (Table 3.2) following 24 hours exposure to LPS concentrations of 1(A), 10(B) and 10,000(C) ng/mL LPS.



3.2.1.1.5.2 *Surface Marker Expression*

3.2.1.1.5.2.1 *Flow Cytometric Analysis*

Purified primary microglia and BV2 cells were assayed for changes in surface CD11b and C5aR by FACS (*as per* Section 2.3.1) after exposure to LPS at different concentrations and time-points (Fig.3.17 A & B). Exposure to 1 μ g/mL LPS caused increases in surface CD11b expression on both primary and BV2 cells, with these changes becoming significant at 12 hours (CD11b MFI at 12hrs = 108.0% and 113.7% Vs baseline, P = 0.008 and 0.008 for BV2 and primary, respectively; CD11b MFI at 6hrs = 101.7% and 105.0% Vs baseline, P = 0.315 and 0.165 for BV2 and primary, respectively) and continuing to increase over the next 36 – 60 hours. The relative increase in surface CD11b was consistently greater for primary microglia, ~2-fold higher than on BV2 cells at each time-point (Table 3.4; Fig.3.17A). Stimulation of primary microglia and BV2 cells with different concentrations of LPS for 48 hours also resulted in increases in surface CD11b and C5aR (Table 3.5; Fig.3.17B). In the case of BV2 cells surface CD11b and C5aR levels continued to increase steadily with LPS concentration across the range tested (0-10 μ g/mL). However, the surface CD11b and C5aR levels on primary cells increased dramatically between LPS doses of 1-10ng/mL and then plateaued and decreased slightly at higher LPS concentrations. These effects closely resembled those observed in the cytokine responses of primary and BV2 cells following stimulation with different concentrations of LPS (Tables 3.2 & 3.3; Fig.3.16). Also mirroring the changes in cytokine production, the increases in surface CD11b and C5aR were greater for primary cells, particularly at the later (\geq 24hr) time-points and higher (\geq 10 ng/mL) LPS concentrations. The scale of the relative changes in surface CD11b and C5aR were comparable between cell types (max increase in CD11b and C5aR MFI ~1.5- and ~2- fold Vs. baseline for BV2 and primary cells, respectively). Histograms depicting CD11b and C5aR staining of untreated and LPS stimulated primary cells illustrate the clear separation between populations stained with fluorophore-conjugated anti-CD11b and anti-C5aR antibodies, with very low background staining with appropriate isotype control antibodies (Fig.3.17C), thus demonstrating specificity of staining and an increase in these surface markers with LPS stimulation.

CD11b MFI % Vs Baseline								
Cell Type	LPS Exposure (Hrs)							
	0	2	4	6	12	24	48	72
BV2	100.0	96.0	100.0	101.7	108.0	114.0	158.7	150.7
Primary	100.0	96.7	100.0	105.0	113.7	136.3	202.3	222.7

Table 3.4: Microglial surface CD11b expression in response to LPS - time-Course. Percent Vs baseline of CD11b MFI (as determined by FACS analysis; N = 3) for BV2 and primary cells following exposure of 2.5×10^5 cells to LPS ($1 \mu\text{g}/\text{mL}$) for time-points ranging from 0-72 hours.

CD11b MFI % Vs Baseline								
Cell Type	LPS Concentration (ng/mL)							
	0	0.1	1	10	100	1000	10,000	
BV2	100.0	101.8	113.3	127.9	136.9	155.5	150.0	
Primary	100.0	107.3	115.9	198.1	174.7	172.7	172.8	

C5aR MFI % Vs Baseline								
Cell Type	LPS Concentration (ng/mL)							
	0	0.1	1	10	100	1000	10,000	
BV2	100.0	102.0	116.5	121.5	137.5	144.0	153.0	
Primary	100.0	96.8	122.2	208.1	220.8	197.5	176.6	

Table 3.5: Microglial surface CD11b and C5aR expression in response to LPS – dose-response. Percent Vs baseline of CD11b and C5aR MFI (as determined by FACS analysis; N = 3) for BV2 and primary cells following exposure (48hr) of 2.5×10^5 cells to LPS concentrations ranging from 0-10,000ng/mL.

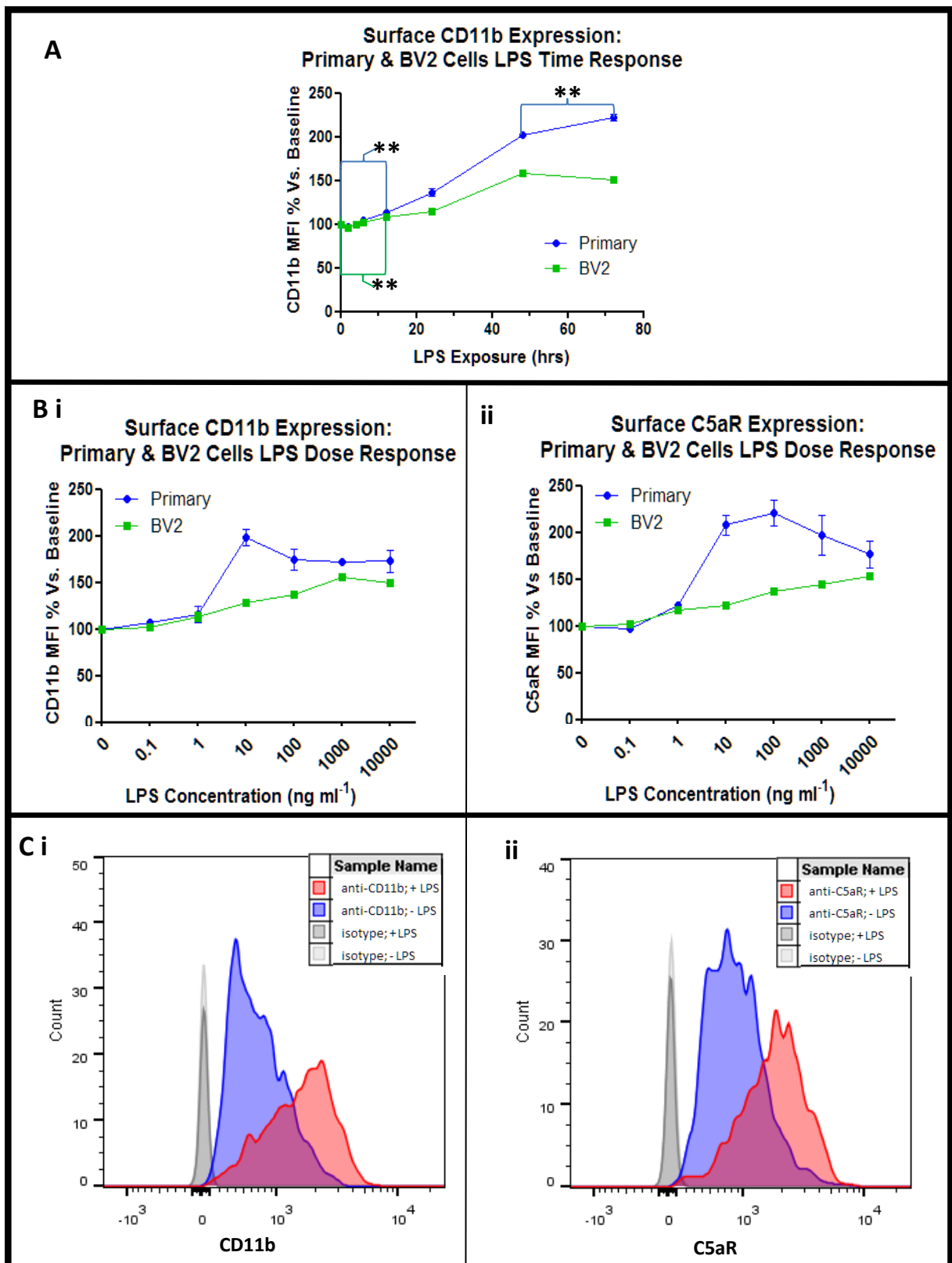
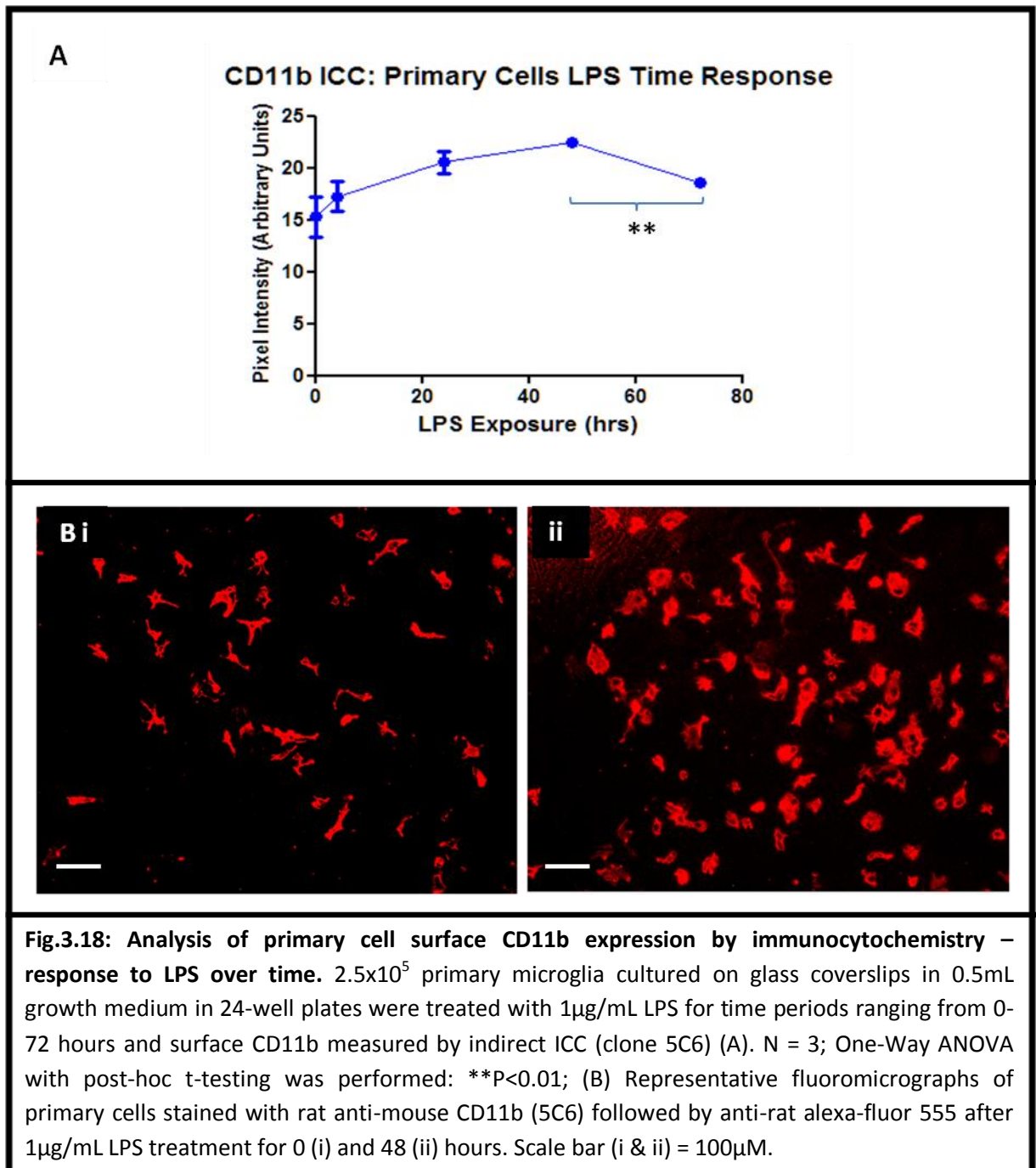


Fig.3.17: Flow cytometric analysis of change in primary and BV2 cell surface markers in response to LPS – dose and time responses. 2.5×10^5 primary microglia or BV2 cells cultured in 0.5mL growth medium in 24-well plates were treated with $1 \mu\text{g}/\text{mL}$ LPS for time periods ranging from 0-72 hours (A) or LPS concentrations ranging from 0-10,000ng/mL for 48 hours (B) and surface CD11b (A & Bi) and C5aR (Bii) measured by flow cytometry. Values are expressed as MFI % vs baseline; $N \geq 3$; bars = means (\pm SDs); One-Way ANOVA with Bonferroni post-testing was performed: $**P < 0.01$ (results of post-tests shown on graph [see Methods 2.5]). ANOVA: Primary – $P < 0.001$, $F = 782.2$; BV2 – $P < 0.001$, $F = 222.3$ (C) Representative histograms of primary cells stained with fluorophore conjugated anti-CD11b (i) or C5aR (ii) antibodies, or appropriate isotype controls, after treatment with or without 10ng/mL LPS for 48 hours.

3.2.1.1.5.2.2 ICC Analysis

Purified primary cells were assayed for changes in surface CD11b expression by fluorescent ICC (*as per* Section 2.3.2) in response to stimulation with 1 μ g/mL LPS for different time periods ranging from 4 to 72 hours. In alignment with the results of FACS analysis detailed above, increased CD11b was detected by ICC in response to LPS exposure (Fig.3.18). The profile of the response over time was similar to that observed through FACS analysis (Table 3.4; Fig.3.17A): increased expression was apparent within a few hours post-LPS treatment and reached a maximum around 48 hours (Fig.3.18A). However, in contrast to FACS analysis, ICC showed a significant decrease in the CD11b signal at 72 hours relative to 48 hours post-LPS treatment (CD11b MFI Vs. baseline 72hr – CD11b MFI Vs baseline 48hr ICC = -25.5%, P = 0.009; CD11b MFI Vs. baseline 72hr – CD11b MFI Vs baseline 48hr FACS (primary) = 20.4%, P = 0.007). Furthermore, the scale of the changes in CD11b levels detected by ICC was significantly reduced, with a maximum increase of less than half that detected by FACS analysis (max. MFI % increase Vs baseline = 47.0% and 122.7% for ICC and FACS, respectively; P = 0.001). BV2 cells were not assayed by ICC since a large proportion of cells were lost from glass coverslips during processing. Although broadly similar, the discrepancy between the results of FACS and ICC quantitative assays of surface CD11b expression is perhaps not surprising given the limitations of microscopy-based techniques for quantitative assessment relative to FACS. Indeed, while ICC/microscopy is ideally suited to-, and of great utility in-, assessing the spatial location along with physical and molecular nature of cellular markers, it is not ideally suited to their quantitative assessment (255), while the inverse is true of conventional FACS analysis (256). Therefore, the FACS based assays of surface markers described previously (Section 3.2.1.1.2) shall be used for further quantitative assessments, whereas microscopy shall be used for any further studies of the parameters mentioned above.



3.2.1.1.5.3 Immune-Related Transcript Expression

BV2 cells were stimulated with $1 \mu\text{g}/\text{mL}$ LPS for 24hrs followed by RNA extraction and Rt-qPCR to assay changes in the transcript/mRNA levels of microglial activation markers, cytokines, inflammatory enzymes and complement components (as described in Section 2.3.4).

To confirm integrity and correct molecular weight, RNA preparations and PCR products from LPS stimulated and control BV2 cells were separated by agarose gel electrophoresis and visualised under UV. Imaging revealed RNA preparations of consistent and expected appearance: lanes showed two sharp bands with molecular weights corresponding to the 28S ($\sim 5\text{Kb}$) and 18S ($\sim 2\text{Kb}$) rRNAs in a ratio of roughly 2:1 (respectively); a faint smear was present between the bands, representing other mRNA species (Fig.3.19).

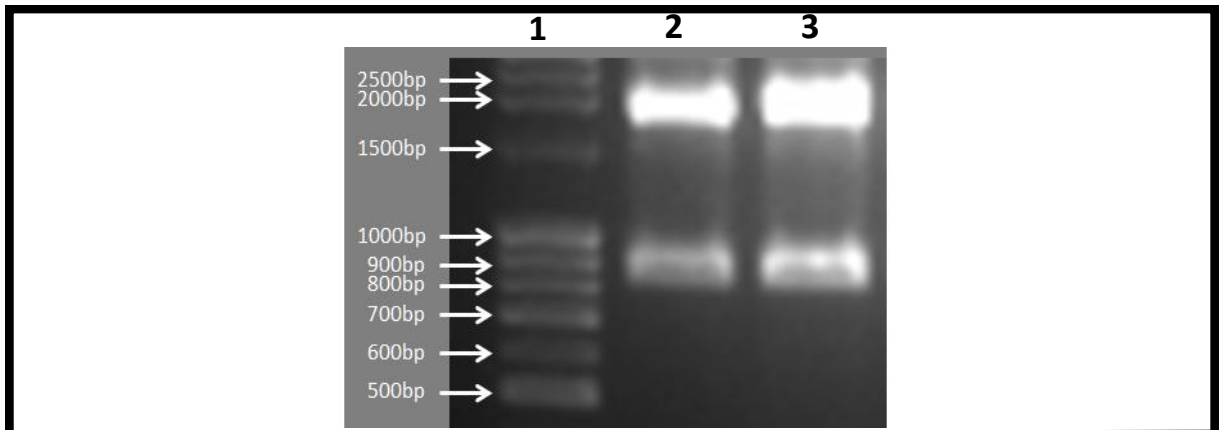


Fig.3.19: Confirmation of RNA integrity. RNA was extracted from 2.5×10^5 untreated BV2 cells cultured in 0.5mL growth medium in 24-well plates or cells treated with $1 \mu\text{g/mL}$ LPS for 24 hours, using the geneElute mammalian total RNA extraction kit (Sigma-Aldrich) and $1 \mu\text{g}$ subjected to agarose gel electrophoresis (1.2% w/v gel) and imaged under UV light (2 & 3, untreated & LPS, respectively). A molecular weight marker was also included (1; dsDNA).

Spectrophotometric analysis was used to determine RNA concentration and assess purity of preparations; 260/280 ratios were consistently of the order of 2.0 indicating suitable purity of RNA preparations. Electrophoretic analyses of PCR products confirmed the generation of a single molecular weight product *per* reaction indicating the specificity of qPCR. Each PCR product was of the expected molecular weight as defined by the source publications of primer sequences and/or primer BLAST analysis (Fig.3.20).

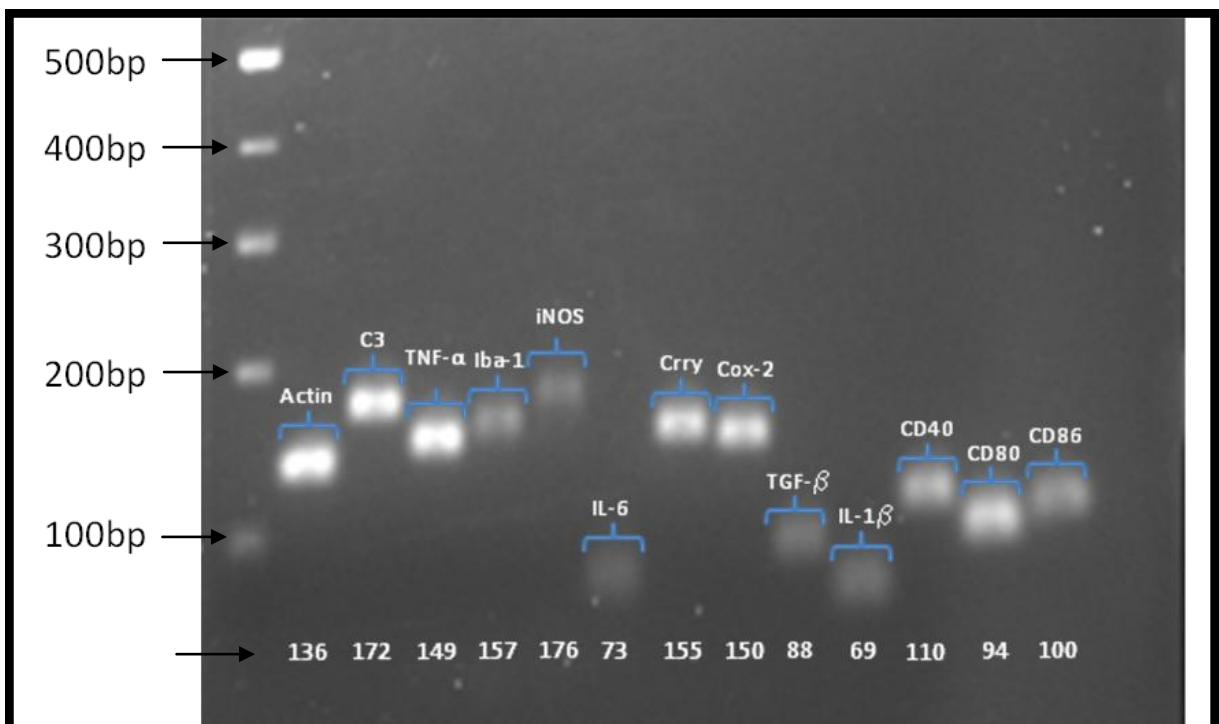


Fig.3.20: Confirmation of PCR specificity. BV2 cell RNA was subjected to RT using the TaqMan RT reagents (Applied Biosystems) and then 32ng RNA equivalent of cDNA was used in qPCR as a template along with gene specific primers (as indicated) in $20 \mu\text{L}$ reactions using SYBR green Jump-Start Taq-ready mix (Sigma-Aldrich). $12.5 \mu\text{L}$ of the PCR product mixed 1:1 with DNA loading dye was then subject to electrophoresis on a 2% (w/v) agarose gel and imaged under UV light. A 100bp-ladder molecular weight marker was also included (1).

With the exception of COX2 and CD86 (57.3% and 8% below baseline, respectively), all of the transcripts assayed increased in relative frequency in response to LPS. The scale of increases in transcript frequencies was broad, ranging from a few percent (e.g. iNOS = 6.5% above baseline) to several-fold (e.g. IL-6, Iba-1 and C3 = 396.8%, 553.8% and 469.5% above baseline, respectively) (Fig.3.21; Table 3.6). Notably, the relative changes detected in the frequency of transcripts for pro-inflammatory cytokines TNF- α and IL-6 in response to LPS treatment in BV2 cells closely mirrored the data obtained for the secreted molecules as determined by ELISA (Table 3.2; Fig.3.16ii). An approximately 4-fold increase in the frequency of IL-6 transcripts was detected compared with a ~2-fold increase for TNF- α (IL-6 and TNF- α transcript frequency = 396.8% and 86.0% above baseline, respectively), while a ~12-fold greater level of IL-6 protein was detected in the BV2 supernatant after 24 hours in response to 1 μ g/mL LPS, compared with a ~2-fold greater level of TNF- α . These results also reflect those obtained by ELISA analyses for TNF- α and IL-6 on supernatant from primary microglia, where a greater increase in the levels of IL-6 from LPS stimulated cells was detected compared with those of TNF- α (e.g. [IL-6] and [TNF] 24hr LPS 1 μ g/mL = 28.9 μ g/mL and 5.8 μ g/mL above baseline, respectively; Table 3.2, Fig.3.16i).

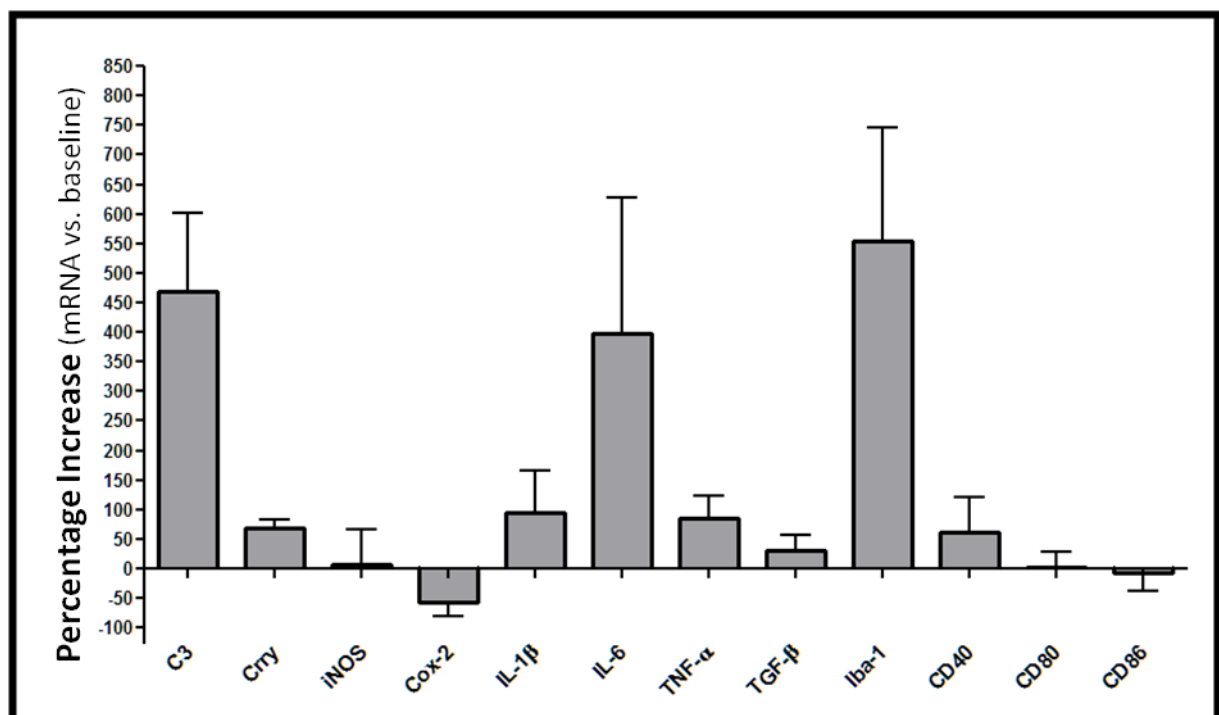


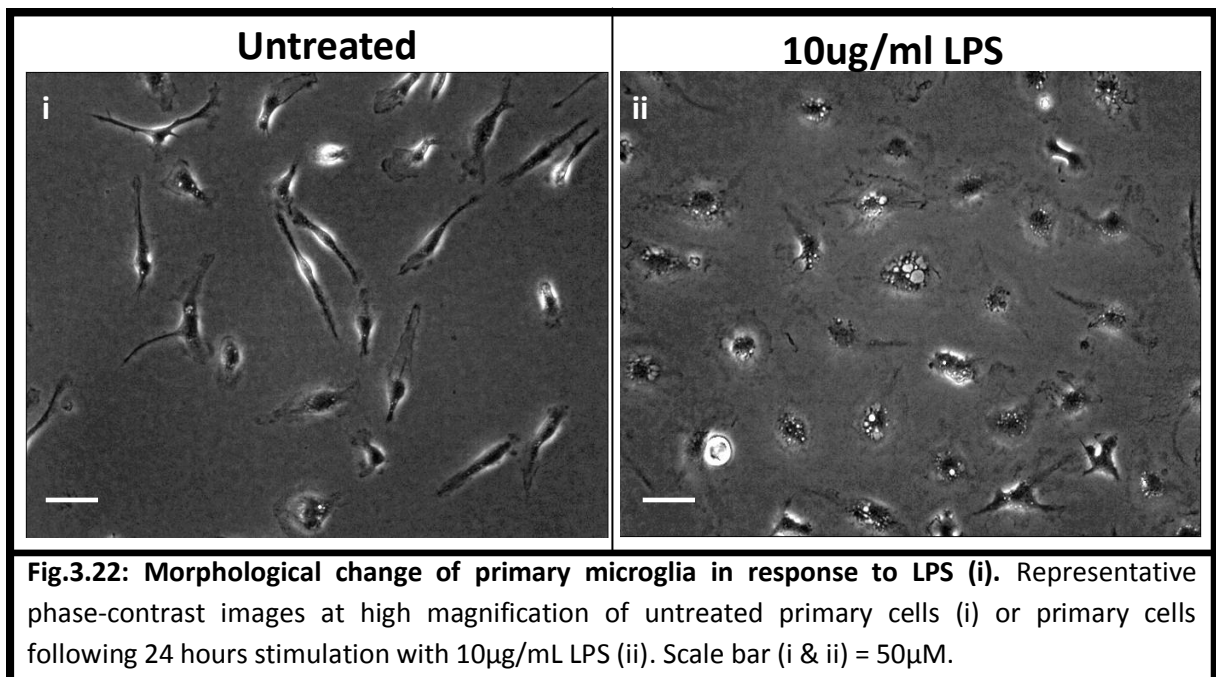
Fig.3.21: Induction of transcripts following microglial LPS treatment. RNA was extracted from 2.5×10^5 untreated BV2 cells cultured in 0.5mL growth medium in 24-well plates or cells treated with 1 μ g/mL LPS for 24 hours and subjected to RT using the TaqMan RT reagents (Applied Biosystems). 32ng RNA equivalent of cDNA was then used in qPCR as a template along with gene specific primers (as indicated) in 20 μ L reactions using SYBR green Jump-Start Taq-ready mix (Sigma-Aldrich). Difference in the relative transcript expression was determined by the $\Delta\Delta C_t$ method (β -Actin served as the reference gene). Mean increase (+/- SD) of LPS treated Vs baseline; N = 4.

BV2 mRNA Mean % Increase in Response to LPS Treatment											
Gene											
C3	Crry	iNOS	COX-2	IL-1 β	IL-6	TNF- α	TGF- β	Iba-1	CD40	CD80	CD86
469.5	68.5	6.5	-57.3	93.8	396.8	86.0	31.3	553.8	61.3	1.0	-8.0

Table 3.6: BV2 transcriptional responses to LPS exposure. Mean percentage increase (Vs baseline/untreated cells) in BV2 cell transcripts (as indicated) following treatment with 1 μ g/mL LPS for 24 hours, as determined by Rt-qPCR (N = 4).

3.2.1.1.5.4 Morphological Change

Purified primary microglia were subjected to LPS exposure (0.1–10,000ng/mL) for 24 hours and assessed for changes in morphology by phase-contrast microscopy. High magnification imaging of unstimulated cells and those treated with the highest LPS dose clearly demonstrated the dramatic effect of LPS exposure on cell morphology (Fig.3.22). LPS treatment resulted in a dose-dependent shift in cell morphology from a ramified form with a relatively small cell body to an amoeboid form with a relatively large cell body, with the transition occurring between doses of 1 and 100ng/mL and becoming global by 1000ng/mL (Fig.3.23). A distinct morphological change was also apparent in images from the fluorescent ICC CD11b expression analysis in response to LPS treatment described above (Fig.3.18B). BV2 cells were not assayed for morphological changes in response to LPS exposure since preliminary experiments showed an absence of any detectable alterations (unsurprising given the properties of activated microglia which they display (241)); the rapidly proliferating BV2 cells continue to proliferate and maintain a rounded morphology even at the highest LPS doses (data not shown).



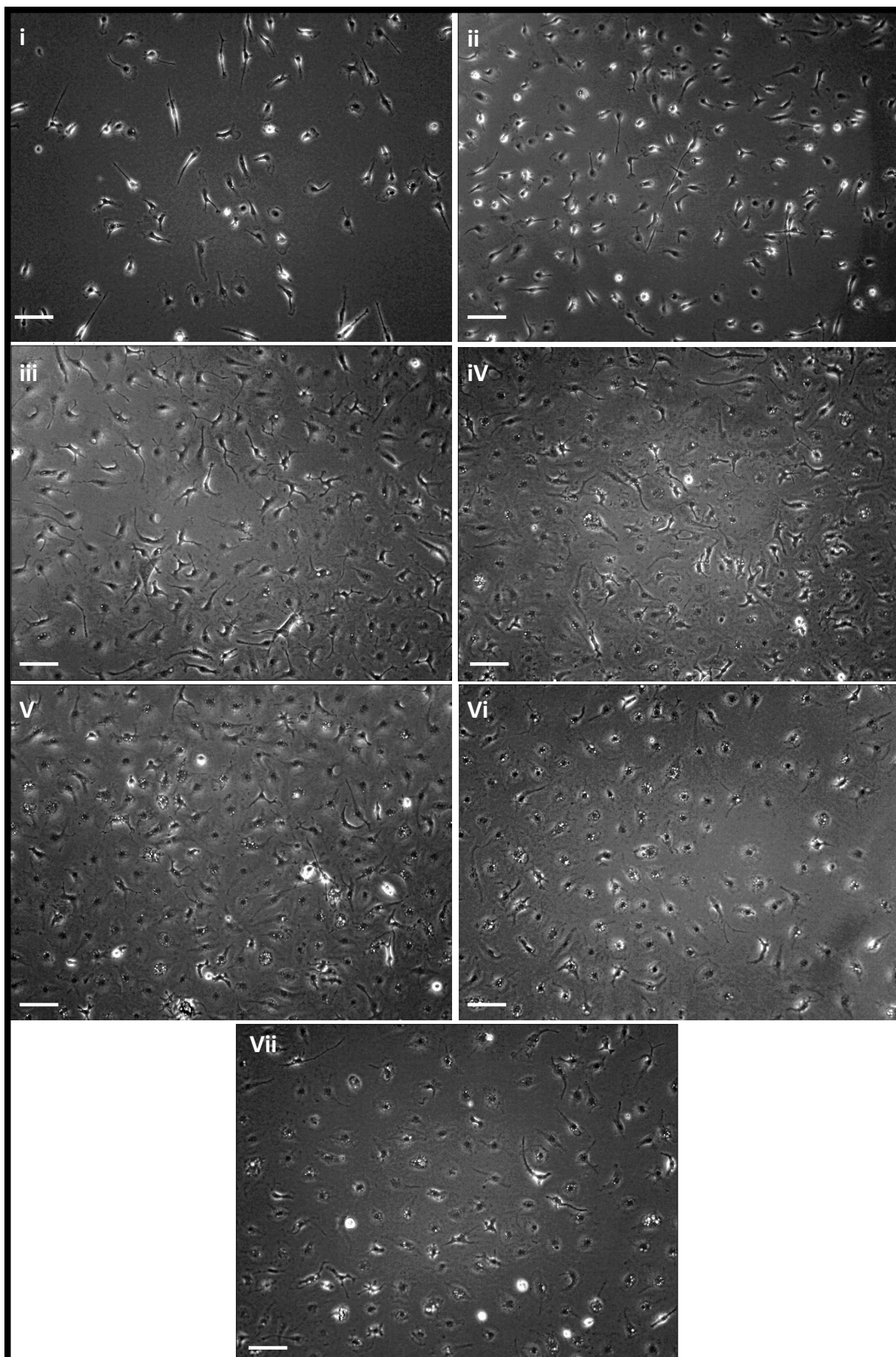


Fig.3.23: Morphological change of primary microglia in response to LPS (ii). Representative phase-contrast images of untreated primary cells (i) or primary cells following stimulation for 24 hours with LPS concentrations starting at 0.1ng/mL and increasing by a factor of Log_{10} up to a maximum of 10 $\mu\text{g/mL}$ (ii-Vii, respectively); Scale bar (i-Vii) = 100 μM .

3.2.2 Mixed Vs Pure Microglial Cultures: Surface CD11b LPS Response

In-order to assess the influence of neuronal-microglial surface interactions in modulating microglial responses, the surface expression of CD11b was assayed by flow cytometry (Section 2.3.1). This was carried out at baseline and following stimulation with LPS for 48 hours at concentrations between 0.1ng/mL and 10 μ g/mL (Section 2.2.1). Both MACS purified primary microglia and primary microglia maintained in mixed CNS cultures were used. This assay was chosen because, unlike those which measure the bulk release of effector molecules (e.g. ELISA), it permits the characterisation of microglial specific responses in a mixed culture system. As shown in Figure 3.1, microglia constituted the majority (~65%) of cells in these mixed CNS cultures, while a significant proportion (~15%), were neurones. Since neurones have a dramatically larger volume than microglia, and neurones occupy more than half the CNS space (257), extensive neuronal-microglial surface interactions can be expected. Little difference was observed in baseline expression of CD11b on microglia in isolation and mixed culture, but the pattern of expression in response to LPS was different in that the increase in CD11b on primary microglia maintained in mixed CNS cultures was ~2-fold greater than that observed on isolated primary microglia at all LPS concentrations tested (Fig.3.24).

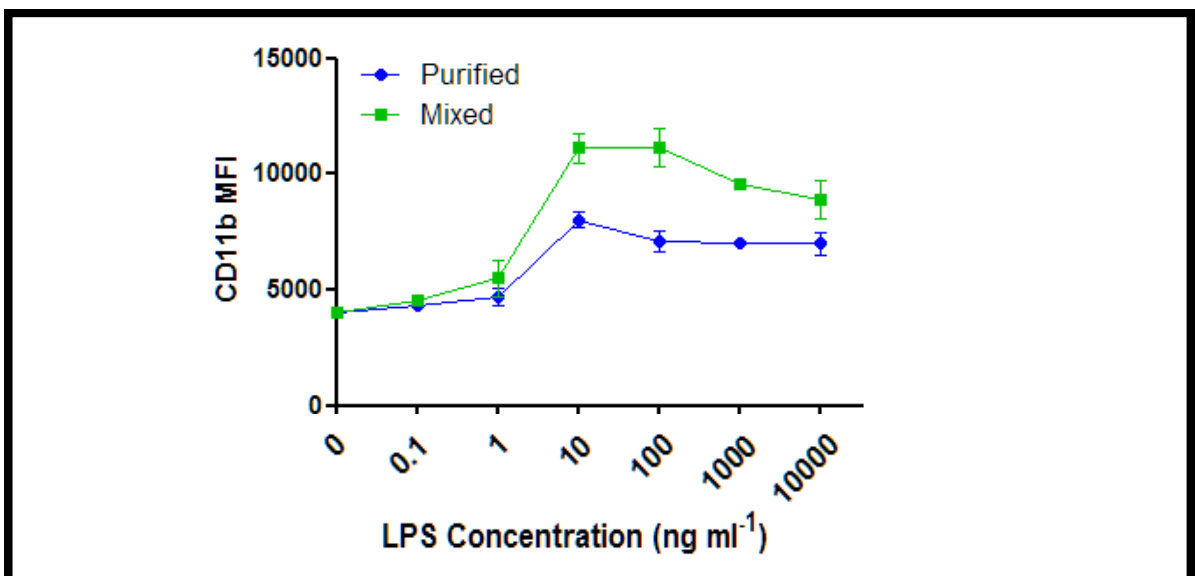


Fig.3.24: Flow cytometric analysis of change in microglial surface CD11b in response to increasing LPS concentration - pure Vs mixed CNS culture. 2.5x10⁵ MACS sorted primary microglia (purified) or mixed CNS cells derived from whole brain homogenate (mixed) in 0.5mL growth media in 24-well plates were treated with LPS concentrations ranging from 0-10,000ng/mL for 48 hours and surface CD11b assayed by flow cytometry (clone M1/70). MFI (+/-SDs); N \geq 3.

3.3 Discussion

3.3.1 Primary Adult Murine Microglia: Culture, Phenotyping and Activation

The principle aims of the work set out in this chapter were to: 1) establish a system for the culture of pure adult murine microglial populations that supported their proliferation and maintenance of a quiescent state; 2) develop assays to characterise cell phenotype and the response to a known activator i.e. LPS; 3) compare primary microglia with a well-described microglial cell line (BV2). These aims were necessary prerequisites to the overarching aims of this thesis relating to the mechanisms of C-mediated microglial priming.

The culture of pure, adult, phenotypically and responsively normal primary microglia over extended periods in sufficient numbers for experimental investigation constitutes a significant challenge. In order to achieve this aim, features of two published adult microglial culture protocols (232, 238) were incorporated into a procedure which also included an immunomagnetic/MACS sorting step. The microglial cultures generated through these modifications of the established procedures were shown by multiple techniques to be of high purity and consisted of cells with a ramified/branching morphology, consistent with that observed in resting microglia *in vivo* (173, 178). These cultured cells were able to survive and gradually proliferate. Cultured primary cells were phenotyped by various assays alongside the widely employed BV2 murine microglial cell line in-order to confirm their identity as microglia and establish similarities and differences with the cell line. Immuno-phenotypic studies demonstrated the presence of numerous microglial cell surface markers on the purified microglia and conversely, an absence of other CNS cell type markers; transcriptome profiling demonstrated the expression of microglial transcripts and an absence of astrocytic transcripts in purified primary cells. Functional studies confirmed that purified primary microglia were phagocytic. Functional responses were also tested by exposing purified primary microglia to LPS, a known myeloid cell activator, at various concentrations and time-points. The data showed dose and time-dependent release of pro-inflammatory effectors (cytokines and NO) together with shifts in the surface expression of multiple activation markers (e.g. CD11b; in-line with previous reports). Morphological studies illustrated an LPS dependent dose-dependent shift of purified primary cells towards an activated, amoeboid form.

A definitive identification of primary microglia to the exclusion of all other cell types, particularly myelomonocytic cells from the periphery, is challenging (173, 183). Nonetheless, the combined morphological, immunophenotypic, transcriptional and functional data, coupled with the inclusion of steps in the culture protocol designed to eliminate cells of non-parenchymal origin, strongly suggests that the purified primary cells are microglia. The combined data illustrate that

both the primary microglia and BV2 cells retain responsiveness to an innate immune cell activator (i.e. LPS). Additionally, a range of cell phenotyping assays have been developed during the course of the investigations delineated in this chapter. These developments are critical for the attainment of the study's further aims which involve the elaboration and detection of microglial responses in cells genetically deficient in specific complement regulatory membrane proteins (i.e. Crry) coupled with an exploration of the effects of C activation products on microglia. The culture systems, activation regimens and phenotyping assays described here will now be taken forward into studies regarding the phenotypic consequences of iC3b ligation of CR3 for naïve microglia and the *in vitro* phenotype of Crry $-/-$ microglia.

3.3.2 Primary Microglia vs BV2 Cells

An inherent aim of the work set out in this chapter was to characterise isolated primary microglia and compare them to a microglial cell line. This comparison would serve as a positive control in phenotyping assays designed to validate the identity of cultured primary microglia. BV2 cells are a widely used murine microglial cell line known to express all common microglial markers (e.g. CD11b, F4/80, CD45, etc.) and functional responses (e.g. phagocytosis, cytokine release, chemotaxis, etc.) (192, 240, 241, 258). Additionally, this comparison would serve to define the similarities and differences between the BV2 cell line and primary murine adult microglia, both as an item of general significance to studies involving the use of cell lines as surrogates for primary microglia, and in-order to establish the suitability of, and appropriate conditions for, the use of BV2 cells in priming experiments.

In all cases investigated, both cell types expressed the markers and functional responses of interest and expected of microglia. However, in some cases, the levels of expression and functional responses were distinctly different between cells types. Several protein markers differed between primary microglia and BV2 in terms of endogenous expression and their relative change in response to LPS treatment (e.g. CD11b). Phagocytosis activity was much higher in primary microglia relative to BV2 cells, while the release of cytokines in response to LPS stimulation was dramatically greater. In line with previous reports concerning the use/suitability of microglial cell lines (192, 240, 241, 258) these combined data indicate that while BV2 cells express all of the key microglial markers, they differ from primary microglia in the extent to which they express these markers. Indeed, this cell line could be considered as possessing a "minimal" microglial phenotype. As others have previously suggested, it seems likely that this effect is a consequence of the transformed nature of the cell line which almost invariably means that compared to primary cells they prioritise progression through the cell cycle over expression of cellular phenotype.

As described previously, a notable feature of the response of primary microglia to LPS exposure was a dramatic increase in the release of pro-inflammatory cytokines. This effect was mirrored by changes in the levels of surface markers (i.e. CD11b and C5aR,) which increased sharply at LPS doses between 1-10ng/mL but then plateaued at higher concentrations, suggesting that in primary microglia a response threshold is reached at this concentration range. However, these threshold effects were not observed in BV2 cells, where changes in surface antigen expression and release of inflammatory effector molecules occurred gradually with LPS concentration across the ranges tested. These observations reveal another distinction between primary microglia and BV2 cells consistent with the premise of the cell line having microglial features/properties which are present but altered. Indeed, recent global gene expression profiling approaches describe a unique microglial signature from which microglial cell lines deviate further than cultured primary microglia (183).

Overall, the retention of all commonly investigated phenotypic features and responses of microglial cells by BV2 cells means that they provide a useful substitute for primary cells in most settings. Furthermore, the intrinsic rapid proliferative properties of the retrovirus-immortalised BV2 cell line means that it provides a readily available source of microglial cells for experimentation; in contrast, extraction of primary microglia from murine tissue gives relatively low yield and the resultant pure cultures have low proliferation rates (192). Availability and ease of culture are the main benefits of the use of microglial cell lines, and the reason behind their original development (192). However, a general reduction in the expression of many microglial phenotypic features and responses, likely a consequence of their rapid proliferation, clearly reduces the suitability of BV2 cells as direct substitutes for primary microglia. This is particularly pertinent in the case of this study given that iC3b engagement of CD11b/CR3 is a major focus, and CD11b/CR3 expression was low on BV2 cells relative to primary microglia. For this reason, I concluded that the only meaningful use of BV2 cells in further experiments intended to address the larger aims of the study would be in preliminary experiments designed to optimise experimental conditions and/or in scenarios where large cell numbers were required or at times when primary cells were unavailable.

3.3.3 Microglial Cultures: Pure Vs Mixed

The final aim of the work described in this chapter was to compare the properties of microglia maintained in isolation with those maintained in mixed CNS cell cultures. As discussed previously, several inhibitory interactions between surface molecules expressed by neurones and microglial receptors have been identified in recent times (e.g. CD200-CD200R, fractalkine-CX3CR1) (173, 246, 249). The significance of the absence of these interactions in isolated microglia culture systems has been identified as an issue. In-order to address this issue, the expression and relative

change in a cell type-specific, microglial surface activation marker (CD11b) in response to LPS stimulation across a range of concentrations was assayed on microglia maintained in isolation, or in mixed cell CNS cultures in which neurones constituted a significant proportion of the total cell population. This approach permitted the specific investigation of microglial responses, even in a mixed population. Assays to measure the bulk release of secreted effector molecules (e.g. cytokines) such as ELISAs cannot distinguish the source of analytes in mixed cultures - microglial or non-microglial origin; hence, the release of cytokines was not investigated in mixed cultures. There was little difference in the baseline CD11b expression level between microglia maintained in isolation or in mixed culture with neurones, and the CD11b response to LPS followed a similar time course; However, the magnitude of CD11b expression changes induced by LPS treatment were increased two-fold in microglia maintained in mixed CNS cultures compared with isolated microglia. These observations indicate that the presence of neurones alongside microglia has important implications for microglial responses and lends strength to the argument that inhibitory surface interactions between neurones and microglia modify microglial activation. This, of-course, has important implications for studies which involve the use of purified culture systems for the investigation of microglial biology. However, this issue is not the main focus of this study and it should be emphasised that only a limited investigation, in which just a single parameter was measured at one time-point. Although additional experimentation to further substantiate the observations and the explanatory model described here was considered beyond the scope of this study, this might have included strategies to interfere with neuronal-microglial surface molecule interaction and distinguish effects mediated by surface interaction from those mediated by secreted molecules (e.g. barrier culture systems, antagonists, etc).

4 iC3b Engagement of Microglial CR3: Phenotypic Consequences

4.1 Introduction

Having established and validated systems for the culture of primary adult murine microglia which are phenotypically normal and responsive alongside a widely utilised murine microglial cell line, these tools were then utilised to further investigate the C3 fragment-dependent mechanism of microglial priming described by Ramaglia *et al.* (2012) in Crry KO mice *in vivo* (1). This chapter thus describes a series of experiments exploring the phenotypic impact of microglial CR3 ligation by its ligand iC3b.

4.1.1 CR3 Discovery and Structure

4.1.1.1 Complement Receptors for Fixed C3: CRs 1, 2, 3 and 4

Since some of the earliest studies concerning the nature of cellular and humoral immunity it has been recognised that factors in serum act as opsonins, promoting the engulfment of microbes by white blood cells; furthermore, it was appreciated that that antibody and C were likely involved in the process (16, 20, 259). However, it wasn't until the latter part of the 20th century that the existence of distinct C receptors and the mechanistic details of C-mediated immune-adherence and (opsono) phagocytosis were properly delineated.

Along with reactions such as agglutination and conglutination, immune haemolysis was among the earliest immunological phenomena described and known to involve antibody and C (20, 259). Its utility as a sensitive and reliable indicator of the activity of these two humoral factors provided an invaluable early clinical and research tool for the diagnosis of disease and immunological investigations (22, 260, 261). Studies of immune haemolysis using antibody sensitised erythrocytes and isolated C components had identified the reaction sequence and requirement for all known C components by the latter part of the 20th century (16) and this was used in the study of C reaction kinetics and the development/formulation of "the One-Hit Theory" of immune-haemolysis by Mayer during the 1950s (262-268). However, the C haemolytic reaction is not dependent on the engagement of effector (as opposed to target i.e. erythrocyte) cells in any way and therefore does not involve the participation of C receptors. Nelson's 1953 description of the phenomenon of immune-adhesion, defined as the adhesion of particles (microbes) sensitized with their individually specific antibody and C to erythrocytes, illustrated the existence of a cellular receptor for particle-bound/fixed C for the first time (269). Additionally, evidenced by the fact that immune-adhesion led to enhanced phagocytosis of the target particle, Nelson postulated that immune-adhesion had a role in the elimination of C opsonised material and thereby host-defence against microbial infection; the demonstration of immune-adhesion in monkeys/*in vivo* within a few years supported this concept (270). The importance of immune-adherence in the

clearance of C opsonised material was subsequently validated and underlies the mechanism of immune-complex clearance *via* the reticuloendothelial system (16). During the 1960s, understanding of the molecular organisation of C was still incomplete. However, by 1963 it had been discovered that the classical third component of C actually consisted of more than one factor which reacted in sequence in immune-haemolysis, and that immune-adhesion was dependent on the sequential reaction of the particle with antibody, followed by C1, C4, C2 and C3c (now known as C3), and that the other factors from the classical third component were not necessary for this interaction (271). Thus, the ligand of a receptor on the surface of erythrocytes for particle-fixed C was identified as activated C3. By the late 1960s it had been shown that in addition to C3, the classical third component also consisted of C5-C9 and that while all of these components are required for immune-haemolysis (272), only the sequential reaction of C1, C4, C2 and C3 with antibody sensitised particle is required for both immune -adherence and -phagocytosis (273). It was also shown at this time that in addition to phagocytes and erythrocytes, lymphocytes express receptors for fixed C3 and furthermore, that these receptors possess distinct characteristics relating to the requirement for divalent cations (274). Thus it was known that at least 2 different C receptors exist on different cell types and that these receptors recognise activated C3.

However, during this period of rapid advancement and divergence in C research, C3, which had been discovered and isolated just a few years previously (275), was still being characterised; this is perhaps unsurprising given the numerous molecules, both C and non-C, with which C3 interacts and the many enzymatic cleavage steps and subsequent conformational changes to which it is subjected during activation and regulation. With the discovery and functional characterisation of the classical pathway C3 convertase (38), including the liberation of a small C3 fragment with anaphylatoxin activity (C3a), along with the discovery and functional characterisation of the C3-inactivator, also known as “conglutininogen-activating factor (KAF)”, and the effects of tryptic and serum protease digestion of C3 (276), in addition to antigenic mapping of C3 during activation (277, 278), it became apparent that C3 undergoes marked conformational change during activation and is split into at least 4 distinct products, native C3 being cleaved into C3a and C3b, and C3b being further cleaved into C3c and C3d. Based on the use of indicator particles (typically erythrocytes) coated with defined C3 fragments along with defined fluid phase C fragments and/or other antagonists, it was shown that erythrocytes, PMNLs, mononuclear phagocytes and a subset of lymphocytes possess a receptor for C3b, while B cells and developing neutrophils and monocytes express a receptor for C3d (279). The receptors for C3b and C3d, which both remain fixed to the target particle *via* the thioester located within the C3d region, were therefore termed CR1 and CR2, respectively (280, 281). However, following the discovery of β 1H globulin (factor H)

and its functional characterisation as a key cofactor for C3b cleavage by factor I, it became apparent that, due to inaccuracy in the comprehension of C3 processing under specific conditions, the results of previous experiments concerning the identity of C receptors on different cell types had been misinterpreted: Previous experiments which had sought to identify C3d specific receptors typically reacted purified factor I/C3b-inactivator with sensitised erythrocytes coated with C1-C3b to generate the C3d ligand; With the completion of C3 breakdown characterisation and the discovery of the existence of iC3b as a fragment intermediate between C3b and C3d, with identical or very similar molecular weight to C3b and no overt fragmentation, it was subsequently appreciated that in this system, significant amounts of iC3b were present on indicator particles, thought previously to harbour only C3d (280, 282, 283). Thus, it was ultimately deduced that receptors exist for the C3b, C3d and iC3b fragments of C3, termed CR1, CR2 and CR3 (respectively), and that monocytes and neutrophils, previously thought to bind C3d and therefore express a receptor akin to B cell CR2, are actually specific for iC3b and therefore express CR3 (not CR2).

Shortly after the identification of CR3 based on the functional property of iC3b binding (283), CR3 was identified as the target of the rat M1/70 monoclonal antibody (284) which had previously been characterised as a mouse macrophage differentiation antigen designated Mac-1 (285). The product of the M1/70 clone was subsequently shown to give the same reactivity with human cells and tissues (286). Later, two additional mouse clones, OKM10 and Mo1, known to target surface antigens on human myeloid cells, were also shown to block CR3-mediated function and to react with antigens with very similar structure to Mac-1 (287, 288).

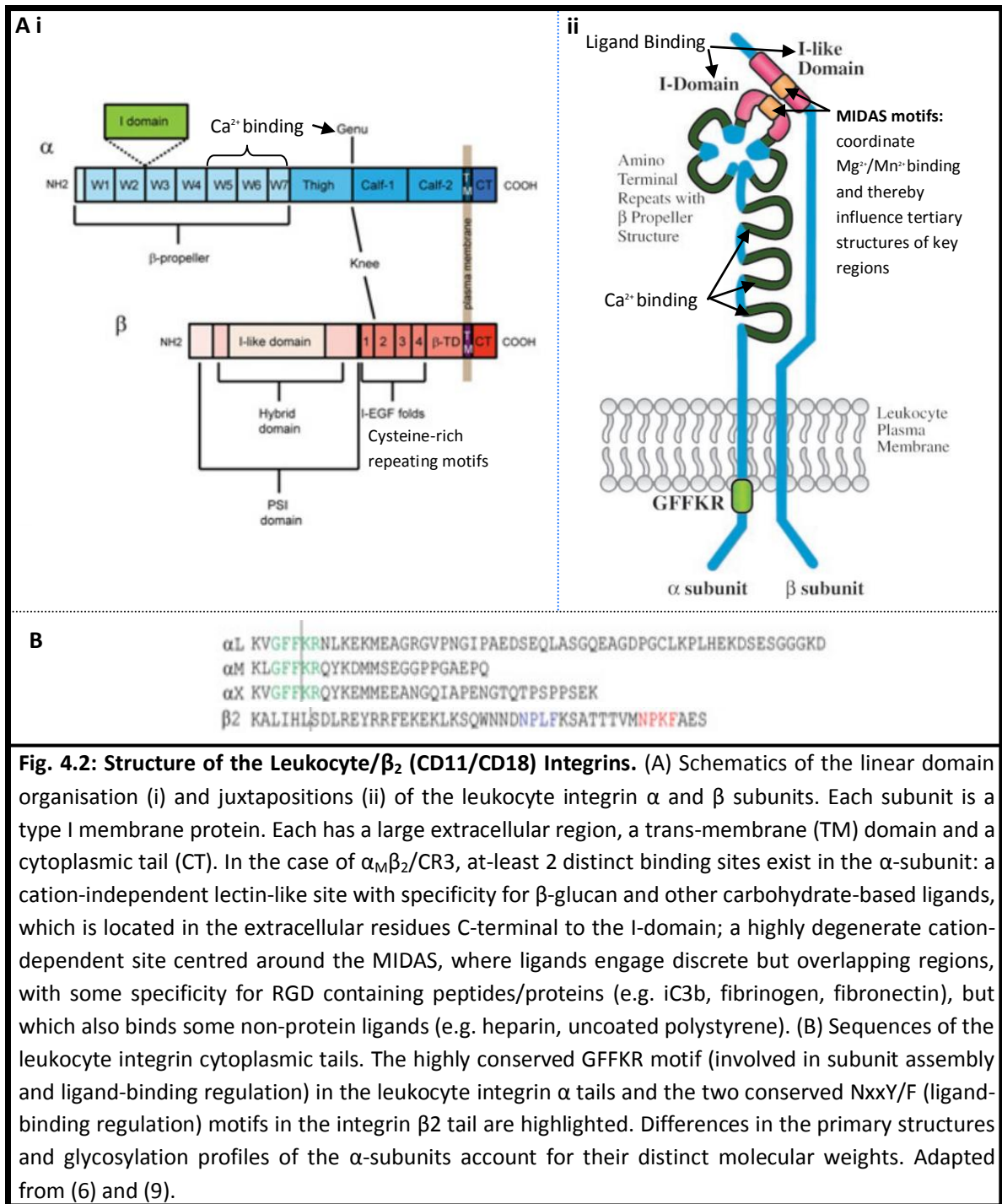
At around the same time as its identification as CR3, Mac-1 was also identified as a structural homolog of lymphocyte function-associated antigen-1 (LFA-1), a surface antigen known to be involved in T-cell cytotoxicity through adhesive interactions (289). Both LFA-1 and Mac-1 molecules were shown to have very similar structures, with non-covalently associated heterodimeric $\alpha\beta$ subunits, with α chains of 175 and 165kD, respectively, and both with β chains of 95kD. Tyrosine mapping of protease digested antigens revealed considerable difference between α subunits but very similar or identical β subunits (290). This finding of a common β subunit and distinct α subunits was subsequently supported by studies using LFA-1/Mac-1 cross reactive and non-cross reactive mAbs (287). Unsurprisingly, interactions which govern unique ligand-specificities were mapped to the divergent α chains (291). The use of LFA-1/Mac-1 cross reactive antibodies against the 95kD β subunit also revealed the existence of another leukocyte membrane protein which shared the common β subunit: the newly identified molecule had an α subunit of 150kD and was therefore designated p150.95. The identification of p150.95 thus defined a family of leukocyte differentiation antigens comprised of 3 members with distinct α and

common β subunits; the α subunits of LFA-1, Mac-1 and p150.95 were designated α_L , α_M and α_X , respectively (287). Despite its known relationship to molecules involved in cell adhesive interactions (LFA-1 and Mac-1) the precise function of p150.95 was initially unknown. However, the discovery of the molecular identity of B-cell CR2 as distinct to another (non CR3) neutrophil receptor for factor I-cleaved C3b, illustrated the existence of CR4 (292). Suggestive of receptor activity, antibody blockade of p150.95 was shown to inhibit C-mediated erythrocyte rosetting to leukocytes and cytotoxic T cell-target adhesion independently of CR1 and CR3 (293). Studies into the molecular interactions of solubilised p150.95 identified it as an iC3b binding protein, but initial attempts to demonstrate iC3b receptor activity of leukocyte surface p150.95 failed. However, subsequent appreciation of the different p150.95 expression levels in different cell types and conditions accounted for these findings and led to the demonstration of iC3b as a ligand for p150.95 in the intact leukocyte membrane, thus defining it as the previously described but unidentified CR4 (293).

At around the same time as the discovery of p150.95 using antibodies against the β polypeptide shared with LFA-1 and Mac-1 (287), patients were described who suffered from frequent severe bacterial infections and whose leukocytes were deficient in the antigens precipitated by antibodies against the α and β chains of LFA-1 and Mac-1 (294). This rare ($1:10^6$) condition, termed "leukocyte adhesion deficiency" (LAD), emphasised the biological importance and clinical relevance of cellular adhesive interactions mediated by adhesion molecules including C receptors in effective immune responses and focused attention on the study of the LFA-1/Mac1/p150.95 family (294-297).

4.1.1.2 CR3 and CR4 as β_2 /CD11:CD18 Integrins

Earlier work on their biosynthesis and assembly had indicated that the α and β subunits of the LFA-1/Mac1/p150.95 family are derived from separate precursors (287). Somatic cell hybrid experiments using leukocytes from a LAD patient had previously mapped the genes encoding the α and shared β subunits of LFA-1 to chromosomes 16 and 21, respectively (298), and following the cloning of the β subunit cDNA its origin from a single gene was subsequently confirmed (299). By the following year, cDNAs for each of the LFA-1, Mac-1 and p150.95 α subunits had been cloned and the chromosomal locations of their genes were mapped to a cluster on the short arm of chromosome 16, between bands p11-p13.1, indicating that they had indeed arisen by gene duplication events (300). The gene encoding the common β subunit was also mapped to band q22 of chromosome 21. In 1987, following the cloning of its cDNA, sequence analysis of the common β chain also revealed that the LFA-1/Mac-1/p150.95 complexes are part of a supergene family



In July 1986, a report by Tamkun *et al.* described and named the fibronectin receptor of chicken embryonic fibroblasts as “integrin”, an integral membrane glycoprotein which integrates/interfaces between the extracellular and intracellular environments through contacts with the cytoskeleton and signalling molecules within the cell, and ligand binding capacity outside the cell (303). Shortly after, in early 1987, separate reports on the nature of molecules with similar structures and ligand binding properties characterised the smaller subunits of the leukocyte LFA-1/Mac-1/p150.95 family members (299) and the platelet/endothelial GP IIIa-IIb

complex (304) and discovered high levels (45-47%) of homology between their primary structures, including complete conservation of 56 cysteine residues and their arrangement into four tandem cysteine-rich domains, thus defining the integrins as a supergene family, with chicken integrin (β_1), the LFA-1/Mac-1/p150.95 proteins (β_2) and the GP IIa-IIIb (β_3) complex as the founding members (305). Shortly afterwards, it was discovered that the 5 very late antigens (VLAs) are β_1 integrins and that the vitronectin receptor is also a β_3 integrin (305). Since that time the number of known α and β subunits has expanded considerably to at least 18 α - and 8 β - forms (6, 306).

Expressed by all nucleated cells, integrins are an extremely widely distributed, almost ubiquitous, family of genetically and structurally related heterodimeric ($\alpha_1\beta_1$) transmembrane adhesion molecules and receptors (307). Structural diversity is achieved through the combination of at least 18 α - and 8 β - subunits which associate non-covalently. The specific combination of α and β subunits, which pair-off in a cell type-specific manner, identifies the integrin species and confers its unique ligand-binding properties (308). Archetypical α subunits associate with just a single type of β subunit and therefore integrin subgroups are designated by their β subunit (i.e. β_1 , β_2 , β_3 , etc.) (308). Through contacts with numerous and diverse ligands, characteristically featuring cell-cell and cell-ECM interactions, integrins participate in a wide range of processes, including the infiltration of leukocytes into inflamed tissue (296). Additionally, through intracellular contacts with cytoplasmic components (e.g. the cytoskeleton, kinases, etc.), integrins convey signals regarding the mechanical and chemical properties of the cell's external environment and modulate responses such as phagocytosis, the release of reactive species (e.g. superoxide/ O_2^- , H_2O_2 , hydroxyl free-radical) during respiratory burst, cytokines and other secreted effectors (e.g. growth factors, proteases, etc.), along with motility/chemotaxis (309).

4.1.2 The Many Ligands of CR3

A unique feature of CR3 is the number and diversity, both structural and functional, of ligands with which it interacts. Indeed, CR3 is the integrin family member with the greatest number of known ligands; more than 30 molecules have been reported to bind CR3 (310-312) (Table. 4.1). CR3 ligands include host cell, microbial cell and extracellular matrix structures, both protein and non-protein (310). The characterisation of iC3b as the receptor's prototypical ligand led to its 'Complement Receptor' ('CR3') designation (313). Given its multiplicity of infection-, inflammation- and pathology- related ligands, along with the identification of a common recognition motif in its ligands (296, 314), CR3 is considered a PRR in addition to being an integrin. The ability of CR3 to recognise so many different ligands, along with its signalling capacity mediated by links with the intracellular environment (310, 311), gives rise to increased complexity of function. Studies using integrin chimeras have implicated a region (Lys[245]-Arg[261]) of the CD11b/ αM I-domain in the uniquely broad ligand binding promiscuity of CR3 (310).

Integrin	Other names	Expression	Ligands
α L β 2	CD11aCD18 or LFA-1	All leucocytes	ICAM-1, ICAM-2, ICAM-3, ICAM-4, ICAM-5 and JAM-1.
α M β 2	CD11bCD18, Mac-1, CR3 or Mo1	Monocytes, macrophages, NK cells, neutrophils and $\gamma\delta$ T-cells	iC3b, fibrinogen, ICAM-1, ICAM-2, ICAM-4, JAM-3, Factor X, heparin, neutrophil inhibitory factor, MBP, high-molecular-mass kininogen, microbial saccharides e.g. LPS, plasminogen, fibronectin, laminin, collagen II and VI, collagen I, tissue growth factor, RAGE, cysteine-rich 61, connective denatured proteins, uPAR and more...
α X β 2	CD11cCD18, p150,95 or CR4	Monocytes, macrophages, dendritic cells and NK cells	Shares many ligands with α M β 2, including iC3b, fibrinogen, ICAM-1, ICAM-4, LPS, collagen I, heparin, denatured proteins. α X β 2 is also a receptor for osteopontin.

Table 4.1: β 2/CD11:CD18 Integrins, their expression and ligands [adapted from (6)].

4.1.3 Cell Signaling of Ligated β 2/CD11:CD18 Integrins

With their numerous ligands (Table 4.1) and expression on many distinct cell types (e.g. phagocytes, lymphocytes, erythrocytes), the precise signalling consequences of leukocyte (β 2) integrin ligation is complex and context-specific (6, 309). In a generalised model of intracellular events which mediate the broad range of β 2-integrin mediated leukocyte functions, ligation results in conformational changes which result in recruitment of members of the SFK family of protein kinase to the cytoplasmic tails of the $\alpha\beta$ 2 chain heterodimers. Recruited SFKs such as HCK, FGR and LCK autophosphorylate upon clustering of ligated $\alpha\beta$ 2 heterodimers resulting in their activation and phosphorylation of ITAM motifs of adaptor proteins such as DAP12. Other protein kinases such as the Syk family member ZAP70 then bind the phosphorylated ITAMs *via* SH2 domains and are then available for phosphorylation by SFKs (315, 316). The activated protein kinases then initiate a sequence of downstream signalling events which culminate in the divergent responses of the leukocyte β 2 integrins (309). Although disparate signalling pathways are employed in a context-specific manner, common end-points include the cytoskeleton (key for adhesion-dependent responses) and transcriptional regulators such as the ERK/MAPK pathway and AP1 (6, 309) (Fig. 4.3). The precise binding-site is key to signalling induced by ligation. For example, CR3/ α M β 2 phagocytosis of I-domain bound ligands is Rho-dependent whereas that of non I-domain bound ligands employs Rac/Cdc42 (317, 318). Vav1/3 (GEFs of RhoGTPases) has also been shown to be important in CR3/ α M β 2-mediated phagocytosis (319, 320). While the β 2 cytoplasmic tail plays an important role in recruitment of signalling molecules to the $\alpha\beta$ 2 heterodimers (Fig.4.3), that of the α chain also has a key role in determining the signalling fate of β 2-integrin ligation. Owing to their varying lengths and sequences (Fig 4.2B), the recruitment of signalling mediators to the ligated complex is thought to vary for the different $\alpha\beta$ 2/CD11:CD18 heterodimer forms (6). For example: Apoptosis was delayed in K562 cells expressing CR3/ α M β 2 that was ligand-bound, but the effect was attenuated by replacing the α M tail with the α L tail

(321); Selective recruitment of the SFK Hck to CR3/ α M β 2 in CHO cell transfectants was abrogated when the α M tail was replaced with that of α L or α X (322); Cross-linking of CR3/ α M β 2, but not α L β 2, on monocytes triggers SFK-dependent phosphorylation and activation of PKC δ (323). The β 2-integrins also interact with other receptor signalling systems to determine the downstream functional consequences of receptor-ligation. For example, CR3/ α M β 2 dampens TLR-induced inflammatory response in macrophages by promoting degradation of TLR effectors MyD88 and TRIF (324).

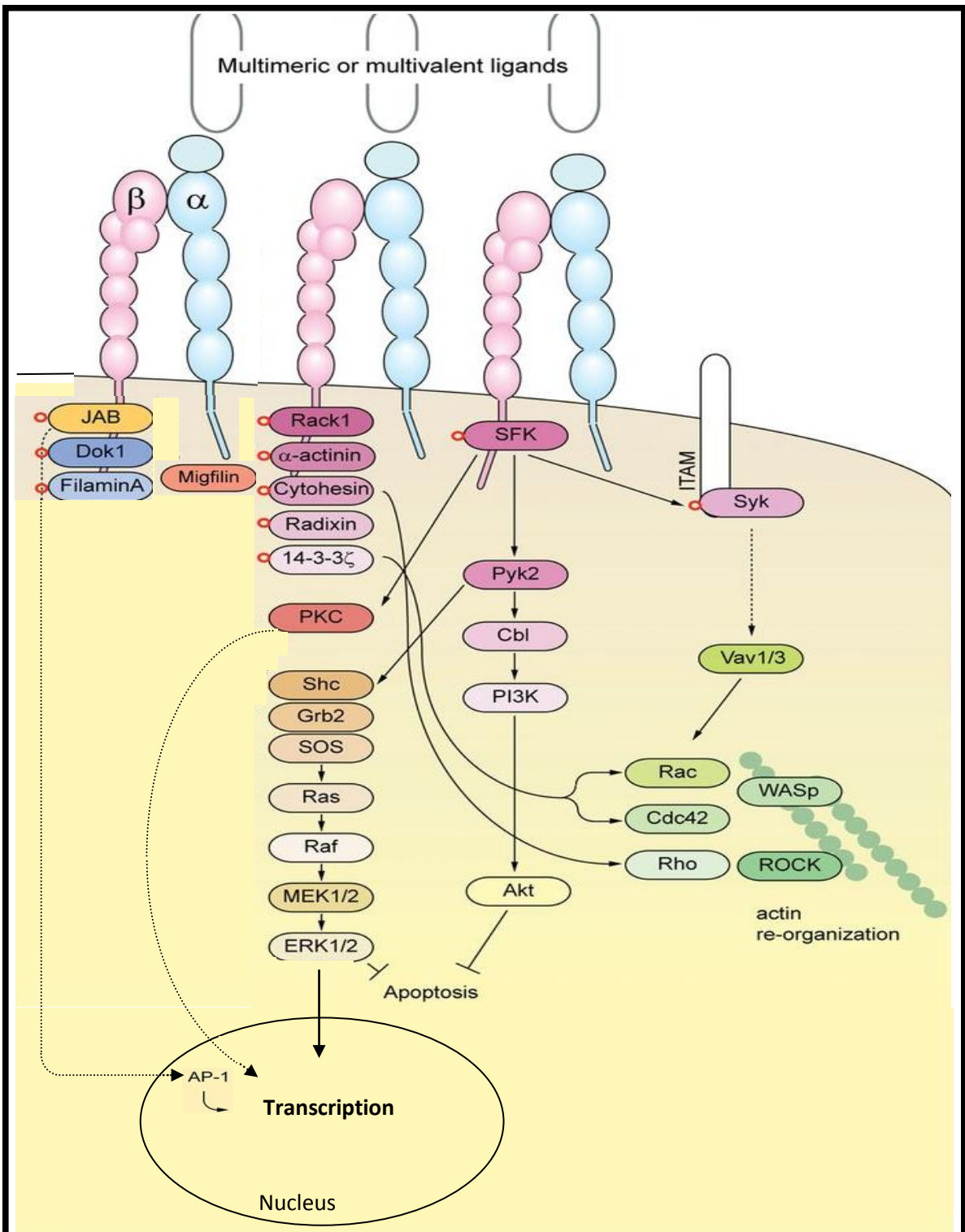


Fig. 4.3: Signal transduction pathways of the $\beta 2$ integrins. The $\beta 2$ integrins modulate gene transcription and cytoskeletal organisation. Clustering of the $\beta 2$ integrins induces SFK activation, leading to ERK1/2 signalling or PKC signalling that can regulate gene transcription. In neutrophils, it has been shown that clustering of the $\beta 2$ integrins induces ERK1/2 signalling and PKB activation, which delay the onset of spontaneous apoptosis. $\beta 2$ integrin-induced SFK activation also regulates actin reorganization via the Syk/Vav1/3 pathway. Other proteins that are reported to directly associate with the integrin $\beta 2$ tail are RACK1, α -actinin, cytohesin 1, radixin, 14-3-3 ζ and Syk. Cytohesin 1 and 14-3-3 ζ can regulate actin reorganization via the RhoGTPases Rac, Cdc42 and Rho. The cytoplasmic tails of the $\beta 2$ integrins are phosphorylated at specific Ser and Thr residues by PKCs. For many of these phosphorylation sites, their functions remain to be determined. The best characterized to date is Thr758 of the $\beta 2$ tail. Phosphorylation of $\beta 2$ Thr758 leads to high-affinity binding with 14-3-3 ζ but not filamin A. This phospho-switch may be one of the mechanisms that regulate the activation status of the $\beta 2$ integrins. When integrin $\alpha\beta 2$ is engaged by ligand, JAB-1 dissociates from the $\beta 2$ tail, translocates into the nucleus and regulates AP-1 transcriptional responses. Red circle indicates that the protein interacts directly with the integrin $\beta 2$ tail. Adapted from (6).

4.1.4 CR3 Functions

4.1.4.1 Phagocytosis and NK Cell Killing

As described above, the ability of CR3 to bind and mediate the uptake of iC3b-bearing particles defined it as a phagocytic receptor for C-opsonised material. *In vitro* studies into the mechanism of CR3 phagocytosis revealed that while iC3b opsonised erythrocytes are bound avidly (*via* CR3) by peripheral myeloid cells (neutrophils and monocytes), activation of a robust phagocytic response requires further stimulation of the cell, such as treatment with PMA (325) or adhesion to a protein coated substratum (326); this multi-hit mechanism of functional regulation mediated by signalling inputs from other cellular sensory systems is characteristic of integrins. Subsequent investigation into the secretory consequences of CR3 activation by iC3b demonstrated that ligation, even under conditions that readily promote phagocytosis, failed to stimulate a respiratory burst (327, 328) or release of eicosanoids (329). In sharp contrast, phagocytosis of zymosan (313, 330) or antibody-coated particles (328) was shown to be constitutive and accompanied by a marked respiratory burst and eicosanoid production. These findings suggest that phagocytosis triggered by iC3b ligation of CR3 is a non-/anti- inflammatory clearance mechanism as opposed to a means of inducing or sustaining a pro-inflammatory response (312, 327-329).

CR3 possesses two distinct binding sites: an adhesion-promoting site for fixed iC3b and a lectin-like site which triggers phagocytosis and release of effector molecules. Studies using a soluble form of β -glucan isolated from zymosan illustrated that ligation of the neutrophil CR3 lectin site results in receptor activation and the avid phagocytosis of iC3b opsonised erythrocytes, which, in the absence of glucan-mediated receptor-activation, adhere to neutrophils but are not engulfed. Similarly, ligation of the lectin site of NK cell CR3 resulted in engulfment and lysis of iC3b opsonised erythrocyte and tumour cell targets which otherwise adhere but are not destroyed (234, 331). These data indicate that while multi-valent ligation of the CR3 α -subunit lectin-like site is sufficient to induce cytotoxic responses directly, ligation of the CR3 iC3b binding site alone is sufficient for adhesion but not cytotoxicity; induction of cytotoxic responses to iC3b-bound ligands requires further stimulus/activation, mediated by signals from within the cell or ligation of the lectin-site by carbohydrates (soluble or membrane-associated). This modality has important *in vivo* implications, since microbes expressing polysaccharides which ligate the CR3 lectin site and which activate C will be killed directly by leukocytes, whereas other host-derived targets which activate C but do not express CR3-ligating polysaccharides (e.g. neoplastic cells) will become bound but will not be destroyed (234, 313, 331). Indeed these observations lend credence to the use of soluble β -glucans as anti-cancer agents (332). Furthermore, the importance of ligand

valency to the functional response indicates that receptor clustering/aggregation influences the signals transduced into the cell by CR3.

4.1.4.2 Adhesion

Early biochemical and immunological studies of CR3 revealed its structural homology with LFA-1, known to have function in T-cell adhesion dependent activities (cytotoxicity and B-cell support), along with the previously unidentified p150.95/CR4 (287). Moreover, cell adhesion studies involving the use of blocking antibodies against each α and the common β subunit of the LFA-1/CR3/CR4 family, along with the identification and characterisation of LAD syndrome, illustrated the role of CR3 in endothelial interactions and diapedesis of neutrophils and monocytes (296, 333). Other leukocyte functions mediated by CR3 include homotypic aggregation of neutrophils, along with monocyte and neutrophil chemotaxis and other general adhesive activities such as attachment to *in vitro* culture substrata (i.e. coated and uncoated plastic and glass) (296, 312).

A notable finding concerning the function of CR3 was the observation that when adherent to *in vitro* culture surfaces coated with proteins (e.g. serum, fibronectin, vitronectin, laminin) or endothelial cell monolayers, but not when in suspension, neutrophils (but not monocytes) respond to treatment with a variety of physiological soluble stimuli (e.g. cytokines, growth factors, chemokines) with a high-level respiratory burst. Moreover, this effect is absent in neutrophils from LAD syndrome patients and is blocked in normal cells by anti-CR3 antibodies (334-336). These findings identified a potentially important physiological mechanism involving CR3 whereby adherence of PMN converts their responsiveness. It has been postulated that upon adhesion to the underlying vasculature or extravasation and adhesion within the ECM at an inflammatory site, this mechanism may render PMN sensitive to stimulation from resident macrophages and infiltrating lymphocytes, thereby directing the immune-response (334-336). These data also provide clear evidence of CR3 transducing extracellular signals that influence the effector functions of discrete surface receptors (i.e. outside-in signalling) and indicate a shared signalling pathway(s) which influences the neutrophil oxidase/respiratory burst activity.

Overall, the consequences of CR3 ligation are heavily context-dependent, with the binding site(s) engaged, valency of ligands, presence of other ligands (both CR3 and non-CR3), adhesive substrates and cell type, all influencing the functional outcome of CR3 binding. The rapid identification of numerous structurally and functionally diverse ligands, leading to a recognition of the importance of allostereism and bidirectional, “outside-in” (the more conventional) and “inside-out” signalling as regulatory mechanisms has underscored the comprehension of CR3 function (and that of integrins generally).

4.1.4.3 Microglial CR3 functions

In the periphery, CR3 is expressed primarily by phagocytic leukocytes, but also by NK cells and subsets of lymphocytes (CD5+ B cells and CD8+ T cells) (337). In the normal CNS parenchyma, only microglia express β_2 integrins, although they are also expressed by infiltrating leukocytes during BBB disruption and by perivascular macrophages (338, 339). Microglial CR3 expression is constitutive and increases with cell activation (173, 340), indicative of an important role in cell function. Despite the known roles of CR3 in modulating aspects of inflammation in the periphery and the importance of microglia in CNS homeostasis, focus on microglial CR3 has been somewhat limited. Studies using an anti CR3 monoclonal antibody (Ox-42) which binds an epitope near the iC3b binding site of rat CR3 revealed roles in microglial proliferation and apoptosis *in vivo* (341) and nitric oxide production *in vitro* (342). C is involved in the phagocytic clearance of various particles in the CNS by microglia, including apoptotic cells, degraded/damaged myelin and β -amyloid deposits (207, 343); available data indicates that similarly to that mediated by CR3 in the periphery, C-mediated phagocytosis by microglial CR3 is non-/anti-inflammatory (173, 207, 339, 343, 344). However, in contrast to these observations, pro-inflammatory and damaging effects are also associated with microglial CR3 (345). CD11b deficient microglia fail to respond with morphological changes when activated *in vitro* and *in vivo* (346, 347), or a respiratory burst when treated with 1-methyl-4-phenyl-pyridium iodide in an animal PD model (347), LPS (346) or mutant α -synuclein protein (348). Further, fibrinogen (a CR3 ligand) is associated with microglial activation, ROS production and axonal damage during BBB disruption (349). Like peripheral phagocytes, microglial treatment with unopsonised zymosan, which engages CR3 *via* the lectin-like site, leads to pro-inflammatory phagocytosis (173, 350).

A recent study into the consequences of microglial CR3 ligation by iC3b demonstrated a C-dependent primed microglial phenotype which was associated with exacerbated inflammatory CNS disease (EAE) in Crry KO mice; co-localisation of iC3b and microglial CR3 indicated that the phenotype was a consequence of iC3b ligation of microglial CR3 (1). In contrast to other studies exploring the function of microglial CR3, this finding concerning the impact of microglial CR3 ligation by iC3b originates from a system of chronic C activation and iC3b generation in the mouse, a feature which could be crucial to the observed effect.

4.1.5 Chapter Aims

The aim of this chapter is to further characterise microglial CR3, specifically the consequences of its engagement by different ligands and the capacity for iC3b-ligation to prime microglia for an enhanced pro-inflammatory response to activating stimuli. *In vitro* strategies were developed to engage CR3 of both primary and immortalised microglia with iC3b; the consequences of this

interaction were then assessed, both at baseline and for the response to a subsequent pro-inflammatory stimulus.

4.2 Results

4.2.1 Fluid-Phase iC3b

Treatment of cells with (particle-) free iC3b (i.e. in the fluid-phase) was investigated as it represents the 'cleanest' possible system for assessing the consequences of its ligation of CR3, free from the interference of additional receptor systems engaged by iC3b-complexed particles/surfaces. Given the technical challenges associated with the *de novo* production of fluid-phase iC3b it was decided that purified preparations available from a reliable commercial source (Complement Technologies Inc. [CompTech], Texas, USA) would be utilised for studies of its effects on *in vitro* microglial phenotypes.

4.2.1.1 Assessment of Commercial iC3b Identity

4.2.1.1.1 Chain Structure and Integrity: SDS-PAGE

In order to first validate the structure and integrity of the iC3b in commercial preparations, iC3b protein was analysed by SDS-PAGE under reducing conditions. Separation and comparison to molecular weight standards revealed the known 3 chain (70kD β , 43kD α'_1 and 65kD α'_2) structure of iC3b (7) with all protein chains localised to sharp bands (i.e. minimal degradation) (Fig. 4.4).

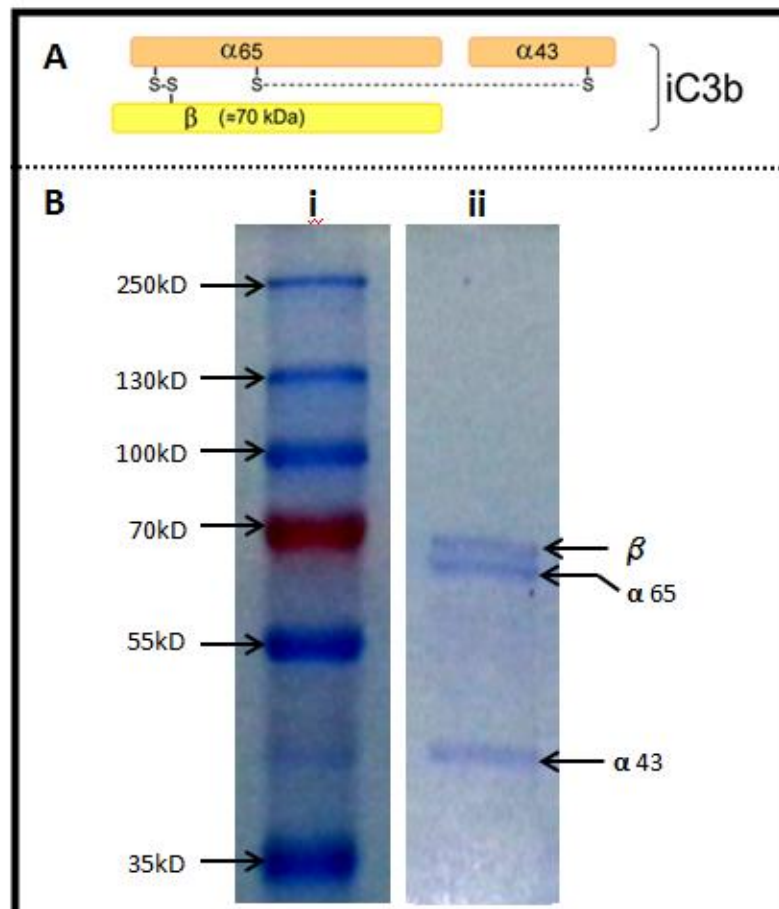


Fig. 4.4: Confirmation of iC3b Chain Structure. (A) Schematic depicting the chain structure of iC3b (adapted from (7)); (B) Protein-stained gel imaged following SDS-PAGE of molecular weight standards (i) or commercial human iC3b (2.5 μ g) under reducing conditions (ii).

4.2.1.1.2 Immuno-Reactivity

In order to further validate the identity of the commercial iC3b protein and confirm its capacity to interact with a known binding partner, a concentration gradient of iC3b protein (unlabelled) was immobilised on the surface of a polystyrene 96-well plate and detected using a concentration gradient of rat monoclonal antibody (clone 9; Hycult Biotech, ND) against human C3g epitope-harboured C(3) activation fragments (i.e. iC3b, C3dg and C3g), followed sequentially by an HRP-conjugated goat anti-rat polyclonal antibody and chromogenic peroxidase substrate (OPD). Detection with this iC3b-specific antibody returned readily detectable signal which correlated with the known concentrations of both immobilised iC3b and anti-iC3b mAb (Fig.4.5). Furthermore, detection using a non-specific antibody of the same isotype (rat IgG1) as a negative control returned no detectable signal above background and no signal above background was detectable when the test antibody was incubated with immobilised C1Inh (a non-target protein) (Fig.4.5). Immobilised C1Inh was readily detectable with a C1Inh specific antibody; the C1Inh specific antibody returned no signal above background when incubated with immobilised iC3b (Fig.4.5). The specificity of the response was thus confirmed. These data therefore provided immunological evidence confirming the identity of the iC3b protein in the commercial preparation, along with its capacity to interact with a known binding partner.

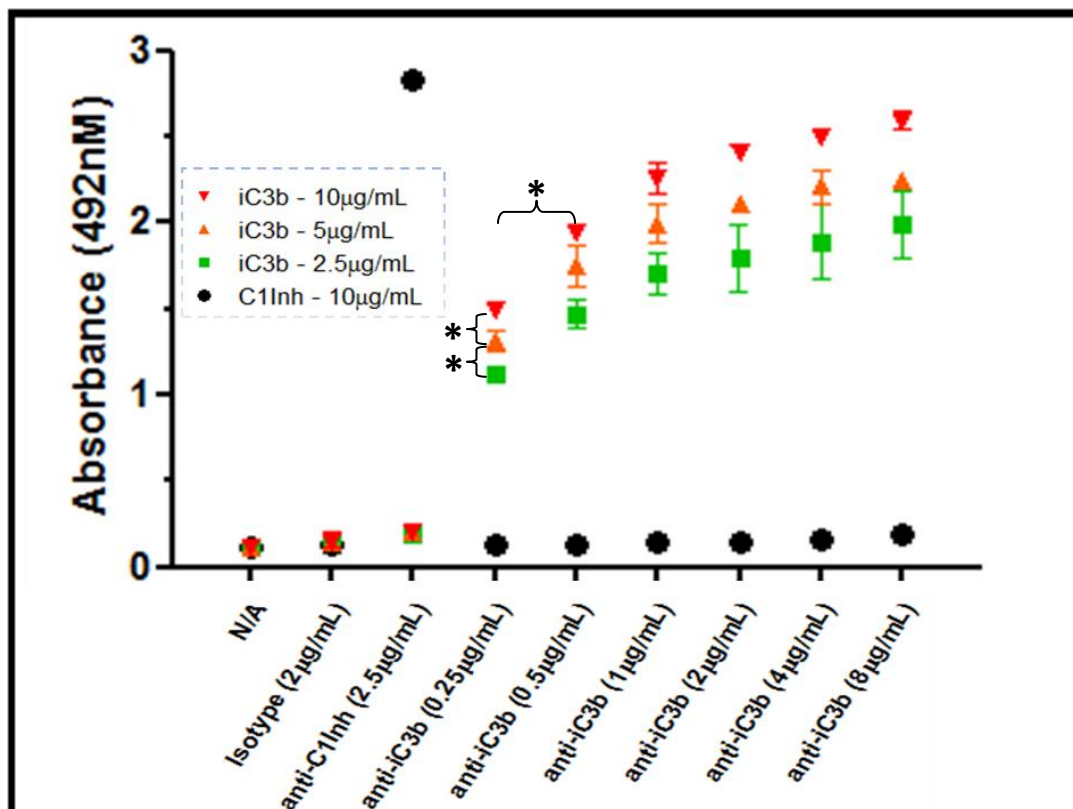


Fig.4.5: Specific immuno-detection of immobilised human iC3b: confirmation of identity and ligand binding capacity. Mean (+/- SD) absorbance values (at 492nm; Y-axis) following immobilisation of purified iC3b (2.5, 5 or 10 -µg/mL) or C1Inh (10µg/mL) in 96-well plates and indirect immuno-detection with rat anti-human iC3b mAb (0.25-8µg/mL), anti-human C1Inh mAb (2.5µg/mL) or IgG1 isotype control mAb (2µg/mL) followed by anti-rat HRP and colourimetric detection (OPD). N = 3; Two-Way ANOVA with Bonferroni post-testing was performed: *P<0.05.

4.2.1.2 Assessment of Human iC3b-Mouse Microglial CR3 Interaction

A prerequisite to these investigations was that they were to be performed using murine microglial cells; however, the only commercially available iC3b was human (generated by the reaction of C3 purified from human serum with factors I and H). Given the species mismatch between the commercially available iC3b and the target cells, questions concerning the capacity of human fluid-phase iC3b to efficiently ligate CR3 on mouse microglia were thus an obvious issue. Moreover, demonstration of ligand-receptor binding would be necessary prior to any further study of the downstream phenotypic consequences resulting from this interaction.

4.2.1.2.1 Fluorescent iC3b

In order to address the above issue, iC3b was labelled with fluorescein *via* N-hydroxysuccinimide-linkage (according to Section 2.2.2.2.1) to generate a fluorescent probe which could then be utilised in binding assays. Earlier studies utilising FITC-labelled soluble molecules to detect ligand binding of cell membrane-associated CR3 validate this experimental approach (337).

4.2.1.2.1.1 Detection of Fluid Phase iC3b-Fluorescein Binding to Immobilised Specific mAb

To confirm successful fluorescent labelling of the iC3b protein and establish its utility as a probe to detect specific binding interactions, the ability of fluorescein-labelled, fluid-phase human iC3b to interact with immobilised clone 9/anti-iC3b mAb (along with the ability to detect this interaction), was assessed (*as per* Section 2.2.2.2.2). A concentration gradient of Clone 9/anti-iC3b mAb was coated to the surface of a 96-well polystyrene plate and was subsequently incubated with a concentration gradient of iC3b-fluorescein. Following washing, fluorescent signal was detected in a fluorescence plate reader. Despite relatively high background, specific signal was readily detectable and correlated with the concentrations of both iC3b-fluorescein and the clone 9 mAb coat (Fig.4.6 Ai). Furthermore, no specific signal was detectable, regardless of concentrations, when iC3b-fluorescein was incubated in wells pre-coated in a non-specific isotype control antibody (Fig.4.6 Bi). Additionally, different concentrations of FITC-labelled anti-rat antibody incubated over a concentration gradient of immobilised clone 9 mAb (Rat IgG1) served as a positive control; Signal was readily detectable and was dependent on the concentrations of both immobilised target and soluble probe (clone 9 mAb and anti-rat igG-FITC, respectively) (Fig.4.6 Ci). Furthermore, assessment of fluorescence prior to washing to remove unbound probe illustrated that in all cases signal related entirely to the concentration of fluorescent probe added to the individual well and was completely unrelated to the type or concentration of the antibody coat (Fig.4.6 A-C ii). These data combined illustrate the validity of the test and clearly demonstrate that all signal detected above background post-wash was indeed a consequence of specific binding. It was therefore established that fluorescently labelled iC3b is capable of specific binding from the fluid-phase with a known binding-partner and that the fluorescent signal could be

detected, thus validating iC3b-fluorescein as a fluorescent probe for the assessment of iC3b-binding partner interactions.

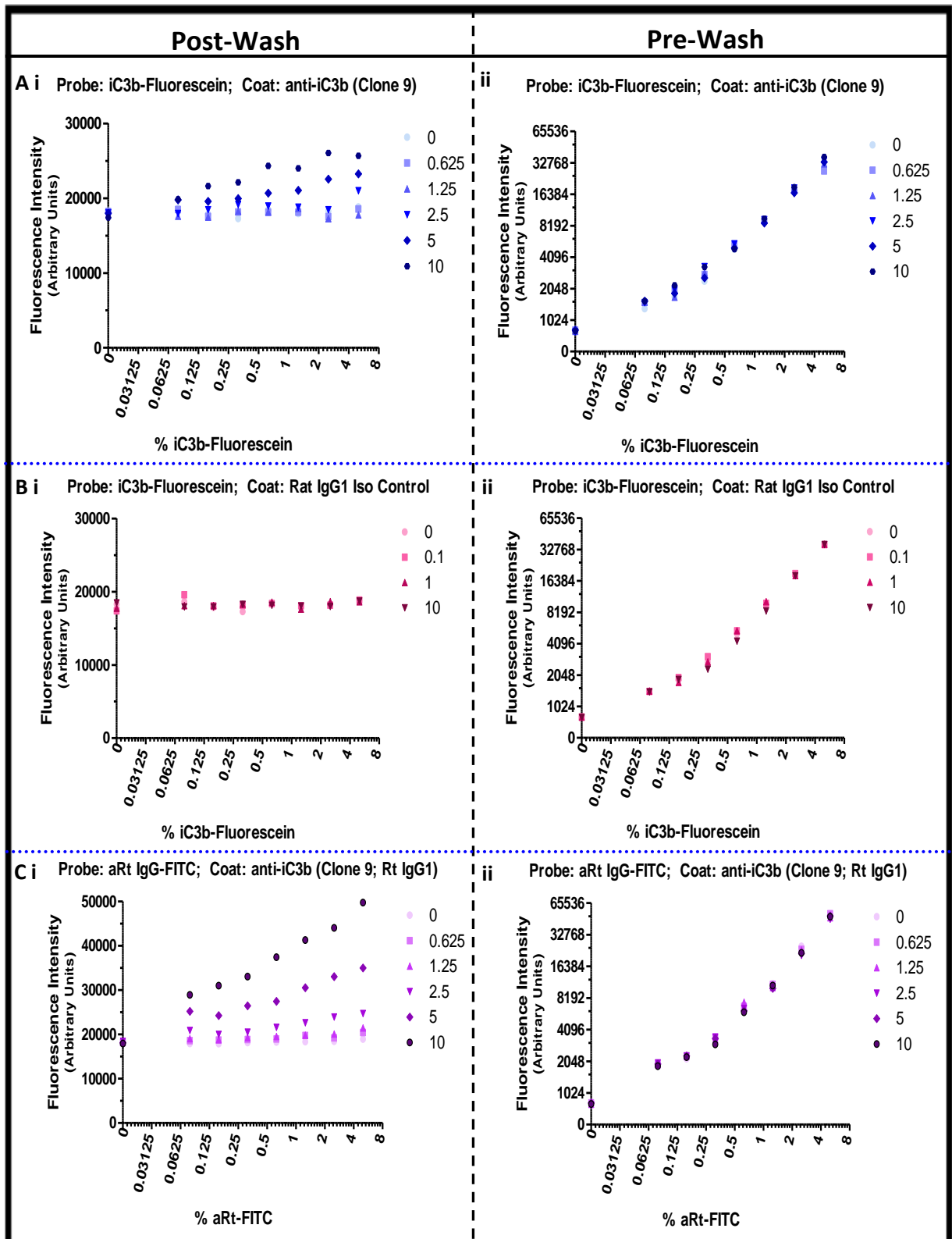


Fig.4.6: Specific fluorescence/immuno-detection of fluid-phase iC3b-Fluorescein by immobilised rat anti-human iC3b mAb: confirmation of fluorescent-labelling and ligand binding capacity from fluid-phase. Fluorescence intensities following immobilisation of rat IgG1 anti-iC3b mAb (clone 9; A and C) or rat IgG1 isotype control mAb (B) (0-10 μ g/mL) in 96-well plates and incubation with iC3b-Fluorescein (A and B; 0-5% in PBS) or anti-rat IgG-FITC (C; 0-50 μ g/mL in PBS), both before and after (ii and i, respectively) washing away of unbound probe. Data points represent individual replicates.

4.2.1.2.1.2 Human iC3b-fluorescein - Mouse Microglial CR3 Binding

To assess the ability of human iC3b to ligate CR3 of mouse microglia, BV2 cells were incubated with increasing concentrations of iC3b-fluorescein with or without the prior addition of an anti-CD11b/CR3 mAb (the same clone [5C6] as used in previous flow cytometry experiments and known to specifically bind CR3 on BV2 cells [see Section 3.2.1.1.2]) which is reported to inhibit iC3b binding (8). Flow cytometric analysis revealed a dose dependent increase in (green) fluorescence following treatment with iC3b-fluorescein. At the highest concentration of iC3b-fluorescein, CD11b/CR3 blocking antibody pre-treatment showed a significant inhibitory effect on binding (~60%, $P < 0.01^{**}$) (Fig.4.7). Overall, these data are consistent with specific binding of human fluid-phase iC3b to mouse microglial CR3. However, fluorescence was relatively weak and CD11b/CR3 antibody blockade failed to completely ablate signal.

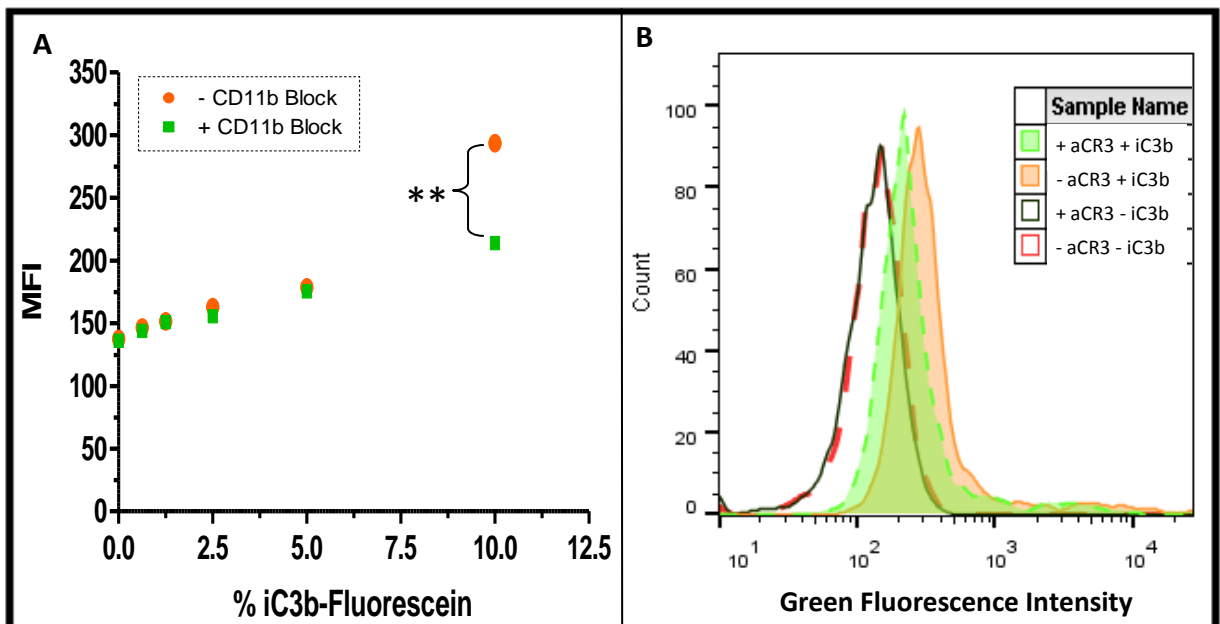


Fig.4.7: Assessment of iC3b-Fluorescein binding to BV2 cell CR3. 10^6 BV2 cells were re-suspended in appropriate volumes of HBSS 1%BSA such that addition of the appropriate volume of the iC3b-fluorescein preparation into the respective cell sample resulted in 100 μ L final-volumes with concentrations of iC3b-fluorescein ranging from 0-10%. Where indicated, harvested cells were first treated with 1 μ g of CR3-blocking mAb [clone 5C6 (8); Bio-Rad] for 30 minutes (4 $^{\circ}$ C) prior to incubation with iC3b-fluorescein. Samples were incubated with iC3b-fluorescein for 1hr (4 $^{\circ}$ C) before iC3b-fluorescein binding was assessed by flow cytometry. N = 3, Two-Way ANOVA with Bonferroni post-testing was performed: $**P < 0.001$; (B) Representative histograms of BV2 cells following incubation with (filled histograms) or without (unfilled histograms) iC3b-Fluorescein (10%) following treatment with (dashed lines) or without (solid lines) anti-CD11b/CR3 blocking antibody (aCR3).

4.5B





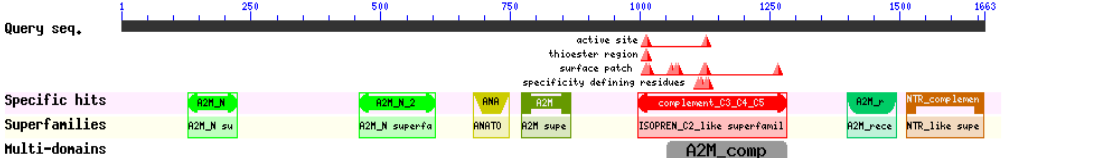

HOME SEARCH GUIDE
NewSearch Structure Home 3D Macromolecular Structures Conserved Domains Pubchem BioSystems

Conserved domains on [gi|115298678|ref|NP_000055.2]

complement C3 preproprotein [Homo sapiens]

View Concise Results ?

Graphical summary Zoom to residue level [show extra options >](#)



Query seq. 250 500 750 1000 1250 1500 1663

active site
thioester region
surface patch
specificity defining residues

Specific hits: A2M_N A2M_N_2 ANA A2M complement_C3_C4_C5 A2M_recep NTR_complemen

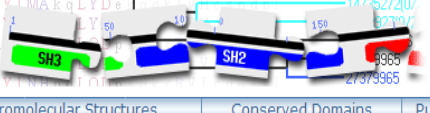
Superfamilies: A2M_su A2M_superfa ANATO A2M_supe ISOPREN_C2_like_superfam1 A2M_recep NTR_like_supe

Multi-domains: A2M_comp

List of domain hits

+	Name	Accession	Description	Interval	E-value
[+]	complement_C3_C4_C5	cd02896	Proteins similar to C3, C4 and C5 of vertebrate complement. The vertebrate complement system, ...	996-1282	5.20e-139
[+]	NTR_complement_C3	cd03583	NTR/C345C domain, complement C3 subfamily; The NTR domain found in complement C3 is also know	1513-1661	6.63e-89
[+]	A2M	pfam00207	Alpha-2-macroglobulin family; This family includes the C-terminal region of the ...	770-866	3.01e-34
[+]	A2M_recep	pfam07677	A-macroglobulin receptor; This family includes the receptor domain region of the ...	1398-1493	6.82e-33
[+]	A2M_N_2	pfam07703	Alpha-2-macroglobulin family N-terminal region; This family includes a region of the ...	458-604	4.55e-29
[+]	ANATO	cd00017	Anaphylatoxin homologous domain; C3a, C4a and C5a anaphylatoxins are protein fragments ...	678-747	2.79e-27
[+]	A2M_N	pfam01835	MG2 domain; This is the MG2 (macroglobulin) domain of alpha-2-macroglobulin.	129-224	4.03e-16
[+]	A2M_comp	pfam07678	A-macroglobulin complement component; This family includes the complement components region of ...	1051-1282	6.39e-64



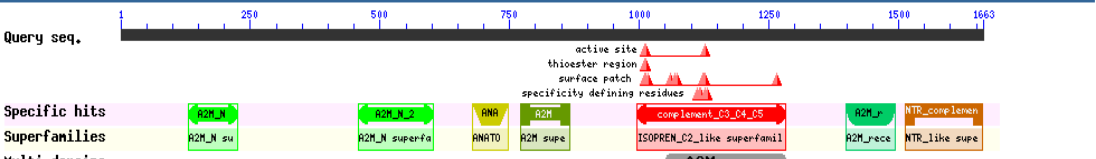
HOME SEARCH GUIDE
NewSearch Structure Home 3D Macromolecular Structures Conserved Domains Pubchem BioSystems

Conserved domains on [gi|126518317|ref|NP_033908.2]

complement C3 preproprotein

View Concise Results ?

Graphical summary Zoom to residue level [show extra options >](#)



Query seq. 250 500 750 1000 1250 1500 1663

active site
thioester region
surface patch
specificity defining residues

Specific hits: A2M_N A2M_N_2 ANA A2M complement_C3_C4_C5 A2M_recep NTR_complemen

Superfamilies: A2M_su A2M_superfa ANATO A2M_supe ISOPREN_C2_like_superfam1 A2M_recep NTR_like_supe

Multi-domains: A2M_comp

List of domain hits

+	Name	Accession	Description	Interval	E-value
[+]	complement_C3_C4_C5	cd02896	Proteins similar to C3, C4 and C5 of vertebrate complement. The vertebrate complement system, ...	996-1282	1.05e-133
[+]	NTR_complement_C3	cd03583	NTR/C345C domain, complement C3 subfamily; The NTR domain found in complement C3 is also know	1513-1661	3.85e-82
[+]	A2M	pfam00207	Alpha-2-macroglobulin family; This family includes the C-terminal region of the ...	770-866	3.47e-35
[+]	A2M_recep	pfam07677	A-macroglobulin receptor; This family includes the receptor domain region of the ...	1398-1493	3.47e-33
[+]	A2M_N_2	pfam07703	Alpha-2-macroglobulin family N-terminal region; This family includes a region of the ...	458-603	1.21e-31
[+]	ANATO	cd00017	Anaphylatoxin homologous domain; C3a, C4a and C5a anaphylatoxins are protein fragments ...	678-747	1.66e-28
[+]	A2M_N	pfam01835	MG2 domain; This is the MG2 (macroglobulin) domain of alpha-2-macroglobulin.	130-225	3.08e-17
[+]	A2M_comp	pfam07678	A-macroglobulin complement component; This family includes the complement components region of ...	1051-1282	5.34e-59

4.5C

BLAST Results
Blast 2 sequences

ref|NM_000064.3| (5148 letters)

RID V3CR3M7E11N (Expires on 08-16 20:17 pm)
Query ID q17269653991ref|NM_000064.3|
Description Homo sapiens complement C3 (C3), mRNA
Molecule type nucleic acid
Query Length 5148

Subject ID q173669943ref|NM_009778.3|
Description Mus musculus complement component 3 (C3), mRNA
Molecule type nucleic acid
Subject Length 5139
Program BLASTN 2.5.0+ > Citation

Other reports: > Search Summary

Graphic Summary

Dot Matrix View

Descriptions

Sequences producing significant alignments:

Select: All None Selected: 0

Alignments Download GenBank Graphics

Table with columns: Description, Max score, Total score, Query cover, E value, Ident, Accession. Row 1: Mus musculus complement component 3 (C3), mRNA, 3528, 3528, 97%, 0.0, 79%, NM_009778.3

Alignments

Mus musculus complement component 3 (C3), mRNA
Sequence ID: ref|NM_009778.3| Length: 5139 Number of Matches: 1

Range: 1:98 to 5133 GenBank Graphics Next Match Previous Match

Score 3528 bits(1910) Expect 0.0 Identities 4033/5076(79%) Gaps 73/5076(1%) Strand Plus/Plus

Main alignment table with columns: Query, Subject, and sequence alignment. Includes a table of alignment statistics at the top right.

iC3b/C3dg/C3g (clone 9; in-house), or an appropriate isotype control (rat IgG1), followed by a fluorophore-labelled anti-rat IgG antibody. Incubation of zymosan particles with NHS resulted in a very rapid acquisition of significant C3-fragment positivity in the assay (2.5min [earliest time-point tested], $P < 0.01^{**}$), reaching a maximum within ~10 minutes (Fig.4.9A); even after 2.5 minutes 100% of particles were positive for deposited C3-activation fragments (Fig.4.9B). Prior treatment of WT serum with EDTA ablated any signal for deposited C3-activation fragments, even after a 1hr incubation period (Fig.4.9). Isotype control primary antibody (i.e. non-specific rat IgG1 mAb) failed to return signal above background, regardless of opsonisation status (Fig.4.9). Together, these data clearly demonstrate the specific detection of C3-activation fragments deposited on zymosan particles when incubated with NHS.

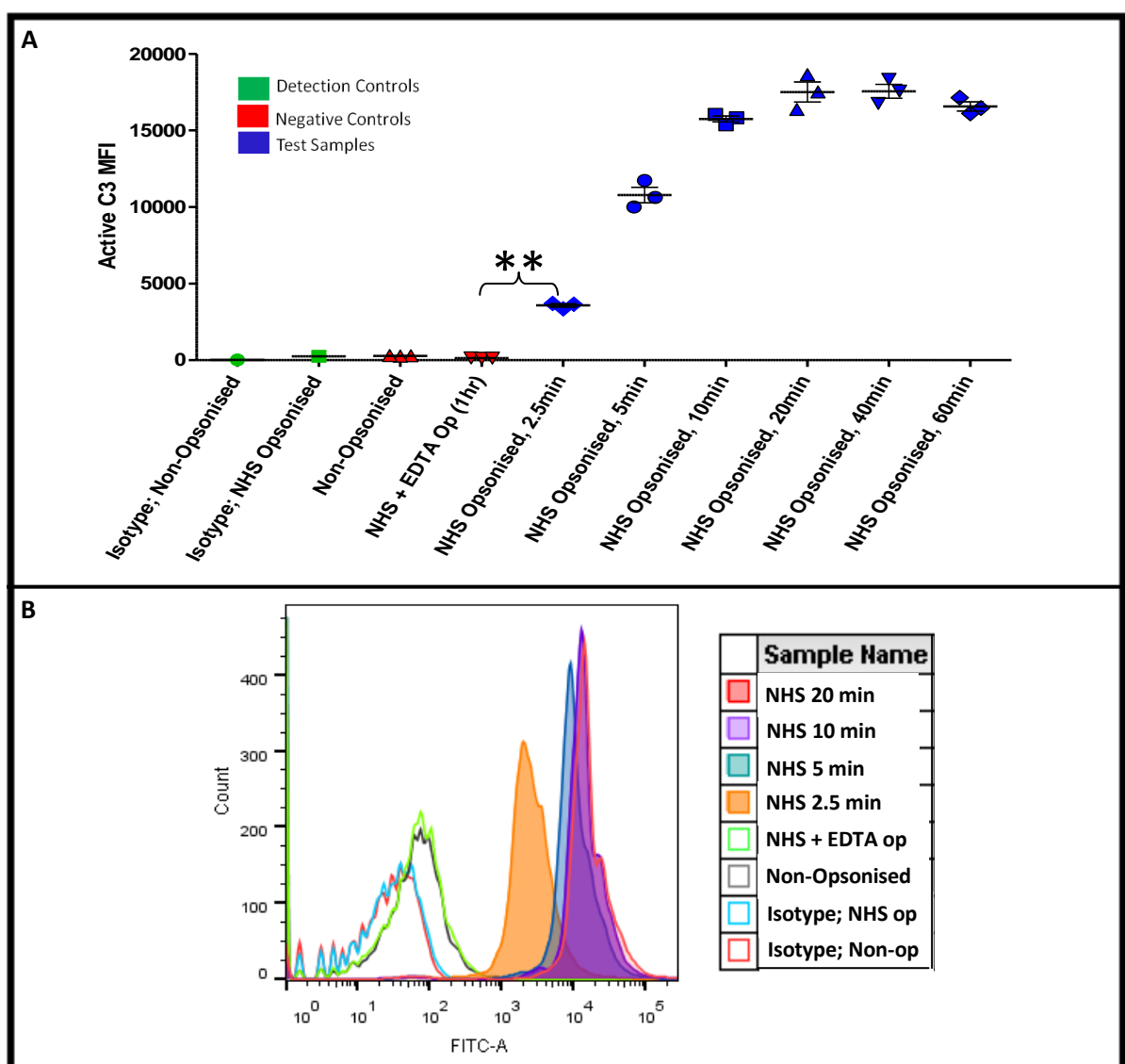


Fig.4.9: Charting C3-activation fragment deposition during NHS-opsonisation of zymosan particles. (A) Zymosan particles (unlabelled) were incubated with NHS for 0-60 minutes at 1mg mL^{-1} , or NHS + 10mM EDTA for 60 mins, before sequential staining with anti-human iC3b/C3dg/C3g mAb (Clone 9, in-house) or appropriate isotype control (rat IgG1, clone R3-34, BD) and AF488-labelled anti-rat Ab (Life Technologies) followed by flow cytometric analysis. Data points represent individual replicates. Bars = MFIs +/- SDs. One-Way ANOVA with post-hoc t-testing was performed: $**P < 0.01$; (B) Representative histograms from (A).

4.2.1.2.3.2 Assay of CR3-Mediated Mouse Microglial Phagocytosis of NHS-Opsonised Zymosan Particles

Untreated fluorescently-labelled (AF488) zymosan particles, or particles incubated with NHS were used in conjunction with an anti-CR3/CD11b mAb which blocks both the iC3b (8) and β -glucan (234) binding sites (clone 5C6 [BioRad], known to specifically bind CR3 on BV2 cells [see Section 3.2.1.1.2]) to assay the specific contribution of CR3 to C-mediated phagocytosis of NHS-opsonised zymosan by BV2 cells (*as per* Section 2.2.3.2.3). As was expected, untreated cells were universally negative for green fluorescence and opsonisation of particles with NHS resulted in a significant ($P < 0.01^{**}$) ~ 3 -fold increase in zymosan uptake (versus non-opsonised) (Fig.4.10). Pre-treatment of cells with CR3/CD11b blocking mAb prior to the addition of NHS-opsonised particles resulted in a significant reduction in opsonic phagocytosis to ~ 2.2 -fold (versus non-opsonic) ($P < 0.01^{**}$; Fig.4.10). Pre-treatment of non-opsonised zymosan-exposed cells with CR3/CD11b blocking mAb significantly reduced the level of uptake to ~ 0.8 -fold baseline ($P < 0.05^*$; Fig.4.10). In contrast, pre-treatment of both NHS-opsonised and non-opsonised zymosan-exposed cells with isotype control mAb (clone RTK4530, BioLegend) had no impact on uptake, illustrating the specificity of the effect resulting from CR3/CD11b mAb-blockade (Fig.4.10). Given that the scale of the impact of CR3/CD11b blockade on the uptake of NHS-opsonised particles is much greater than on that of non-opsonised particles (~ 4 -fold; Fig.4.10), these data combined illustrate that mouse microglial CR3 has a role in opsonic phagocytosis of NHS-opsonised zymosan and must therefore be able to engage human C3-derived ligands (albeit immobilised forms).

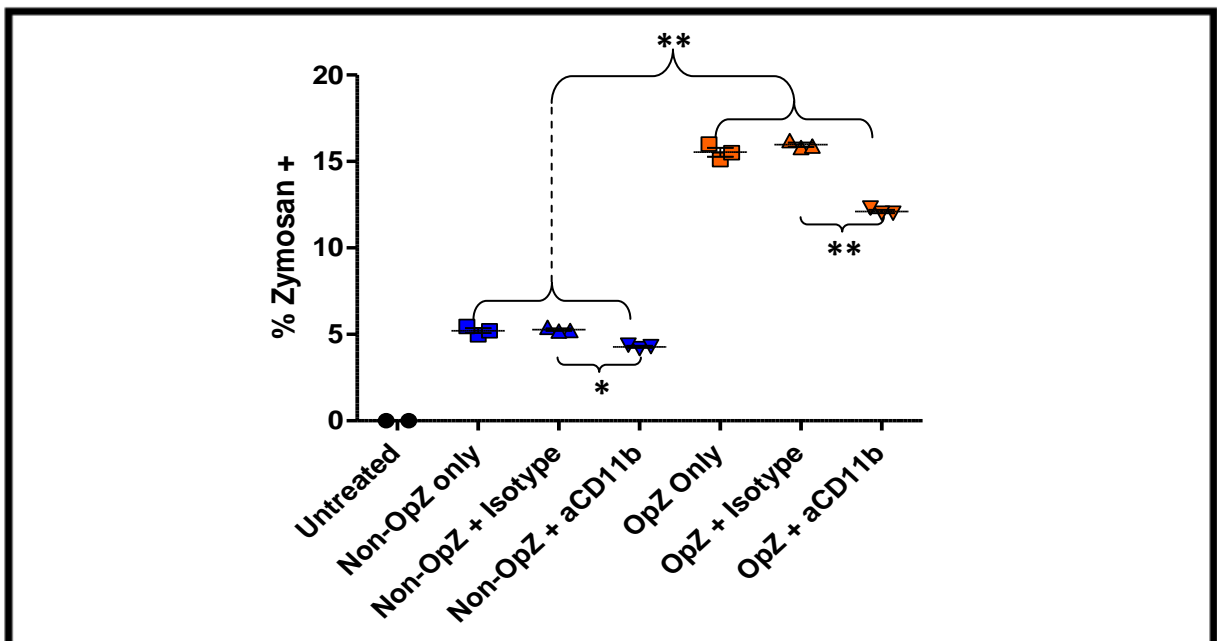


Fig.4.10: Assessment of CR3-mediated mouse microglial phagocytosis of NHS-opsonised and non-opsonised zymosan particles. 2.5×10^5 non-opsonised or NHS-opsonised particles were added directly to 5×10^4 BV2 cells cultured in 0.5mL growth medium in 24-well plates and incubated for ~ 1 hr (37°C , 5% CO_2 , humidified atmosphere). Where indicated, cells were treated with $2\mu\text{g}$ CR3-blocking Ab (Clone 5C6) or appropriate isotype control for ~ 15 minutes prior to zymosan treatment. Cells were then harvested and fluorescently stained (4°C , 30 mins) for surface CD11b (M1/70; $1\mu\text{g}/\text{mL}$) and viability (7-AAD; $2.5\mu\text{g}/\text{mL}$), before analysis by flow cytometry. Bars = means (\pm SDs); Data points represent individual replicates; One-Way ANOVA with post-hoc t-testing was performed: * $P < 0.05$, ** $P < 0.01$.

4.2.1.3 Effect of iC3b Treatment on Cell Phenotype

Microglia were treated overnight with iC3b (unlabelled) or left untreated and then activated with LPS or left un-stimulated, before assessment of surface expression of CD11b and C5aR by FACS and NO release by Griess assay.

An iC3b concentration of $1\mu\text{g mL}^{-1}$ was selected for these experiments based on published studies of CR3-ligand interactions which demonstrate specific CR3 binding and blockade of C receptor function by fluid-phase iC3b at this concentration (283, 351). Based on the results described in Chapter 3 and previous reports concerning the time-scale of changes in microglial surface markers (173), an LPS dose of 10ng/mL and a time point of 48 hours were also selected. Primary microglia were used throughout.

4.2.1.3.1 Surface Markers and Secreted Effector Molecules

Similar to the results described in Chapter 3, LPS treatment resulted in a significant (~1.5-fold) increase in baseline surface expression of both CD11b and C5aR (CD11b: $P < 0.05^*$, MFI = 1.43 x baseline; C5aR: $P < 0.001^{***}$, MFI = 1.48 x baseline) (Fig.4.11A), and robust induction of NO release ($P < 0.001^{***}$, supernatant [nitrite] = 15.5 x baseline) (Fig.4.11B). iC3b treatment alone had no effect on the basal expression of surface CD11b and C5aR and did not trigger NO release (Fig.4.11). Pre-treatment with iC3b did however modestly enhance the LPS dependent increase in both surface markers (CD11b MFI: iC3b + LPS = 1.57 x baseline Vs LPS alone = 1.43 x baseline; C5aR MFI: iC3b + LPS = 1.56 x baseline Vs LPS alone = 1.48 x baseline), although this did not achieve significance ($P = 0.32$ and 0.17 for CD11b and C5aR, respectively) (Fig.4.11A). Pre-treatment with iC3b had no effect on NO release in response to LPS (Fig.4.11B).

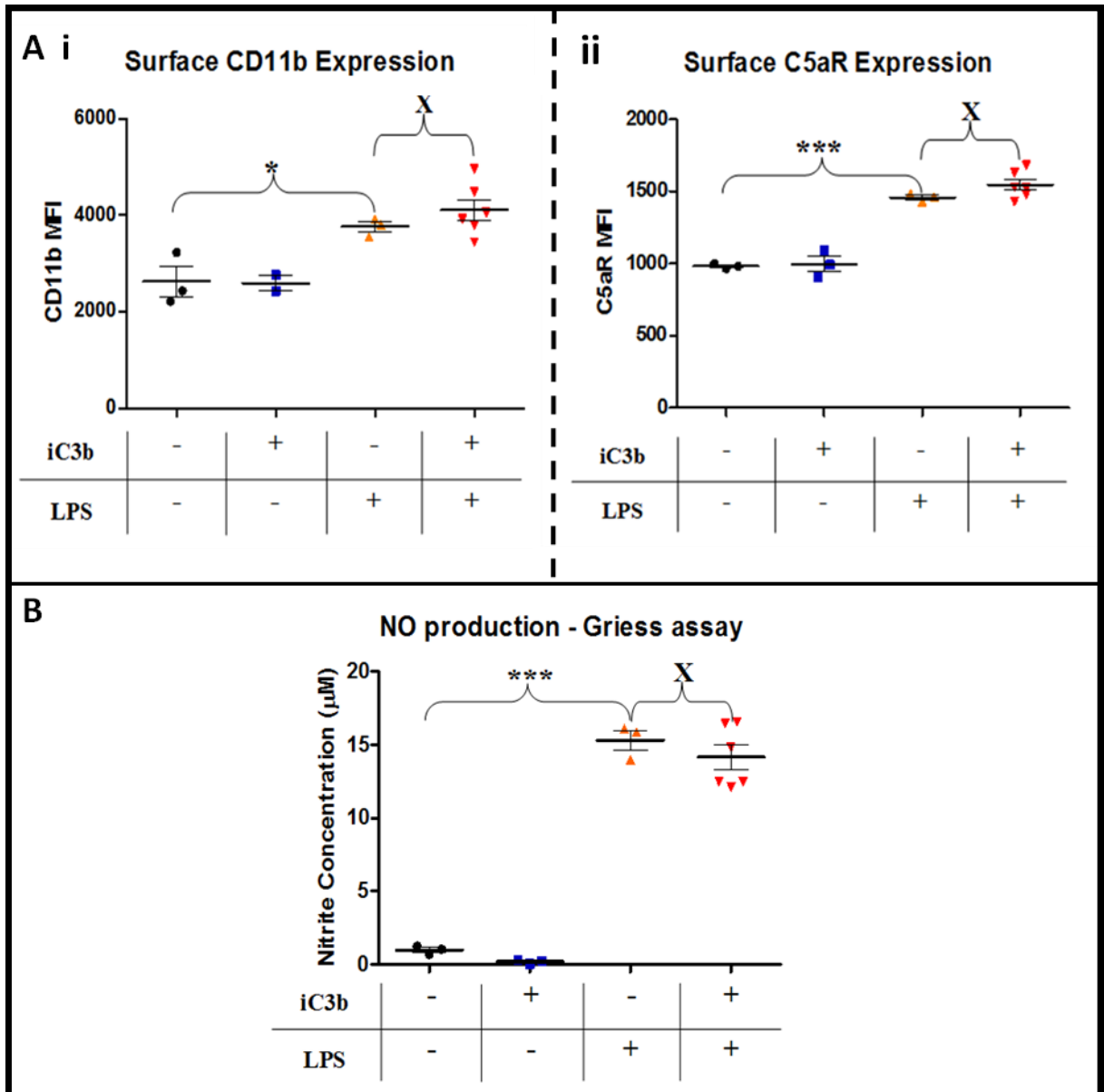


Fig.4.11: Effects of fluid-phase iC3b on basal and LPS-activated microglial phenotype – surface markers and NO production. 2.5×10^5 MACS sorted primary microglia cultured in 24-well plates were left untreated or incubated with $1 \mu\text{g}/\text{mL}$ iC3b overnight before treatment with or without $100 \mu\text{g}/\text{mL}$ LPS for 48 hours. Cells were then assayed for (A) surface CD11b (i) and C5aR (ii) by flow cytometry and (B) nitric oxide production by Griess assay of supernatants. Data points represent individual replicates; bars = means \pm SDs; Two-Way ANOVA with post-hoc t-testing was performed: * $P < 0.05$, *** $P < 0.001$, X $P > 0.05$. Individual variables: +/- LPS – $P < 0.0001$, $F = 66.04$; +/- iC3b – $P = 0.3015$, $F = 1.22$.

4.2.2 Zymosan

In view of the issue of species mismatch between iC3b in the commercial fluid-phase preparation (human) and the test cells (mouse), along with the inability to definitively demonstrate specific CR3-mediated ligand-target/cell binding, other approaches to engage microglial CR3 with iC3b were adopted. Having already demonstrated the significant role of CR3 in C-mediated phagocytosis of the well-characterised C-activator, zymosan (344), following opsonisation with NHS (as part of investigations into the ability of human C3-activation products to ligate cell-borne mouse CR3; Section 4.2.1.2.3), this strategy was again employed using mouse serum (in-place of NHS). This approach circumvents the issue of species mismatch and, owing to the local availability of C3 KO mice, benefits from the capacity to use C3-deficient serum as a negative control.

4.2.2.1 The Role of CR3 in Microglial Zymosan Phagocytosis

As a prerequisite to assays addressing the effect of CR3 engagement by zymosan-borne iC3b on cell phenotype, it was necessary to demonstrate the deposition of mouse C3-activation fragments on zymosan particles following incubation with mouse serum and to test the specific contributions of both CR3 and C3 to microglial zymosan phagocytosis.

4.2.2.1.1 Detection of Mouse C3-Activation Fragment Deposition on Zymosan Particles

Unlabelled zymosan particles were incubated with neat WT or C3 KO mouse serum for 0-60 minutes, with or without the prior addition of 10mM EDTA to the serum, and the deposition of C3-activation fragments assayed by flow cytometry using a rat monoclonal antibody (clone 2/11; Hycult Biotech, ND) against mouse C3b/iC3b/C3c, or an appropriate isotype control (rat IgG1), followed by a fluorophore-labelled anti-rat IgG antibody. Similarly to results with NHS (Section 4.2.1.2.3.1), incubation of zymosan particles with neat wild-type serum resulted in a very rapid acquisition of significant C3-fragment positivity in the assay (2.5min [earliest time-point tested], $P < 0.01^{**}$), reaching a maximum within ~10 minutes (Fig.4.12A). Incubation with C3 KO serum for any length of time failed to return any signal above very low background fluorescence (Fig.4.12), prior treatment of WT serum with EDTA ablated any signal for deposited C3-activation fragments, even after a 1hr incubation period (Fig.4.12), and isotype control primary antibody (i.e. non-specific rat IgG1 mAb) failed to return signal above background, regardless of opsonisation status (Fig.4.12). Together, these data clearly demonstrate the specific detection of murine C3-activation fragments (iC3b and C3b) deposited on zymosan particles when incubated with WT mouse serum.

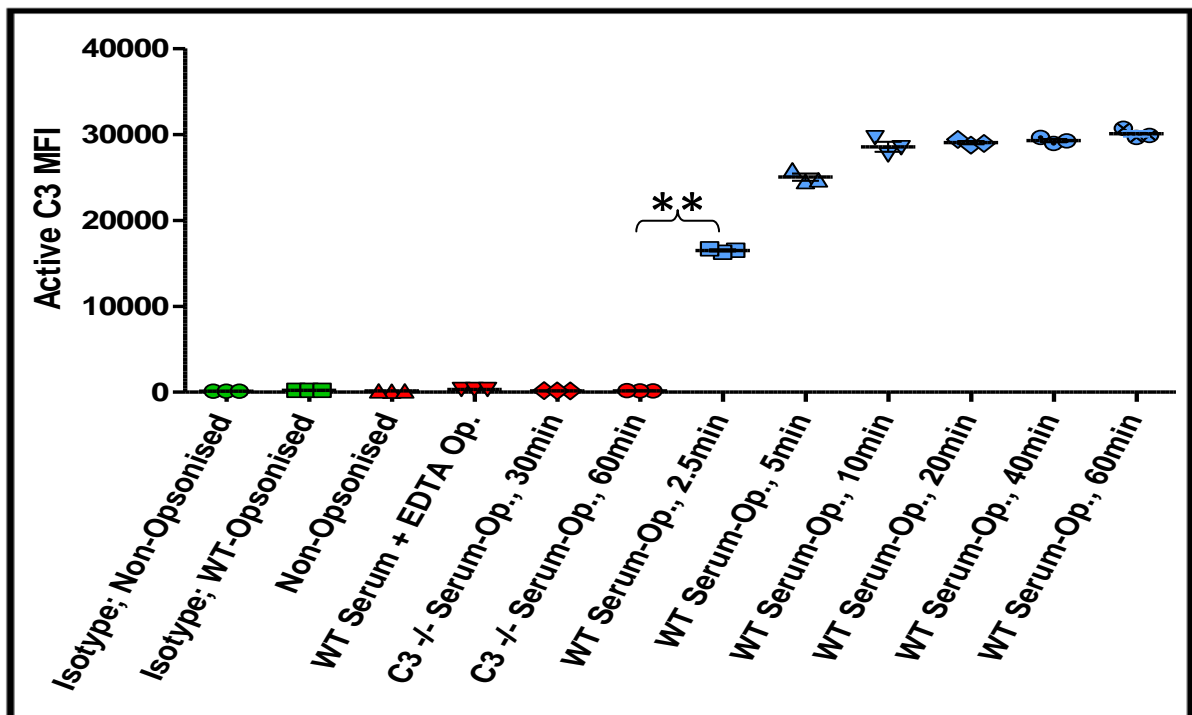


Fig.4.12: Charting C3-activation fragment deposition during mouse serum-opsonisation of zymosan particles. (A) Zymosan particles (unlabelled) were incubated with WT or C3 KO mouse serum for 0-60 minutes at 1mg mL^{-1} , or WT serum + 10mM EDTA for 60 mins, before sequential staining (4°C , 30 mins) with anti-mouse C3b/iC3b/C3c mAb (clone 2/11) or appropriate isotype control and AF488-labelled anti-rat Ab, followed by flow cytometric analysis. Data points represent individual replicates; bars = means \pm SDs; One-Way ANOVA with post-hoc t-testing was performed: $***P < 0.01$.

4.2.2.1.2 Assay of the Contribution of iC3b-CR3 Binding to Microglial Phagocytosis

Untreated fluorescently-labelled (AF488) zymosan particles, or particles incubated with WT or C3 KO mouse serum were used in conjunction with an anti-CR3 mAb which blocks both the iC3b (8) and β -glucan (234) binding sites (clone 5C6, BioRad UK) to assay the specific contribution of CR3 and C3 to both non-opsonic and opsonic phagocytosis of zymosan by BV2 cells (*as per* Section 2.2.3.2.3). Untreated cells were universally negative for green fluorescence (Fig.4.13). Opsonisation of particles with WT serum resulted in a significant ~ 2.3 -fold increase ($P < 0.01^{**}$) in zymosan uptake (versus non-opsonised) (Fig.4.13). Pre-treatment of cells with CR3 blocking Ab prior to the addition of WT serum-opsonised particles resulted in a significant reduction in opsonic phagocytosis to ~ 1.7 x baseline/non-opsonised ($P < 0.01^{**}$; Fig.4.13); this difference (resulting from blockade of both the iC3b and β -glucan binding-sites of CR3) represents the total contribution of CR3 to both opsonic (C/iC3b binding site-mediated) and non-opsonic (β -glucan binding site mediated) phagocytosis of WT serum opsonised zymosan ($\sim 25\%$). Pre-treatment of non-opsonised zymosan-exposed cells with CR3 blocking Ab significantly reduced the level of uptake to ~ 0.85 -fold baseline ($P < 0.05^{*}$; Fig.4.13); this reduction represents the contribution of the

CR3 β -glucan binding site to particle uptake. Opsonisation of particles with C3 KO serum (which precludes phagocytosis *via* the iC3b-binding site of CR3) resulted in a \sim 1.85-fold increase in particle uptake (versus non-opsonised); pre-treatment of cells with CR3-blocking Ab significantly reduced this level to \sim 1.7-fold baseline ($P < 0.05^*$) – the same as that of cells treated with CR3-blocking Ab prior to the addition of WT serum opsonised particles (Fig.4.13).

To summarise, these data combined demonstrate the specific detection of C3 (mouse)-activation fragment deposition on zymosan particles following incubation with WT mouse serum and define the specific contributions of both CR3 and C3 to opsonic (and non-opsonic) zymosan phagocytosis by BV2 cells: A large proportion (\sim 35-40%) of opsonic uptake of serum-opsonised zymosan by BV2 cells is mediated by fixed-C3, although other serum factors (e.g. Abs) and membrane receptors (e.g. Fc γ R) make an important contribution to the process; all C3-mediated microglial zymosan uptake proceeds *via* CR3; a minor proportion (10-15%) of non-opsonic zymosan phagocytosis is mediated by another CR3 binding site (i.e. lectin-like).

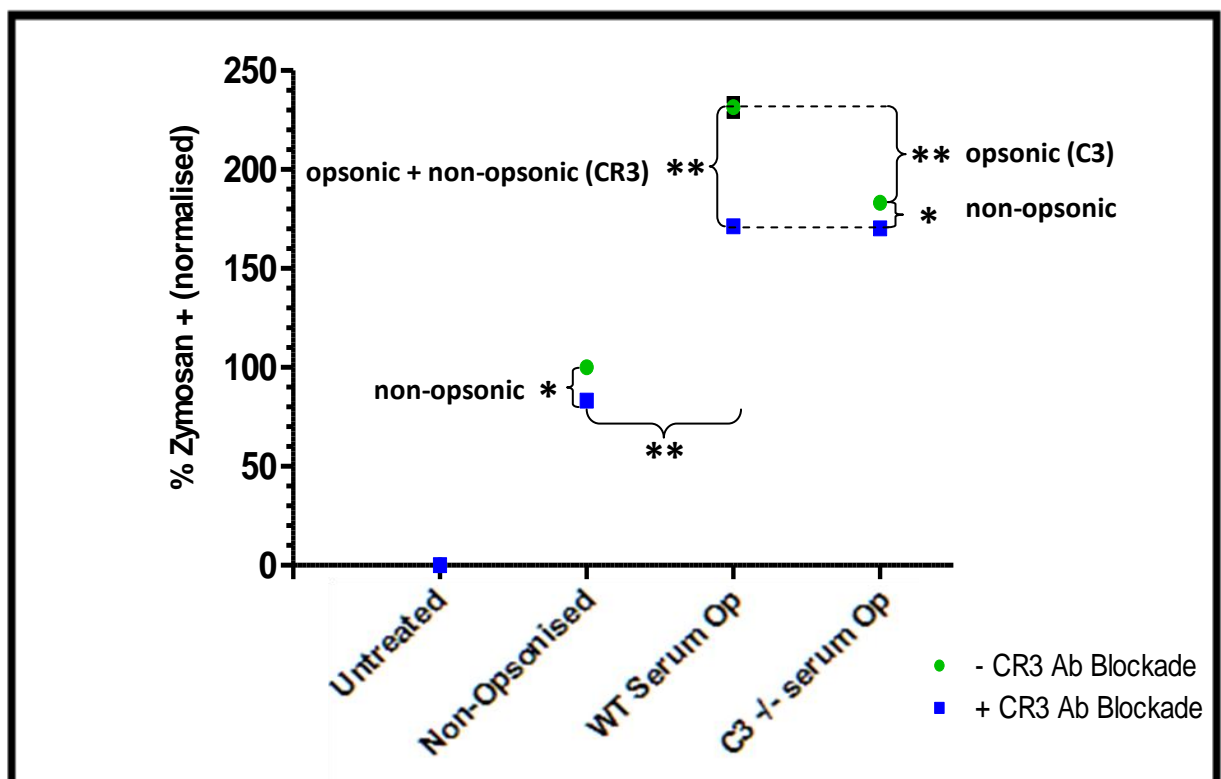


Fig.4.13: Assessment of the specific contributions of CR3 and C3 to opsonic and non-opsonic microglial zymosan phagocytosis. 2.5×10^5 non-opsonised or WT or C3 KO mouse serum- opsonised AF488-labelled zymosan particles were added directly to 5×10^4 BV2 cells cultured in 0.5mL growth medium in 24-well plates and incubated for \sim 1hr (37°C, 5% CO₂, humidified atmosphere) before fluorescent cell surface CD11b (M1/70; 1 μ g/mL) and viability (7-AAD; 2.5 μ g/mL) staining (4°C, 30 mins) followed by flow cytometric analysis. Where indicated, CR3 was blocked prior to zymosan treatment by incubation with 2 μ g CR3-blocking mAb (5C6) for 15 mins. Values are normalised to the uptake of non-opsonised particles without any mAb blockade (to permit inter-assay comparisons). Bars = means (\pm SDs); N = 3; Two-Way ANOVA with Bonferroni post-testing was performed: * $P < 0.05$, ** $P < 0.01$. Individual variables: \pm CR3 Ab Blockade – $p < 0.0001$, F = 100.6; Zymosan treatment-status – $P < 0.0001$, F = 1663.0.

The use of WT and C3 KO mouse serum-opsonised particles, alongside untreated zymosan and CR3 blockade thus permits the consequences of iC3b engagement of CR3 to be investigated and, furthermore, dissected from those resulting from engagement of the same receptor by other ligands (e.g. β -glucan), along with other receptors (opsonic [e.g. FcR] and non-opsonic/scavenger [e.g. dectin-1]), whilst also circumventing issues of species mismatch. Both CR3-blockade (using mAb) and the use of C3 KO serum as an opsonising reagent provide a means to eliminate particle uptake mediated by iC3b-CR3 binding, but given that CR3 blockade also eliminates its minor role in non-opsonic uptake, coupled with the finding that opsonic phagocytosis mediated by fixed-C3 occurs exclusively *via* CR3 in BV2 cells, it is determined that the use of C3 KO serum as an opsonising reagent provides the optimal means to control for off-target effects resulting from zymosan uptake *via* non-iC3b-CR3 interactions (e.g. β -glucan-CR3, IgG-Fc γ R).

4.2.2.2 CR3 Binding of Zymosan-Borne iC3b and Microglial Phenotype

4.2.2.2.1 Basal Phenotype - Rt-qPCR

In-order to investigate the effects on microglial phenotype of CR3 engagement by iC3b generated on the surface of zymosan particles (as a consequence of sequential C activation and regulation during serum opsonisation), BV2 cells were exposed to an excess of un-opsonised zymosan, or particles opsonised with normal or heat inactivated WT, or C3 KO serum, and assayed for changes in mRNA/transcript levels of pro-inflammatory cytokines (IL-6, TNF- α and IL-1 β) by Rt-qPCR. Cells were also treated with LPS as a pro-inflammatory immune cell activator (whose effects on microglial phenotypes were characterised and described in Chapter 3).

LPS treatment resulted in a robust mRNA/transcript induction for all genes tested (TNF- α , IL-6 and IL-1 β) (Fig.4.14) and in the case of IL-6 (Fig.4.14A) and TNF- α (Fig.4.14B) caused the greatest response among all conditions investigated. Similarly to LPS, treatment with non-opsonised zymosan particles was potently pro-inflammatory, resulting in a robust increase for all cytokines tested (Fig.4.14). In the case of IL-6 this increase was \sim 40% of the magnitude of that observed following LPS treatment and in the case of TNF- α was \sim 75% (both significantly reduced Vs LPS, $P < 0.01^{**}$; Fig.4.14 A & B, respectively), while being slightly greater in the case of IL-1 β (Fig.4.14C). Treatment of cells with zymosan particles incubated with WT serum which had been heat inactivated resulted in a response profile very similar to that of non-opsonised particles (Fig.4.14). In contrast, when cells were treated with normal WT serum-opsonised particles the mRNA/transcript levels for IL-6 (Fig.4.14A) and TNF- α (Fig.4.14B) were barely above baseline (significantly reduced Vs heat-inactivated serum, $P < 0.01^{**}$). In the case of IL-1 β , however, the response relative to that for LPS, non-opsonised and heat-inactivated WT serum opsonised particles was significantly greater by some \sim 30% ($P < 0.01^{**}$; Fig.4.14C). For all genes tested,

treatment of cells with zymosan opsonised with C3 KO serum resulted in a response intermediate between that observed following stimulation with non-opsonised and WT serum-opsonised particles (significantly different Vs WT serum-opsonised particles, IL-6 & TNF- α [increased] $P < 0.01^{**}$, IL-1 β [reduced] $P < 0.05^*$; Fig.4.14).

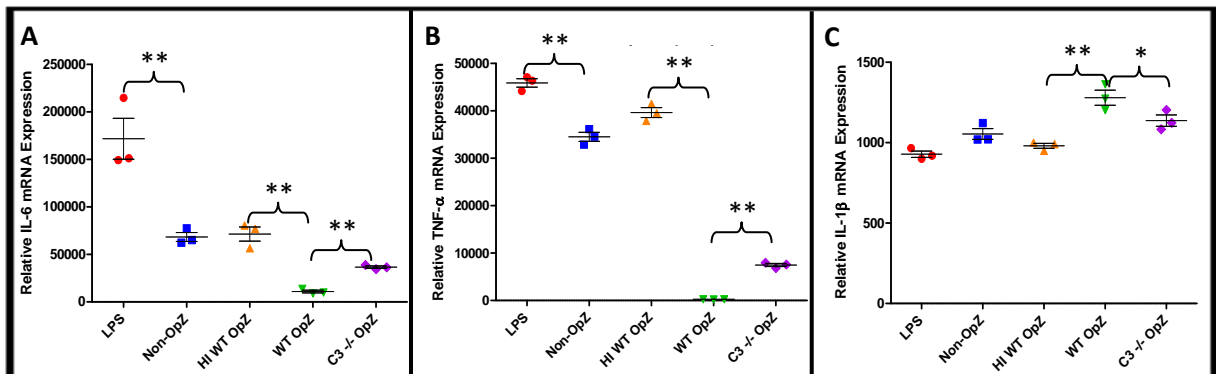


Fig.4.14: Impact of opsonic and non-opsonic zymosan exposure on microglial cytokine mRNA production—the role of zymosan borne iC3b. 5×10^4 BV2 cells were seeded into individual wells of a 24-well plate and cultured overnight in 0.5mL growth medium. Cells were then treated for 24 hours with $1 \mu\text{g/mL}$ LPS, or 2.5×10^6 un-opsonised zymosan particles (unlabelled), or particles opsonised (1mg/mL , 37°C , 1hr) with HI or normal WT or C3 KO serum. RNA was then extracted and subjected to DNase I (Ambion) digest prior to RT ($20 \mu\text{g/mL}$) using the TaqMan RT reagents (Applied Biosystems). Quantitative PCR was then performed using 32ng RNA equivalent of cDNA as a template along with gene specific primers (as indicated) in $20 \mu\text{L}$ reactions using SYBR green Jump-Start Taq-ready mix (Sigma-Aldrich). Data points represent individual replicates; bars = means \pm SDs; One-Way ANOVA with post-hoc t-testing was performed: * $P < 0.05$, ** $P < 0.01$.

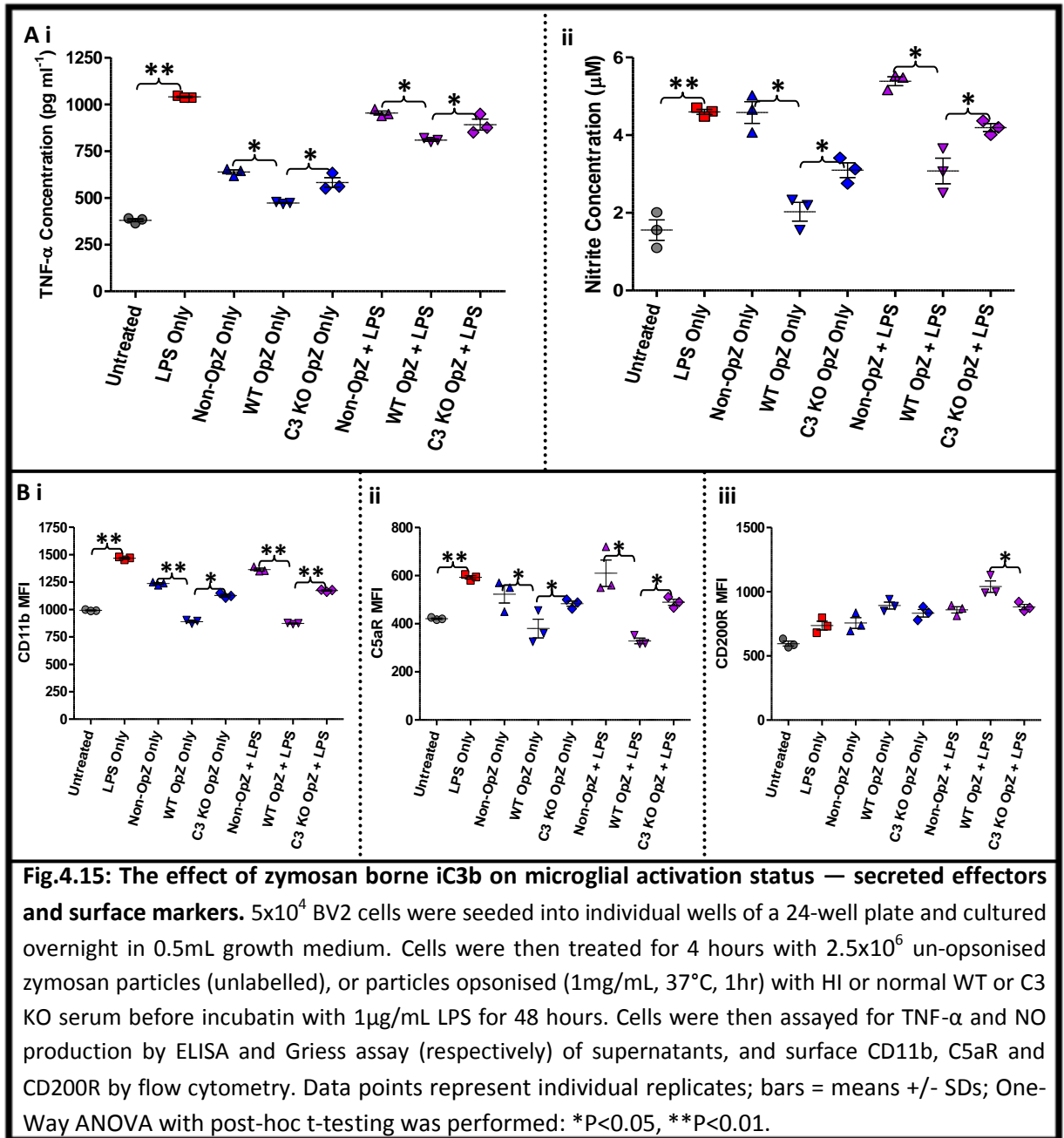
4.2.2.2.2 Activation Response - Secreted Effectors and Surface Markers

In-order to investigate the specific effects of CR3 engagement by iC3b generated on the surface of zymosan particles on the magnitude of microglial functional responses to subsequent activating stimuli, BV2 cells were stimulated with an excess of un-opsonised zymosan, or particles opsonised with (normal) WT, or C3 KO serum, before subsequent treatment with or without LPS; Cells were then assayed for changes in the release of pro-inflammatory effector molecules (TNF- α and NO, by ELISA and Griess assay, respectively) and cell-surface markers (CD11b, C5aR and CD200R, FACS).

Release of TNF- α (Fig.4.15Ai) into the supernatant in response to LPS alone was significantly increased ~ 3 -fold ($P < 0.01^{**}$); although readily detectable, the TNF- α response to non-opsonised zymosan alone was $\sim 60\%$ lower (somewhat surprising given that the mRNA/transcript changes were similar for these triggers [Fig.4.14B]). In contrast, treatment with particles opsonised with WT serum had little impact on basal TNF- α secretion, resulting in a significant reduction in the TNF- α level relative to non-opsonised particle-treatment ($P < 0.05^*$). Treatment with zymosan opsonised with C3 KO serum elicited an intermediate response which was significantly greater than basal levels ($P < 0.05^*$). Pre-treatment with the different forms of zymosan caused moderate

(~20-40%) reductions in the TNF- α response to LPS exposure; the largest effect was with WT serum opsonised zymosan (significantly reduced Vs non-opsonised particles, $P < 0.05^*$) while C3 KO serum-opsonised particles again had an intermediate effect (significantly increased Vs WT serum-opsonised particles, $P < 0.05^*$).

Very similar relationships were observed in the changes in the other parameters investigated following treatment with the different zymosan forms and/or LPS, although for all other parameters there was a smaller, or no difference in the response to non-opsonised zymosan versus LPS alone (Fig.4.15 Aii & B). Additionally: in the case of surface CD11b (Fig.4.15Bi) and C5aR (Fig.4.15Bii), in-contrast to treatment with LPS or non-opsonised zymosan in isolation or sequential combination, treatment with WT serum opsonised particles resulted in a change to levels which were actually below baseline and the response continued to shift in this direction following subsequent LPS treatment; in the case of surface CD200R (Fig.4.15Biii), treatment with WT serum opsonised zymosan resulted in a response relative to LPS which was inverted compared with that detected for the other parameters (i.e. CD200R WT opZ > CD200R LPS; C5aR, CD11b, TNF- α , NO WT opZ < C5aR, CD11b, TNF- α , NO LPS) and which continued to shift in this direction following subsequent LPS treatment.



4.2.3 C3-Activation Fragments Immobilised on Tissue Culture Plastic

4.2.3.1 System Development

In-view of the issues associated with the use of zymosan as a 'carrier' for serum-derived activated C3, namely its intrinsic nature as a potent PAMP, other approaches were explored to specifically engage microglial CR3 with iC3b. Having validated the concept of activating serum C to achieve C3-fixation on surfaces, along with assays for its specific detection and the use of C3 KO serum as a negative control (Section 4.2.2.1), a method based on this principle (i.e. activation and fixation of serum C3) was sought. The very earliest formal recognition of C was that of the ability of complexed Ab to sensitise an Ag to C activation (2, 16, 20). Furthermore, as a basis for many common lab assays (e.g. ELISAs), it is long established that bio-molecules can be adsorbed to plastic surfaces (352): Based on these fundamental principles, the possibility of utilising a C-fixing Ab-Ag interaction to activate and immobilise serum-derived C3 to TC plastic was explored.

Well characterised in-house C-fixing anti-MOG mouse mAbs (353-355) along with recombinant MOG were utilised as a foundation for the investigation of C3-fixation described above.

4.2.3.1.1 Demonstrating Specificity of rMOG : anti-MOG Binding

As a starting point for optimising the activation of C3 on TC plastic, 3 mouse anti-MOG mAbs (Z4, Z12 and Y10) were tested together with mouse anti-C1Inh monoclonal Ab as a control. Target antigen (i.e. rMOG or C1Inh) was immobilised onto TC plastic and then incubated sequentially with a concentration gradient of either Z4, Z12, Y10 or anti-C1Inh, followed by HRP-labelled anti-mouse Ab. Binding was detected by colourimetric means (*as per* Section 2.2.4.1.1). When rMOG was immobilised (Fig.4.16A), each of the anti-rMOG antibodies returned strong signal at the highest Ab concentrations. However, as concentrations of Abs decreased, signal for Y10 decreased rapidly, becoming undetectable at the lowest concentrations, whereas that of Z4 and Z12 remained relatively stable throughout the concentration range tested. Anti-C1Inh mAb returned no signal above background for binding to immobilised rMOG, regardless of concentration. When C1Inh was immobilised (Fig.4.16B), Anti-C1Inh mAb returned strong signal at the highest concentrations, which declined with decreasing Ab concentration but remained above background throughout. No signal was detectable for Y10 binding to C1Inh at any of the concentrations tested. A modest signal for non-specific binding of Z4 and, more strongly, Z12 to C1Inh was detectable at the highest Ab concentrations tested, but this fell away with decreasing concentration. These data indicate all 3 anti-MOG Abs specifically bind rMOG (albeit with different affinities and specificities).

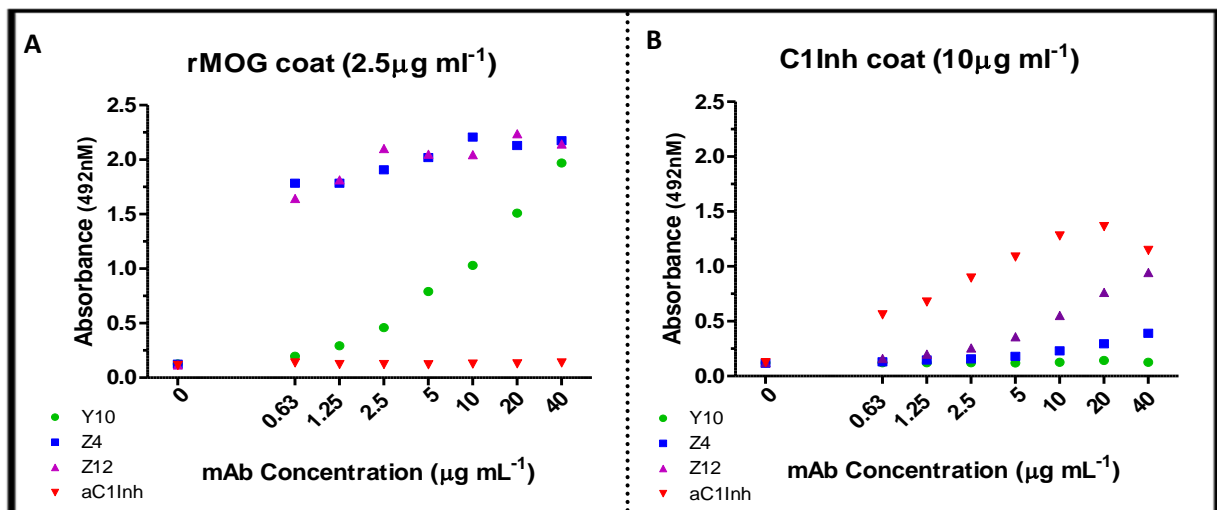
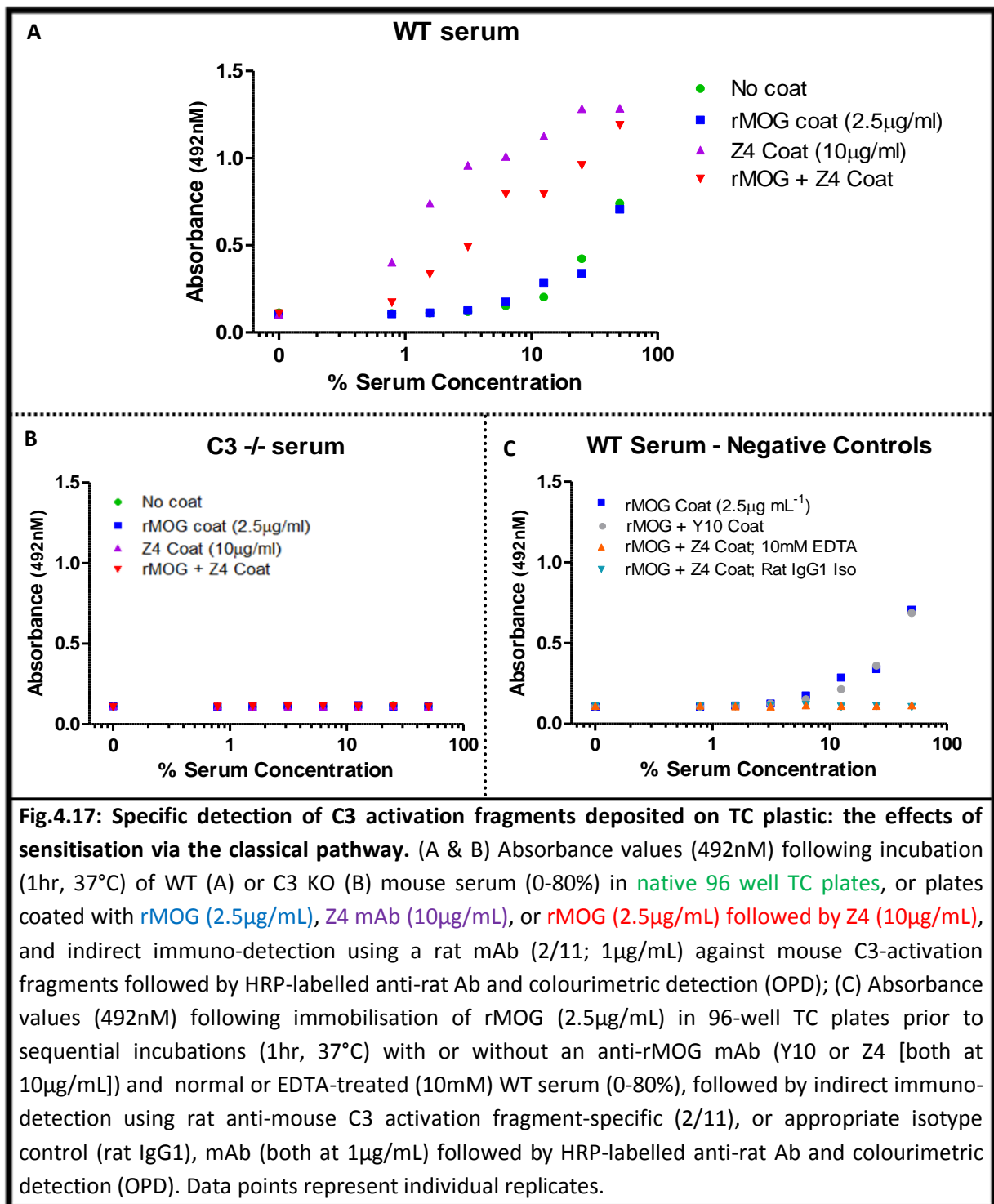


Fig.4.16: Specific binding of anti-rMOG mAbs to immobilised Ag. Absorbance (492nm) values following immobilisation of rMOG (2.5µg/mL; A) or C1Inh (10µg/mL; B) in 96-well plates and detection using a concentration gradient of a mouse anti-rMOG (Y10, Z4 or Z12) or anti-C1Inh mAb (0-40µg/mL) followed by anti-mouse HRP and colourimetric detection (OPD). Data points represent individual replicates.

4.2.3.1.2 Demonstrating C-Activation by anti-MOG mAb: C-Fixing (Z4) Vs Non C-Fixing (Y10)

The C-fixing capacity of the in-house anti-MOG mAbs has previously been determined (354): Z4 is a C-fixing mAb with high affinity and specificity for immobilised MOG (Fig.4.16); Y10 is non C-fixing and was included as a negative control. rMOG was immobilised and then incubated with (or without) Z4 or Y10 anti-rMOG mAbs prior to incubation with doubling-dilutions of WT or C3 KO or EDTA (10mM)-treated WT serum. Z4 mAb alone was also immobilised directly to the TC plastic (i.e. without any target Ag) and incubated (as above) with serum. Fixation of activated C3 was then assayed using a rat anti-C3b/iC3b/C3c mAb (clone 2/11), or an appropriate isotype control (rat IgG1), followed by anti-rat HRP and colourimetric detection (*as per* Section 2.2.4.1.2). Incubation of WT serum with untreated TC plastic (Fig.4.17A) or plastic coated with unbound Ag/rMOG alone (Fig.4.17 A & C) failed to result in any detectable C3-fixation at the lowest serum concentrations, but appreciable levels of signal were detectable at the highest serum concentrations (i.e. >10%). Binding of Y10 mAb to rMOG failed to promote C3-activation fragment deposition, confirming its non-C-activating nature [Fig.4.17C; (354)]. In contrast, binding of Z4 mAb to rMOG enhanced the deposition of C3-activation fragments, confirming its C-activating nature [Fig.4.17A; (354)]. Given that Ag binding and orientation are important determinants in terms of an antibody's ability to fix C (2, 20), an unexpected finding was that the sensitisation conditions which yielded the greatest signal for activated-C3 deposition were those when Z4 was immobilised directly to untreated TC plastic (Fig.4.17A). When C3 KO (Fig.4.147B), or EDTA inhibited WT serum or a non-specific rat IgG1 monoclonal primary C3-detection Ab (Fig.4.17C) were utilised as negative controls, no signal for deposited C3-activation fragments was detectable under any conditions.



These data illustrate the ability to specifically detect C activation and deposition on TC plastic and to utilise a C-fixing Ag-Ab interaction to enhance this process/sensitise the substrate. Additionally, they demonstrate that a level of C activation (and C3-deposition) occurs without requiring any sensitisation of TC plastic, becoming appreciable at the highest serum concentrations, and also show that C3 KO serum can act as a suitable control for any off target effects resulting from incubation of TC plastic with serum. Moreover, they illustrate that the most effective design in this system of C activation with the reagents in use is the direct immobilisation of Z4 mAb to the TC surface with subsequent incubation with WT serum.

4.2.3.2 Effects of TC-Plastic Immobilised C3-Activation Fragments on Microglia

4.2.3.2.1 Z4 mAb

Having developed methods for the deposition of C3 activation fragments on TC plastic, the impact on microglial phenotype was investigated. TC wells were coated with C3 activation fragments as described above (Section 4.2.3.1.2); C3 KO serum was used as control. After thorough washing, BV2 cells were seeded onto the wells then treated with or without LPS. After 48 hours, cells and supernatants were harvested and assayed for expression of surface markers (CD11b, C5aR & CD200R; *as per* Section 2.3.1) and levels of secreted effectors (cytokines [TNF- α , IL-6] and NO; *as per* Section 2.3.3), respectively.

4.2.3.2.1.1 Secreted Effectors

As a pro-inflammatory control stimulus, LPS treatment alone resulted in a clear, significant increase in detectable levels of each secreted effector assayed in the culture supernatant (Fig.4.18): in the case of TNF- α ($P < 0.01^{**}$; Fig.4.18i) and NO ($P < 0.05^*$; Fig.4.18iii), levels following LPS treatment were roughly 2-fold baseline; in the case of IL-6 (Fig.4.18ii), where no cytokine was detectable at baseline, LPS treatment resulted in an increase from 0-25pg mL⁻¹ ($P < 0.01^{**}$). Exposure of cells to a Z4 mAb-coated surface caused a 2-fold increase in TNF- α levels compared to baseline (Fig.18i), while smaller increases in the levels of IL-6 (Fig.18ii) and NO (Fig.4.18iii) were detected. Pre-incubation of serum with the Z4 coated substrate modified the effects of the antibody coat-alone, significantly reducing the levels of each analyte ($P < 0.05^*$; Fig.4.18); in the case of NO, this reduced production to below basal levels. The effects of WT serum mirrored almost exactly those of C3 KO serum (Fig.4.18).

LPS treatment of cells seeded onto a Z4 mAb-coated substrate resulted in the highest recorded levels of TNF- α (Fig.4.18i) and IL-6 (Fig.4.18ii). In the case of NO release, however, levels were very similar to those following exposure of cells to a Z4-coated substrate alone (Fig.4.18iii). LPS treatment of cells seeded on serum-preincubated Z4-coated substrate resulted in an increase in all analytes relative to baseline or following exposure of cells to Z4 coated surface, with or without prior incubation with serum (WT or C3 KO) (Fig.4.18). In the case of TNF- α (Fig.4.18i) and IL-6 (Fig.4.18ii), levels were significantly reduced ($P < 0.05^*$) compared with those following LPS treatment of cells seeded onto Z4-coated substrate, being roughly equal with those detected following isolated LPS treatment; In the case of NO release however, levels were significantly greater than those following LPS treatment of cells seeded onto wells coated with Z4 mAb ($P < 0.05^*$; Fig.4.18iii). As observed in the absence of LPS treatment, the effects of incubation of WT serum with a Z4 coated substrate prior to seeding and treatment of cells with LPS mirrored almost exactly those observed following incubation with C3 KO serum (Fig.4.18).

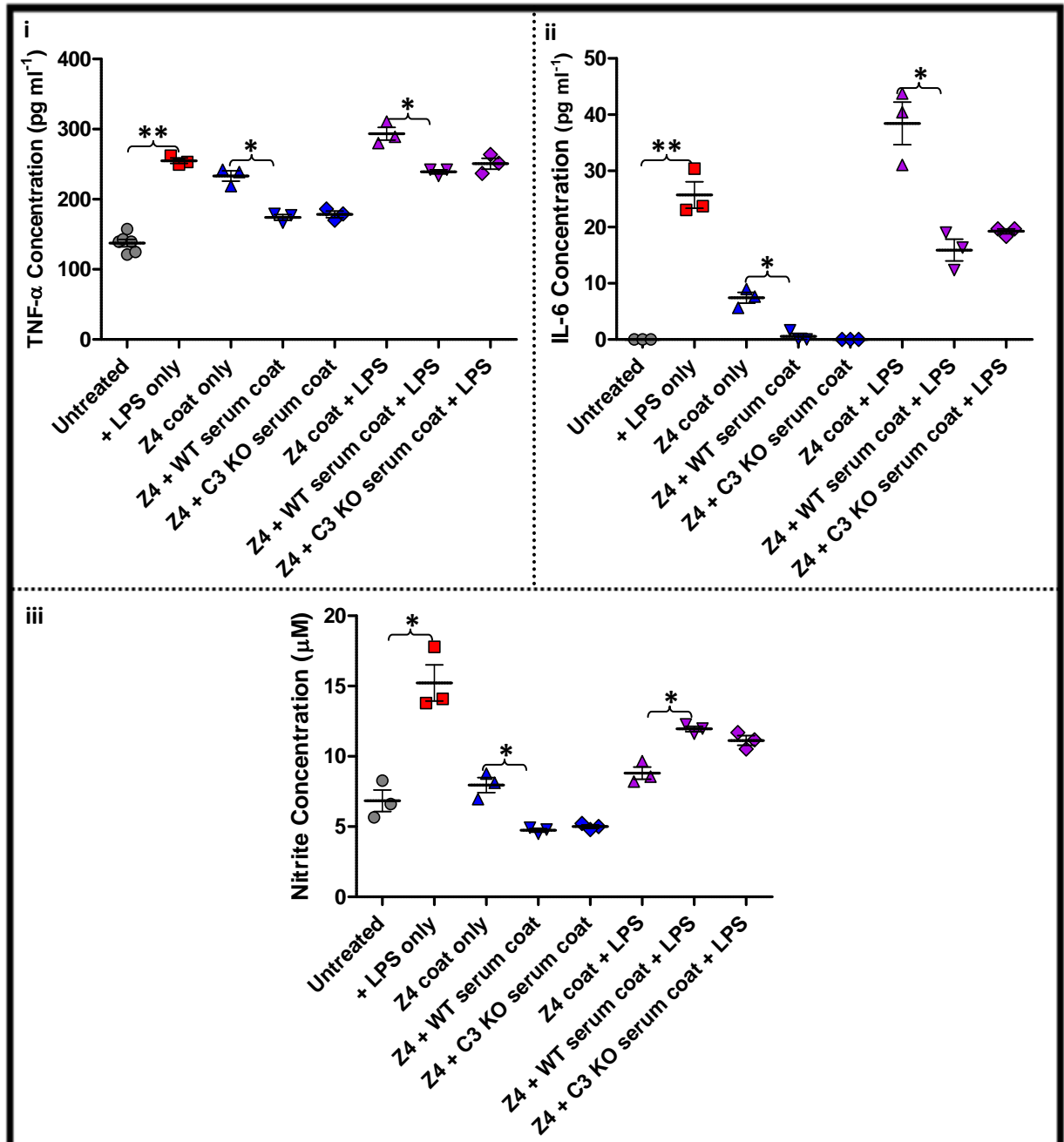


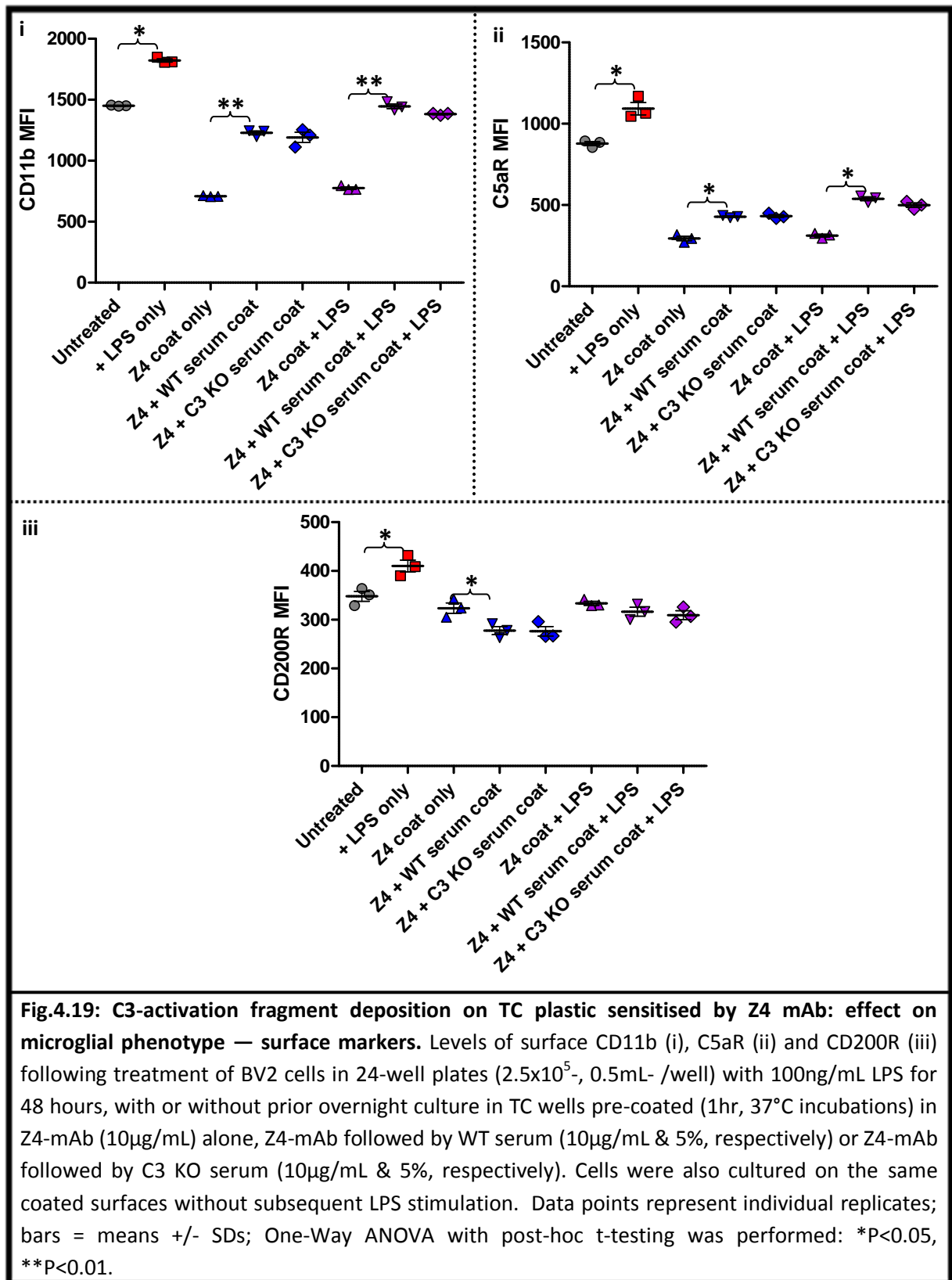
Fig.4.18: C3-activation fragment deposition on TC plastic sensitised by Z4 mAb: effect on microglial phenotype — secreted effectors. Levels of supernatant TNF- α (i), IL-6 (ii) and NO (iii) as determined by ELISA (cytokines) and Griess assay (NO) following treatment of BV2 cells in 24-well plates (2.5×10^5 , 0.5mL /well) with 100ng/mL LPS for 48 hours, with or without prior overnight culture in TC wells pre-coated (1hr, 37°C incubations) in Z4-mAb (10 μ g/mL) alone, Z4-mAb followed by WT serum (10 μ g/mL & 5%, respectively) or Z4-mAb followed by C3 KO serum (10 μ g/mL & 5%, respectively). Cells were also cultured on the same coated surfaces without subsequent LPS stimulation. Data points represent individual replicates; bars = means \pm SDs; One-Way ANOVA with post-hoc t-testing was performed: *P<0.05, **P<0.01.

4.2.3.2.1.2 *Surface Markers*

In the case of both CD11b (Fig.4.19i) and C5aR (Fig.4.19ii) surface levels increased significantly following LPS treatment (~25%, $P < 0.05^*$). In contrast, culture of cells on Z4-coated TC plastic resulted in a dramatic reduction in expression of these markers (~55-70%). Incubation of serum in Z4-coated wells prior to cell seeding resulted in a significant shift in both markers back towards baseline levels, which was more pronounced in the case of CD11b (CD11b: ~50%, $P < 0.01^{**}$; C5aR: ~15%, $P < 0.05^*$). Subsequent LPS treatment of cells seeded on Z4-coated wells incubated without serum had little effect on surface CD11b and C5aR responses to the mAb-coat. In the case of serum-incubated Z4-coated wells however, there was a significant increase in both (CD11b, $P < 0.01^{**}$, C5aR, $P < 0.05^*$), exceeding the levels under the same conditions without subsequent LPS stimulation.

In the case of CD200R (Fig.4.19iii), LPS treatment alone significantly increased expression over basal levels (~20%, $P < 0.05^*$). In contrast to CD11b (Fig.4.19i) and C5aR (Fig.4.19ii), culture of cells on a Z4-coated substrate resulted in a slight (non-significant, $P > 0.05$) decrease in basal surface CD200R levels, while exposure to serum-treated Z4-coated wells resulted in a further decrease which achieved significance ($P < 0.05^*$). LPS treatment of cells seeded onto Z4-coated TC plastic had no discernible effect on the surface CD200R response to the mAb-coat, while LPS treatment of cells seeded onto serum-treated Z4-coated wells resulted in a slight decrease (although not as great as the same conditions in the absence of LPS-treatment).

As observed for secreted effectors (Fig.4.18) the effects of incubation of WT serum with a Z4-coated substrate prior to seeding, with or without LPS treatment, were virtually identical to those detected when using C3 KO serum (Fig.4.19).



These data illustrate a complex relationship between microglial activation and exposure to the different triggers employed here. The lack of difference between WT and C3-deficient serum opsonisation indicates that C3-activation fragments had no specific effects on microglial inflammatory effector release and surface maker expression. Instead these data show that the

observed alterations from the normal basal and activated phenotypes are consequences of the mAb-coated substrate and the presence of serum-derived factors other than C3 and its activation products.

4.2.3.2.2 Non-Sensitised TC Plastic: BV2 Microglial Cell Line

Given the powerful observed effects of the Z4 mAb-substrate coat on cell phenotype (Section 4.2.3.2.1), it appears evident that, as shown above for zymosan (Section 4.2.2), the Ab-coated surface provides a powerful activation trigger that may mask effects of iC3b-CR3 interaction. Guided by the demonstration that C3-activation fragments are deposited even on untreated TC substrate when incubated with high serum concentrations (Fig.4.17), this simple system was utilised to achieve C activation and C3-activation fragment deposition in the absence of the confounding presence of the mAb substrate-coat.

Previously untreated TC plastic was left untreated or incubated with 35% WT or C3 KO serum prior to seeding of BV2 cells and treatment with or without LPS; Cells and supernatants were then harvested and assayed for surface markers (CD11b and C5aR; *as per* Section 2.3.1) and secreted effectors (IL-6 and NO; *as per* Section 2.3.3), respectively.

4.2.3.2.2.1 Secreted Effectors

In the case of both IL-6 and NO, LPS treatment alone resulted in a significant increase, with NO levels in supernatant increasing ~2-fold and IL-6 levels from undetectable to ~80pg/mL ($P < 0.01^{**}$; Fig.4.20A). In the case of IL-6, incubation of the wells with serum (either WT or C3 KO) failed to significantly alter basal levels or the response to LPS (Fig.4.20Aii). In the case of NO however, serum pre-incubation significantly reduced basal levels to ~50% ($P < 0.01^{**}$), although no difference was observed between the effects of WT or C3 KO serum (Fig.4.20Ai). Pre-incubation with serum (WT or C3-deficient) failed to modify the normal IL-6 response to LPS treatment (Fig.4.20Aii). However, while pre-incubation with C3 KO serum also failed to modify the normal NO response to LPS treatment, pre-incubation with WT serum significantly enhanced it (~40%, $P < 0.05^*$; Fig.4.20Ai). These results are compatible with previous reports of iC3b-CR3 modulation of microglial priming (1).

4.2.3.2.2.2 Surface Markers

LPS treatment of cells in untreated wells resulted in a significant increase in surface expression of both CD11b and C5aR (~20-25%, $P < 0.05^*$; Fig.4.20B). Incubation of cells in wells pre-incubated with C3 KO serum resulted in a small increase in basal CD11b and C5aR expression, while WT serum resulted in a reduction, with a significant difference between the serum-treatment groups ($P < 0.05^*$; Fig.4.20B). When cells cultured in wells pre-incubated with serum were subsequently treated with LPS, expression of both markers was further increased above that caused by LPS

alone; this effect was seen for both WT and C3-deficient serum but in the case of CD11b was significantly more pronounced for C3-deficient serum ($P < 0.05^*$) (Fig.4.20B).

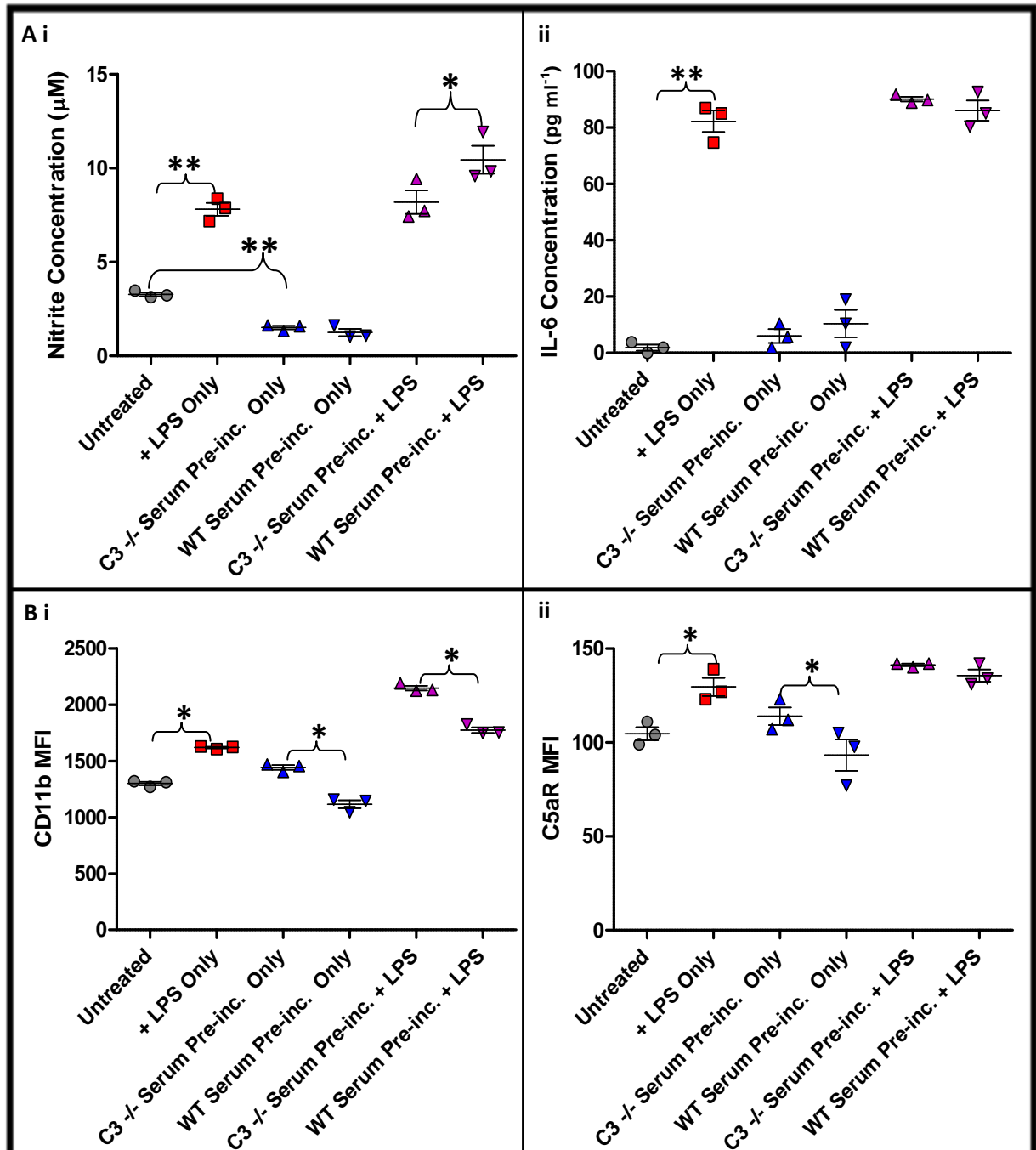


Fig.4.20: C3-activation fragment deposition on non-sensitised TC plastic: effect on microglial phenotype — secreted effectors and surface markers. (A) Levels of supernatant IL-6 (i) and NO (ii) as determined by ELISA & Griess assay, respectively, and (B) surface CD11b (i) and C5aR (ii) as determined by flow cytometry, following treatment of BV2 cells in 24-well plates (2.5×10^5 , 0.5 mL/well) with 100 ng/mL LPS for 48 hours, with or without prior overnight culture in TC wells pre-coated in 35% WT or C3 KO serum (1hr, 37°C). Cells were also cultured on the same coated surfaces without subsequent LPS stimulation. Data points represent individual replicates; bars = means \pm SDs, One-Way ANOVA with post-hoc t-testing was performed: $*P < 0.05$, $**P < 0.01$.

4.2.3.2.3 Non-Sensitised TC Plastic: Primary Adult Murine Microglia

In-light of their observed effects on the secretion responses of BV2 microglial cells and their consistency with a primed phenotype (specifically, LPS-stimulated NO production), the effect of serum-derived deposited C3-activation fragment exposure on the phenotype of primary microglial cells was explored. Again, TC wells were either left untreated or incubated with C3 KO or WT serum prior to cell seeding, followed by treatment with or without LPS. Cells and supernatants were harvested and assayed for surface markers (CD11b, C5aR and CD200R) and secreted effectors (TNF- α , IL-6 and NO), respectively; additionally, to assess for morphological changes (which are far clearer in primary Vs BV2 microglial cells [Chapter 3]) cells were imaged by phase contrast microscopy following culture on the different surfaces.

4.2.3.2.3.1 *Morphology*

Pre-incubation of wells with WT (Fig.4.21iii) but not C3 KO (Fig.4.21ii) serum resulted in striking morphological changes compared to cells cultured in untreated wells (Fig.4.21i). Cells cultured on plastic pre-treated with WT serum were larger with longer, more distinct processes, and fewer adopted an 'amoeboid' morphology.

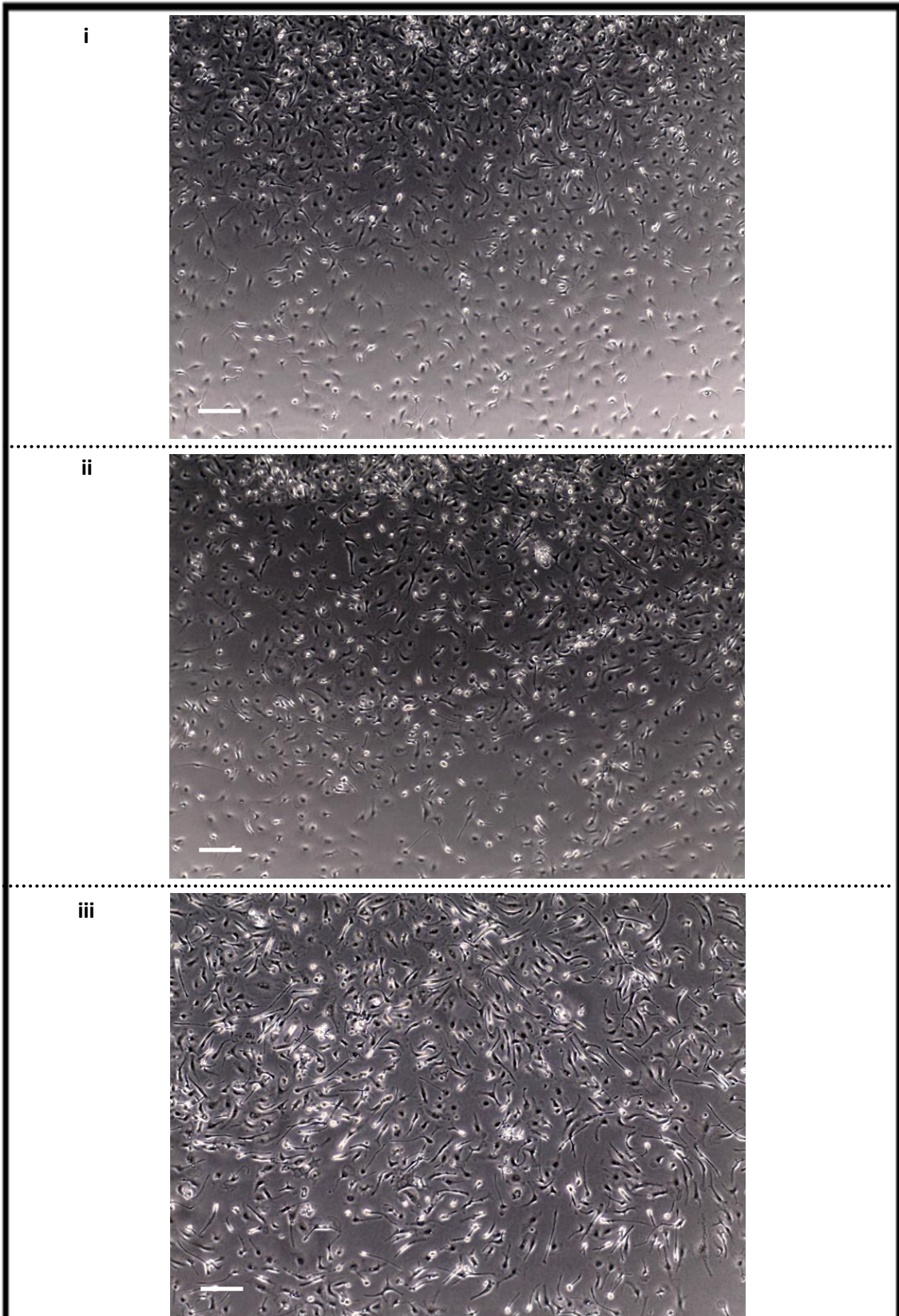


Fig.4.21: C3-activation fragment deposition on non-sensitised TC plastic: effect on primary microglial cell phenotype — morphology. Representative photomicrographs of MACS sorted primary microglial cells following overnight culture in TC plates (24-well, 1.25×10^5 /well) pre-incubated with HBSS alone (i), or 35% C3 KO (ii) or WT (iii) serum in HBSS for 1hr at 37°C. Scale bars = 200μM.

4.2.3.2.3.2 Secreted Effectors

After culture in untreated wells or wells pre-incubated with serum (either WT or C3 KO) without LPS treatment, levels of TNF- α (Fig.4.22i), IL-6 (Fig.4.22ii) and NO (Fig.4.22iii) were barely detectable or undetectable, with no significant differences between groups. LPS treatment resulted in a robust increase in secretion of TNF- α ($P < 0.01^{**}$, Fig.4.22i) and IL-6 ($P < 0.001^{***}$, Fig.4.22ii). Incubation of wells with C3 KO serum prior to cell seeding had no effect on the TNF- α and IL-6 responses to LPS treatment. Pre-incubation with WT serum, however, increased significantly their LPS-triggered secretion (TNF- α , $P < 0.01^{**}$, Fig.4.22i; IL-6, $P < 0.001^{***}$, Fig.4.22ii). In the case of NO (Fig.4.22iii), isolated LPS treatment resulted in a slight increase ($\sim 1.5\mu\text{M}$) in detectable levels. Cells cultured in wells pre-incubated with WT serum had markedly greater NO responses when exposed to LPS (~ 10 -fold increase). Wells pre-incubated with C3-deficient serum also significantly increased the NO response to LPS (~ 3 -fold; $P < 0.01^{**}$) albeit to a significantly smaller degree ($P < 0.001^{***}$).

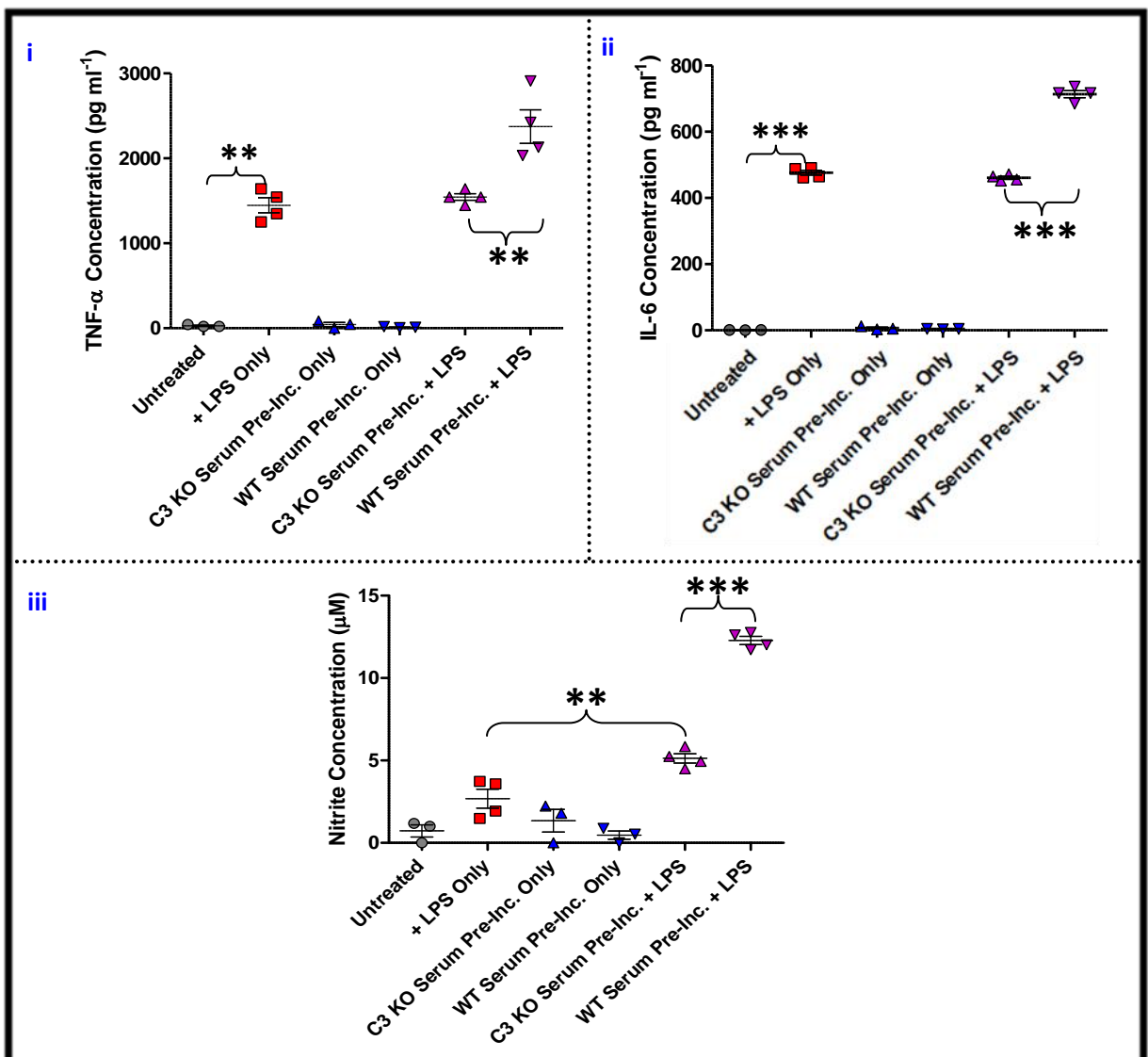
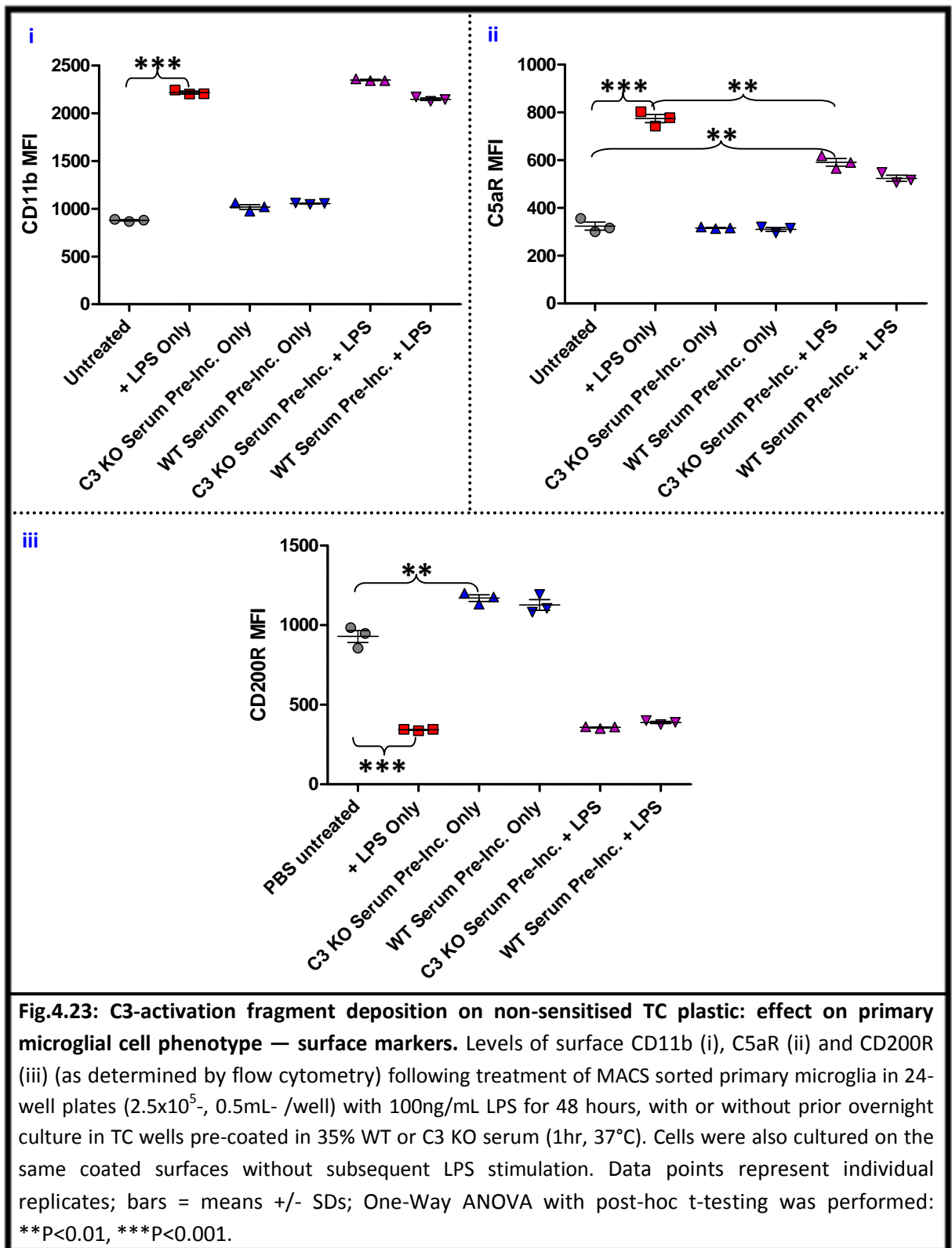


Fig.4.22: C3-activation fragment deposition on non-sensitised TC plastic: effect on primary microglial cell phenotype — secreted effectors. Levels of supernatant TNF- α (i), IL-6 (ii) and NO (iii) (as determined by ELISA [cytokines] and Griess assay [NO]) following treatment of MACS sorted primary microglia in 24-well plates (2.5×10^5 , 0.5mL- /well) with 100ng/mL LPS for 48 hours, with or without prior overnight culture in TC wells pre-coated in 35% WT or C3 KO serum (1hr, 37°C). Cells were also cultured on the same coated surfaces without subsequent LPS stimulation. Data points represent individual replicates; bars = means \pm SDs; One-Way ANOVA with post-hoc t-testing was performed: $^{**}P < 0.01$, $^{***}P < 0.001$.

4.2.3.2.3.3 *Surface Markers*

In the case of surface CD11b (Fig.4.23i) and C5aR (Fig.4.23ii), culture in wells pre-incubated with WT or C3 KO serum had little effect on baseline levels. Isolated LPS treatment, however, resulted in a clear increase in both markers to >2-fold baseline levels ($P<0.001^{***}$). Pre-incubation of wells with serum (either WT or C3 KO) had little effect on the CD11b response to LPS, but significantly reduced the LPS-dependent increase in surface C5aR by ~40-60% ($P<0.01^{**}$). Basal CD200R expression (Fig.4.23iii) was modestly increased by culture in wells pre-incubated with either WT or C3 KO serum (~20%, $P<0.01^{**}$). LPS treatment caused a major reduction in surface CD200R (~65%, $P<0.001^{***}$) that was not altered by serum pre-incubation (WT or C3 deficient). The effects of WT serum closely matched those of C3 KO serum.



These data demonstrate a clear effect of C3-activation fragment deposition on cell morphology (Fig.4.21) and on the capacity of primary microglia to release cytokines in response to LPS activation; surfaces pre-incubated with WT serum markedly enhanced the response while C3-deficient serum coated surfaces did not (Fig.4.22). The data are compatible with the induction of a

'primed' microglial phenotype mediated by iC3b-CR3 signalling (1). In the case of surface markers, while effects were clearly evident, they appeared predominantly as a consequence of LPS exposure, with smaller contributions from serum factors other than C3 (and its derivatives) and only minor specific effects due to C3-activation products (Fig.4.23).

4.3 Discussion

The results described in this chapter which, prompted by an earlier report (1), aim to characterise the *in vitro* phenotypic effects of microglial CR3 engagement by iC3b, illustrate some clear impacts on cellular responses in the systems investigated. However, the precise nature of the observed phenotypic effects appeared variable (and not necessarily consistent with a primed phenotype), although this is perhaps unsurprising given the differences in the systems employed to achieve CR3 engagement.

4.3.1 Fluid-phase iC3b

As the simplest treatment-system possible, with the potential to achieve specific iC3b-CR3 ligation in the absence of any other confounding ligand-receptor interaction, purified fluid-phase iC3b was initially investigated. Given the technical issues associated with the production of significant quantities of highly purified murine iC3b, commercially available preparations of human fluid-phase iC3b were employed. Electrophoretic analysis and immuno-detection of immobilised protein confirmed the structural integrity and identity of the commercial protein. In a subsequent attempt to illustrate specific ligand-receptor binding, the fluid-phase human protein was fluorescently labelled and retention of its ability to specifically bind a solid-phase target (in the form of immobilised anti-human iC3b antibody) was confirmed. In FACS-based cell binding assays using the fluorescently labelled protein as a probe, data consistent with specific binding of fluid-phase human iC3b to murine microglial CR3 were obtained, although these were not definitive. Previous studies have utilised fluid-phase iC3b to inhibit other CR3 ligand interactions (283, 351, 356), thus illustrating the ability of fluid-phase iC3b to actually engage its cognate receptor on the cell surface. Furthermore, previous studies using other fluid-phase fluorescently labelled CR3 ligands (e.g. soluble β -glucan) and FACS to demonstrate specific binding to cell surface receptor provide proof of concept of the experimental approach employed (337). Sequence alignment indicates a high degree of homology (~75-80% identity) between human and mouse C3 protein and gene transcript sequences, including retention of all major domains (e.g. TED, CUB), suggestive of inter-species compatibility. Moreover, phagocytosis assays clearly demonstrated the ability of mouse microglial CR3 to mediate uptake of zymosan opsonised with human serum-derived C3-activation fragments, thus demonstrating the ability of human iC3b to interact functionally with mouse CR3; it is important to emphasise, however, that this interaction occurs with immobilised iC3b in the presence of numerous other cell surface receptor-ligands and thus is

highly distinct to that of fluid-phase iC3b. In-light of this there appears to be no barrier to human iC3b in the fluid-phase ligating murine CR3 on the cell surface, and while the results of the binding assay do not definitively demonstrate this specific interaction, they are compatible with such. Nonetheless, no clear phenotypic impact of fluid-phase iC3b treatment on microglia was detected. However, previous studies have illustrated that the physical state of CR3 ligands (e.g. fibronectin) can have important impacts on subsequent cell responses; specifically, only immobilised ligands have phenotypic effects (334-336, 356) and multivalent receptor occupation is required to achieve signalling (331, 356-359). Given these combined observations it seems probable that the absence of any overt impact of fluid-phase iC3b treatment on detected microglial responses is a consequence of the inability of iC3b to exert significant phenotypic effects when in the fluid-phase, rather than the xenogeneic fluid-phase ligand simply failing to engage the receptor.

Given the issue of the ability of fluid-phase human iC3b to bind murine microglial CR3 and the problems associated with this in terms of interpreting the results of experiments designed to assess its impact on cell phenotype, it would be desirable to explore other systems to assess the fidelity of this interaction. Given that the preliminary experiments utilising immobilised specific mAbs in a plate-based system coupled with fluorescence detection clearly demonstrated specific binding of fluorescein-labelled fluid-phase human iC3b, utilising the same detection system with adherent murine microglial cells (in place of immobilised mAb) appears to provide a viable option. This approach would also have the added benefit of assessing binding in the native, adherent state, as opposed to the state of suspension necessitated by the FACS-based assay; indeed, a key difference between this and the earlier study assessing cell-borne receptor binding of fluorescently-conjugated soluble CR3 ligand by FACS is that the original study assessed binding to cells which naturally exist in suspension i.e. leukocytes: monocytes, neutrophils and NK cells (337). Furthermore, to supplement data from cell binding assays, the ability of human fluid-phase iC3b to induce the intracellular signalling responses associated with CR3/CD11b:CD18 integrin ligation could be investigated (e.g. phosphorylation of SFKs, ERK/MAPK, Rho-GTPases, etc.; see Section 4.1.3). Indeed, this strategy would prove valuable in all systems where the demonstration of specific and/or functional iC3b-CR3 binding is desirable.

4.3.2 Zymosan

Given the issues of species-mismatch and the inability to definitively demonstrate specific ligand-receptor binding between fluid-phase human iC3b and mouse microglial CR3, coupled with an apparent absence of significant phenotypic effects of treatment, other strategies to engage murine microglial CR3 with syngeneic iC3b were pursued. As a well characterised particulate C activator which becomes abundantly coated in C3 activation fragments during the activation

process (344), zymosan was employed alongside WT and C3 KO mouse serum and CR3 blockade to dissect the specific role of iC3b-CR3 binding in mediating particle-cell interactions and subsequent phenotypic effects.

4.3.2.1 Particle-Cell Interaction: Dependence on iC3b-CR3 Binding

Having first specifically demonstrated the rapid deposition of C3-activation fragments on the particle surface following incubation of zymosan with serum, in order to subsequently establish the relative contribution of iC3b-CR3 binding to microglial-zymosan interactions, uptake assays were performed utilising fluorescently-labelled particles. Consistent with previous reports in the same and other cell types (344, 360), these assays revealed an important role for iC3b-CR3 binding in mediating opsonic microglial zymosan uptake; although other serum factors contribute to this process, iC3b-CR3 binding was responsible for roughly 40%. Again, consistent with previous reports (344, 361), CR3 was also shown to have a minor role in non-opsonic microglial zymosan uptake. The ability to demonstrate the specific role of iC3b-CR3 binding in the dramatic enhancement of particle uptake which occurs upon serum opsonisation established a key precedent (which was absent in the case of fluid-phase iC3b), namely that exposure of microglia to WT serum opsonised zymosan particles definitively results in the engagement of CR3. Furthermore, the use of C3 KO serum alongside specific CR3 blockade also established that all, if not the vast majority of, C3-mediated microglial zymosan uptake occurs *via* CR3; this had important implications given that CR3 also has a minor role in non-opsonic zymosan uptake, in that it demonstrated the use of C3 KO serum opsonised particles, as opposed to (total) CR3 blockade, represented the optimal choice to control for the off-target (i.e. non iC3b-CR3 mediated) effects of serum-opsonised zymosan exposure.

4.3.2.2 Phenotypic Effects Attributable to iC3b-CR3 Binding

In-contrast to fluid-phase iC3b, exposure of cells to zymosan particles, both serum-opsonised and non-opsonised, had marked phenotypic effects. The effects of non-opsonised zymosan exposure clearly result in a pro-inflammatory microglial phenotype, comparable to that observed for LPS. In contrast, initial effects of treatment with iC3b-bearing zymosan, which include an absence of a major induction and/or release of pro-inflammatory effector molecules or increase in surface activation molecules, despite a clear immunological challenge (i.e. opsonic zymosan exposure), are compatible with a primed phenotype (1). These findings are in alignment with those of previous studies concerning the consequences of opsonic versus non-opsonic phagocytosis in the context of inflammation (312, 327-329, 362-364). However, the impact on a subsequent activation response, which results in reduced release of pro-inflammatory effector molecules and reduced expression of surface activation markers, along with increased expression of immune inhibitory receptors (i.e. CD200R), indicates that exposure to zymosan-borne iC3b results in a

state of dampened inflammatory potential (preceded by a non-inflammatory response i.e. to zymosan particles). The specific elimination of the zymosan-iC3b-CR3-microglial interaction during exposure of cells to serum-opsonised particles *via* removal of C3 from the opsonising agent (i.e. through use of C3 KO serum) reverted the detected cellular responses back towards those observed for pro-inflammatory stimuli (i.e. LPS, non-opsonised and heat-inactivated WT serum opsonised particles), illustrative of specific phenotypic effects attributable to it.

The finding that microglial CR3 signalling triggered *via* receptor engagement by particle-borne iC3b, in conjunction with other undefined signalling events triggered by other serum-derived opsonic factors, results in a minimal or absent pro-inflammatory response upon exposure to zymosan (which otherwise triggers a potent proinflammatory response), coupled with a notably reduced functional response to subsequent exposure to a pro-inflammatory activator, raises interesting possibilities regarding the use of iC3b-opsonised zymosan as a prophylactic: In cases where a CNS lesion is inevitable, for example during brain surgery, iC3b-/WT serum-opsonised zymosan (or a refinement of this agent) could be previously administered to quell microglial reactivity, leading to a net reduction in the subsequent pro-inflammatory response and reduced side-effects. Given the potentially pro-inflammatory nature of the iC3b-bearing particle (i.e. zymosan) however it would be critical to ensure correct opsonisation. In this regard, the use of other, less intrinsically pro-inflammatory parent/barer particles would merit investigation. Indeed, in-order to validate this strategy at the very earliest pre-clinical stages, the use of different parent/barer molecules and opsonising agents along with the effects on other cell-types would require further investigation. Also, as mentioned above, the contribution of serum-derived C3-activation fragments to the effects of serum-opsonisation on microglial responses, although important, is only partial, indicating that other serum factors also contribute to the anti-/non-inflammatory effect mediated by serum opsonisation. What remains unclear however is whether all serum-derived opsonins orientate cellular responses in a non-/anti-inflammatory direction, or whether some actually promote a pro-inflammatory response. Suggestive of the latter, natural antibodies against zymosan exist and FcR-mediated cellular interactions are generally characterised as pro-inflammatory (312, 327, 363, 365-368). It is possible that an optimised opsonisation reagent could enhance the inflammation-dampening effect observed following treatment of cells with WT serum opsonised particles.

While results of the studies into phenotypic consequences of microglial zymosan exposure reveal distinctive effects attributable to iC3b-CR3 interaction, these effects are not compatible with a primed phenotype previously hypothesised to be induced by microglial iC3b-CR3 engagement (1). Nonetheless, other, highly contrasting phenotypic effects were identified for other interactions in this system, interactions which that of iC3b-CR3 binding can only occur in the presence of;

furthermore, in this particle-based system, iC3b-CR3 interaction occurs exclusively in the context of phagocytosis, a complex cellular event which invariably stimulates numerous signalling pathways during the processing of the phagocytic compartment (20, 102, 259). Given the somewhat degenerate nature of cell signalling, where multiple discrete pathways ultimately feed-in to common pathways which govern different major aspects of cellular behaviour (369), it is likely that these other interactions and signalling events exert a strong degree of influence over the net effect of zymosan-iC3b-CR3-microglial signalling. Indeed, the zymosan carbohydrate ligands present in this system are known to impact CR3 functional responses through direct interactions (331, 350) and also exert cellular effects through other receptor systems (344). Additionally, natural antibodies capable of binding zymosan would have been present and FcR interactions are also known to influence CR3 functional responses along with having CR3-independent effects (363, 366). In the model of priming reported by Ramaglia *et al.*, microglial iC3b-CR3 interaction was a consequence of the intrinsic sensitivity of the cell to C activation and subsequent C3-activation fragment deposition (resulting from Crry deficiency) (1) and therefore occurred in the absence of the plethora of confounding interactions present in the zymosan-based system. With this in mind, despite the demonstration of clear phenotypic effects, the consequences of microglial iC3b-CR3 binding described in this section do not accurately mimic the scenario of C-dependent priming reported previously (1); the exploration of other simplified, particle-free systems for the engagement of microglial CR3 was thus necessitated.

4.3.3 C3-Activation Fragments Immobilised on Tissue Culture Plastic

The ability to exploit the interaction between a C-fixing mAb and its specific antigen as a means to sensitise TC substrate to C3-activation fragment deposition was explored. Under the presumption that Ag binding and Ab orientation would be key to achieving sensitisation, it was assumed that a design in which the antibody bound to its immobilised antigen (i.e. *via* F(Ab)₂) would yield the greatest degree of C3-activation fragment deposition; However, analysis of all possible antigen, antibody combinations revealed that the greatest level of deposition occurred in a system design where the C-fixing antibody was immobilised directly to the substrate in the absence of antigen, and this design was therefore selected to achieve C3-activation fragment deposition. This also had the added benefit of simplifying the design, although removal of the rMOG antigen eliminated a potentially interesting feature from this CNS-orientated system.

In a parallel to the scenario regarding the zymosan-based system described above, the factor included in the system design to stimulate C-activation (i.e. Z4 mAb Vs zymosan) had a pro-inflammatory effect which was absent when the C source (i.e. serum) was included; furthermore, the inclusion of the C source led to a reduction in the overall pro-inflammatory activation response. Again, while the use of this system to explore the phenotypic effects of microglial iC3b-

CR3 engagement revealed some clear impacts on inflammatory cell responses, the use of a mAb-coat acting to sensitise the TC substratum is complicated by the intrinsic stimulatory nature of the C-activating agent (i.e. mAb, zymosan), which may mask effects of isolated iC3b-CR3 interaction (363, 366-368). In this case, however, the observed effects on the cellular responses appeared to be entirely due to serum factors other than C3 and its derivatives. While the findings relating to the use of this system are not compatible with the induction of a primed microglial phenotype, they do provide further evidence in a different setting suggesting that highly controlled elective microglial activation regimes which promote a transient non-/anti- inflammatory phenotype may have potential to reduce responses to unavoidable pro-inflammatory activation triggers (e.g. surgery, drugs, etc.).

Simplification of the system to its most basic elements (i.e. serum, culture substrate and cells) eliminated the confounding effects of inclusion of the C-fixing mAb in the design; it is important to emphasise however, that even in this most simplified system, numerous other non-C serum factors are deposited on the TC plastic during incubation. Under such conditions, significant effects on microglial functional responses were detected in both adult primary and immortalised cells, which, importantly, were almost entirely dependent on iC3b-CR3 signalling (as demonstrated through the use of C3 KO serum) and consistent with a primed phenotype. These findings therefore support those reported and the mechanism proposed by Ramaglia *et al.* (1).

4.3.4 General

The overriding theme which emerges from the studies presented in this chapter is that the consequences of microglial CR3 engagement by iC3b are heavily context dependent: while this event exerts a non-/anti- inflammatory effect over the multi-factorial process of innate immune-phagocytosis, in isolation (or at least, in the absence of an intrinsically stimulatory C-activator) it appears to promote an overt yet apparently benign basal phenotype which progresses to an overly reactive phenotype in response to a robust pro-inflammatory trigger i.e. a 'primed' phenotype. Nonetheless, questions still remain: while the use of C3 KO serum can control for the off target effects resulting from the use of serum as a C source, it remains unclear whether or to what extent other non-C3-derived serum factors influence the specific interaction between iC3b and microglial CR3 and the consequences thereof; Furthermore, it remains unclear as to whether monomeric iC3b is able to exert an effect on microglial phenotype from the fluid phase, or, as suggested by other studies of CR3 ligation (331, 334-336, 356-359), if such effects can only be mediated by the immobilised protein or through multivalent receptor occupation. To address these issues, future work would seek to utilise purified iC3b protein and/or a minimal system of C3 activation and processing utilising purified components and regulators (e.g. C3, factors B, D, H, I and P) to generate soluble iC3b and to immobilise iC3b to surfaces and particles, in-order to

assess the effects of iC3b-CR3 interactions which differ in terms of their isolation, phase and valency.

Other possible avenues to be explored by future work pertaining to the cellular consequence of iC3b-CR3 engagement include the adoption of other strategies to achieve (and demonstrate) this key binding event, both as an isolated interaction and in systems of mixed (and presumably more physiological) interactions. To this end attempts could include: blockade of key microglial C regulators (e.g. Crry) to achieve sensitisation to C activation and iC3b deposition on the cell surface; the use of mAbs (whole IgG, F(ab)₂ and F(ab)) which specifically ligate the iC3b binding site of CR3 (e.g. clones M1/70 and OX42) to stimulate receptor signalling.

5 The *In Vitro* Crry KO Microglial Phenotype

5.1 Introduction

The C3-dependent mechanism of microglial priming described by Ramaglia *et al.* (2012) in Crry KO mice *in vivo* (1) is the central focus of this study. The previous chapter sought to further investigate this mechanism through the development of *in vitro* systems to recreate the key interaction which is proposed to underpin it - i.e. ligation of microglial CR3 by iC3b. This chapter is intended to further explore this mechanism through the investigation of the Crry KO microglial phenotype *in vitro*; this will address the question of whether the primed Crry KO microglial phenotype reported *in vivo* is retained *in vitro*, or whether it is lost due to the absence of the chronic C activation which occurs in the live animal, or possibly the isolation and culture process *per se* and/or absence of the plethora of other factors with which microglial cells interact *in vivo*.

5.1.1 Biological Role of Crry

Following the discovery (85, 87, 145, 147-149, 151-154) and functional characterisation of Crry as an inhibitor of the classical and alternative activation (but not the terminal) pathways, with both decay-acceleration and fi-cofactor activity (155-157), attention focused on its biological roles. These studies identified a number of roles and potential therapeutic uses for Crry. Use of Crry-based pharmacological inhibitors of C-activation has proven to be protective against anti-phospholipid Ab induced foetal-loss in a murine model of lupus pregnancy failure (98) and to ameliorate tissue damage in models of mesenteric ischemia-reperfusion injury (370) and antibody-induced glomerulonephritis (371). Crry-based therapeutics have been shown to reduce atherosclerosis in mice (372) and inhibit the development of a rat model of myasthenia gravis (EAMG) (373). Furthermore Crry-based therapeutic agents block tubulointerstitial injury and renal dysfunction in a rat model of puromycin-induced nephrosis (374), and IgG deposition and elevated aquaporin-4 expression (associated with cerebral oedema) in a mouse model of lupus cerebritis (375). Use of transgenic mice with systemic soluble Crry over-expression has also shown that Crry can be protective in the same model of antibody-induced glomerulonephritis (376). The development of global Crry KO mice immediately revealed a critical role for Crry in murine fetomaternal tolerance, revealing that Crry is essential for protecting the developing foetus from C-mediated injury and subsequent pregnancy failure (169). Establishing ways to circumvent the embryonic lethal Crry KO phenotype led to increased understanding of C homeostatic mechanisms (170). The subsequent use of global Crry KOs has revealed roles for Crry in modulating, among other things, immunological processes in EAMG (377). Tissue-specific Crry KOs have been used to study T-cell dynamics (378), platelet dynamics and C sensitivity (379), and renal ischemia-reperfusion injury (380). To circumvent the issue of C-insufficiency intrinsic to the

Crry-deficient phenotype and also intrinsic to some earlier models of global Crry KO (i.e. C3 or factor B $-/-$ or $+/-$), adoptive transfer models were developed where Crry $-/-$ cells or tissues were transferred to a syngeneic C-sufficient host: these studies revealed the critical role for Crry in protecting cells (erythrocytes) (164) and tissue (renal) (381) from C-mediated injury. Studies of T-cell biology have also identified an unexpected role for Crry in cell signalling, independent of its C-regulatory function (382-386).

Another key observation emerging from studies of Crry function is that of its primary importance over other membrane C-regulators in protection of a variety of cell types against C-mediated injury. Cell types include: T-cells (378, 387, 388); erythrocytes (163, 164); platelets (379); tubular epithelial cells (389). Additionally, it appears that Crry's ability to function as a C regulator is specific to homologous C, with reports of no difference in sensitivity of mouse cells to C from other closely related species (e.g. rat) regardless of Crry expression-status, despite clear differences in sensitivity to mouse C (156, 157, 164).

5.1.2 Crry and the CNS

Despite its status as the chief membrane regulator of C activation in the mouse (84, 390) and the availability of pharmacological agents capable of modulating Crry function (e.g. sCrry, Crry-Ig, Crry-CR2) (84) along with both Crry KO (global (1, 377, 391) and conditional (378-380)) and over-expression (376, 392, 393) transgenic mice strains, relatively few studies have directly addressed the question of Crry function in the CNS. In-terms of KO animals, a highly valuable resource for the investigation of gene function, the embryonic lethality of the Crry KO phenotype (169) has probably contributed to the limited use of this mode of investigation; the relatively recent development of ways to circumvent this whilst maintaining an otherwise intact C system (170, 171) has seen the situation change somewhat. Among the earliest CNS-specific studies of Crry, around the turn of the millennium, were characterisations of its expression at a cellular level (394, 395), since previous studies had merely noted its presence in the CNS and expression relative to other tissues (396, 397). It was found that microglia and astrocytes express both Crry mRNA and protein, with microglia possessing more surface Crry than astrocytes, whereas neurones, under physiological conditions, express the gene only at the transcript level (394, 395). In parallel, the same investigators assessed the effect of sCrry over-expression in the CNS driven by the GFAP promoter in transgenic mice and found that this was protective against MOG-induced EAE (392). Later, the phenotype of the same transgenic mice was assessed in the cuprizone model, where de-myelination, featuring an inflammatory infiltrate, occurs in certain CNS white-matter tracts (e.g. *corpus callosum*), followed by a period of re-myelination upon withdrawal of the copper-chelating, oligodendrotoxic drug. The Crry-over-expressing transgenics were protected against de-myelination; interestingly, the same animals were found to have a mild degree de-myelination

during the recovery-phase of the model in-which the diseased white-matter tracts of WT animals were repairing, suggesting that C has a role in neural regeneration as well as destruction (398). In addition to de-myelinating inflammatory diseases of the CNS, the role of Crry has also been investigated in TBI models: transgenic mice which express Crry under the control of the astrocytic GFAP promoter were employed and assessed for pathology and neurological deficits following TBI and were found to be protected (393); In a follow-up study by the same group, Crry-Ig was used to assess the potential for pharmacological C inhibition as a treatment for TBI and was also found to be protective (399). Crry-Ig has also been used to investigate the effects of pharmacological C-inhibition on parameters of inflammation and cerebral oedema (IgG deposition and aquaporin-4 expression, respectively) in a mouse model of lupus cerebritis: chronic Crry-Ig treatment was shown to have a beneficial effect (375). Most recently, the status of the Crry KO CNS has been investigated with respect to markers of Alzheimer's disease pathology: in a basic investigation designed to assess the presence of tau-235 (serine)-phosphate and fH in hippocampal homogenates it was found that these markers were both significantly reduced in Crry KO mice (391).

5.1.2.1 The Microglial Phenotype of Crry KO Mice

As discussed in previous chapters, a 2012 report by Ramaglia *et al.* (1) described a CNS-specific investigation of Crry function where the Crry KO CNS was examined. This investigation identified a C-dependent primed microglial phenotype unique to Crry KOs (i.e. not present in another system of C3 dysregulation [fH KO]) and based on co-localisation of fixed C3-activation fragments (C3b/iC3b) and microglial CR3, along with the local nature of C activation and primary effect, attributed this phenotype to locally accumulated iC3b ligating CR3 and triggering microglial priming in the Crry^{-/-} CNS. Furthermore, the relevance of this mechanism of C-mediated microglial priming was demonstrated in a human inflammatory and degenerative CNS disease (MS). Nonetheless, while this report detailed a molecular mechanism of *in vivo* microglial priming for the first time, implicating C along with its regulators and receptors in microglial membranes, no other studies have addressed the question of the phenotypic consequences of Crry function in the CNS at the cellular level, beyond that of inferred sensitivity to C-activation. Furthermore, despite methods for *in vitro* microglial characterisation being long-established, the Crry KO primed microglial phenotype reported by Ramaglia *et al.* (1) was based solely on *in vivo* investigations. A detailed *in vitro* study of the Crry KO microglial phenotype is therefore proposed here and will feature as the subject of this chapter.

5.1.3 Chapter Aims

The aim of this chapter is the further characterisation of the Crry KO microglial phenotype through *in vitro* investigation. Microglial cells from Crry KO and WT mice will be isolated and

cultured. The absence/presence of the key regulator (i.e. Crry) on the cell surface shall be specifically determined and the sensitivity to C activation (both syngeneic and xenogeneic) assessed. The methods described in chapter 3 shall be employed to assess cell phenotype, both at baseline and following exposure to C and/or activation.

5.2 Results

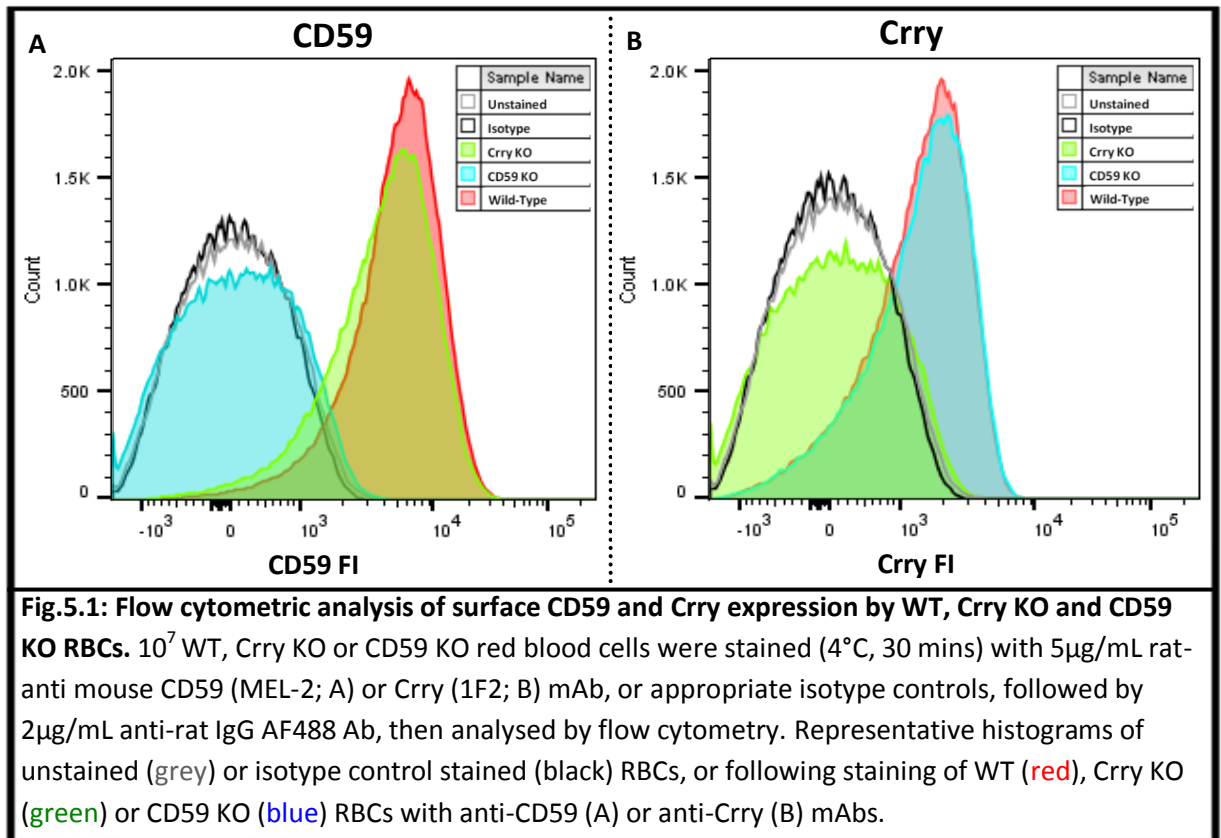
5.2.1 Specific Detection of Surface Crry Expression

As a prerequisite to any further studies concerning their *in vitro* phenotype, it was essential to formally establish the phenotype, with regards to surface Crry expression, of the primary microglial cells cultured following isolation from both Crry KO and WT CNS tissues. The FACS-based assay of surface Crry expression described in chapter 3 was therefore employed for this purpose.

5.2.1.1 Red Blood Cells

In order to validate the assay designed to specifically demonstrate cell surface expression of Crry, a cell type which is known to express high levels of membrane-bound Crry, i.e. erythrocyte (163, 164, 400), was first assayed to serve as a positive control. In addition, to demonstrate the specificity of staining and serve as a further control, red blood cells from Crry KO and WT mice were also assayed for CD59 expression, in-addition to those from CD59 KO mice.

Cells were assayed by FACS *as per* Section 2.3.1. In all cases, cells stained with isotype control antibodies returned signal which was undetectable over levels obtained from unstained cells (Fig.5.1). As expected, while CD59 expression was readily detectable and equivalent on WT and Crry KO erythrocytes, it was undetectable on CD59 KO cells, where signal was equivalent to that of cells of (any genotype) stained with an isotype control antibody primary mAb (Fig.5.1A). Similarly, Crry expression was readily detectable and equivalent on WT and CD59 KO erythrocytes, but was undetectable on Crry KO cells, (the same situation applied in-relation to isotype control staining) (Fig.5.1B). These data thus validated the FACS-based assay for surface Crry expression and enabled its expression by primary cells derived from other (i.e. CNS) tissues to be assessed with confidence. This assay was then applied to primary microglial cells cultured following isolation from both Crry KO and WT CNS tissues.



5.2.1.2 Primary Microglial Cells

Primary microglial cells isolated from WT and Crry KO mice were assayed for surface Crry expression by FACS. In addition, to demonstrate the specificity of staining and serve as a positive control, cells were also assayed for surface F4/80 antigen expression. In all cases, cells stained with isotype control antibodies returned signal which was barely detectable over that returned by unstained cells (Fig.5.2). As expected, while F4/80 expression was readily detectable above background and equivalent on WT and Crry KO cells (Fig.5.2A), Crry expression was readily detectable on WT microglia, but was undetectable on Crry KO cells, (the same situation applied in-relation to isotype control staining) (Fig.5.2B). These data thus clearly demonstrate the specific detection of Crry on the surface of primary microglial cells purified from WT sources, and conversely, its absence on that of microglial cells purified from Crry KO sources.

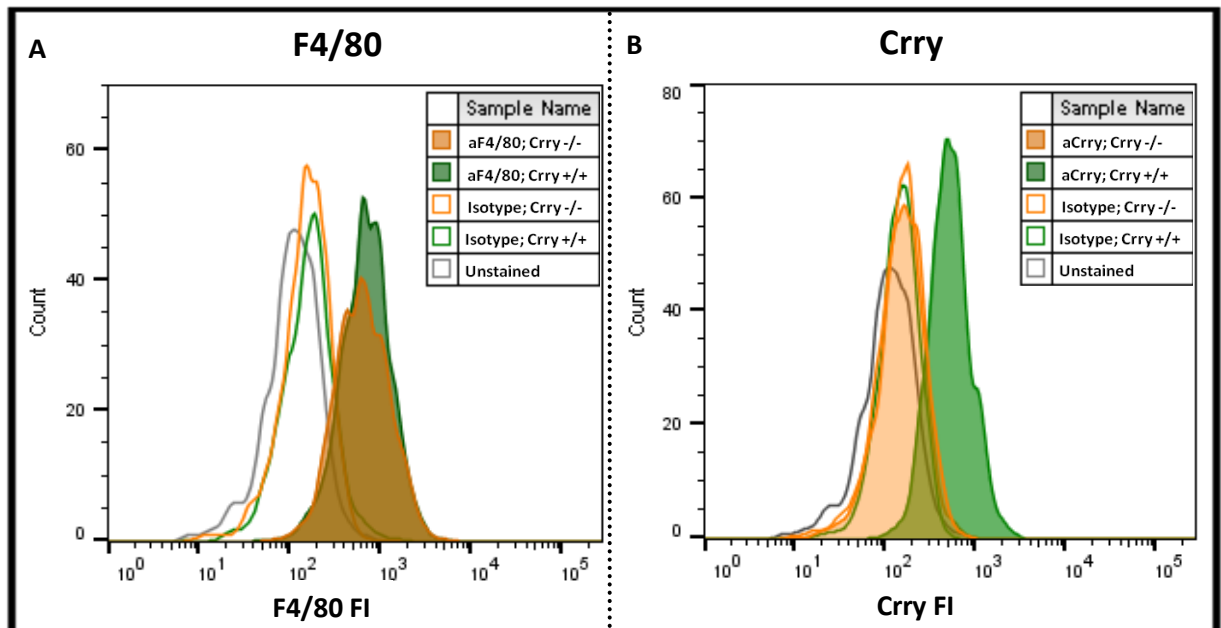


Fig.5.2: Flow cytometric analysis of surface F4/80 Ag and Crry expression by WT and Crry KO primary microglia. 5×10^5 WT, Crry KO or CD59 KO MACS sorted microglia were stained (4°C , 30 mins) with rat-anti mouse F4/80 (Cl:A3-1, $10\mu\text{g}/\text{mL}$; A) or Crry (1F2, $5\mu\text{g}/\text{mL}$; B) mAb, or appropriate isotype controls, followed by $2\mu\text{g}/\text{mL}$ anti-rat IgG AF488 Ab (4°C , 30 mins), then analysed by flow cytometry. Representative histograms of unstained cells (grey, open) or cultured primary microglia isolated from WT (green) or Crry KO (yellow) CNS tissue following incubation with isotype control mAb (open histograms) or test mAbs (filled histograms) against F4/80 antigen (A) or Crry (B).

5.2.2 *In Vitro* Phenotype of Crry KO Microglia

In-order to examine and define the phenotype of Crry KO microglia *in vitro*, primary microglia isolated from Crry KO and WT mouse tissue were assayed for expression of surface markers and release of cytokines at baseline and following exposure to a concentration gradient of LPS. The results showed that regardless of genotype, treatment of cells with increasing LPS concentrations resulted in dose-dependent changes in the release of secreted effector molecules and levels of surface markers (Fig.5.3). Furthermore, the profile of these changes broadly resembled those in chapter 3 which describe the initial characterisation of systems for *in vitro* assessment of microglial responses to LPS (e.g. greatest effect between $1\text{-}10\text{ng mL}^{-1}$ LPS). However, despite the primed Crry KO microglial phenotype reported *in vivo* (1), no dramatic differences in the profile of cytokine release and surface markers were observed between Crry KO and WT microglia, at baseline or in response to LPS treatment (Fig.5.3). These data indicate that when removed from the *in vivo* environment and taken into culture, Crry KO microglia are no longer hyper-responsive relative to WT cells.

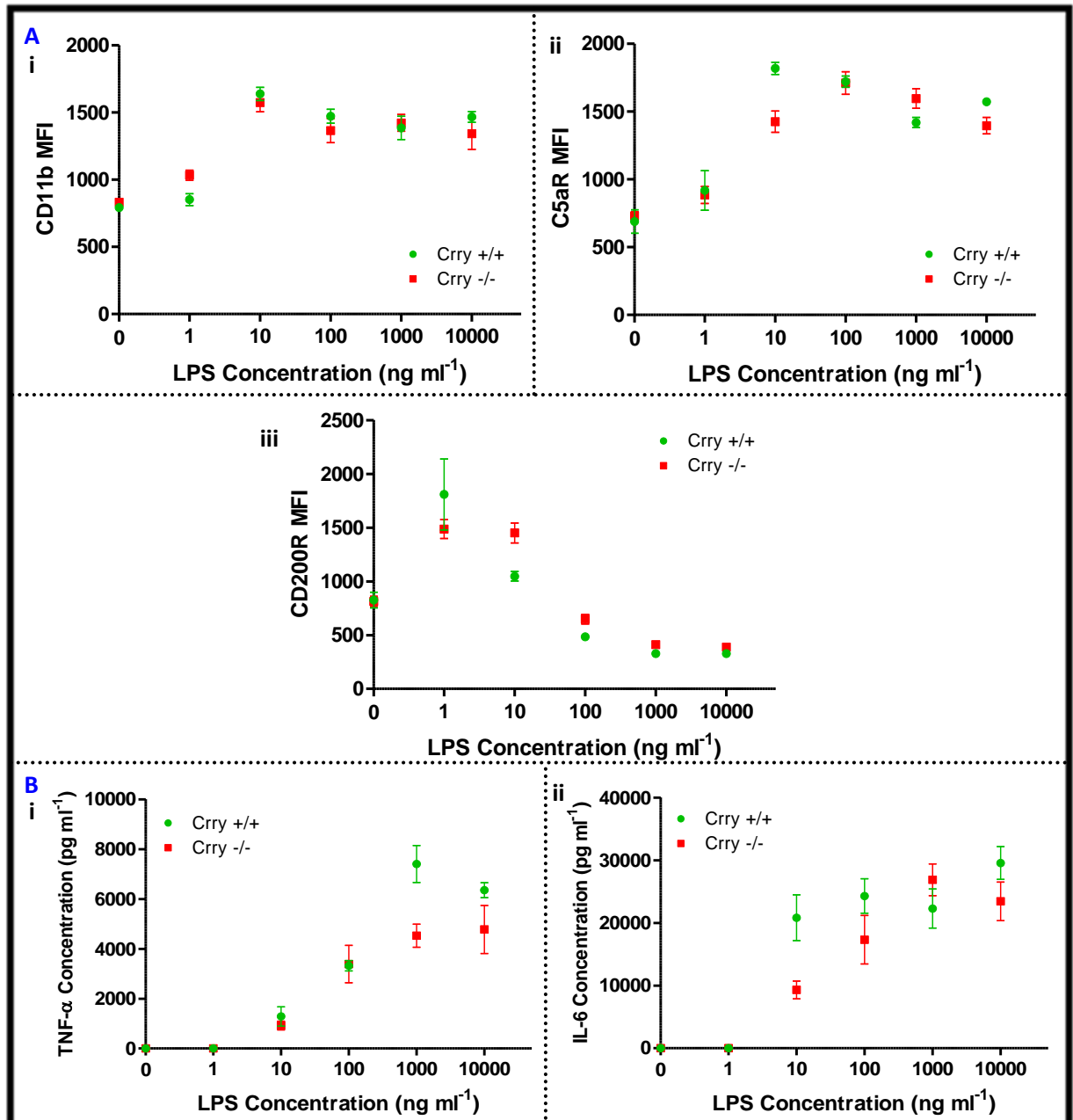


Fig.5.3: Assessment of the *in vitro* Crry KO microglial phenotype. 2.5×10^5 WT (green) and Crry KO (red) MACS sorted primary microglia (per well, 24 well-plates, 0.5mL medium) were incubated with increasing concentrations (0-10 μ g/mL) of LPS for 48 hours before: (A) flow cytometric assessment of surface CD11b (i), C5aR (ii) and CD200R (iii); (B) ELISA of supernatant TNF- α and IL-6 (N = 4; bars = means \pm SDs). (N = 4; bars = means \pm SDs).

5.2.3 Sensitivity to C Activation: C3-Activation Fragment Deposition and MAC-Mediated Lysis

In-light of the absence of any detectable difference between the basal- and activated- WT and Crry KO *in vitro* microglial phenotype in the absence of any previous cell exposure/treatment, and given that the Crry KO primed microglial phenotype is proposed to be a consequence of the intrinsic sensitivity of these cells to C-activation resulting in the chronic local presence of C-

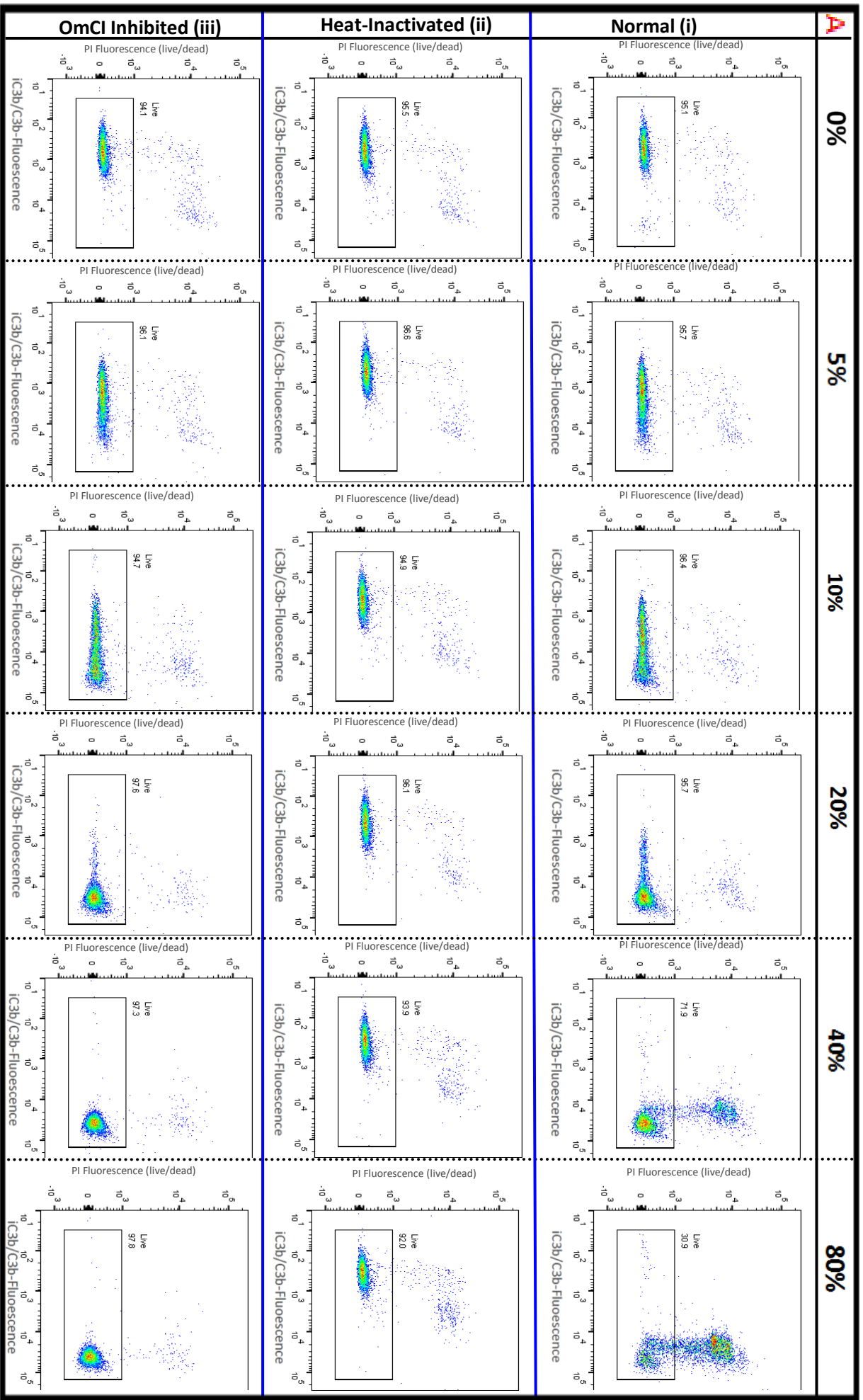
derived CR3 ligands (which ligate the receptor), an attempt was made to recreate this proposed mechanism of *in vivo* priming *in vitro*. In-order to achieve this, assays to chart the activation of C and the deposition of C-activation products (C3b/iC3b; MAC) on the surface of murine microglial cells, along with their viability, were developed.

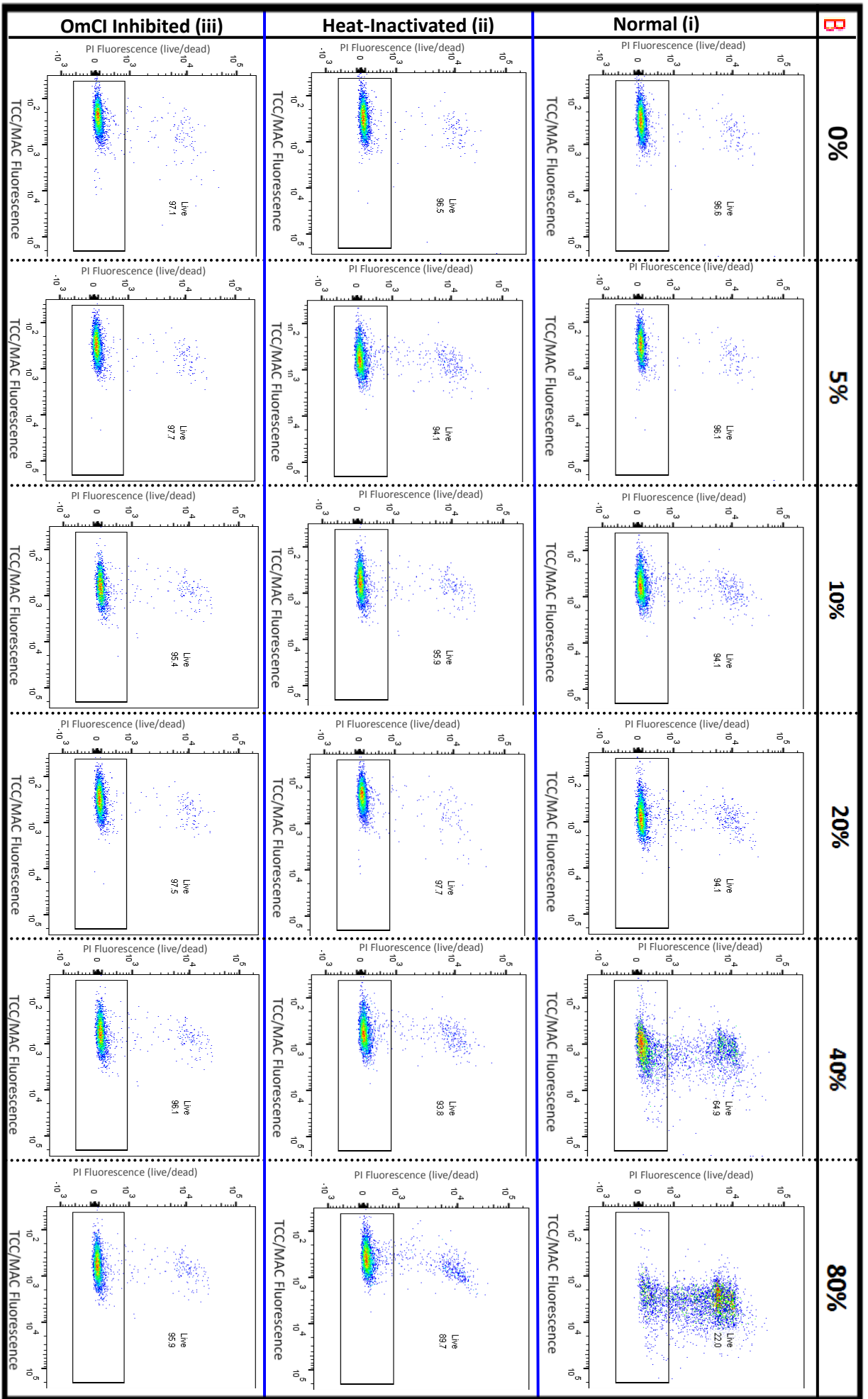
5.2.3.1 Human Serum as C Source

5.2.3.1.1 BV2 Cells

Given the ready availability of the BV2 murine microglial cell line relative to primary murine microglial cells, along with its close approximation to primary cells (as detailed in chapter 3), coupled with the ready availability of fresh normal human serum relative to that of mouse, BV2 cells and human serum were employed in an initial attempt to establish an assay of C deposition on murine microglial cells.

BV2 cells were incubated with increasing concentrations of normal or heat inactivated human serum, with or without the addition of the C5-activation blocking agent (derived from the saliva of the tick, *Ornithodoros moubata*), OmCI, and then assayed for C3 activation fragment deposition along with MAC formation and viability (see Section 2.2.5). Incubation of BV2 cells with normal serum resulted in a dose dependent increase in C3 deposition which was detectable at the lowest serum concentration tested (5%) and, although at ~95% maximal signal at 40% serum, continued to increase up to the highest serum dose tested (80%) (Fig. 5.4A & 5.4Ci). Although very low levels of MAC formation appeared to be detectable at the lower serum concentrations of 10% and 20% serum, which coincided with emergence of a rapid increase in the levels of detectable deposited C3, a dramatic increase in the levels of detectable MAC formation occurred between 20-40% and 40-80% serum; this increase coincided with a dramatic decrease in viability (from ~95% to ~20%) as assessed by staining with the fluorescent dye, PI (impermeant to an intact cell membrane) (Fig.5.4Bi, Fig.5.4C ii & iii). As expected, when cells were incubated with heat inactivated human serum, no change in C3 deposition, MAC formation or viability was detected (Fig.5.4 Aii, Bii & C), confirming ablation of all serum C factors. Notably, when cells were incubated with normal serum which had been pre-treated with OmCI, while the same change in C3 deposition occurred as described for cells incubated with normal serum, no change in MAC formation or viability was detected (Fig.5.4 Aiii, Biii & C), illustrating successful and specific blockade of C5-activation and confirming that MAC formation was responsible for the observed cell death.





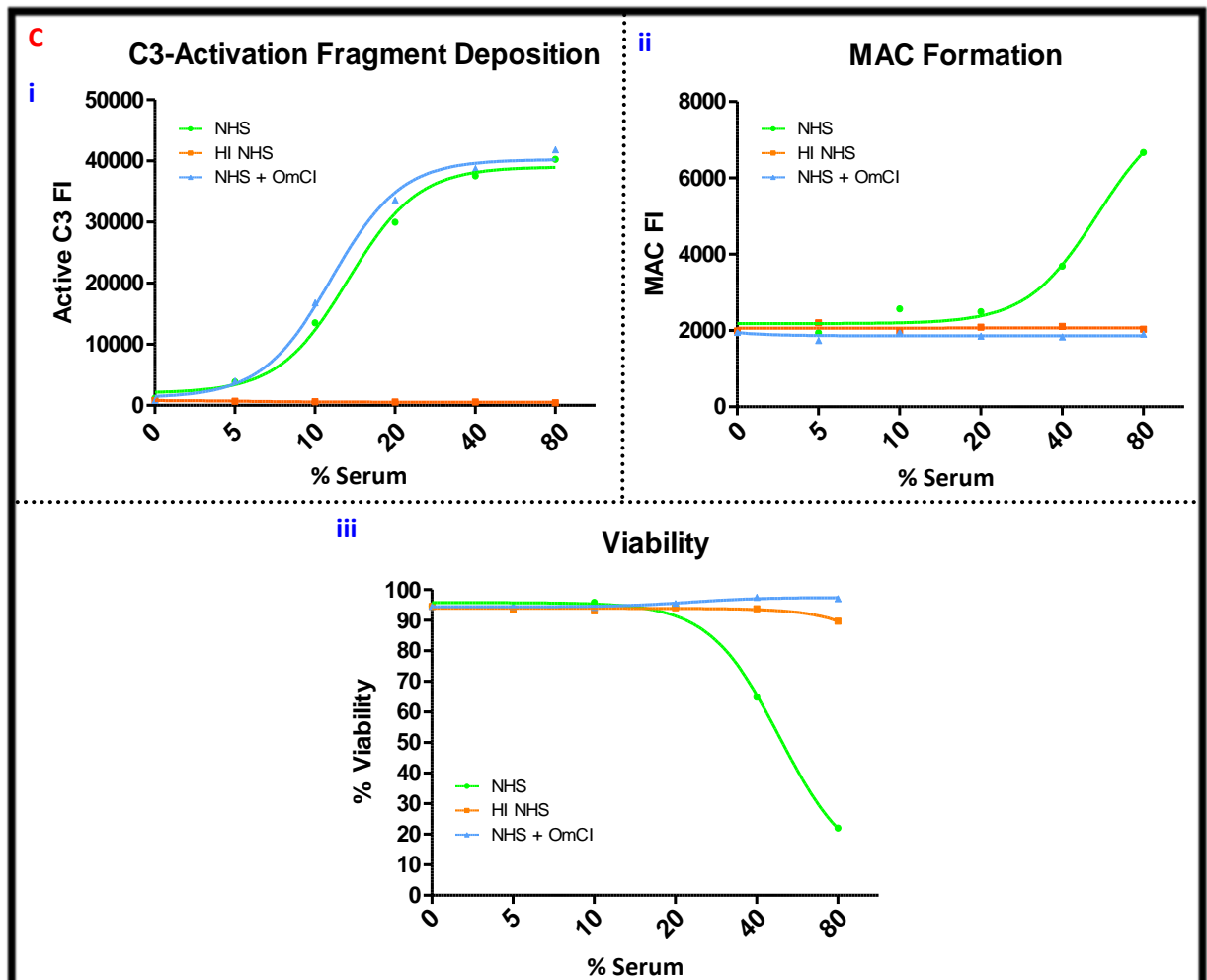


Fig.5.4: Activated C3 deposition and MAC formation on BV2 cells: development of assay of murine microglial C activation. BV2 cells seeded at 5×10^4 per well in 24-well plates were treated with NHS, HI NHS, or NHS pre-incubated with OmCl ($10 \mu\text{g mL}^{-1}$, RT, 15 mins) at concentrations ranging from 0-80% (1hr, 37°C ; all experimental media/serum volumes = 0.5mL). Cells were then stained (4°C , 30 mins) with rat anti-human iC3b/C3dg/C3g (Clone 9, in-house; $9 \mu\text{g/mL}$) or mouse anti-human TCC (aE11; $1 \mu\text{g/mL}$) mAbs followed by AF488/FITC-labelled anti-rat or mouse IgG (as appropriate; $1 \mu\text{g/mL}$), before PI staining ($2.5 \mu\text{g/mL}$; 5 mins, 4°C) and flow cytometric analysis. Prior to mouse anti-human TCC mAb use, cells were pre-treated (10mins, 4°C) with rat-anti-mouse Fc blocking Ab (2.4G2; $5 \mu\text{g/mL}$) and secondary Ab was used which had been cross-adsorbed against rat serum proteins (to prevent binding to rat Fc blocking Ab instead of mouse anti-human TCC target). **(A & B)** Representative fluorescence dotplots (Y axis **A & B** = PI fluorescence; X-axis **A** = fluorescence due to C3 deposition, X-axis **B** = fluorescence due to MAC formation) of BV2 cells following incubation with increasing concentrations (0-80%) of normal, heat-inactivated or OmCl pre-treated human serum; **(C)** Quantification/Combined graphical illustration of fluorescence depicted in **A** and **B** showing signal due to C3-activation fragment (i) and MAC (ii) deposition, along with calculated viability (iii).

These data thus demonstrate proof of concept in terms of achieving C activation on murine microglial cells combined with specifically and quantitatively detected the process. Regardless of previous reports indicating the species-restricted function of Crry (156, 157, 164), in-light of the success of the assay detailed here, this assay of human C activation and membrane deposition was applied to both Crry KO and WT primary microglial cells, in an attempt to detect differences in sensitivity to C activation based on the presence of the membrane regulator (i.e. Crry).

5.2.3.1.2 Primary Microglial Cells: Crry KO Vs WT

In a similar manner to BV2 cells, exposure of WT primary microglia to increasing concentrations of human serum resulted in a dose-dependent increase in C3-deposition which was readily detectable even at the lowest serum concentration tested (25%) and which continued to increase in parallel with serum concentration up to the highest serum concentration tested (100%) (Fig.5.5A). Again, similarly to BV2 cells, very low levels of MAC formation appeared to be detectable at the lower serum concentrations ($\leq 50\%$), with a dramatic increase occurring at the higher serum concentrations tested ($>50\%$) (Fig.5.5B) which coincided with a dramatic decrease in viability (from $\sim 90\%$ to $\sim 35\%$) (Fig.5.5C). The profile of C3-deposition, MAC formation and viability for Crry KO primary microglial cells in response to increasing concentrations of human serum mirrored almost exactly that of WT cells (Fig.5.5A-C).

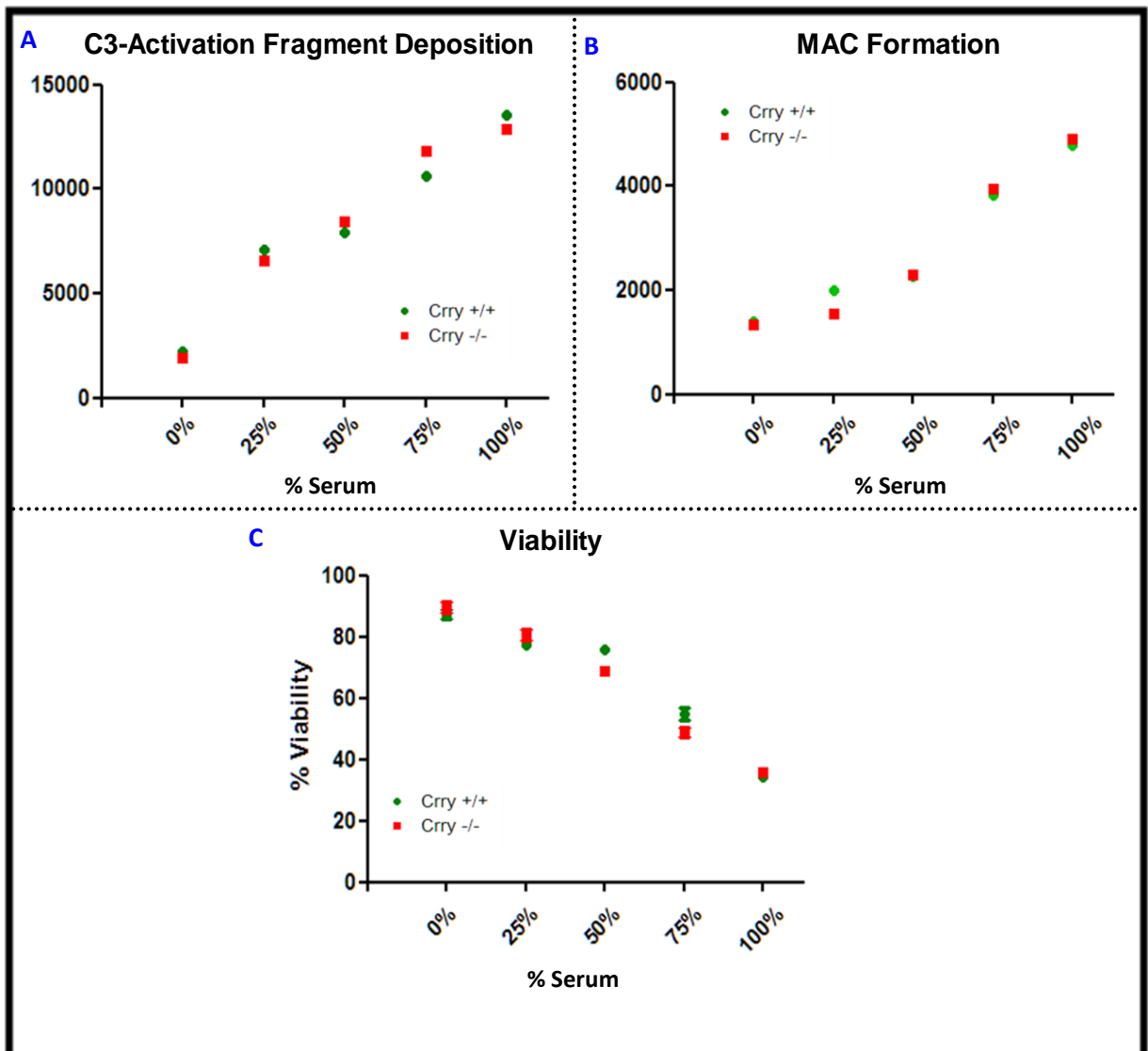


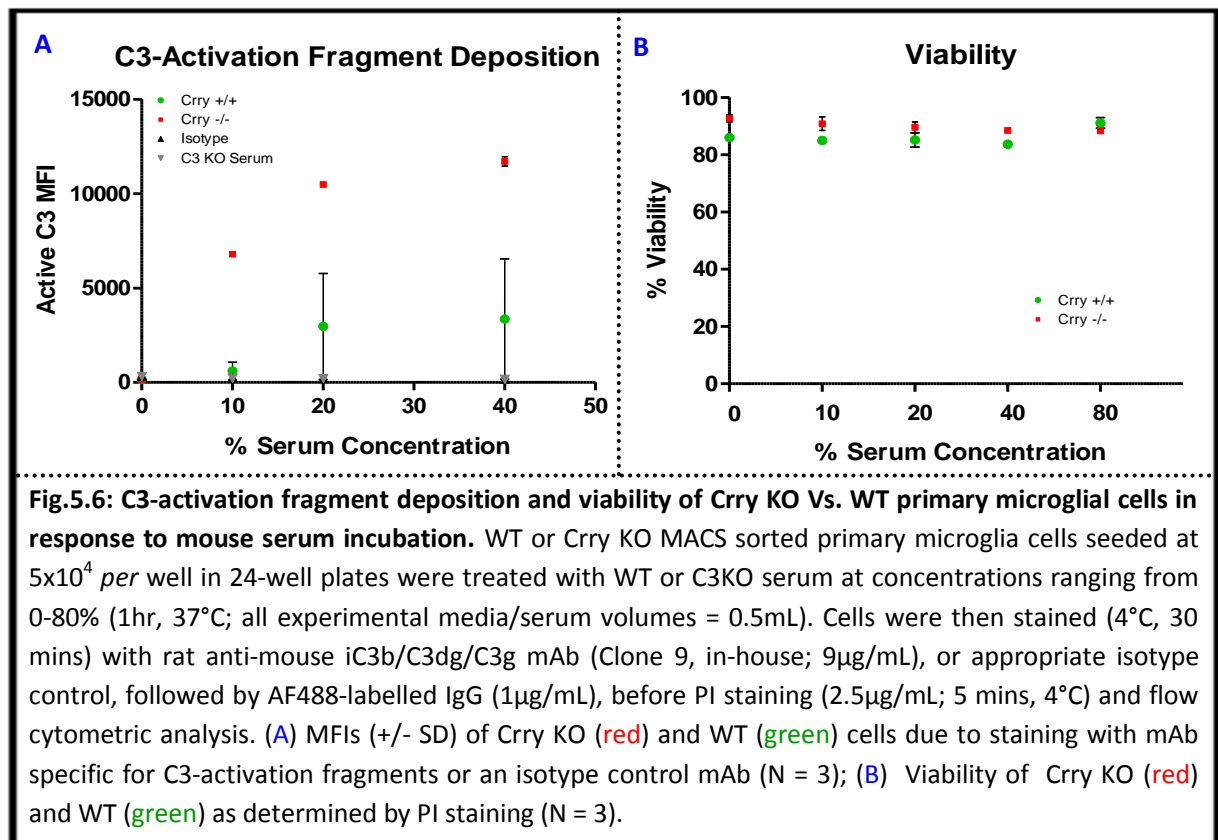
Fig.5.5: C3-activation fragment deposition and MAC formation on Crry KO Vs WT primary microglial cells: human serum. WT or Crry KO MACS sorted primary microglia cells seeded at 5×10^4 per well in 24-well plates were treated with NHS at concentrations ranging from 0-100% (1hr, 37°C; all experimental media/serum volumes = 0.5mL). Cells were then stained (4°C, 30 mins) with rat anti-human iC3b/C3dg/C3g (Clone 9, in-house; 9µg/mL) or mouse anti-human TCC (aE11; 1µg/mL) mAbs followed by AF488/FITC-labelled anti-rat or mouse IgG (as appropriate; 1µg/mL), before PI staining (2.5µg/mL; 5 mins, 4°C) and flow cytometric analysis. Prior to mouse anti-human TCC mAb use, cells were pre-treated (10mins, 4°C) with rat-anti-mouse Fc blocking Ab (2.4G2; 5µg/mL) and secondary Ab was used which had been cross-adsorbed against rat serum proteins (to prevent binding to rat Fc blocking Ab instead of mouse anti-human TCC target). MFIs (+/- SDs) of Crry KO (red) and WT (green) primary cells due to staining of C3-activation fragments (A) or TCC/MAC (B), or viability (means +/- SDs) as determined by PI staining (C) (N = 3).

5.2.3.2 Mouse Serum as C Source

C3-activation fragment deposition and cell viability (which parallels MAC formation; Fig.5.4 & Fig.5.5) was next assayed by FACS for Crry KO and WT primary microglial cells following incubation with increasing concentrations of mouse C (using WT serum as a C source). As controls, to

demonstrate the specificity of the responses, microglia were incubated with serum obtained from C3 KO mice. Assay controls also included appropriate isotype control mAb (in place of the mouse C3-activation fragment specific primary mAb i.e. clone 2/11).

Incubation of Crry KO cells in normal mouse serum resulted in a dose dependent increase in C3-activation fragment deposition which was readily detectable even at the lowest serum concentration tested (10%) (Fig.5.6A). However, in-contrast to human serum (Fig.5.5) and despite the noted C3-deposition effect, incubation in normal mouse serum at any concentration tested failed to have any effect on cell viability (Fig.5.6B). Incubation of WT microglial cells in low concentrations of normal mouse serum ($\leq 10\%$) resulted in C3-deposition which, while still detectable, was never on the same scale as that detected on Crry KO cells (Deposited C3 MFI at 10% serum: WT $\sim 10\%$ that of Crry KO). Incubation of WT cells in higher serum concentrations ($>10\%$) resulted in a level of C3 deposition which never exceeded $\sim 1/2$ that observed for Crry KO cells at the equivalent serum dose (Fig.5.6A). Similarly to Crry KO cells, no effect on viability was detected for WT cells regardless of serum concentration (Fig.5.6B).



5.2.4 Phenotypic Effects of C Activation on Crry KO Microglia *in Vitro*

In-order to further characterise the phenotype of Crry KO microglia *in vitro*, including the capacity of C-derived CR3 ligands to elicit an activation response consistent with a primed phenotype (1), primary microglia isolated from Crry KO and WT mouse tissue were assayed for expression of surface markers and release of cytokines at baseline and following exposure to 10% WT or C3 KO mouse serum or LPS alone, or 10% WT or C3 KO mouse serum with the subsequent addition of LPS.

The data show that WT and Crry KO cells had a very similar basal cytokine and surface marker profile (Fig.5.7); treatment with LPS alone resulted in comparable, readily-detectable increases in the release of pro-inflammatory cytokines and levels of surface markers (Fig.5.7 A, Bi & Bii), with the exception of surface CD200R which (as expected) decreased slightly (Fig.5.7Biii). Moreover, treatment of cells of either genotype with 10% WT or C3 KO mouse serum alone failed to significantly modify their basal cytokine and surface marker profiles (Fig.5.7). Furthermore, no dramatic differences in the response to LPS were detected between WT and Crry KO cells following previous exposure to 10% mouse serum (C3 KO or WT) (Fig.5.7), despite the C3-dependent primed Crry KO microglial phenotype reported *in vivo* (1) along with the clear and specific demonstration of C3-deposition on Crry KO microglia upon incubation with 10% WT mouse serum (Section 5.2.3.2).

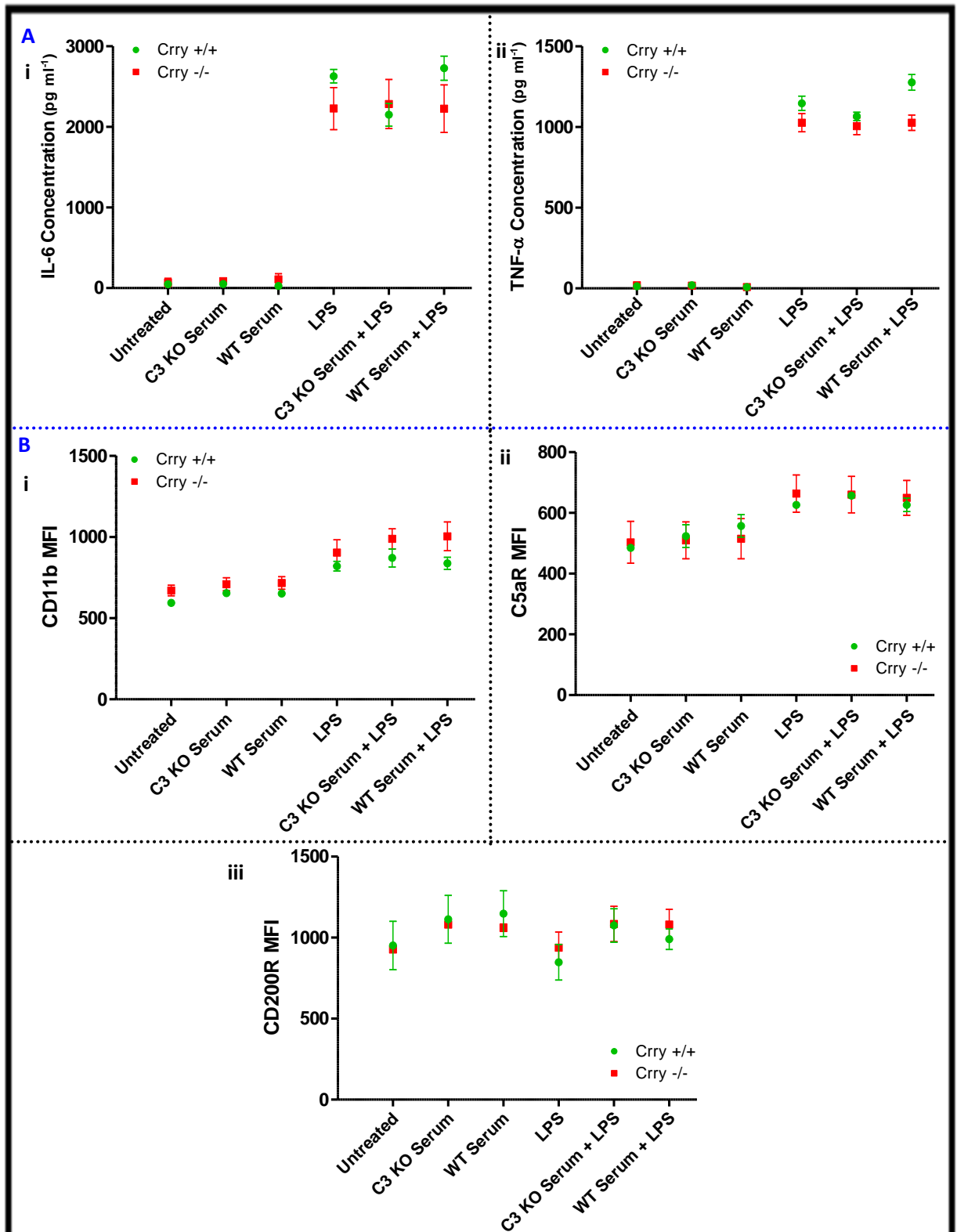


Fig.5.7: Assessment of the *in vitro* Crry KO microglial phenotype in response to C3-activation fragment deposition resulting from sensitivity to autologous C activation. 2.5×10^5 WT or Crry KO MACS sorted primary microglia were seeded *per well* in 24-well plates (0.5mL media). After 24 hours, cells were incubated with 10% WT or C3KO mouse serum (37°C, 1hr) before thorough washing (2 PBS followed-by 2 complete-media washes) and treatment with or without 10ng/mL LPS for 48 hours. Some wells were also left untreated or treated with LPS alone. Cytokine (IL-6 and TNF- α) production was determined by ELISA of supernatants + cell surface markers (CD11b, C5aR, and CD200R) were assayed by flow cytometry. (A) IL-6 (i) and TNF- α (ii) supernatant concentrations; (B) Fluorescence intensities due to CD11b (i), C5aR (ii) and CD200R (iii) staining. WT: green, Crry KO: red; Bars = Means +/- SDs; N \geq 3.

5.3 Discussion

5.3.1 The *in Vitro* Crry KO Microglial Phenotype and the Mechanism of C-dependent Priming

The work described in this chapter was conducted in-order to further characterise the mechanism of C-dependent microglial priming reported *in vivo* in Crry KO mice. Given that the original study which identified this mechanism was based solely on data gathered from *in vivo* and *in situ* observations, the intrinsic complexity of the experimental systems means that the fine details of this mechanism remained veiled. For example, the question of whether the Crry KO primed microglial phenotype is lost in the absence of the plethora of other factors with which microglial cells interact *in vivo* and/or the chronic C activation which occurs in the live animal, remains to be fully investigated.

As a key starting point, expression and deficiency of surface Crry protein was demonstrated for microglial cells isolated from WT and Crry KO CNS tissue, respectively, confirming the *in vitro* retention of the innate difference between cells of the different genotypes. Initial phenotypic characterisation experiments failed to show any evidence of a primed phenotype in Crry KO cells in the form of pro-inflammatory hyper-reactivity. This is perhaps unsurprising given that through pharmacological C-inhibition, Ramaglia *et al.*, found evidence to suggest that in the absence of chronic local C-activation, the *in vivo* primed Crry KO microglial phenotype is lost (1). However, the possibility cannot be excluded that the isolation and culture process *per se* and/or the absence of other *in vivo* interaction partners, and not that of chronic local C-activation is responsible for the initial loss of distinction between WT and Crry KO microglial cells in-terms of pro-inflammatory reactivity.

Given the absence of any detectable differences in basal pro-inflammatory responses consistent with a primed phenotype for cultured Crry KO microglia, an attempt was made to recreate the mechanism of *in vivo* priming in the Crry KO CNS, in the context of the sensitivity of the Crry KO microglia to C-activation. C-deposition assays were developed which were employed to demonstrate the specific sensitivity of Crry KO cells to autologous C activation and C3-deposition. Based on the results of these assays a system was designed which, analogous to the mechanism of C-dependent priming reported *in vivo*, resulted in readily detectable C3-deposition on Crry KO cells, whilst C3-deposition on WT cells remained undetectable. Given that the intrinsic sensitivity of Crry KO microglia to C activation and C3-deposition, leading to microglial CR3-ligation by C3-activation products, is proposed to underlie the mechanism of C-dependent priming, the effect of this design on microglial pro-inflammatory activation responses was subsequently investigated. These experiments revealed no evidence to support the role of C3-activation fragments in the

promotion of a primed phenotype in microglia derived from Crry KO mice. This was somewhat surprising given the initial report describing the priming mechanism (1), together with the results presented in the previous chapter implicating C3-derived CR3 ligands in the induction of a primed phenotype in WT microglia (Section 4.2.3.2).

Given previous reports implicating serum factors which enter the parenchyma upon BBB disruption in microglial activation (173, 401, 402), the lack of any phenotypic effects resulting from direct treatment of cultured cells with serum, albeit dilute, is notable. Nonetheless, even under pathological conditions leading to a disruption in BBB integrity, some selectivity for entry of blood-borne factors into the tissue remains since BBB disruption occurs at a degree along a spectrum (ranging from minimal to severe) and cannot simply be considered as an 'all or nothing event'. It therefore follows that while the direct treatment of cultured primary microglial cells with serum results in their exposure to the entire serum load, the exposure to blood-borne factors experienced by *in vivo* microglia during BBB-disruption will vary depending on the extent to which the barrier is compromised. It is therefore possible that the inability to observe any pro-inflammatory effects associated with exposure of cultured primary microglia (WT or Crry KO) to serum is a consequence of the presence of serum factors beyond those typically experienced by microglia during BBB disruption. The results of phenotyping experiments using opsonised zymosan (Section 4.2.2.2) and immobilised serum proteins (Section 4.2.3) further highlight the potential for non-/anti- inflammatory responses to be elicited by serum factors. The possibility cannot, of course, be excluded that the observed altered responsiveness is simply a product of the *in vitro* microglial environment. These data further emphasise the importance of context in the vectoring of cellular responses.

5.3.1.2 *The Inability to Detect a Primed Crry KO Microglial Phenotype in Vitro*

A possible explanation for this apparent inability of C3-derived CR3 ligands to induce a primed phenotype in Crry KO microglia *in vitro* is that having been already primed by C *in vivo*, Crry KO cells, unlike WT, fail to respond to subsequent C3-CR3 ligation with a priming effect. The importance of the context-differences of the systems employed must also be emphasised: the study of Crry KO cells attempted to closely mimic the original *in vivo* study, utilising the intrinsic sensitivity of Crry KO cells to achieve C-activation and C3-deposition on them by adding autologous normal serum directly to the cells in culture; the results described in the previous chapter (Section 4.2.3.2.3) seeded WT cells directly onto C3-activation fragment coated TC plastic surfaces, obtained by incubation of autologous normal serum in plastic TC wells followed by multiple washes. Crry KO cells were therefore exposed, albeit briefly, to a plethora of other serum factors (including CR3 ligands e.g. fibrinogen) which have potential to modify the phenotypic response to CR3-ligation by C3-derived products. In contrast, in the experiments detailed in the

previous chapter, the relative abundance of C3-derived CR3 ligands would be dramatically increased, since C3-activation fragments actively attach to activating surfaces through covalent bonding *via* the TED, whereas other serum factors attach passively through adsorption. Furthermore, the probable differences in the scale of the exposures should also be emphasised: in the results described in the previous chapter, although a higher serum concentration was used (35% Vs 10%), the vast majority of serum factors, including C3-activation fragments, would fail to adhere and subsequently be washed away; in the experiments with Crry KO cells, cells would invariably be exposed to the entirety of the serum load. It is therefore likely that the scale of the exposures in the different systems varied widely both quantitatively and qualitatively and may well account for the apparent discrepancy of between the phenotypic effects of C3-derived CR3 ligands observed therein. Indeed, given that the CNS is shielded from peripheral C by the BBB, the level of C activation to which Crry KO cells are exposed *in vivo* is likely to be very low (albeit chronic).

A key point, however, is the duration of exposure to C3-derived CR3 ligands required to induce a phenotypic response when deposited on Crry KO cells during autologous C activation. Given that in the *in vivo* scenario C activation in the Crry KO microglial locality is chronic (although probably low-grade), iC3b ligation of CR3 is presumably continuous over the lifetime of the animal (1). In the *in vitro* investigation of Crry KO microglia described in this chapter, the phenotypic effects of just a single, acute C (1hr) exposure were tested, distancing the experimental system in its approximation of the *in vivo* Crry KO setting. This also presents a key difference between the results of the previous chapter where priming was successfully demonstrated (Section 4.2.3.2.3), where priming-trigger exposure was overnight. On reviewing the data, it seems clear that the length of time between the iC3b-CR3 ligation event (i.e. the priming-trigger) and the LPS exposure (i.e. the activator) is of pivotal importance for the elaboration of any priming phenotype. Indeed, on reflection it appears highly likely that a period of at-least several hours would be necessary for the cellular phenotypic consequences of iC3b-microglial CR3 ligation to become fully initiated, since the process of priming is likely to involve mid-longer term cellular responses (i.e. changes in gene expression beginning at the level of transcription, proliferation). It is therefore possible that the requirement for a more prolonged C exposure (due to autologous C activation) than was employed here underlies the inability to induce a primed phenotype in Crry KO microglia *in vitro*. Future work should revisit this key point and investigate the effects of longer-term exposures to C3-derived CR3 ligands on Crry KO microglia resulting from uncontrolled C-activation. Although the investigation of a system which re-created the *in vivo* scenario was the aim of the studies presented here, future work could also investigate the use of Crry KO primary microglia in the same experimental system utilised in the previous chapter (Section 4.2.3.2.3) to successfully

achieve priming in WT cells. This would address questions concerning both the timings of the priming and activation triggers and the quantitative and qualitative differences between the factors present in the different systems designed to achieve iC3b-CR3 ligation.

A fundamental way in which the *in vitro* experimental system employed here differs from the *in vivo* Crry KO scenario is the absence of countless of the *in vivo* factors with which microglial cells interact in the live animal. Given the accumulating evidence (including results presented in Section 3.2.2) that other CNS cell types have important effects on microglial activation, particularly the inhibitory effect of neuronal-microglial ligand-receptor partners (e.g. CD200-CD200R, CX3CL1-CX3CR1) (173, 246, 249), it is conceivable that in their absence important aspects of normative microglial biology would be perturbed enough to prevent the elaboration of normal (including C-induced priming) responses. Indeed, this is perhaps a more obvious explanation for the inability to detect a C-dependent primed phenotype in Crry KO microglia than any consideration of the fine details of the nature of the C exposure and CR3 ligation. However, the results presented in the previous chapter, where C3-derived CR3 ligands were found to induce a primed phenotype in isolated WT microglia, indicate that the absence of other CNS cell types does not necessarily exclude the induction of a primed phenotype by C3-derived CR3-ligands. Experiments involving mixed CNS cell cultures would be required to assess the influence of other CNS cell types on microglial priming.

Moreover, in the absence of clear phenotypic effects attributable specifically to the presence of C3-activation fragments in the system, it remains unclear whether C3-activation fragments deposited on Crry KO cells *in vitro* actually functionally engage CR3: While the presence of C3-activation products specifically on Crry KO microglia was definitively demonstrated, the engagement of microglial CR3 by these products was not, thus raising the possibility that C3-activation fragment mediated CR3-signalling was not induced or was insufficient to have a priming effect. Indeed, in-contrast to the 3-dimensional situation *in vivo*, the microglial culture systems employed here had a standard 2-dimensional, planar nature and thus, although pure populations were used, the sum of total microglia-microglia interactions would be expected to be reduced relative to the scenario *in vivo*. It is unknown whether an individual cell can reposition CRs in its membrane to engage a C3-derived ligand deposited thereon, although presumably some ligand could be deposited directly upon a receptor, or in sufficiently close proximity to be engaged by it (at a frequency dependant on the densities of both the receptor and ligand). Although this issue of 'auto-signalling' applies equally *in vitro* and *in vivo*, it is therefore impossible to delineate the relative contributions of 'auto-signalling' (i.e. CR3 in a membrane engaging C3-derived ligands deposited therein) and 'juxta-signalling' (i.e. CR3 in a membrane engaging C3-derived ligands deposited on the membrane of a neighbouring cell) to the induction of the primed microglial

phenotype reported in Crry KO mice *in vivo*. As stated previously (Section 4.3.1) the induction of the intracellular signalling responses associated with CR3/CD11b:CD18 integrin ligation could be investigated (e.g. phosphorylation of SFKs, ERK/MAPK, Rho-GTPases, etc.) as a means to assess functional engagement of CR3 in a system dependent on its ligation.

To summarise: through isolating the cells *in vitro*, the effect of C withdrawal on the Crry KO microglial phenotype was tested. The lack of distinction between Crry KO and WT microglia *in vitro* under basal conditions would appear to further indicate that in the absence of C3-derived CR3 ligands, the primed Crry KO-specific phenotype is lost. However, when the intrinsic sensitivity of Crry KO microglia to C-activation was exploited *in vitro* to recreate the mechanism of priming proposed based on *in vivo* observations (1), a phenotypic effect consistent with priming failed to emerge. In-light of the results presented in the previous chapter (where C3-derived CR3 ligands were found to induce a primed phenotype in isolated WT microglia; Section 4.2.3.2.3), along with those of the original report of C-dependent microglial priming in the Crry KO *in vivo* setting (1), it seems logical to conclude that the failure to detect a C-induced primed phenotype in Crry KO microglia *in vitro* is either a consequence of the cells being resistant or intolerant having already been primed by C *in vivo*, an inability to adequately mimic the *in vivo* Crry KO scenario (with timing of CR3-ligand exposure being a key issue), and/or an inability to detect the primed response. Additionally, given the accumulating evidence of the importance of interactions with other CNS cell types for microglial responses (173, 177, 246-249) the very nature of the highly purified cultured cells employed may have conspired against the ultimate goal of these experiments and precluded the stimulation of a primed microglial phenotype by C. These observations do not exclude a role for C activation in the promotion of a primed phenotype *in vivo* but demand a more careful consideration of how to study and elicit these responses *in vitro*, particularly in terms of the issue of timing between the priming and the activatin triggers.

5.3.2 Crry as the Key Regulator of Microglial Sensitivity to Autologous C Activation

The results presented in this chapter clearly show that Crry is critical for protection from autologous C3 activation, but ineffective against heterologous C. These findings support previous reports of species restriction of Crry function (156, 157, 164). However, to my knowledge, this is the first time sensitivity of microglial cells to C activation has been assessed *in vitro*. These findings reveal that, similarly to other murine cell types, Crry is critical for microglial protection from autologous C activation and indicates that functional redundancy is not achieved through other C-regulators. Furthermore, while Crry KO cells were clearly far more sensitive to C3 deposition, in-contrast to the results with human serum, autologous serum had no effect on

viability. Since viability appears to be directly related to MAC formation (based on results with human serum on both BV2 and primary cells) it seems reasonable to summarise that: a) the primary cells are protected against MAC formation; b) the level of C3 deposition achieved on Crry KO cells, although readily detectable, was insufficient to trigger sufficient C5-covertase formation and C5-activation to trigger MAC-mediated lysis, and/or; c) the known decreased terminal pathway activity of mouse Vs human serum (144, 403) resulted in a failure to trigger lysis, regardless of abundant deposition of C3-activation fragments. Given the results described in chapter 3, it appears that BV2 and primary microglial cells express similarly low levels of CD59, suggesting that differential expression of MAC-regulators isn't responsible for the difference in sensitivity to lysis by autologous Vs heterologous serum. Based on this evidence, coupled with the sensitivity of primary microglial cells (both WT and Crry KO) to MAC-mediated lysis in the presence of human C (Fig.5.4), it seems likely that the well documented species difference in the lytic activity of serum from human and mouse (144, 403) underlies the failure of incubation with autologous serum to result in the lysis of primary microglial cells, regardless of Crry expression status and sensitivity to C3-deposition. This issue could readily be further investigated by assaying C activation on BV2 cells using WT mouse serum as the C source and/or attempting to further increase the level of autologous C activation (and thus achieve MAC-mediated lysis) by sensitising cells with a C-fixing Ab. Moreover, since the main aim of this study was to explore the consequences of microglial CR3-ligation by iC3b resulting from unrestricted C3 activation and deposition, specifically on Crry KO microglia i.e. Ramaglia *et al.*, 2012 (1), the failure of autologous serum to result in lysis at any concentration, coupled with the Crry KO-specific sensitivity to C3-deposition, was beneficial in-terms of the requirement to balance maximal C3-deposition on Crry KO cells against minimal cell death.

6 Discussion

6.1 Study Outline

Microglia, the sole-resident innate immune cells within the highly specialised and sensitive environment of the CNS parenchyma, interact with their environment through a wide variety of receptor-based detection systems (173). Prompted by a previous *in vivo* investigation in Crry KO mice (1), this study chiefly sought to characterise *in vitro* the consequences of ligation of the hetero-dimeric integrin receptor CR3 with its archetypical ligand [the iC3b fragment of C (284)] on the microglial immune response, specifically in the context of the induction of a primed/hyper-responsive state. Furthermore, the *in vitro* phenotype of Crry KO microglia, previously shown to be functionally 'primed' *in vivo* (1), was a focus of this project. The results presented in this thesis further illustrate the potential for C-derived CR3 ligands to induce exaggerated microglial inflammatory responses, whilst also further emphasising the importance of the context of interactions for cell fate.

Additionally, through the use of BV2 cells in validating the identity of primary microglial cells isolated from adult mouse CNS tissue, a mouse microglial cell line was compared directly with primary mouse microglia in-order to assess their resemblance and thereby determine the suitability of cell lines as a substitute for primary microglia. In-view of increasing awareness of the importance of microglial interactions with other CNS cell types (173, 177, 246-249), the phenotype of microglia maintained in isolation or in mixed CNS cultures was also investigated.

6.2 Summary of Main Findings

6.2.1 The Influence of C on *In Vitro* Microglial Phenotypes

6.2.1.1 Purified Fluid-Phase Human iC3b

In an initial attempt to define the consequences of microglial CR3 ligation by iC3b in the simplest possible system of cell treatments, commercially-available purified fluid-phase human iC3b was used as an agonist of CR3 on cultured primary microglial cells. Although interaction could be detected, binding studies using fluorescently labelled ligand (iC3b-fluorescein) along with blocking antibody directed against the iC3b-binding site of CR3 were unable to definitively demonstrate specific binding of fluid-phase human iC3b to mouse microglial CR3. Coupled with the absence of any overt phenotypic effects, it therefore remained unclear whether the xenogeneic ligand can engage the receptor in this system, or whether iC3b is simply unable to exert significant phenotypic effects when in the fluid-phase. Nonetheless, previous studies demonstrate the ability of fluid-phase iC3b to bind its cell-borne receptor (283, 351, 356) along with the ability to use fluorescently labelled soluble CR3 ligands to demonstrate specific binding (337). Combined with

the results of sequence comparisons (Section 4.2.1.2.2) and binding studies using zymosan opsonised with NHS alongside mouse microglia (Section 4.2.1.2.3), these data indicate that there should be no intrinsic impediment to fluorescent human fluid-phase iC3b ligating mouse cell-borne CR3 and detecting this interaction through the method employed. Furthermore, it has been illustrated that the physical state of CR3 ligands (e.g. fibronectin) can have important impacts on subsequent cell responses, specifically that only immobilised ligands have phenotypic effects (334-336, 356) and that multivalent receptor occupation is required to achieve signalling (331, 356-359). The data presented in this thesis is broadly in line with these studies, indicating that monomeric fluid-phase iC3b is incapable of inducing a significant effect on the microglial activation response.

6.2.1.2 *Zymosan*

In-light of the difficulties associated with the use of fluid-phase xenogeneic iC3b, alternative approaches were sought which would circumvent these issues. The well-characterised particulate C-activator, zymosan (233, 404), was thus employed to generate fixed C3-derived CR3 ligands. These studies were aided by the commercial availability of fluorescently-labelled zymosan for use in binding assays, along with the ability to utilise WT mouse serum as a C-source in-parallel with C3 KO serum as a negative control to account for non-specific effects of serum opsonisation. Using non-opsonised fluorescently labelled (AF488) zymosan, along with particles opsonised with WT or C3 KO serum, in combination with anti-CR3 blocking reagent, the specific contribution of CR3 to both opsonic and non-opsonic microglia zymosan phagocytosis was characterised. Importantly, it was determined that C3-dependent microglial opsonic zymosan phagocytosis is exclusively CR3-mediated and that this represents a significant proportion (~25%) of total zymosan phagocytosis. Phenotyping assays demonstrated clear effects specific to iC3b-CR3 interactions; however, the specific effects of iC3b-CR3 interactions on microglial responses (both basal and to LPS) were masked greatly in this system by the major intrinsic activating effects of the β glucan-rich zymosan particles used to bear iC3b. Nonetheless, in alignment with studies concerning the consequences of CR3-mediated opsonic and non-opsonic phagocytosis in other cell types (312, 327-329, 362-364), non-opsonic CR3-mediated (i.e. β -glucan site-mediated) microglial phagocytosis was found to be potently pro-inflammatory, whilst in sharp contrast, opsonic CR3-mediated (iC3b site-mediated) zymosan phagocytosis was found to be non-inflammatory. Furthermore, it was shown that the non-inflammatory effects of iC3b-CR3-mediated phagocytosis can lead to a net reduction in inflammation upon secondary exposure to an activating trigger (Section 4.2.2.2.2).

6.2.1.3 *C3-Activation Fragments Immobilised on TC Plastic*

6.2.1.3.1 Using C-Fixing mAb

The complexities associated with the use of zymosan as an iC3b-bearing particle called for the pursuit of other strategies to achieve specific engagement of microglial CR3. A design based on the classical C activation pathway was employed where a C-fixing in-house mouse mAb (354) was utilised alongside WT mouse serum (as a C-source) to achieve deposition of C3-activation fragments on TC plastic, in-parallel with C3 KO serum (as a negative control). In similar vein to the results seen with zymosan, the activation of serum-borne C resulted in specific effects on microglial responses, however, the presence of the C-fixing mAb-coat itself had a potentially pro-inflammatory activating effect on the basal microglial phenotype which prevented assessment of the isolated effects of iC3b-CR3 interaction. These data are also in alignment with other studies concerning the consequences of FcR-ligation on microglia along with other cells (367, 368).

6.2.1.3.2 Native TC Plastic

Although use of the C-fixing mAb-based system described above yielded the greatest deposition of C3-activation fragments on TC plastic, it was noted that even on native TC plastic, signal for deposited C3-activation fragments was readily detectable and, at higher serum titres, was comparable with that achieved using the C-fixing mAb (Fig.4.11). The mAb was therefore removed from the design, yielding a system devoid of other factors beyond TC plastic and those found in (mouse) serum; through use of WT and C3 KO mouse serum, it was therefore possible to isolate the specific effects of iC3b-CR3 ligation on basal microglial responses. Marked phenotypic effects, specific to the presence of C-derived CR3 ligands, which are consistent with priming (e.g. changes in basal morphology in the absence of pro-inflammatory effector release; exaggerated pro-inflammatory LPS-response) were observed, particularly in primary microglia. Coupled with the finding that CR3 is the principle microglial receptor for C3-activation fragments, these data demonstrate that ligation of microglial CR3 by its archetypical ligand (iC3b), can induce a primed phenotype in this *in vitro* setting of relatively isolated CR3 ligation.

6.2.1.4 *Crry KO Microglia*

Investigations using cultured Crry KO microglia showed that the sensitivity of these cells to C activation at the C3-level is clearly elevated, in a similar manner to that seen *in vivo* (1). While other studies have investigated the expression of membrane C-regulators (i.e. DAF, Crry, CD59) by CNS cells (394, 395) and thereby inferred that Crry is the chief microglial form, to my knowledge this is the first time that the sensitivity of microglial cells to C activation has been assessed *in vitro*, and certainly the first time that the deposition of C3-activation fragments (along with viability) has been charted directly and shown to be altered as a function of differences in

membrane C-regulator expression. Nonetheless, unlike *in vivo* (1), investigations of the *in vitro* Crry KO microglial phenotype failed to show any consequence of Crry expression status, even when the intrinsic sensitivity of Crry KO cells to C3 activation and deposition was exploited, thus mimicking the *in vivo* scenario (including the potential for iC3b ligation of CR3). While perhaps somewhat surprising, this result further illustrates the critical importance of context in determining the outcome of microglial CR3 engagement by its cognate ligand, iC3b..

6.2.1.5 *Summary*

Overall, specific effects attributable to the interaction of iC3b with microglial CR3 have been demonstrated, some of which are compatible with the induction of a primed microglial phenotype while others are associated with non-/anti- inflammatory responses. The picture that has emerged is that the effects of CR3 ligation are heavily influenced by the combination of the binding site(s) engaged, valency of ligands, presence of other ligands (both CR3 and non-CR3), adhesive substrates and cell type. The interactions of these numerous factors culminate in a spectrum of CR3 functional responses, the range of which is striking: from non-/anti-inflammatory (e.g. iC3b-CR3-mediated phagocytosis) to the potentially pro-inflammatory (e.g. β glucan-CR3-mediated phagocytosis).

The findings presented here which centre on the binding of microglial CR3 by iC3b make novel contributions to the understanding of the phenotypic consequences of ligation of C receptors for the larger (i.e. non-C3a) fragments of activated C3, including the concept of C-dependent priming. Furthermore, they also contribute to the broader theme which is emerging in recent times regarding the important influence that C has on microglia and other CNS cells and how these interactions are involved in diverse processes ranging from developmental, homeostatic and protective to ageing and degenerative (96, 178, 222, 405-409).

6.2.2 *Microglial Culture Systems*

6.2.2.1 *Primary Vs Cell Lines*

A comparison of primary mouse microglial cells with a widely utilised microglial cell line derived from the same species (BV2) was performed. This initially served as a comparator and validation tool for the isolated primary cells, but by the same token, subsequently served as a means to assess the degree to which this cell line approximates its intended replacement (i.e. primary mouse microglial cells) and thus its suitability for its purpose. This comparison revealed that while all aspects of microglial biology investigated were retained in BV2 cells, many were suppressed (e.g. level of surface marker expression, cytokine secretion) or otherwise altered (e.g. morphology, proliferation rate) relative to primary cells. These findings are in alignment with those of others who have investigated the same issues (183, 192, 240, 258) and lead to the

conclusion that while BV2 cells are a useful tool for investigations pertaining to microglial biology, they are an imperfect replacement for primary cells. This is particularly true in the case of functional studies (i.e. dependent on cellular responsiveness), where relatively low gene expression levels and rapid-turnover rate of BV2 cells Vs primary microglia reduces their ability to faithfully mimic key aspects of microglial biology. This is exemplified by the experiments involving the culture of microglia on C3-activation fragment-coated TC plastic prior to LPS activation (described in Sections 4.2.3.2.2 and 4.2.3.2.3), where priming was far more evident in primary microglia Vs BV2 cells.

6.2.2.2 *Isolated Microglial Vs Mixed CNS Cultures*

Given the emerging theme of the importance of inhibitory surface interactions of microglia with other CNS cell types (particularly neurones) for the maintenance of a resting/basal phenotype (173, 177, 246-249) a minor investigation into the activation response of primary microglia maintained in isolation or in mixed CNS culture was conducted. This revealed distinct differences in the profile of surface CD11b expression during microglial activation, illustrating detectable changes in microglial phenotype which are dependent on the presence of other CNS cell types. This is one of the very few experimental studies to-date which has directly addressed the question of how microglia maintained in isolation differ from those cultured in mixed populations and provided some quantitative measure to this end. The concept of taking measures to restore microglial culture systems to a closer approximation of their *in vivo* environment in-terms of interactions with other CNS cells (e.g. through supplementing the culture medium with neurone-derived ligands) has recently been established (249) and could become an important and popular tool for *in vitro* microglial research in future; This work therefore contributes towards the development of this concept.

6.2.2.3 *Summary*

Combined with *in vivo* models for the study of CNS cell biology and neuroinflammation, methods for the *in vitro* culture of microglia (and other CNS cells) will continue to be an important tool for research into all aspects of their biology for the foreseeable future. The findings related to microglial culture systems presented here (i.e. cell lines Vs primary cells; isolated Vs mixed) contribute to the ongoing development of this important resource. With increasing recognition and manifestation of the current and future global mental health burden leading to emphasis on research into neuro-inflammatory mechanisms, *in vitro* experimentation with microglia (and other CNS cells) will likely feature even more prominently in future, thus increasing the value of such design improvements.

6.3 Future Directions

6.3.1 Purified iC3b

Investigations using commercially available purified human iC3b in the fluid-phase were confounded by the inability to determine with certainty whether the interaction of the soluble protein with mouse microglial cells was specifically mediated by CR3, leading to difficulties in making definitive conclusions regarding the lack of overt functional effects of soluble iC3b treatment. Since a system utilising purified iC3b provides the 'cleanest' possible approach to the exploration of the isolated effects of microglial CR3 ligation by C, it would be desirable to employ this strategy with greater effectiveness having established the fundamental element of specific interaction between ligand and receptor. Although the technical difficulties (including acquiring the necessary volume of C-sufficient mouse serum) coupled with the commercial availability of soluble human iC3b preparations meant an attempt to purify mouse iC3b was never made, soluble iC3b could be generated and purified from fresh mouse serum. This purified mouse iC3b could then be employed, initially in attempts to establish the specificity of binding, then in experiments concerning the functional consequences of treatment. This approach would (of-course) circumvent the issues associated with species-mismatch and would determine if this underlies the failure to definitively show binding specificity. Furthermore, in a further attempt to assess binding specificity, a plate-based system for detection of interaction of the fluorescently-labelled soluble ligand with an immobilised binding partner (i.e. microglial CR3), similar to that used to assess the ability of fluorescently-labelled soluble human iC3b to bind immobilised specific mAb (Section 4.2.1.2.1.1), could be employed. This approach has the distinct benefit over the FACS based assay used to assess specific ligand – cell-borne receptor binding in this study of the ability to assess binding while the cells remain in their native state (i.e. adherent). Furthermore, based on the results of the comparative assessment between the BV2 microglial cell line employed and primary microglial cells (Section 3.2.1.1), along with those which demonstrate more pronounced effects of iC3b-CR3 interaction in primary microglia Vs BV2 cells (Section 4.2.3.2), it appears that primary microglia express greater levels of surface CR3 and are thereby more responsive to iC3b ligands. Although, primary cells were used for phenotypic/functional experiments, BV2 cells were employed to assess specific ligand-receptor binding. Therefore, in-order to definitively demonstrate the specificity of ligand-cell borne receptor binding, future work would be best served by employing primary cells. Moreover, in-order to demonstrate specific and/or functional iC3b-CR3 binding, the ability to detect activation of CR3/CD11b:CD18 integrin-linked intracellular-signalling mediators (Section 4.1.3) would be highly valuable.

Additionally, based on the known potential importance of the physical state of CR3 ligands (331, 334-336, 356-359), and the interesting results from experiments using fresh mouse serum to

achieve immobilisation of C3-activation fragments on TC plastic (Section 4.2.3.2), future work using purified iC3b preparations could seek to immobilise the ligand onto TC plastic and then seed microglial cells onto this opsonised/coated surface, in-order to investigate the potential phenotypic effects. This avenue was briefly explored in preliminary investigations using immobilised purified human iC3b and BV2 cells. However, as attempts to demonstrate specific binding through adhesion assays failed, this approach was not pursued further, although in hindsight there is a possibility that this failure to exhibit specific interaction was simply a consequence of the relatively low expression levels of CR3 by BV2 cells.

6.3.2 The Priming Effect of Immobilised Mouse iC3b Derived from Serum Borne C3

The most positive finding to emerge from this study in support of the C3-dependent mechanism of microglial priming reported by Ramaglia *et al.* (based on observations in Crry KO mice) (1) is that concerning the phenotypic effects of C3-activation products immobilised on TC plastic generated from serum-borne mouse C3 (Section 4.2.3.2). However, this remained largely undefined. Thus a clear objective of future work could be to explore the fine details of the C-primed state, including its functional consequences. To this end, attempts to define the molecular hallmarks of C-mediated microglial priming would perhaps be best served by the employment of systems biology approaches such as global gene expression analyses (e.g. oligonucleotide microarray, RNA sequencing technology, quantitative mass-spectrometry/TMT) which have the interrogative power to detect differences in cellular factors involved in every aspect of cell function. This will likely be necessary to distinguish between the C-primed microglial phenotype and those induced in other non-physiological settings (e.g. other modes of priming and dysfunction such as: activation through P/DAMPs such as LPS, β -glucan and β -amyloid; aging; CD200 deficiency; prion-infection). Indeed, in other scenarios of priming (i.e. ageing and neurodegeneration), Holtman *et al.* have recently reported the application of such global approaches to phenotyping (oligonucleotide microarray) and provide what is probably the most detailed picture to-date of its molecular hallmarks in the form of a distinctive transcriptomic profile (235). Having initially being defined through functional readout of soluble inflammatory effector release in different contexts, this represents a significant step forward in the characterisation of the primed microglial phenotype.

Perhaps the most interesting potential avenue of future research stemming from this study is that concerning the consequences of C-mediated *in vitro* priming in a wider context than the simple measurement of inflammatory effector molecule release, such as those for neuronal and (thereby) cognitive integrity. In pursuit of a greater understanding of this, future studies could employ mixed systems where C-primed microglia are cultured alongside neurones and the effect of a subsequent insult assessed on parameters of neuronal function and viability. In an *in vivo*

setting, C-primed microglia could be transferred to a host CNS before or alongside an inflammatory insult (e.g. TBI, ischaemia, infection, LPS-administration) and the effect on the clinical profile, along with parameters derived from tissue analysis (e.g. histology, RNA profile/gene expression, protein expression) assessed. Furthermore, particularly since microglial priming is thought to be a common event/process which occurs with ageing and contributes to the cognitive decline and diseases (e.g. Alzheimer's) associated with it (223), future research pursuing therapies to modulate neuro-inflammation should consider the development of strategies to reverse priming.

6.3.3 Crry KO Microglia

The failure to demonstrate any difference in the activation profile between cultured Crry KO and WT microglial cells, even under conditions which exploit the clear C-sensitivity of Crry KO cells and thereby closely approximate the *in vivo* setting in which the initial report of their primed phenotype originates (1) (Chapter 5), is perhaps surprising, especially given the priming effect achieved with WT cells and immobilised serum-derived C3-activation products discussed above. Several possible explanations exist for this inability (see Section 5.3.1.2) and should be explored in more depth, with the issue of timing between the priming and activation triggers believed to be of particular importance. Such studies should continue to explore the magnitude of the Crry KO microglial activation response and determine definitively if the inability to show an altered phenotype [such as that described *in vivo* (1)] is a genuine feature of Crry KO microglia *in vitro* or was due to some inaccuracy or imprecision in the fidelity of the experimental design or artefact.

6.3.4 The Assessment of IL-1 β as a Priming Marker

Initial studies into microglial priming using *in vivo* prion disease models identified dramatic increases in IL-1 β expression as an important feature of the activation-profile of primed microglia (217, 221). Research involving the same investigators also linked IL-1 β production to systemic infection and cognitive decline in Alzheimer's disease patients (229). Other investigators have also noted exaggerated IL-1 β production as a central feature following the activation of primed microglia (1). While other major soluble pro-inflammatory mediators were measured, including TNF- α , IL-6 and NO, all of which have been implicated as components of the primed microglial activation profile (1, 217, 221), the measurement of this key cytokine was omitted during experiments involving the measurement of cytokine release of microglial cells exposed to priming stimuli. It is possible that the inclusion of IL-1 β as an analyte would have revealed a far different picture of the relationship between iC3b-CR3 ligation and microglial priming. Future studies concerned with this research theme should undoubtedly include IL-1 β as a primary analyte of interest. Furthermore, the production and release of IL-1 β has an important and emerging link to the inflammasome, which analogous to priming, also features a 'two-hit'

functional model. An area with great research potential is that of the links between the functional stages in microglial priming (i.e. primed and activated), and the step-wise synthesis and release of IL-1 β *via* the inflammasome.

6.3.5 Exploiting CR3 Non-Inflammatory Responses

A notable finding in this study was the striking spectrum of responses elicited by microglial CR3 ligation ranging from distinctly pro-inflammatory (e.g. β -glucan binding-site mediated phagocytosis) to non-inflammatory (e.g. iC3b binding-site mediated phagocytosis). Furthermore, it was shown that the non-inflammatory effects of iC3b-CR3-mediated phagocytosis can lead to a net reduction in inflammation upon secondary exposure to an activating trigger (Section 4.2.2.2.2). Previous studies have considered the potential to exploit the mechanistic quirks of CR3 ligation by promoting β -glucan site ligation to induce pro-inflammatory responses to iC3b-bearing targets (i.e. cancer cells) (313). An interesting possibility which further employs this concept of exploiting CR3 mechanisms would be the potential to promote non-inflammatory iC3b-CR3 mediated phagocytosis leading to a net inflammatory reduction in pathological conditions in which predictable pro-inflammatory mechanisms (e.g. FcR- and CR3 β -glucan site- mediated) prevail (e.g. relapsing Ab-driven autoimmunity and hypersensitivity, surgery, infection and sepsis). In-order to explore the viability of this approach a common animal model of *in vivo* inflammation could be employed: particles which possess minimal inflammatory potential such as latex beads (unlike e.g. zymosan) could be opsonised with iC3b and then transferred to the peritoneal cavity of an experimental animal; the effects of this treatment on the net response to a subsequent pro-inflammatory trigger could then be investigated, through measures such as the dynamics and phenotypic/functional status of immune cell populations found therein, systemic levels of inflammatory effectors (e.g. cytokines), etc.

6.4 Concluding Remarks

As the sole resident innate immune cells within the CNS parenchyma which are unique in origin to all other cell types normally resident therein (along with resident innate immune cell populations in peripheral organs e.g. macrophages and dendritic cells), microglia are highly specialised cells, both in-terms of function and development, in a very sensitive organ. They exist to support and maintain the normal CNS physiology but intrinsically, due to their function and nature as fully competent innate immune cells, possess the potential for non-discriminatory damage and destruction of their host tissue which they are intended to protect. With the accumulation of insults through normal ageing, local pathology (e.g. trauma, infection, ischaemia) and inflammatory signals delivered from the periphery (e.g. arising from systemic infection or trauma), the balance of microglial responses is tipped in-favour of a pro-inflammatory, intrinsically self-destructive nature. Questions concerning the fine details of the molecular

mechanisms which mediate these changes are only just coming into the focus of the research community and attempts to answer them will likely lead to important developments in the understanding of neuro- inflammatory and degenerative conditions, and potentially the emergence of new therapeutic targets to combat the cognitive decline which is a sequela of these pathologies. The work presented in this thesis makes a small contribution towards understanding the role of C in this process. The development of validated therapeutic targets to modulate the activities of microglia in disease processes will almost certainly be of extreme importance for the development of therapies for neuro- inflammatory and degenerative conditions. Indeed, the challenge of, and potential for, therapeutic microglial targeting is also coming to the fore in the field of neuroscience research (182, 410-412). Perhaps the greatest hope in this sphere of interest is that future work in the vein of understanding microglial function in health and disease along with therapeutic targeting reaches a level of sophistication where efficacious microglia-orientated therapies are developed. This is particularly true for the most common and debilitating form of CNS disease for-which no effective therapy is available and the burden is forecast to increase greatly in coming decades (i.e. Alzheimer's) (224). Although major progress is required before any sort of microglia-targeted/specific therapy is sufficiently developed to enter clinical (or even pre-clinical) use, we should perhaps take heart from the fact that this avenue of research is still in its infancy and many stones yet lay unturned.

References

1. Ramaglia V, Hughes TR, Donev RM, Ruseva MM, Wu X, Huitinga I, et al. C3-dependent mechanism of microglial priming relevant to multiple sclerosis. *Proc Natl Acad Sci U S A*. 2012;109(3):965-70.
2. Paul WE. *Fundamental immunology*. 7th ed. Philadelphia: Wolters Kluwer Health/Lippincott Williams & Wilkins; 2013. xviii, 1283 p. p.
3. Penfield W. *Cytology & cellular pathology of the nervous system*. New York,: P.B. Hoeber, Inc.; 1932.
4. Parkhurst CN, Gan WB. Microglia dynamics and function in the CNS. *Curr Opin Neurobiol*. 2010;20(5):595-600.
5. Walport MJ. Complement. First of two parts. *N Engl J Med*. 2001;344(14):1058-66.
6. Tan SM. The leucocyte beta2 (CD18) integrins: the structure, functional regulation and signalling properties. *Biosci Rep*. 2012;32(3):241-69.
7. Alcorlo M, Martinez-Barricarte R, Fernandez FJ, Rodriguez-Gallego C, Round A, Vega MC, et al. Unique structure of iC3b resolved at a resolution of 24 Å by 3D-electron microscopy. *Proc Natl Acad Sci U S A*. 2011;108(32):13236-40.
8. Rosen H, Gordon S. Monoclonal antibody to the murine type 3 complement receptor inhibits adhesion of myelomonocytic cells in vitro and inflammatory cell recruitment in vivo. *J Exp Med*. 1987;166(6):1685-701.
9. Harris ES, McIntyre TM, Prescott SM, Zimmerman GA. The leukocyte integrins. *J Biol Chem*. 2000;275(31):23409-12.
10. Kinoshita T. Biology of complement: the overture. *Immunol Today*. 1991;12(9):291-5.
11. Morgan BP, Harris CL. *Complement regulatory proteins*. San Diego: Academic Press; 1999. xiv, 382 p. p.
12. Morley BJ, Walport M. *The complement factsbook*. San Diego, CA: Academic Press; 2000. viii, 228 p. p.
13. Müller-Eberhard HJ, Miescher PA. *Complement*. Berlin ; New York: Springer-Verlag; 1985. vi, 474 p. p.
14. Janeway CA, Travers P, Walport M, Shlomchik MJ. *Immuno Biology: The Immune System In Health and Disease*: Garland Science Pub.; 2005.
15. Muller-Eberhard HJ. Molecular organization and function of the complement system. *Annu Rev Biochem*. 1988;57:321-47.
16. Ross GD. *Immunobiology of the complement system : an introduction for research and clinical medicine*. Orlando: Academic Press; 1986. xi, 273 p. p.
17. Lambris JD, Holers VM, Ricklin D. *Complement therapeutics*. New York: Springer; 2013. viii, 320 p. p.
18. Morgan BP, Gasque P. Extrahepatic complement biosynthesis: where, when and why? *Clin Exp Immunol*. 1997;107(1):1-7.
19. Ramadori G, Rasokat H, Burger R, Meyer Zum Buschenfelde KH, Bitter-Suermann D. Quantitative determination of complement components produced by purified hepatocytes. *Clin Exp Immunol*. 1984;55(1):189-96.
20. Cruse JM, Lewis RE. *Atlas of immunology*. 3rd ed. Boca Raton, FL: CRC Press/Taylor & Francis; 2010. 940 p. p.
21. Lambris JD. *Current topics in complement II*. New York ; London: Springer; 2008. xxx, 316 p. p.
22. Craig CF. Observations Upon the Noguchi Modification of the Wassermann Complement Fixation Test in the Diagnosis of Lues in the Military Service. *J Exp Med*. 1910;12(6):726-45.
23. Bordet J. The Cameron Prize Lecture ON MICROBIC TRANSMISSIBLE AUTOLYSIS: Given before the University of Edinburgh, 1922. *Br Med J*. 1923;1(3240):175-8.
24. Pillemer L, Blum L, Lepow IH, Ross OA, Todd EW, Wardlaw AC. The properdin system and immunity. I. Demonstration and isolation of a new serum protein, properdin, and its role in immune phenomena. *Science*. 1954;120(3112):279-85.
25. Pillemer L. The properdin system. *Trans N Y Acad Sci*. 1955;17(7):526-30.

26. Pillemer L, Schoenberg MD, Blum L, Wurz L. Properdin system and immunity. II. Interaction of the properdin system with polysaccharides. *Science*. 1955;122(3169):545-9.
27. Pillemer L, Blum L, Lepow IH, Wurz L, Todd EW. The properdin system and immunity. III. The zymosan assay of properdin. *J Exp Med*. 1956;103(1):1-13.
28. Turner MW. Mannose-binding lectin: the pluripotent molecule of the innate immune system. *Immunol Today*. 1996;17(11):532-40.
29. Nonaka M. Origin and evolution of the complement system. *Curr Top Microbiol Immunol*. 2000;248:37-50.
30. Nonaka M. Evolution of the complement system. *Curr Opin Immunol*. 2001;13(1):69-73.
31. Nonaka M, Yoshizaki F. Evolution of the complement system. *Mol Immunol*. 2004;40(12):897-902.
32. Nonaka M, Kimura A. Genomic view of the evolution of the complement system. *Immunogenetics*. 2006;58(9):701-13.
33. Nonaka M. Evolution of the complement system. *Subcell Biochem*. 2014;80:31-43.
34. Chen G, Tan CS, Teh BK, Lu J. Molecular mechanisms for synchronized transcription of three complement C1q subunit genes in dendritic cells and macrophages. *J Biol Chem*. 2011;286(40):34941-50.
35. Reid KB, Porter RR. Subunit composition and structure of subcomponent C1q of the first component of human complement. *Biochem J*. 1976;155(1):19-23.
36. Kishore U, Reid KB. C1q: structure, function, and receptors. *Immunopharmacology*. 2000;49(1-2):159-70.
37. Strang CJ, Siegel RC, Phillips ML, Poon PH, Schumaker VN. Ultrastructure of the first component of human complement: electron microscopy of the crosslinked complex. *Proc Natl Acad Sci U S A*. 1982;79(2):586-90.
38. Muller-Eberhard HJ, Polley MJ, Calcott MA. Formation and functional significance of a molecular complex derived from the second and the fourth component of human complement. *J Exp Med*. 1967;125(2):359-80.
39. Lucisano Valim YM, Lachmann PJ. The effect of antibody isotype and antigenic epitope density on the complement-fixing activity of immune complexes: a systematic study using chimaeric anti-NIP antibodies with human Fc regions. *Clin Exp Immunol*. 1991;84(1):1-8.
40. Bindon CI, Hale G, Bruggemann M, Waldmann H. Human monoclonal IgG isotypes differ in complement activating function at the level of C4 as well as C1q. *J Exp Med*. 1988;168(1):127-42.
41. Bindon CI, Hale G, Waldmann H. Importance of antigen specificity for complement-mediated lysis by monoclonal antibodies. *Eur J Immunol*. 1988;18(10):1507-14.
42. Diebolder CA, Beurskens FJ, de Jong RN, Koning RI, Strumane K, Lindorfer MA, et al. Complement is activated by IgG hexamers assembled at the cell surface. *Science*. 2014;343(6176):1260-3.
43. de Jong RN, Beurskens FJ, Verploegen S, Strumane K, van Kampen MD, Voorhorst M, et al. A Novel Platform for the Potentiation of Therapeutic Antibodies Based on Antigen-Dependent Formation of IgG Hexamers at the Cell Surface. *PLoS Biol*. 2016;14(1):e1002344.
44. Lindorfer MA, Cook EM, Tupitza JC, Zent CS, Burack R, de Jong RN, et al. Real-time analysis of the detailed sequence of cellular events in mAb-mediated complement-dependent cytotoxicity of B-cell lines and of chronic lymphocytic leukemia B-cells. *Mol Immunol*. 2016;70:13-23.
45. Eggleton P, Reid KB, Tenner AJ. C1q--how many functions? How many receptors? *Trends Cell Biol*. 1998;8(11):428-31.
46. Rother K, Till GO, Hänsch GM. The complement system. 2nd rev. ed. Berlin ; New York: Springer; 1998. xx, 564 p. p.
47. Pangburn MK. Activation of complement via the alternative pathway. *Fed Proc*. 1983;42(1):139-43.
48. Pangburn MK, Muller-Eberhard HJ. Initiation of the alternative complement pathway due to spontaneous hydrolysis of the thioester of C3. *Ann N Y Acad Sci*. 1983;421:291-8.

49. Bexborn F, Andersson PO, Chen H, Nilsson B, Ekdahl KN. The tick-over theory revisited: formation and regulation of the soluble alternative complement C3 convertase (C3(H₂O)Bb). *Mol Immunol.* 2008;45(8):2370-9.
50. Pangburn MK, Schreiber RD, Muller-Eberhard HJ. Formation of the initial C3 convertase of the alternative complement pathway. Acquisition of C3b-like activities by spontaneous hydrolysis of the putative thioester in native C3. *J Exp Med.* 1981;154(3):856-67.
51. Fishelson Z, Pangburn MK, Muller-Eberhard HJ. C3 convertase of the alternative complement pathway. Demonstration of an active, stable C3b, Bb (Ni) complex. *J Biol Chem.* 1983;258(12):7411-5.
52. Lambris JD, Muller-Eberhard HJ. The multifunctional role of C3: structural analysis of its interactions with physiological ligands. *Mol Immunol.* 1986;23(11):1237-42.
53. Nilsson B, Nilsson Ekdahl K. The tick-over theory revisited: is C3 a contact-activated protein? *Immunobiology.* 2012;217(11):1106-10.
54. Lachmann PJ, Halbwachs L. The influence of C3b inactivator (KAF) concentration on the ability of serum to support complement activation. *Clin Exp Immunol.* 1975;21(1):109-14.
55. Nicol PA, Lachmann PJ. The alternate pathway of complement activation. The role of C3 and its inactivator (KAF). *Immunology.* 1973;24(2):259-75.
56. Schreiber RD, Pangburn MK, Lesavre PH, Muller-Eberhard HJ. Initiation of the alternative pathway of complement: recognition of activators by bound C3b and assembly of the entire pathway from six isolated proteins. *Proc Natl Acad Sci U S A.* 1978;75(8):3948-52.
57. Platts-Mills TA, Ishizaka K. Activation of the alternate pathway of human complements by rabbit cells. *J Immunol.* 1974;113(1):348-58.
58. Hummell DS, Swift AJ, Tomasz A, Winkelstein JA. Activation of the alternative complement pathway by pneumococcal lipoteichoic acid. *Infect Immun.* 1985;47(2):384-7.
59. Schreiber RD, Muller-Eberhard HJ. Assembly of the cytolytic alternative pathway of complement from 11 isolated plasma proteins. *J Exp Med.* 1978;148(6):1722-7.
60. Leijh PC, van den Barselaar MT, van Zwet TL, Daha MR, van Furth R. Requirement of extracellular complement and immunoglobulin for intracellular killing of micro-organisms by human monocytes. *J Clin Invest.* 1979;63(4):772-84.
61. Kluin-Nelemans HC, van Velzen-Blad H, van Helden HP, Daha MR. Functional deficiency of complement factor D in a monozygous twin. *Clin Exp Immunol.* 1984;58(3):724-30.
62. Vasta GR, Ahmed H. *Animal lectins : a functional view.* Boca Raton: CRC Press; 2009. xxii, 558 p., 16 p. of plates p.
63. Gupta GS, Gupta A, Gupta RK. *Animal lectins : form, function and clinical applications.* Vienna ; New York: Springer; 2012. 2 volumes (liv, 1108 pages) p.
64. Matsushita M, Fujita T. Activation of the classical complement pathway by mannose-binding protein in association with a novel C1s-like serine protease. *J Exp Med.* 1992;176(6):1497-502.
65. Lambris JD. *Current topics in innate immunity.* Berlin: Springer; 2007. xxv, 432 p. p.
66. Thiel S. Complement activating soluble pattern recognition molecules with collagen-like regions, mannan-binding lectin, ficolins and associated proteins. *Mol Immunol.* 2007;44(16):3875-88.
67. Wallis R. Interactions between mannose-binding lectin and MASPs during complement activation by the lectin pathway. *Immunobiology.* 2007;212(4-5):289-99.
68. Eisen DP, Minchinton RM. Impact of mannose-binding lectin on susceptibility to infectious diseases. *Clin Infect Dis.* 2003;37(11):1496-505.
69. Ezekowitz RA. Role of the mannose-binding lectin in innate immunity. *J Infect Dis.* 2003;187 Suppl 2:S335-9.
70. Super M, Thiel S, Lu J, Levinsky RJ, Turner MW. Association of low levels of mannan-binding protein with a common defect of opsonisation. *Lancet.* 1989;2(8674):1236-9.
71. Hadders MA, Bubeck D, Roversi P, Hakobyan S, Forneris F, Morgan BP, et al. Assembly and regulation of the membrane attack complex based on structures of C5b6 and sC5b9. *Cell Rep.* 2012;1(3):200-7.

72. Chakravarti DN, Chakravarti B, Parra CA, Muller-Eberhard HJ. Structural homology of complement protein C6 with other channel-forming proteins of complement. *Proc Natl Acad Sci U S A*. 1989;86(8):2799-803.
73. Whaley K, Loos M, Weiler JM. *Complement in health and disease*. 2nd ed. Dordrecht ; Boston: Kluwer Academic Publishers; 1993. x, 383 p. p.
74. Kock MA, Hew BE, Bammert H, Fritzing DC, Vogel CW. Structure and function of recombinant cobra venom factor. *J Biol Chem*. 2004;279(29):30836-43.
75. Merle NS, Church SE, Fremeaux-Bacchi V, Roumenina LT. Complement System Part I - Molecular Mechanisms of Activation and Regulation. *Front Immunol*. 2015;6:262.
76. Harris CL, Rushmere NK, Morgan BP. Molecular and functional analysis of mouse decay accelerating factor (CD55). *Biochem J*. 1999;341 (Pt 3):821-9.
77. Schwaebler W, Dippold WG, Schafer MK, Pohla H, Jonas D, Luttig B, et al. Properdin, a positive regulator of complement activation, is expressed in human T cell lines and peripheral blood T cells. *J Immunol*. 1993;151(5):2521-8.
78. Dahlback B, Stenflo J. High molecular weight complex in human plasma between vitamin K-dependent protein S and complement component C4b-binding protein. *Proc Natl Acad Sci U S A*. 1981;78(4):2512-6.
79. Kinoshita T, Nussenzweig V. Regulatory proteins for the activated third and fourth components of complement (C3b and C4b) in mice. I. Isolation and characterization of factor H: the serum cofactor for the C3b/C4b inactivator (factor I). *J Immunol Methods*. 1984;71(2):247-57.
80. Law SK, Fearon DT, Levine RP. Action of the C3b-inactivator on the cell-bound C3b. *J Immunol*. 1979;122(3):759-65.
81. Bhakdi S, Bhakdi-Lehnen B, Tranum-Jensen J. Proteolytic transformation of SC5b-9 into an amphiphilic macromolecule resembling the C5b-9 membrane attack complex of complement. *Immunology*. 1979;37(4):901-12.
82. Podack ER, Muller-Eberhard HJ. SC5b-9 complex of complement: formation of the dimeric membrane attack complex by removal of S-protein. *J Immunol*. 1980;124(4):1779-83.
83. C1 esterase inhibitor (human). *P T*. 2010;35(7 Section 2):2-3.
84. Kim DD, Song WC. Membrane complement regulatory proteins. *Clin Immunol*. 2006;118(2-3):127-36.
85. Kinoshita T, Takeda J, Hong K, Kozono H, Sakai H, Inoue K. Monoclonal antibodies to mouse complement receptor type 1 (CR1). Their use in a distribution study showing that mouse erythrocytes and platelets are CR1-negative. *J Immunol*. 1988;140(9):3066-72.
86. Edberg JC, Tomic L, Taylor RP. Immune adherence and the processing of soluble complement-fixing antibody/DNA immune complexes in mice. *Clin Immunol Immunopathol*. 1989;51(1):118-32.
87. Holers VM, Kinoshita T, Molina H. The evolution of mouse and human complement C3-binding proteins: divergence of form but conservation of function. *Immunol Today*. 1992;13(6):231-6.
88. Hillmen P, Young NS, Schubert J, Brodsky RA, Socie G, Muus P, et al. The complement inhibitor eculizumab in paroxysmal nocturnal hemoglobinuria. *N Engl J Med*. 2006;355(12):1233-43.
89. Rother RP, Rollins SA, Mojciak CF, Brodsky RA, Bell L. Discovery and development of the complement inhibitor eculizumab for the treatment of paroxysmal nocturnal hemoglobinuria. *Nat Biotechnol*. 2007;25(11):1256-64.
90. Hillmen P, Elebute M, Kelly R, Urbano-Ispizua A, Hill A, Rother RP, et al. Long-term effect of the complement inhibitor eculizumab on kidney function in patients with paroxysmal nocturnal hemoglobinuria. *Am J Hematol*. 2010;85(8):553-9.
91. Mevorach D. Paroxysmal nocturnal hemoglobinuria (PNH) and primary p.Cys89Tyr mutation in CD59: Differences and similarities. *Mol Immunol*. 2015;67(1):51-5.
92. Dunkelberger JR, Song WC. Complement and its role in innate and adaptive immune responses. *Cell Res*. 2010;20(1):34-50.

93. Pepys MB. Role of complement in induction of antibody production in vivo. Effect of cobra factor and other C3-reactive agents on thymus-dependent and thymus-independent antibody responses. *J Exp Med.* 1974;140(1):126-45.
94. Pepys MB. Role of complement in the induction of immunological responses. *Transplant Rev.* 1976;32:93-120.
95. Stevens B, Allen NJ, Vazquez LE, Howell GR, Christopherson KS, Nouri N, et al. The classical complement cascade mediates CNS synapse elimination. *Cell.* 2007;131(6):1164-78.
96. Rutkowski MJ, Sughrue ME, Kane AJ, Mills SA, Fang S, Parsa AT. Complement and the central nervous system: emerging roles in development, protection and regeneration. *Immunol Cell Biol.* 2010;88(8):781-6.
97. Cho H. Complement regulation: physiology and disease relevance. *Korean J Pediatr.* 2015;58(7):239-44.
98. Holers VM, Girardi G, Mo L, Guthridge JM, Molina H, Pierangeli SS, et al. Complement C3 activation is required for antiphospholipid antibody-induced fetal loss. *J Exp Med.* 2002;195(2):211-20.
99. Wright A, Douglas SR. An experimental investigation of the role of blood fluids in connection with phagocytosis. London: s.n.; 1903. p. 357 -70 p.
100. Bajic G, Degen SE, Thiel S, Andersen GR. Complement activation, regulation, and molecular basis for complement-related diseases. *EMBO J.* 2015;34(22):2735-57.
101. Krych M, Atkinson JP, Holers VM. Complement receptors. *Curr Opin Immunol.* 1992;4(1):8-13.
102. Rosales C. Molecular mechanisms of phagocytosis. Georgetown, Tex.

New York: Landes Bioscience/Eurekah.com ;

Springer Science+Business Media; 2005. 154 p. p.

103. Nauta AJ, Castellano G, Xu W, Woltman AM, Borrias MC, Daha MR, et al. Opsonization with C1q and mannose-binding lectin targets apoptotic cells to dendritic cells. *J Immunol.* 2004;173(5):3044-50.
104. Bobak DA, Gaither TA, Frank MM, Tenner AJ. Modulation of FcR function by complement: subcomponent C1q enhances the phagocytosis of IgG-opsonized targets by human monocytes and culture-derived macrophages. *J Immunol.* 1987;138(4):1150-6.
105. Bobak DA, Frank MM, Tenner AJ. C1q acts synergistically with phorbol dibutyrate to activate CR1-mediated phagocytosis by human mononuclear phagocytes. *Eur J Immunol.* 1988;18(12):2001-7.
106. Ghebrehiwet B, Peerschke EI. cC1q-R (calreticulin) and gC1q-R/p33: ubiquitously expressed multi-ligand binding cellular proteins involved in inflammation and infection. *Mol Immunol.* 2004;41(2-3):173-83.
107. Ricklin D, Lambris JD. Complement in immune and inflammatory disorders: pathophysiological mechanisms. *J Immunol.* 2013;190(8):3831-8.
108. Stegert M, Bock M, Trendelenburg M. Clinical presentation of human C1q deficiency: How much of a lupus? *Mol Immunol.* 2015;67(1):3-11.
109. van Schaarenburg RA, Schejbel L, Truedsson L, Topaloglu R, Al-Mayouf SM, Riordan A, et al. Marked variability in clinical presentation and outcome of patients with C1q immunodeficiency. *J Autoimmun.* 2015;62:39-44.
110. Handin RI, Lux SE, Stossel TP. *Blood : principles and practice of hematology.* 2nd ed. Philadelphia, Pa.: Lippincott Williams & Wilkins; 2003. xii, 2304 p. p.
111. Magendie Fo. *Phénomènes physiques de la vie : leçons professées au collège de France.* Paris: Chez J.-B. Baillière; 1842.
112. Humphrey JH, Dourmashkin RR. The lesions in cell membranes caused by complement. *Adv Immunol.* 1969;11:75-115.
113. Hesketh TR, Dourmashkin RR, Payne SN, Humphrey JH, Lachmann PJ. Lesions due to complement in lipid membranes. *Nature.* 1971;233(5322):620-3.

114. Rosado CJ, Kondos S, Bull TE, Kuiper MJ, Law RH, Buckle AM, et al. The MACPF/CDC family of pore-forming toxins. *Cell Microbiol.* 2008;10(9):1765-74.
115. August JT. *Biological response mediators and modulators.* New York: Academic Press; 1983. xix, 254 p. p.
116. Bhakdi S, Trandum-Jensen J. On the cause and nature of C9-related heterogeneity of terminal complement complexes generated on target erythrocytes through the action of whole serum. *J Immunol.* 1984;133(3):1453-63.
117. Bhakdi S, Trandum-Jensen J. Membrane damage by complement. *Biochim Biophys Acta.* 1983;737(3-4):343-72.
118. Trandum-Jensen J, Bhakdi S. Freeze-fracture analysis of the membrane lesion of human complement. *J Cell Biol.* 1983;97(3):618-26.
119. Bhakdi S, Trandum-Jensen J. Mechanism of complement cytolysis and the concept of channel-forming proteins. *Philos Trans R Soc Lond B Biol Sci.* 1984;306(1129):311-24.
120. Lewis LA, Ram S. Meningococcal disease and the complement system. *Virulence.* 2014;5(1):98-126.
121. Rautemaa R, Meri S. Complement-resistance mechanisms of bacteria. *Microbes Infect.* 1999;1(10):785-94.
122. Holers VM. The spectrum of complement alternative pathway-mediated diseases. *Immunol Rev.* 2008;223:300-16.
123. Litman GW, Rast JP, Fugmann SD. The origins of vertebrate adaptive immunity. *Nat Rev Immunol.* 2010;10(8):543-53.
124. Hirano M, Das S, Guo P, Cooper MD. The evolution of adaptive immunity in vertebrates. *Adv Immunol.* 2011;109:125-57.
125. Walport MJ. Complement. Second of two parts. *N Engl J Med.* 2001;344(15):1140-4.
126. Marchbank KJ, Watson CC, Ritsema DF, Holers VM. Expression of human complement receptor 2 (CR2, CD21) in Cr2^{-/-} mice restores humoral immune function. *J Immunol.* 2000;165(5):2354-61.
127. Fearon DT, Carter RH. The CD19/CR2/TAPA-1 complex of B lymphocytes: linking natural to acquired immunity. *Annu Rev Immunol.* 1995;13:127-49.
128. Karp CL, Wysocka M, Wahl LM, Ahearn JM, Cuomo PJ, Sherry B, et al. Mechanism of suppression of cell-mediated immunity by measles virus. *Science.* 1996;273(5272):228-31.
129. Astier AL. T-cell regulation by CD46 and its relevance in multiple sclerosis. *Immunology.* 2008;124(2):149-54.
130. Rutkowski MJ, Sughrue ME, Kane AJ, Mills SA, Parsa AT. Cancer and the complement cascade. *Mol Cancer Res.* 2010;8(11):1453-65.
131. Barbu A, Hamad OA, Lind L, Ekdahl KN, Nilsson B. The role of complement factor C3 in lipid metabolism. *Mol Immunol.* 2015;67(1):101-7.
132. Rooney IA, Oglesby TJ, Atkinson JP. Complement in human reproduction: activation and control. *Immunol Res.* 1993;12(3):276-94.
133. Miwa T, Nonaka M, Okada N, Wakana S, Shiroishi T, Okada H. Molecular cloning of rat and mouse membrane cofactor protein (MCP, CD46): preferential expression in testis and close linkage between the mouse Mcp and Cr2 genes on distal chromosome 1. *Immunogenetics.* 1998;48(6):363-71.
134. Qian YM, Qin X, Miwa T, Sun X, Halperin JA, Song WC. Identification and functional characterization of a new gene encoding the mouse terminal complement inhibitor CD59. *J Immunol.* 2000;165(5):2528-34.
135. Hong MH, Jin CH, Sato T, Ishimi Y, Abe E, Suda T. Transcriptional regulation of the production of the third component of complement (C3) by 1 alpha,25-dihydroxyvitamin D3 in mouse marrow-derived stromal cells (ST2) and primary osteoblastic cells. *Endocrinology.* 1991;129(5):2774-9.
136. Mestas J, Hughes CC. Of mice and not men: differences between mouse and human immunology. *J Immunol.* 2004;172(5):2731-8.

137. Cockburn IA, Mackinnon MJ, O'Donnell A, Allen SJ, Moulds JM, Baisor M, et al. A human complement receptor 1 polymorphism that reduces Plasmodium falciparum rosetting confers protection against severe malaria. *Proc Natl Acad Sci U S A*. 2004;101(1):272-7.
138. Moulds JM, Reveille JD, Arnett FC. Structural polymorphisms of complement receptor 1 (CR1) in systemic lupus erythematosus (SLE) patients and normal controls of three ethnic groups. *Clin Exp Immunol*. 1996;105(2):302-5.
139. Ong GL, Mattes MJ. Mouse strains with typical mammalian levels of complement activity. *J Immunol Methods*. 1989;125(1-2):147-58.
140. Meo T, Krasteff T, Shreffler DC. Immunochemical characterization of murine H-2 controlled Ss (serum substance) protein through identification of its human homologue as the fourth component of complement. *Proc Natl Acad Sci U S A*. 1975;72(11):4536-40.
141. Shreffler DC, David CS. Studies on recombination within the mouse H-2 complex. I. Three recombinants which position the Ss locus within the complex. *Tissue Antigens*. 1972;2(3):232-40.
142. Ebanks RO, Jaikaran AS, Carroll MC, Anderson MJ, Campbell RD, Isenman DE. A single arginine to tryptophan interchange at beta-chain residue 458 of human complement component C4 accounts for the defect in classical pathway C5 convertase activity of allotype C4A6. Implications for the location of a C5 binding site in C4. *J Immunol*. 1992;148(9):2803-11.
143. Ebanks RO, Isenman DE. Evidence for the involvement of arginine 462 and the flanking sequence of human C4 beta-chain in mediating C5 binding to the C4b subcomponent of the classical complement pathway C5 convertase. *J Immunol*. 1995;154(6):2808-20.
144. Ebanks RO, Isenman DE. Mouse complement component C4 is devoid of classical pathway C5 convertase subunit activity. *Mol Immunol*. 1996;33(3):297-309.
145. Kurtz CB, O'Toole E, Christensen SM, Weis JH. The murine complement receptor gene family. IV. Alternative splicing of Cr2 gene transcripts predicts two distinct gene products that share homologous domains with both human CR2 and CR1. *J Immunol*. 1990;144(9):3581-91.
146. Quigg RJ, Alexander JJ, Lo CF, Lim A, He C, Holers VM. Characterization of C3-binding proteins on mouse neutrophils and platelets. *J Immunol*. 1997;159(5):2438-44.
147. Wong WW, Fearon DT. p65: A C3b-binding protein on murine cells that shares antigenic determinants with the human C3b receptor (CR1) and is distinct from murine C3b receptor. *J Immunol*. 1985;134(6):4048-56.
148. Kingsmore SF, Vik DP, Kurtz CB, Leroy P, Tack BF, Weis JH, et al. Genetic organization of complement receptor-related genes in the mouse. *J Exp Med*. 1989;169(4):1479-84.
149. Paul MS, Aegerter M, O'Brien SE, Kurtz CB, Weis JH. The murine complement receptor gene family. Analysis of mCRY gene products and their homology to human CR1. *J Immunol*. 1989;142(2):582-9.
150. Dierich MP, Pellegrino MA, Ferrone S, Reisfeld RA. Evaluation of C3 receptors on lymphoid cells with different complement sources. *J Immunol*. 1974;112(5):1766-73.
151. Kinoshita T, Lavoie S, Nussenzweig V. Regulatory proteins for the activated third and fourth components of complement (C3b and C4b) in mice. II. Identification and properties of complement receptor type 1 (CR1). *J Immunol*. 1985;134(4):2564-70.
152. Aegerter-Shaw M, Cole JL, Klickstein LB, Wong WW, Fearon DT, Lalley PA, et al. Expansion of the complement receptor gene family. Identification in the mouse of two new genes related to the CR1 and CR2 gene family. *J Immunol*. 1987;138(10):3488-94.
153. Kurtz CB, Paul MS, Aegerter M, Weis JJ, Weis JH. Murine complement receptor gene family. II. Identification and characterization of the murine homolog (Cr2) to human CR2 and its molecular linkage to Crry. *J Immunol*. 1989;143(6):2058-67.
154. Paul MS, Aegerter M, Cepek K, Miller MD, Weis JH. The murine complement receptor gene family. III. The genomic and transcriptional complexity of the Crry and Crry-ps genes. *J Immunol*. 1990;144(5):1988-96.
155. Kim YU, Kinoshita T, Molina H, Hourcade D, Seya T, Wagner LM, et al. Mouse complement regulatory protein Crry/p65 uses the specific mechanisms of both human decay-accelerating factor and membrane cofactor protein. *J Exp Med*. 1995;181(1):151-9.

156. Molina H, Wong W, Kinoshita T, Brenner C, Foley S, Holers VM. Distinct receptor and regulatory properties of recombinant mouse complement receptor 1 (CR1) and Crry, the two genetic homologues of human CR1. *J Exp Med*. 1992;175(1):121-9.
157. Foley S, Li B, Dehoff M, Molina H, Holers VM. Mouse Crry/p65 is a regulator of the alternative pathway of complement activation. *Eur J Immunol*. 1993;23(6):1381-4.
158. Tsujimura A, Shida K, Kitamura M, Nomura M, Takeda J, Tanaka H, et al. Molecular cloning of a murine homologue of membrane cofactor protein (CD46): preferential expression in testicular germ cells. *Biochem J*. 1998;330 (Pt 1):163-8.
159. Jacobson AC, Weis JH. Comparative functional evolution of human and mouse CR1 and CR2. *J Immunol*. 2008;181(5):2953-9.
160. Schifferli JA, Ng YC, Peters DK. The role of complement and its receptor in the elimination of immune complexes. *N Engl J Med*. 1986;315(8):488-95.
161. Fearon DT. Identification of the membrane glycoprotein that is the C3b receptor of the human erythrocyte, polymorphonuclear leukocyte, B lymphocyte, and monocyte. *J Exp Med*. 1980;152(1):20-30.
162. Reinagel ML, Taylor RP. Transfer of immune complexes from erythrocyte CR1 to mouse macrophages. *J Immunol*. 2000;164(4):1977-85.
163. Molina H, Miwa T, Zhou L, Hilliard B, Mastellos D, Maldonado MA, et al. Complement-mediated clearance of erythrocytes: mechanism and delineation of the regulatory roles of Crry and DAF. Decay-accelerating factor. *Blood*. 2002;100(13):4544-9.
164. Miwa T, Zhou L, Hilliard B, Molina H, Song WC. Crry, but not CD59 and DAF, is indispensable for murine erythrocyte protection in vivo from spontaneous complement attack. *Blood*. 2002;99(10):3707-16.
165. Kameyoshi Y, Matsushita M, Okada H. Murine membrane inhibitor of complement which accelerates decay of human C3 convertase. *Immunology*. 1989;68(4):439-44.
166. Spicer AP, Seldin MF, Gendler SJ. Molecular cloning and chromosomal localization of the mouse decay-accelerating factor genes. Duplicated genes encode glycosylphosphatidylinositol-anchored and transmembrane forms. *J Immunol*. 1995;155(6):3079-91.
167. Hourcade D, Holers VM, Atkinson JP. The regulators of complement activation (RCA) gene cluster. *Adv Immunol*. 1989;45:381-416.
168. Powell MB, Marchbank KJ, Rushmere NK, van den Berg CW, Morgan BP. Molecular cloning, chromosomal localization, expression, and functional characterization of the mouse analogue of human CD59. *J Immunol*. 1997;158(4):1692-702.
169. Xu C, Mao D, Holers VM, Palanca B, Cheng AM, Molina H. A critical role for murine complement regulator crry in fetomaternal tolerance. *Science*. 2000;287(5452):498-501.
170. Wu X, Spitzer D, Mao D, Peng SL, Molina H, Atkinson JP. Membrane protein Crry maintains homeostasis of the complement system. *J Immunol*. 2008;181(4):2732-40.
171. Ruseva MM, Hughes TR, Donev RM, Sivasankar B, Pickering MC, Wu X, et al. Crry deficiency in complement sufficient mice: C3 consumption occurs without associated renal injury. *Mol Immunol*. 2009;46(5):803-11.
172. Blanchong CA, Chung EK, Rupert KL, Yang Y, Yang Z, Zhou B, et al. Genetic, structural and functional diversities of human complement components C4A and C4B and their mouse homologues, Slp and C4. *Int Immunopharmacol*. 2001;1(3):365-92.
173. Kettenmann H, Hanisch UK, Noda M, Verkhratsky A. Physiology of microglia. *Physiol Rev*. 2011;91(2):461-553.
174. Prinz M, Priller J. Microglia and brain macrophages in the molecular age: from origin to neuropsychiatric disease. *Nat Rev Neurosci*. 2014;15(5):300-12.
175. Prinz M, Tay TL, Wolf Y, Jung S. Microglia: unique and common features with other tissue macrophages. *Acta Neuropathol*. 2014;128(3):319-31.
176. Prinz M, Mildner A. Microglia in the CNS: immigrants from another world. *Glia*. 2011;59(2):177-87.
177. Tremblay ME, Stevens B, Sierra A, Wake H, Bessis A, Nimmerjahn A. The role of microglia in the healthy brain. *J Neurosci*. 2011;31(45):16064-9.

178. Tremblay M-Ev, Sierra A. *Microglia in health and disease*. New York: Springer; 2014. xiv, 486 pages p.
179. Wake H, Moorhouse AJ, Jinno S, Kohsaka S, Nabekura J. Resting microglia directly monitor the functional state of synapses in vivo and determine the fate of ischemic terminals. *J Neurosci*. 2009;29(13):3974-80.
180. Nimmerjahn A, Kirchhoff F, Helmchen F. Resting microglial cells are highly dynamic surveillants of brain parenchyma in vivo. *Science*. 2005;308(5726):1314-8.
181. Davalos D, Grutzendler J, Yang G, Kim JV, Zuo Y, Jung S, et al. ATP mediates rapid microglial response to local brain injury in vivo. *Nat Neurosci*. 2005;8(6):752-8.
182. Chiu IM, Morimoto ET, Goodarzi H, Liao JT, O'Keefe S, Phatnani HP, et al. A neurodegeneration-specific gene-expression signature of acutely isolated microglia from an amyotrophic lateral sclerosis mouse model. *Cell Rep*. 2013;4(2):385-401.
183. Butovsky O, Jedrychowski MP, Moore CS, Cialic R, Lanser AJ, Gabriely G, et al. Identification of a unique TGF-beta-dependent molecular and functional signature in microglia. *Nat Neurosci*. 2014;17(1):131-43.
184. Jordan CA, Watkins BA, Kufta C, Dubois-Dalcq M. Infection of brain microglial cells by human immunodeficiency virus type 1 is CD4 dependent. *J Virol*. 1991;65(2):736-42.
185. Kanmogne GD, Kennedy RC, Grammas P. Infection of baboon microglia with SIV-HIV recombinant viruses: role of CD4 and chemokine receptors. *AIDS Res Hum Retroviruses*. 2002;18(8):557-65.
186. Wake H, Fields RD. Physiological function of microglia. *Neuron Glia Biol*. 2011;7(1):1-3.
187. Wake H, Moorhouse AJ, Nabekura J. Functions of microglia in the central nervous system-beyond the immune response. *Neuron Glia Biol*. 2011;7(1):47-53.
188. Del Rio-Hortega P. Art and artifice in histologic science. *Tex Rep Biol Med*. 1949;7(3):363-90.
189. Blinzinger K, Kreutzberg G. Displacement of synaptic terminals from regenerating motoneurons by microglial cells. *Z Zellforsch Mikrosk Anat*. 1968;85(2):145-57.
190. Giulian D, Baker TJ. Characterization of ameboid microglia isolated from developing mammalian brain. *J Neurosci*. 1986;6(8):2163-78.
191. Fischer HG, Reichmann G. Brain dendritic cells and macrophages/microglia in central nervous system inflammation. *J Immunol*. 2001;166(4):2717-26.
192. Stansley B, Post J, Hensley K. A comparative review of cell culture systems for the study of microglial biology in Alzheimer's disease. *J Neuroinflammation*. 2012;9:115.
193. Schilling T, Eder C. Ion channel expression in resting and activated microglia of hippocampal slices from juvenile mice. *Brain Res*. 2007;1186:21-8.
194. Boucsein C, Kettenmann H, Nolte C. Electrophysiological properties of microglial cells in normal and pathologic rat brain slices. *Eur J Neurosci*. 2000;12(6):2049-58.
195. Schipke CG, Boucsein C, Ohlemeyer C, Kirchhoff F, Kettenmann H. Astrocyte Ca²⁺ waves trigger responses in microglial cells in brain slices. *FASEB J*. 2002;16(2):255-7.
196. Boucsein C, Zacharias R, Farber K, Pavlovic S, Hanisch UK, Kettenmann H. Purinergic receptors on microglial cells: functional expression in acute brain slices and modulation of microglial activation in vitro. *Eur J Neurosci*. 2003;17(11):2267-76.
197. Jung S, Aliberti J, Graemmel P, Sunshine MJ, Kreutzberg GW, Sher A, et al. Analysis of fractalkine receptor CX(3)CR1 function by targeted deletion and green fluorescent protein reporter gene insertion. *Mol Cell Biol*. 2000;20(11):4106-14.
198. Hirasawa T, Ohsawa K, Imai Y, Ondo Y, Akazawa C, Uchino S, et al. Visualization of microglia in living tissues using Iba1-EGFP transgenic mice. *J Neurosci Res*. 2005;81(3):357-62.
199. Kreutzberg GW. Microglia: a sensor for pathological events in the CNS. *Trends Neurosci*. 1996;19(8):312-8.
200. Sierra A, Tremblay ME, Wake H. Never-resting microglia: physiological roles in the healthy brain and pathological implications. *Front Cell Neurosci*. 2014;8:240.
201. Barnum SR. Complement biosynthesis in the central nervous system. *Crit Rev Oral Biol Med*. 1995;6(2):132-46.

202. Stahel PF, Barnum SR. Bacterial meningitis: complement gene expression in the central nervous system. *Immunopharmacology*. 1997;38(1-2):65-72.
203. Gasque P, Fontaine M, Morgan BP. Complement expression in human brain. Biosynthesis of terminal pathway components and regulators in human glial cells and cell lines. *J Immunol*. 1995;154(9):4726-33.
204. Morgan BP, Gasque P, Singhrao SK, Piddlesden SJ. Role of complement in inflammation and injury in the nervous system. *Exp Clin Immunogenet*. 1997;14(1):19-23.
205. Thomas A, Gasque P, Vaudry D, Gonzalez B, Fontaine M. Expression of a complete and functional complement system by human neuronal cells in vitro. *Int Immunol*. 2000;12(7):1015-23.
206. Veerhuis R, Nielsen HM, Tenner AJ. Complement in the brain. *Mol Immunol*. 2011;48(14):1592-603.
207. Brennan FH, Anderson AJ, Taylor SM, Woodruff TM, Ruitenbergh MJ. Complement activation in the injured central nervous system: another dual-edged sword? *J Neuroinflammation*. 2012;9:137.
208. Kulkarni AP, Kellaway LA, Kotwal GJ. Herbal complement inhibitors in the treatment of neuroinflammation: future strategy for neuroprotection. *Ann N Y Acad Sci*. 2005;1056:413-29.
209. Persson M, Pekna M, Hansson E, Ronnback L. The complement-derived anaphylatoxin C5a increases microglial GLT-1 expression and glutamate uptake in a TNF-alpha-independent manner. *Eur J Neurosci*. 2009;29(2):267-74.
210. Heese K, Hock C, Otten U. Inflammatory signals induce neurotrophin expression in human microglial cells. *J Neurochem*. 1998;70(2):699-707.
211. Brouns R, Wauters A, De Surgeloose D, Marien P, De Deyn PP. Biochemical markers for blood-brain barrier dysfunction in acute ischemic stroke correlate with evolution and outcome. *Eur Neurol*. 2011;65(1):23-31.
212. Chodobski A, Zink BJ, Szmydynger-Chodobska J. Blood-brain barrier pathophysiology in traumatic brain injury. *Transl Stroke Res*. 2011;2(4):492-516.
213. Sierra A, Beccari S, Diaz-Aparicio I, Encinas JM, Comeau S, Tremblay ME. Surveillance, phagocytosis, and inflammation: how never-resting microglia influence adult hippocampal neurogenesis. *Neural Plast*. 2014;2014:610343.
214. Perry VH, Nicoll JA, Holmes C. Microglia in neurodegenerative disease. *Nat Rev Neurol*. 2010;6(4):193-201.
215. Hoek RM, Ruuls SR, Murphy CA, Wright GJ, Goddard R, Zurawski SM, et al. Down-regulation of the macrophage lineage through interaction with OX2 (CD200). *Science*. 2000;290(5497):1768-71.
216. Henry CJ, Huang Y, Wynne AM, Godbout JP. Peripheral lipopolysaccharide (LPS) challenge promotes microglial hyperactivity in aged mice that is associated with exaggerated induction of both pro-inflammatory IL-1beta and anti-inflammatory IL-10 cytokines. *Brain Behav Immun*. 2009;23(3):309-17.
217. Combrinck MI, Perry VH, Cunningham C. Peripheral infection evokes exaggerated sickness behaviour in pre-clinical murine prion disease. *Neuroscience*. 2002;112(1):7-11.
218. Dilger RN, Johnson RW. Aging, microglial cell priming, and the discordant central inflammatory response to signals from the peripheral immune system. *J Leukoc Biol*. 2008;84(4):932-9.
219. Frank MG, Thompson BM, Watkins LR, Maier SF. Glucocorticoids mediate stress-induced priming of microglial pro-inflammatory responses. *Brain Behav Immun*. 2012;26(2):337-45.
220. Murray C, Sanderson DJ, Barkus C, Deacon RM, Rawlins JN, Bannerman DM, et al. Systemic inflammation induces acute working memory deficits in the primed brain: relevance for delirium. *Neurobiol Aging*. 2012;33(3):603-16 e3.
221. Cunningham C, Wilcockson DC, Champion S, Lunnon K, Perry VH. Central and systemic endotoxin challenges exacerbate the local inflammatory response and increase neuronal death during chronic neurodegeneration. *J Neurosci*. 2005;25(40):9275-84.

222. Zabel MK, Kirsch WM. From development to dysfunction: microglia and the complement cascade in CNS homeostasis. *Ageing Res Rev.* 2013;12(3):749-56.
223. Perry VH, Holmes C. Microglial priming in neurodegenerative disease. *Nat Rev Neurol.* 2014;10(4):217-24.
224. Brookmeyer R, Johnson E, Ziegler-Graham K, Arrighi HM. Forecasting the global burden of Alzheimer's disease. *Alzheimers Dement.* 2007;3(3):186-91.
225. Peila R, Launer LJ. Inflammation and dementia: epidemiologic evidence. *Acta Neurol Scand Suppl.* 2006;185:102-6.
226. Wyss-Coray T, Rogers J. Inflammation in Alzheimer disease—a brief review of the basic science and clinical literature. *Cold Spring Harb Perspect Med.* 2012;2(1):a006346.
227. Montero-Menei CN, Sindji L, Garcion E, Mege M, Couez D, Gamelin E, et al. Early events of the inflammatory reaction induced in rat brain by lipopolysaccharide intracerebral injection: relative contribution of peripheral monocytes and activated microglia. *Brain Res.* 1996;724(1):55-66.
228. Holmes C, Cunningham C, Zotova E, Woolford J, Dean C, Kerr S, et al. Systemic inflammation and disease progression in Alzheimer disease. *Neurology.* 2009;73(10):768-74.
229. Holmes C, El-Okli M, Williams AL, Cunningham C, Wilcockson D, Perry VH. Systemic infection, interleukin 1 β , and cognitive decline in Alzheimer's disease. *J Neurol Neurosurg Psychiatry.* 2003;74(6):788-9.
230. Hannestad J, Gallezot JD, Schafbauer T, Lim K, Kloczynski T, Morris ED, et al. Endotoxin-induced systemic inflammation activates microglia: [(1)(1)C]PBR28 positron emission tomography in nonhuman primates. *Neuroimage.* 2012;63(1):232-9.
231. Blasi E, Barluzzi R, Bocchini V, Mazzolla R, Bistoni F. Immortalization of murine microglial cells by a v-raf/v-myc carrying retrovirus. *J Neuroimmunol.* 1990;27(2-3):229-37.
232. Yip PK, Kaan TK, Fenesan D, Malcangio M. Rapid isolation and culture of primary microglia from adult mouse spinal cord. *J Neurosci Methods.* 2009;183(2):223-37.
233. Leon MA. Quantitative studies of the properdin-complement system. III. Kinetics of the reaction between C'3 and the properdin-zymosan complex. *J Immunol.* 1958;81(1):23-8.
234. Xia Y, Vetvicka V, Yan J, Hanikyrova M, Mayadas T, Ross GD. The beta-glucan-binding lectin site of mouse CR3 (CD11b/CD18) and its function in generating a primed state of the receptor that mediates cytotoxic activation in response to iC3b-opsonized target cells. *J Immunol.* 1999;162(4):2281-90.
235. Holtman IR, Raj DD, Miller JA, Schaafsma W, Yin Z, Brouwer N, et al. Induction of a common microglia gene expression signature by aging and neurodegenerative conditions: a co-expression meta-analysis. *Acta Neuropathol Commun.* 2015;3:31.
236. Norden DM, Muccigrosso MM, Godbout JP. Microglial priming and enhanced reactivity to secondary insult in aging, and traumatic CNS injury, and neurodegenerative disease. *Neuropharmacology.* 2015;96(Pt A):29-41.
237. Moussaud S, Draheim HJ. A new method to isolate microglia from adult mice and culture them for an extended period of time. *J Neurosci Methods.* 2010;187(2):243-53.
238. Ponomarev ED, Novikova M, Maresz K, Shriver LP, Dittel BN. Development of a culture system that supports adult microglial cell proliferation and maintenance in the resting state. *J Immunol Methods.* 2005;300(1-2):32-46.
239. Nikodemova M, Watters JJ. Efficient isolation of live microglia with preserved phenotypes from adult mouse brain. *J Neuroinflammation.* 2012;9:147.
240. Henn A, Lund S, Hedtjarn M, Schratzenholz A, Porzgen P, Leist M. The suitability of BV2 cells as alternative model system for primary microglia cultures or for animal experiments examining brain inflammation. *ALTEX.* 2009;26(2):83-94.
241. Bocchini V, Mazzolla R, Barluzzi R, Blasi E, Sick P, Kettenmann H. An immortalized cell line expresses properties of activated microglial cells. *J Neurosci Res.* 1992;31(4):616-21.
242. Cardona AE, Pioro EP, Sasse ME, Kostenko V, Cardona SM, Dijkstra IM, et al. Control of microglial neurotoxicity by the fractalkine receptor. *Nat Neurosci.* 2006;9(7):917-24.

243. Frank MG, Wieseler-Frank JL, Watkins LR, Maier SF. Rapid isolation of highly enriched and quiescent microglia from adult rat hippocampus: immunophenotypic and functional characteristics. *J Neurosci Methods*. 2006;151(2):121-30.
244. de Haas AH, Boddeke HW, Brouwer N, Biber K. Optimized isolation enables ex vivo analysis of microglia from various central nervous system regions. *Glia*. 2007;55(13):1374-84.
245. Elmore MR, Najafi AR, Koike MA, Dagher NN, Spangenberg EE, Rice RA, et al. Colony-stimulating factor 1 receptor signaling is necessary for microglia viability, unmasking a microglia progenitor cell in the adult brain. *Neuron*. 2014;82(2):380-97.
246. Biber K, Neumann H, Inoue K, Boddeke HW. Neuronal 'On' and 'Off' signals control microglia. *Trends Neurosci*. 2007;30(11):596-602.
247. de Haas AH, van Weering HR, de Jong EK, Boddeke HW, Biber KP. Neuronal chemokines: versatile messengers in central nervous system cell interaction. *Mol Neurobiol*. 2007;36(2):137-51.
248. Pocock JM, Kettenmann H. Neurotransmitter receptors on microglia. *Trends Neurosci*. 2007;30(10):527-35.
249. Neiva I, Malva JO, Valero J. Can we talk about microglia without neurons? A discussion of microglial cell autonomous properties in culture. *Front Cell Neurosci*. 2014;8:202.
250. Wes PD, Holtman IR, Boddeke EW, Moller T, Eggen BJ. Next generation transcriptomics and genomics elucidate biological complexity of microglia in health and disease. *Glia*. 2016;64(2):197-213.
251. Tam WY, Ma CH. Bipolar/rod-shaped microglia are proliferating microglia with distinct M1/M2 phenotypes. *Sci Rep*. 2014;4:7279.
252. Taylor SE, Morganti-Kossmann C, Lifshitz J, Ziebell JM. Rod microglia: a morphological definition. *PLoS One*. 2014;9(5):e97096.
253. Brown GC, Neher JJ. Microglial phagocytosis of live neurons. *Nat Rev Neurosci*. 2014;15(4):209-16.
254. Neniskyte U, Vilalta A, Brown GC. Tumour necrosis factor alpha-induced neuronal loss is mediated by microglial phagocytosis. *FEBS Lett*. 2014;588(17):2952-6.
255. Burry RW. *Immunocytochemistry : a practical guide for biomedical research*. New York: Springer; 2010. xv, 223 p. p.
256. Sobti RC, Krishan A. *Advanced flow cytometry : applications in biological research*. Dordrecht ; Boston: Kluwer Academic Publishers; 2003. 114 p. p.
257. Squire LR. *Fundamental neuroscience*. 3rd ed. Amsterdam ; Boston: Elsevier / Academic Press; 2008. xx, 1256 p. p.
258. Horvath RJ, Nutile-McMenemy N, Alkaitis MS, Deleo JA. Differential migration, LPS-induced cytokine, chemokine, and NO expression in immortalized BV-2 and HAPI cell lines and primary microglial cultures. *J Neurochem*. 2008;107(2):557-69.
259. Paul WE. *Fundamental immunology*. 6th ed. Philadelphia: Wolters Kluwer/Lippincott Williams & Wilkins; 2008. xviii, 1603 p., 16 p. of plates p.
260. Kahn RL. The Wassermann Test in the Public Health Laboratory. *Am J Public Health (N Y)*. 1921;11(5):410-5.
261. Pillemer L, Seifter S, Chu F, Ecker EE. Function of Components of Complement in Immune Hemolysis. *J Exp Med*. 1942;76(1):93-101.
262. Mayer MM, Croft CC, Gray MM. Kinetic studies on immune hemolysis; a method. *J Exp Med*. 1948;88(4):427-44.
263. Bowman WM, Mayer MM, Rapp HJ. Kinetic studies on immune hemolysis. II. The reversibility of red cell-antibody combination and the resultant transfer of antibody from cell to cell during hemolysis. *J Exp Med*. 1951;94(2):87-110.
264. Levine L, Mayer MM. Kinetic studies on immune hemolysis. V. Formation of the complex EAC'x and its reaction with C'y. *J Immunol*. 1954;73(6):426-34.
265. Levine L, Mayer MM, Rapp HJ. Kinetic studies on immune hemolysis. VI. Resolution of the C'y reaction step into two successive processes involving C'2 and C'3. *J Immunol*. 1954;73(6):435-42.

266. Mayer MM, Levine L. Kinetic studies on immune hemolysis. IV. Rate determination of the Mg⁺⁺ and terminal reaction steps. *J Immunol.* 1954;72(6):516-30.
267. Mayer MM, Levine L. Kinetic studies on immune hemolysis. III. Description of a terminal process which follows the Ca⁺⁺ and Mg⁺⁺ reaction steps in the action of complement on sensitized erythrocytes. *J Immunol.* 1954;72(6):511-5.
268. Mayer MM, Levine L, Rapp HJ, Marucci AA. Kinetic studies on immune hemolysis. VII. Decay of EAC'1, 4, 2, fixation of C'3, and other factors influencing the hemolytic action of complement. *J Immunol.* 1954;73(6):443-54.
269. Nelson RA, Jr. The immune-adherence phenomenon; an immunologically specific reaction between microorganisms and erythrocytes leading to enhanced phagocytosis. *Science.* 1953;118(3077):733-7.
270. Nelson RA, Jr. The immune-adherence phenomenon; a hypothetical role of erythrocytes in defence against bacteria and viruses. *Proc R Soc Med.* 1956;49(1):55-8.
271. Nishioka K, Linscott WD. Components of Guinea Pig Complement. I. Separation of a Serum Fraction Essential for Immune Hemolysis and Immune Adherence. *J Exp Med.* 1963;118:767-93.
272. Nelson RA, Jr., Jensen J, Gigli I, Tamura N. Methods for the separation, purification and measurement of nine components of hemolytic complement in guinea-pig serum. *Immunochemistry.* 1966;3(2):111-35.
273. Gigli I, Nelson RA, Jr. Complement dependent immune phagocytosis. I. Requirements for C'1, C'4, C'2, C'3. *Exp Cell Res.* 1968;51(1):45-67.
274. Lay WH, Nussenzweig V. Receptors for complement of leukocytes. *J Exp Med.* 1968;128(5):991-1009.
275. Muller-Eberhard HJ, Nilsson U. RELATION OF A beta(1)-GLYCOPROTEIN OF HUMAN SERUM TO THE COMPLEMENT SYSTEM. *J Exp Med.* 1960;111(2):217-34.
276. Lachmann PJ, Muller-Eberhard HJ. The demonstration in human serum of "conglutinin-activating factor" and its effect on the third component of complement. *J Immunol.* 1968;100(4):691-8.
277. West C, Davis NC, Forristal J, Herbst J, Spitzer R. Antigenic determinants of human beta-1c and beta-1g-globulins. *J Immunol.* 1966;96(4):650-8.
278. Spitzer RE, Stitzel AE, Pauling VL, Davis NC, West CD. The antigenic and molecular alterations of C3 in the fluid phase during an immune reaction in normal human serum. Demonstration of a new conversion product, C3x. *J Exp Med.* 1971;134(3 Pt 1):656-80.
279. Holers VM. Complement receptors. *Year Immunol.* 1989;4:231-40.
280. Pangburn MK, Schreiber RD, Muller-Eberhard HJ. Human complement C3b inactivator: isolation, characterization, and demonstration of an absolute requirement for the serum protein beta1H for cleavage of C3b and C4b in solution. *J Exp Med.* 1977;146(1):257-70.
281. Ross GD, Polley MJ, Rabellino EM, Grey HM. Two different complement receptors on human lymphocytes. One specific for C3b and one specific for C3b inactivator-cleaved C3b. *J Exp Med.* 1973;138(4):798-811.
282. Gitlin JD, Rosen FS, Lachmann PJ. The mechanism of action of the C3b inactivator (conglutinin-activating factor) on its naturally occurring substrate, the major fragment of the third component of complement (C3b). *J Exp Med.* 1975;141(5):1221-6.
283. Ross GD, Lambris JD. Identification of a C3bi-specific membrane complement receptor that is expressed on lymphocytes, monocytes, neutrophils, and erythrocytes. *J Exp Med.* 1982;155(1):96-110.
284. Beller DI, Springer TA, Schreiber RD. Anti-Mac-1 selectively inhibits the mouse and human type three complement receptor. *J Exp Med.* 1982;156(4):1000-9.
285. Springer T, Galfre G, Secher DS, Milstein C. Mac-1: a macrophage differentiation antigen identified by monoclonal antibody. *Eur J Immunol.* 1979;9(4):301-6.
286. Ault KA, Springer TA. Cross-reaction of a rat-anti-mouse phagocyte-specific monoclonal antibody (anti-Mac-1) with human monocytes and natural killer cells. *J Immunol.* 1981;126(1):359-64.

287. Sanchez-Madrid F, Nagy JA, Robbins E, Simon P, Springer TA. A human leukocyte differentiation antigen family with distinct alpha-subunits and a common beta-subunit: the lymphocyte function-associated antigen (LFA-1), the C3bi complement receptor (OKM1/Mac-1), and the p150,95 molecule. *J Exp Med*. 1983;158(6):1785-803.
288. Wilson ME, Pearson RD. Roles of CR3 and mannose receptors in the attachment and ingestion of *Leishmania donovani* by human mononuclear phagocytes. *Infect Immun*. 1988;56(2):363-9.
289. Springer TA, Davignon D, Ho MK, Kurzinger K, Martz E, Sanchez-Madrid F. LFA-1 and Lys-2,3, molecules associated with T lymphocyte-mediated killing; and Mac-1, an LFA-1 homologue associated with complement receptor function. *Immunol Rev*. 1982;68:171-95.
290. Kurzinger K, Springer TA. Purification and structural characterization of LFA-1, a lymphocyte function-associated antigen, and Mac-1, a related macrophage differentiation antigen associated with the type three complement receptor. *J Biol Chem*. 1982;257(20):12412-8.
291. Sanchez-Madrid F, Simon P, Thompson S, Springer TA. Mapping of antigenic and functional epitopes on the alpha- and beta-subunits of two related mouse glycoproteins involved in cell interactions, LFA-1 and Mac-1. *J Exp Med*. 1983;158(2):586-602.
292. Frade R, Myones BL, Barel M, Krikorian L, Charriaut C, Ross GD. gp140, a C3b-binding membrane component of lymphocytes, is the B cell C3dg/C3d receptor (CR2) and is distinct from the neutrophil C3dg receptor (CR4). *Eur J Immunol*. 1985;15(12):1192-7.
293. Myones BL, Dalzell JG, Hogg N, Ross GD. Neutrophil and monocyte cell surface p150,95 has iC3b-receptor (CR4) activity resembling CR3. *J Clin Invest*. 1988;82(2):640-51.
294. Kishimoto TK, Hollander N, Roberts TM, Anderson DC, Springer TA. Heterogeneous mutations in the beta subunit common to the LFA-1, Mac-1, and p150,95 glycoproteins cause leukocyte adhesion deficiency. *Cell*. 1987;50(2):193-202.
295. Harlan JM. Leukocyte adhesion deficiency syndrome: insights into the molecular basis of leukocyte emigration. *Clin Immunol Immunopathol*. 1993;67(3 Pt 2):S16-24.
296. Granger DN, Schmid-Schönbein GW. Physiology and pathophysiology of leukocyte adhesion. New York: Oxford University Press; 1995. xvi, 501 p. p.
297. Gahmberg CG, Tolvanen M, Kotovuori P. Leukocyte adhesion--structure and function of human leukocyte beta2-integrins and their cellular ligands. *Eur J Biochem*. 1997;245(2):215-32.
298. Marlin SD, Morton CC, Anderson DC, Springer TA. LFA-1 immunodeficiency disease. Definition of the genetic defect and chromosomal mapping of alpha and beta subunits of the lymphocyte function-associated antigen 1 (LFA-1) by complementation in hybrid cells. *J Exp Med*. 1986;164(3):855-67.
299. Law SK, Gagnon J, Hildreth JE, Wells CE, Willis AC, Wong AJ. The primary structure of the beta-subunit of the cell surface adhesion glycoproteins LFA-1, CR3 and p150,95 and its relationship to the fibronectin receptor. *EMBO J*. 1987;6(4):915-9.
300. Corbi AL, Larson RS, Kishimoto TK, Springer TA, Morton CC. Chromosomal location of the genes encoding the leukocyte adhesion receptors LFA-1, Mac-1 and p150,95. Identification of a gene cluster involved in cell adhesion. *J Exp Med*. 1988;167(5):1597-607.
301. Bernard A, Institut national de la santé et de la recherche médicale (France), World Health Organization., IUIS. Leucocyte typing : human leucocyte differentiation antigens detected by monoclonal antibodies : specification, classification, nomenclature = Typage leucocytaire : antigènes de différenciation leucocytaire humains révélés par les anticorps monoclonaux. Berlin ; New York: Springer-Verlag; 1984. xxiv, 814 p. p.
302. McMichael AJ. Leucocyte typing III : white cell differentiation antigens. Oxford ; New York: Oxford University Press; 1987. xxxiv, 1050 p. p.
303. Tamkun JW, DeSimone DW, Fonda D, Patel RS, Buck C, Horwitz AF, et al. Structure of integrin, a glycoprotein involved in the transmembrane linkage between fibronectin and actin. *Cell*. 1986;46(2):271-82.
304. Fitzgerald LA, Steiner B, Rall SC, Jr., Lo SS, Phillips DR. Protein sequence of endothelial glycoprotein IIIa derived from a cDNA clone. Identity with platelet glycoprotein IIIa and similarity to "integrin". *J Biol Chem*. 1987;262(9):3936-9.

305. DeSimone DW, Stepp MA, Patel RS, Hynes RO. The integrin family of cell surface receptors. *Biochem Soc Trans.* 1987;15(5):789-91.
306. Schwartz M. Sticking to it: tracking the paths of integrin signalling. *Nat Cell Biol.* 2014;16(6):487.
307. Wrighton KH. Cell adhesion: the 'ins' and 'outs' of integrin signalling. *Nat Rev Mol Cell Biol.* 2013;14(12):752.
308. Danen EHJ. Integrins and development. Georgetown, Tex.: Landes Bioscience/Eurekah.com; 2006. 221 p. p.
309. Hogg N, Patzak I, Willenbrock F. The insider's guide to leukocyte integrin signalling and function. *Nat Rev Immunol.* 2011;11(6):416-26.
310. Yakubenko VP, Lishko VK, Lam SC, Ugarova TP. A molecular basis for integrin alphaMbeta 2 ligand binding promiscuity. *J Biol Chem.* 2002;277(50):48635-42.
311. Mobberley-Schuman PS, Weiss AA. Influence of CR3 (CD11b/CD18) expression on phagocytosis of *Bordetella pertussis* by human neutrophils. *Infect Immun.* 2005;73(11):7317-23.
312. Lambris JD. Current topics in complement. New York: Springer; 2006. xxii, 406 p. p.
313. Todd RF, 3rd. The continuing saga of complement receptor type 3 (CR3). *J Clin Invest.* 1996;98(1):1-2.
314. Wright SD, Levin SM, Jong MT, Chad Z, Kabbash LG. CR3 (CD11b/CD18) expresses one binding site for Arg-Gly-Asp-containing peptides and a second site for bacterial lipopolysaccharide. *J Exp Med.* 1989;169(1):175-83.
315. Abtahian F, Bezman N, Clemens R, Sebzda E, Cheng L, Shattil SJ, et al. Evidence for the requirement of ITAM domains but not SLP-76/Gads interaction for integrin signaling in hematopoietic cells. *Mol Cell Biol.* 2006;26(18):6936-49.
316. Mocsai A, Abram CL, Jakus Z, Hu Y, Lanier LL, Lowell CA. Integrin signaling in neutrophils and macrophages uses adaptors containing immunoreceptor tyrosine-based activation motifs. *Nat Immunol.* 2006;7(12):1326-33.
317. Caron E, Hall A. Identification of two distinct mechanisms of phagocytosis controlled by different Rho GTPases. *Science.* 1998;282(5394):1717-21.
318. Le Cabec V, Carreno S, Moisand A, Bordier C, Maridonneau-Parini I. Complement receptor 3 (CD11b/CD18) mediates type I and type II phagocytosis during nonopsonic and opsonic phagocytosis, respectively. *J Immunol.* 2002;169(4):2003-9.
319. Bustelo XR. Regulatory and signaling properties of the Vav family. *Mol Cell Biol.* 2000;20(5):1461-77.
320. Hall AB, Gakidis MA, Glogauer M, Wilsbacher JL, Gao S, Swat W, et al. Requirements for Vav guanine nucleotide exchange factors and Rho GTPases in FcgammaR- and complement-mediated phagocytosis. *Immunity.* 2006;24(3):305-16.
321. Pluskota E, Soloviev DA, Szpak D, Weber C, Plow EF. Neutrophil apoptosis: selective regulation by different ligands of integrin alphaMbeta2. *J Immunol.* 2008;181(5):3609-19.
322. Tang RH, Law SK, Tan SM. Selective recruitment of src family kinase Hck by leukocyte integrin alphaMbeta2 but not alphaLbeta2 or alphaXbeta2. *FEBS Lett.* 2006;580(18):4435-42.
323. Xue ZH, Zhao CQ, Chua GL, Tan SW, Tang XY, Wong SC, et al. Integrin alphaMbeta2 clustering triggers phosphorylation and activation of protein kinase C delta that regulates transcription factor Foxp1 expression in monocytes. *J Immunol.* 2010;184(7):3697-709.
324. Han C, Jin J, Xu S, Liu H, Li N, Cao X. Integrin CD11b negatively regulates TLR-triggered inflammatory responses by activating Syk and promoting degradation of MyD88 and TRIF via Cbl-b. *Nat Immunol.* 2010;11(8):734-42.
325. Wright SD, Silverstein SC. Tumor-promoting phorbol esters stimulate C3b and C3b' receptor-mediated phagocytosis in cultured human monocytes. *J Exp Med.* 1982;156(4):1149-64.
326. Wright SD, Craigmyle LS, Silverstein SC. Fibronectin and serum amyloid P component stimulate C3b- and C3bi-mediated phagocytosis in cultured human monocytes. *J Exp Med.* 1983;158(4):1338-43.
327. Wright SD, Silverstein SC. Receptors for C3b and C3bi promote phagocytosis but not the release of toxic oxygen from human phagocytes. *J Exp Med.* 1983;158(6):2016-23.

328. Yamamoto K, Johnston RB, Jr. Dissociation of phagocytosis from stimulation of the oxidative metabolic burst in macrophages. *J Exp Med*. 1984;159(2):405-16.
329. Aderem AA, Wright SD, Silverstein SC, Cohn ZA. Ligated complement receptors do not activate the arachidonic acid cascade in resident peritoneal macrophages. *J Exp Med*. 1985;161(3):617-22.
330. Ross GD, Cain JA, Myones BL, Newman SL, Lachmann PJ. Specificity of membrane complement receptor type three (CR3) for beta-glucans. *Complement*. 1987;4(2):61-74.
331. Vetvicka V, Thornton BP, Ross GD. Soluble beta-glucan polysaccharide binding to the lectin site of neutrophil or natural killer cell complement receptor type 3 (CD11b/CD18) generates a primed state of the receptor capable of mediating cytotoxicity of iC3b-opsonized target cells. *J Clin Invest*. 1996;98(1):50-61.
332. Akramiene D, Kondrotas A, Didziapetriene J, Kevelaitis E. Effects of beta-glucans on the immune system. *Medicina (Kaunas)*. 2007;43(8):597-606.
333. Smith CW, Marlin SD, Rothlein R, Toman C, Anderson DC. Cooperative interactions of LFA-1 and Mac-1 with intercellular adhesion molecule-1 in facilitating adherence and transendothelial migration of human neutrophils in vitro. *J Clin Invest*. 1989;83(6):2008-17.
334. Nathan CF. Neutrophil activation on biological surfaces. Massive secretion of hydrogen peroxide in response to products of macrophages and lymphocytes. *J Clin Invest*. 1987;80(6):1550-60.
335. Nathan C, Srimal S, Farber C, Sanchez E, Kabbash L, Asch A, et al. Cytokine-induced respiratory burst of human neutrophils: dependence on extracellular matrix proteins and CD11/CD18 integrins. *J Cell Biol*. 1989;109(3):1341-9.
336. Nathan CF. Respiratory burst in adherent human neutrophils: triggering by colony-stimulating factors CSF-GM and CSF-G. *Blood*. 1989;73(1):301-6.
337. Ross GD, Vetvicka V. CR3 (CD11b, CD18): a phagocyte and NK cell membrane receptor with multiple ligand specificities and functions. *Clin Exp Immunol*. 1993;92(2):181-4.
338. Akiyama H, McGeer PL. Brain microglia constitutively express beta-2 integrins. *J Neuroimmunol*. 1990;30(1):81-93.
339. Milner R, Campbell IL. The integrin family of cell adhesion molecules has multiple functions within the CNS. *J Neurosci Res*. 2002;69(3):286-91.
340. Kloss CU, Bohatschek M, Kreutzberg GW, Raivich G. Effect of lipopolysaccharide on the morphology and integrin immunoreactivity of ramified microglia in the mouse brain and in cell culture. *Exp Neurol*. 2001;168(1):32-46.
341. Reid DM, Perry VH, Andersson PB, Gordon S. Mitosis and apoptosis of microglia in vivo induced by an anti-CR3 antibody which crosses the blood-brain barrier. *Neuroscience*. 1993;56(3):529-33.
342. Goodwin JL, Kehrli ME, Jr., Uemura E. Integrin Mac-1 and beta-amyloid in microglial release of nitric oxide. *Brain Res*. 1997;768(1-2):279-86.
343. van Beek J, Elward K, Gasque P. Activation of complement in the central nervous system: roles in neurodegeneration and neuroprotection. *Ann N Y Acad Sci*. 2003;992:56-71.
344. Hadas S, Reichert F, Rotshenker S. Dissimilar and similar functional properties of complement receptor-3 in microglia and macrophages in combating yeast pathogens by phagocytosis. *Glia*. 2010;58(7):823-30.
345. Block ML, Zecca L, Hong JS. Microglia-mediated neurotoxicity: uncovering the molecular mechanisms. *Nat Rev Neurosci*. 2007;8(1):57-69.
346. Pei Z, Pang H, Qian L, Yang S, Wang T, Zhang W, et al. MAC1 mediates LPS-induced production of superoxide by microglia: the role of pattern recognition receptors in dopaminergic neurotoxicity. *Glia*. 2007;55(13):1362-73.
347. Hu X, Zhang D, Pang H, Caudle WM, Li Y, Gao H, et al. Macrophage antigen complex-1 mediates reactive microgliosis and progressive dopaminergic neurodegeneration in the MPTP model of Parkinson's disease. *J Immunol*. 2008;181(10):7194-204.

348. Zhang W, Dallas S, Zhang D, Guo JP, Pang H, Wilson B, et al. Microglial PHOX and Mac-1 are essential to the enhanced dopaminergic neurodegeneration elicited by A30P and A53T mutant alpha-synuclein. *Glia*. 2007;55(11):1178-88.
349. Davalos D, Ryu JK, Merlini M, Baeten KM, Le Moan N, Petersen MA, et al. Fibrinogen-induced perivascular microglial clustering is required for the development of axonal damage in neuroinflammation. *Nat Commun*. 2012;3:1227.
350. Ross GD, Cain JA, Lachmann PJ. Membrane complement receptor type three (CR3) has lectin-like properties analogous to bovine conglutinin as functions as a receptor for zymosan and rabbit erythrocytes as well as a receptor for iC3b. *J Immunol*. 1985;134(5):3307-15.
351. Gordon DL, Johnson GM, Hostetter MK. Characteristics of iC3b binding to human polymorphonuclear leucocytes. *Immunology*. 1987;60(4):553-8.
352. Crowther JR. *The ELISA guidebook*. 2nd ed. New York, NY: Humana Press; 2009. xv, 566 p. p.
353. Piddlesden S, Lassmann H, Laffafian I, Morgan BP, Linington C. Antibody-mediated demyelination in experimental allergic encephalomyelitis is independent of complement membrane attack complex formation. *Clin Exp Immunol*. 1991;83(2):245-50.
354. Piddlesden SJ, Lassmann H, Zimprich F, Morgan BP, Linington C. The demyelinating potential of antibodies to myelin oligodendrocyte glycoprotein is related to their ability to fix complement. *Am J Pathol*. 1993;143(2):555-64.
355. Piddlesden SJ. *Antibody-mediated demyelination in experimental allergic encephalomyelitis*. Cardiff: S.J. Piddlesden; 1991. 226p. illus bibliog. p.
356. Bartok I, Walport MJ. Comparison of the binding of C3S and C3F to complement receptors types 1, 2, and 3. *J Immunol*. 1995;154(10):5367-75.
357. Fearon DT, Kaneko I, Thomson GG. Membrane distribution and adsorptive endocytosis by C3b receptors on human polymorphonuclear leukocytes. *J Exp Med*. 1981;153(6):1615-28.
358. Ferkol T, Perales JC, Mularo F, Hanson RW. Receptor-mediated gene transfer into macrophages. *Proc Natl Acad Sci U S A*. 1996;93(1):101-5.
359. Smolny M, Rogers ML, Shafton A, Rush RA, Stebbing MJ. Development of non-viral vehicles for targeted gene transfer into microglia via the integrin receptor CD11b. *Front Mol Neurosci*. 2014;7:79.
360. Wolf HM, Mannhalter JW, Salzmann HC, Gottlicher J, Ahmad R, Eibl MM. Phagocytosis of serum-opsonized zymosan down-regulates the expression of CR3 and FcRI in the membrane of human monocytes. *J Immunol*. 1988;141(10):3537-43.
361. Le Cabec V, Cols C, Maridonneau-Parini I. Nonopsonic phagocytosis of zymosan and *Mycobacterium kansasii* by CR3 (CD11b/CD18) involves distinct molecular determinants and is or is not coupled with NADPH oxidase activation. *Infect Immun*. 2000;68(8):4736-45.
362. Amarilyo G, Verbovetski I, Atallah M, Grau A, Wisner G, Gil O, et al. iC3b-opsonized apoptotic cells mediate a distinct anti-inflammatory response and transcriptional NF-kappaB-dependent blockade. *Eur J Immunol*. 2010;40(3):699-709.
363. Zhou MJ, Brown EJ. CR3 (Mac-1, alpha M beta 2, CD11b/CD18) and Fc gamma RIII cooperate in generation of a neutrophil respiratory burst: requirement for Fc gamma RIII and tyrosine phosphorylation. *J Cell Biol*. 1994;125(6):1407-16.
364. Berton G, Laudanna C, Sorio C, Rossi F. Generation of signals activating neutrophil functions by leukocyte integrins: LFA-1 and gp150/95, but not CR3, are able to stimulate the respiratory burst of human neutrophils. *J Cell Biol*. 1992;116(4):1007-17.
365. Ehlenberger AG, Nussenzweig V. The role of membrane receptors for C3b and C3d in phagocytosis. *J Exp Med*. 1977;145(2):357-71.
366. Huang ZY, Hunter S, Chien P, Kim MK, Han-Kim TH, Indik ZK, et al. Interaction of two phagocytic host defense systems: Fc gamma receptors and complement receptor 3. *J Biol Chem*. 2011;286(1):160-8.
367. Aderem A, Underhill DM. Mechanisms of phagocytosis in macrophages. *Annu Rev Immunol*. 1999;17:593-623.

368. Aderem A. Phagocytosis and the inflammatory response. *J Infect Dis.* 2003;187 Suppl 2:S340-5.
369. Hancock JT. *Cell signalling.* 3rd ed. Oxford ; New York: Oxford University Press; 2010. xxii, 341 p. p.
370. Rehrig S, Fleming SD, Anderson J, Guthridge JM, Rakstang J, McQueen CE, et al. Complement inhibitor, complement receptor 1-related gene/protein γ -Ig attenuates intestinal damage after the onset of mesenteric ischemia/reperfusion injury in mice. *J Immunol.* 2001;167(10):5921-7.
371. Quigg RJ, Kozono Y, Berthiaume D, Lim A, Salant DJ, Weinfeld A, et al. Blockade of antibody-induced glomerulonephritis with Crry-Ig, a soluble murine complement inhibitor. *J Immunol.* 1998;160(9):4553-60.
372. Liu F, Wu L, Wu G, Wang C, Zhang L, Tomlinson S, et al. Targeted mouse complement inhibitor CR2-Crry protects against the development of atherosclerosis in mice. *Atherosclerosis.* 2014;234(1):237-43.
373. Hepburn NJ, Chamberlain-Banoub JL, Williams AS, Morgan BP, Harris CL. Prevention of experimental autoimmune myasthenia gravis by rat Crry-Ig: A model agent for long-term complement inhibition in vivo. *Mol Immunol.* 2008;45(2):395-405.
374. He C, Imai M, Song H, Quigg RJ, Tomlinson S. Complement inhibitors targeted to the proximal tubule prevent injury in experimental nephrotic syndrome and demonstrate a key role for C5b-9. *J Immunol.* 2005;174(9):5750-7.
375. Alexander JJ, Bao L, Jacob A, Kraus DM, Holers VM, Quigg RJ. Administration of the soluble complement inhibitor, Crry-Ig, reduces inflammation and aquaporin 4 expression in lupus cerebritis. *Biochim Biophys Acta.* 2003;1639(3):169-76.
376. Quigg RJ, He C, Lim A, Berthiaume D, Alexander JJ, Kraus D, et al. Transgenic mice overexpressing the complement inhibitor crry as a soluble protein are protected from antibody-induced glomerular injury. *J Exp Med.* 1998;188(7):1321-31.
377. Soltys J, Wu X. Complement regulatory protein Crry deficiency contributes to the antigen specific recall response in experimental autoimmune myasthenia gravis. *J Inflamm (Lond).* 2012;9(1):20.
378. Miwa T, Zhou L, Kimura Y, Kim D, Bhandoola A, Song WC. Complement-dependent T-cell lymphopenia caused by thymocyte deletion of the membrane complement regulator Crry. *Blood.* 2009;113(12):2684-94.
379. Barata L, Miwa T, Sato S, Kim D, Mohammed I, Song WC. Deletion of Crry and DAF on murine platelets stimulates thrombopoiesis and increases factor H-dependent resistance of peripheral platelets to complement attack. *J Immunol.* 2013;190(6):2886-95.
380. Miao J, Leshner AM, Miwa T, Sato S, Gullipalli D, Song WC. Tissue-specific deletion of Crry from mouse proximal tubular epithelial cells increases susceptibility to renal ischemia-reperfusion injury. *Kidney Int.* 2014;86(4):726-37.
381. Bao L, Wang Y, Chang A, Minto AW, Zhou J, Kang H, et al. Unrestricted C3 activation occurs in Crry-deficient kidneys and rapidly leads to chronic renal failure. *J Am Soc Nephrol.* 2007;18(3):811-22.
382. Fernandez-Centeno E, de Ojeda G, Rojo JM, Portoles P. Crry/p65, a membrane complement regulatory protein, has costimulatory properties on mouse T cells. *J Immunol.* 2000;164(9):4533-42.
383. Arsenovic-Ranin N, Vucevic D, Okada N, Dimitrijevic M, Colic M. A monoclonal antibody to the rat Crry/p65 antigen, a complement regulatory membrane protein, stimulates adhesion and proliferation of thymocytes. *Immunology.* 2000;100(3):334-44.
384. Antic Stankovic J, Vucevic D, Majstorovic I, Vasilijic S, Colic M. The role of rat Crry, a complement regulatory protein, in proliferation of thymocytes. *Life Sci.* 2004;75(25):3053-62.
385. Jimenez-Perianez A, Ojeda G, Criado G, Sanchez A, Pini E, Madrenas J, et al. Complement regulatory protein Crry/p65-mediated signaling in T lymphocytes: role of its cytoplasmic domain and partitioning into lipid rafts. *J Leukoc Biol.* 2005;78(6):1386-96.

386. Ojeda G, Pini E, Eguiluz C, Montes-Casado M, Broere F, van Eden W, et al. Complement regulatory protein Crry/p65 costimulation expands natural treg cells with enhanced suppressive properties in proteoglycan-induced arthritis. *Arthritis Rheum.* 2011;63(6):1562-72.
387. Hanna S, Spiller O, Linton SM, Mead RJ, Morgan B. Rat T cells express neither CD55 nor CD59 and are dependent on Crry for protection from homologous complement. *Eur J Immunol.* 2002;32(2):502-9.
388. Li Q, Nacion K, Bu H, Lin F. Mouse CD4⁺ CD25⁺ T regulatory cells are protected from autologous complement mediated injury by Crry and CD59. *Biochem Biophys Res Commun.* 2009;382(1):223-6.
389. Renner B, Coleman K, Goldberg R, Amura C, Holland-Neidermyer A, Pierce K, et al. The complement inhibitors Crry and factor H are critical for preventing autologous complement activation on renal tubular epithelial cells. *J Immunol.* 2010;185(5):3086-94.
390. Molina H. The murine complement regulator Crry: new insights into the immunobiology of complement regulation. *Cell Mol Life Sci.* 2002;59(2):220-9.
391. Killick R, Hughes TR, Morgan BP, Lovestone S. Deletion of Crry, the murine ortholog of the sporadic Alzheimer's disease risk gene CR1, impacts tau phosphorylation and brain CFH. *Neurosci Lett.* 2013;533:96-9.
392. Davoust N, Nataf S, Reiman R, Holers MV, Campbell IL, Barnum SR. Central nervous system-targeted expression of the complement inhibitor sCrry prevents experimental allergic encephalomyelitis. *J Immunol.* 1999;163(12):6551-6.
393. Rancan M, Morganti-Kossmann MC, Barnum SR, Saft S, Schmidt OI, Ertel W, et al. Central nervous system-targeted complement inhibition mediates neuroprotection after closed head injury in transgenic mice. *J Cereb Blood Flow Metab.* 2003;23(9):1070-4.
394. Rogers CA, Gasque P, Piddlesden SJ, Okada N, Holers VM, Morgan BP. Expression and function of membrane regulators of complement on rat astrocytes in culture. *Immunology.* 1996;88(1):153-61.
395. Davoust N, Nataf S, Holers VM, Barnum SR. Expression of the murine complement regulatory protein crry by glial cells and neurons. *Glia.* 1999;27(2):162-70.
396. Li B, Sallee C, Dehoff M, Foley S, Molina H, Holers VM. Mouse Crry/p65. Characterization of monoclonal antibodies and the tissue distribution of a functional homologue of human MCP and DAF. *J Immunol.* 1993;151(8):4295-305.
397. Quigg RJ, Lo CF, Alexander JJ, Sneed AE, 3rd, Moxley G. Molecular characterization of rat Crry: widespread distribution of two alternative forms of Crry mRNA. *Immunogenetics.* 1995;42(5):362-7.
398. Briggs DT, Martin CB, Ingersoll SA, Barnum SR, Martin BK. Astrocyte-specific expression of a soluble form of the murine complement control protein Crry confers demyelination protection in the cuprizone model. *Glia.* 2007;55(14):1405-15.
399. Leinhase I, Schmidt OI, Thurman JM, Hossini AM, Rozanski M, Taha ME, et al. Pharmacological complement inhibition at the C3 convertase level promotes neuronal survival, neuroprotective intracerebral gene expression, and neurological outcome after traumatic brain injury. *Exp Neurol.* 2006;199(2):454-64.
400. Kim DD, Miwa T, Song WC. Retrovirus-mediated over-expression of decay-accelerating factor rescues Crry-deficient erythrocytes from acute alternative pathway complement attack. *J Immunol.* 2006;177(8):5558-66.
401. Hanisch UK, Kettenmann H. Microglia: active sensor and versatile effector cells in the normal and pathologic brain. *Nat Neurosci.* 2007;10(11):1387-94.
402. Hernandez-Ontiveros DG, Tajiri N, Acosta S, Giunta B, Tan J, Borlongan CV. Microglia activation as a biomarker for traumatic brain injury. *Front Neurol.* 2013;4:30.
403. Ooi YM, Colten HR. Genetic defect in secretion of complement C5 in mice. *Nature.* 1979;282(5735):207-8.
404. Harboe M, Garred P, Lindstad JK, Pharo A, Muller F, Stahl GL, et al. The role of properdin in zymosan- and *Escherichia coli*-induced complement activation. *J Immunol.* 2012;189(5):2606-13.

405. Lian H, Yang L, Cole A, Sun L, Chiang AC, Fowler SW, et al. NFkappaB-activated astroglial release of complement C3 compromises neuronal morphology and function associated with Alzheimer's disease. *Neuron*. 2015;85(1):101-15.
406. Granados-Duran P, Lopez-Avalos MD, Hughes TR, Johnson K, Morgan BP, Tamburini PP, et al. Complement system activation contributes to the ependymal damage induced by microbial neuraminidase. *J Neuroinflammation*. 2016;13(1):115.
407. Hong S, Beja-Glasser VF, Nfonoyim BM, Frouin A, Li S, Ramakrishnan S, et al. Complement and microglia mediate early synapse loss in Alzheimer mouse models. *Science*. 2016;352(6286):712-6.
408. Lian H, Litvinchuk A, Chiang AC, Aithmitti N, Jankowsky JL, Zheng H. Astrocyte-Microglia Cross Talk through Complement Activation Modulates Amyloid Pathology in Mouse Models of Alzheimer's Disease. *J Neurosci*. 2016;36(2):577-89.
409. Lui H, Zhang J, Makinson SR, Cahill MK, Kelley KW, Huang HY, et al. Progranulin Deficiency Promotes Circuit-Specific Synaptic Pruning by Microglia via Complement Activation. *Cell*. 2016;165(4):921-35.
410. Walter HL, van der Maten G, Antunes AR, Wieloch T, Ruscher K. Treatment with AMD3100 attenuates the microglial response and improves outcome after experimental stroke. *J Neuroinflammation*. 2015;12:24.
411. Biber K, Moller T, Boddeke E, Prinz M. Central nervous system myeloid cells as drug targets: current status and translational challenges. *Nat Rev Drug Discov*. 2016;15(2):110-24.
412. Tremblay ME, Zhang I, Bisht K, Savage JC, Lecours C, Parent M, et al. Remodeling of lipid bodies by docosahexaenoic acid in activated microglial cells. *J Neuroinflammation*. 2016;13(1):116.

Appendix

Company Addresses

Ambion, Life Technologies Ltd., Paisley, UK

Applied Biosystems, Life Technologies Ltd, Paisley, UK

Becton Dickinson, Oxford, UK

BioLegend, London, UK

Biomers.net GmbH, Ulm, Germany

Bio-Rad Laboratories Ltd, Hemel Hempstead, UK

BMG Labtech, Aylesbury, UK

Complement Technology, Inc., Tyler, Texas, USA

Corning B.V Life Sciences, Amsterdam, Netherlands

eBioscience Inc., San Diego, USA

Fisher Scientific, Loughborough, UK

Gibco, Life Technologies Ltd, Paisley, UK

GraphPad Software Inc, San Diego, CA, USA

Greiner, Stonehouse, Gloucestershire, UK

Hycult Biotech, Uden, Netherlands

Invitrogen, Life Technologies Ltd, Paisley, UK

Jackson Immuno Research Europe Ltd, Suffolk, England

Millipore (U.K.) Ltd, Watford, UK

Miltenyi Biotec, Surrey, UK

MJ Research Inc., St. Bruno, Canada

New England Biolabs, Ipswich, Massachusetts, USA

NIH, Maryland, USA

Nikon Corp., Tokyo, Japan

Nunc International, New York, USA

Promega Ltd, Southampton, UK

R&D Systems, Abingdon, Oxfordshire, UK

Sigma-Aldrich, Dorset, UK

Starlab, Milton Keynes, USA

Thermo Fisher Scientific, Waltham, USA

Treestar, Inc./FlowJo, L.L.C., Ashland, Oregon, USA

Vector Laboratories, Peterborough, UK

Viropharma Inc., Exton, Pennsylvania, USA